

**INVESTIGATION OF FACTORS
AFFECTING THE
REGION OF ORIGIN ESTIMATE IN
BLOODSTAIN PATTERN ANALYSIS**

**A thesis
submitted in partial fulfilment
of the requirements for the Degree
of
Master of Science
in
Medical Physics
by
Joanna K. Wells**

**University of Canterbury
2006**

ABSTRACT

The causes of errors in the angle of impact calculation were investigated including the surface type, falling velocity and the method used to fit an ellipse to a bloodstain. As had been cited previously the angle of impact was generally underestimated, especially at acute angles and the reason for this was determined to be due to an overestimation of the length of a bloodstain. The surface type was found to significantly affect the accuracy of an angle of impact calculation and as the falling velocity increased, the angle of impact calculation became more accurate. High-speed photography was used to further investigate the formation of bloodstains on surfaces. It was found that the formation of the bloodstain varied depending on the surface type and the angle of the surface.

Bloodstain pattern analysis involves the application of scientific techniques to reconstruct events that resulted in a bloodstain pattern. The position of the blood source in three-dimensional space is a fundamental element of this application. Currently little is known about the methods used by bloodstain pattern analysts to select bloodstains when determining the region of origin. Fourteen analysts worldwide were surveyed in order to ascertain this information. It was found that the methods used were variable and were often not based on scientific research. Research was therefore undertaken into bloodstain selection and in particular, which bloodstains should be selected for a region of origin analysis. As a result of these experiments, two sets of selection criteria were established, one for use when the region of origin is being calculated manually and one for when directional analysis is being used.

ACKNOWLEDGEMENTS

This work has been accomplished at the Institute for Environmental Science and Research Limited (ESR), Christchurch. I would firstly like to thank my supervisor from ESR, Dr Michael Taylor for his enthusiasm, patient guidance and for the many opportunities he presented to me throughout this journey.

I would also like to thank my University of Canterbury supervisor Dr Richard Watts, for whom this area of research was mostly novel. I appreciate your input especially in the physics related experiments. Thanks for your effort to always explain things simply to me.

To the forensic team, Gary, Wendy J, Roz, Lauren, Gillian, Wendy L, Paulette and Janine, thank you for your kind support and interest in my project this year.

To Emma Ross, another MSc student for the proofreading, the use of your camera during the first part of the research and for all the interesting discussions on the physics of BPA this year.

To Stuart Brown from Alliance Meatworks for providing the blood used in the experiments every week.

To Nicolas Oliver of the Chemistry department, University of Canterbury for constructing the mechanical device used to create impact spatter patterns for the research.

To my parents Trisha and Mike Wells for the support and encouragement you have provided me. Thanks for always believing in me - not only throughout this year but every year of my education.

To all of my friends, thank you for your awesome support throughout this year. Finally, I would like to give a special thank you to Owen. Thanks for always being there for me - your love and support is greatly appreciated.

TABLE OF CONTENTS

ABSTRACT.....	II
ACKNOWLEDGEMENTS	III
TABLE OF CONTENTS	IV
LIST OF TABLES	IX
LIST OF FIGURES	X
LIST OF ABBREVIATIONS	XVI
SUMMARY OF RESEARCH FINDINGS.....	XVII
Blood dynamics	XVII
Angle of impact	XVII
Selection of bloodstains.....	XVIII
 CHAPTER ONE: INTRODUCTION.....	 1
1.1 <i>Introduction.....</i>	1
1.1.1 Classification of bloodstain patterns.....	1
1.1.2 Impact patterns.....	2
1.1.3 Information from an impact pattern.....	2
1.2 <i>Background to the region of origin.....</i>	3
1.2.1 Directionality of bloodstains.....	4
1.2.2 2D Area of convergence	6
1.2.3 Angle of impact.....	7
1.2.4 Ellipse fitted to a bloodstain	8
1.2.5 Determination of the region of origin	9
1.2.5.1 Stringing.....	9
1.2.5.2 Tangent method	10
1.2.5.3 Directional analysis.....	11
1.2.5.1.1 BackTrack™	12
1.2.6 The result	13
1.3 <i>Stain selection criteria and estimation of error.....</i>	14
1.4 <i>Scope and layout of this thesis</i>	17
 CHAPTER TWO: FACTORS THAT MAY CONTRIBUTE TO UNCERTAINTIES IN THE REGION OF ORIGIN	 19
2.1 <i>Errors relating to the flight path calculation.....</i>	19
2.1.1 Determination of the angle of impact	19
2.1.1.1 ‘Normal’ measurement errors.....	19
2.1.1.2 Asymmetric nature of a bloodstain	20
2.1.1.3 Additional systematic error.....	21
2.1.1.4 Oscillations	24
2.1.2 Determination of direction.....	25
2.1.2.1 ‘Normal’ measurement error.....	25
2.1.3 The effect of gravity and air resistance.....	25
2.1.4 Secondary effects	26
2.2 <i>Errors relating to the method of convergence</i>	26
2.3 <i>The effect of errors on the region of origin.....</i>	27

2.3.1	Systematic errors.....	27
2.3.1.1	Errors in alpha.....	27
2.3.1.2	Gravity and air resistance.....	27
2.3.1.3	Different methods of convergence.....	28
2.3.2	Random errors.....	28
2.3.2.1	Errors in gamma.....	28
2.4	Avoiding errors.....	28
	Angle of impact	28
	Gamma	29
	Air resistance and gravity	29
	Method of convergence	29
CHAPTER THREE: GENERAL METHODS AND MATERIALS.....		30
3.1	Laboratories.....	30
3.2	Blood.....	30
3.3	Angle board and dropping pipette	31
3.4	Generation of impact spatter patterns	34
3.4.1	Hammer and wooden block method	34
3.4.2	Impact device	35
3.5	Photography.....	37
3.6	Health and safety procedures	38
CHAPTER FOUR: BLOOD DYNAMICS.....		39
4.1	Droplet impact with a target surface.....	39
4.1.1	Introduction.....	39
4.1.2	Method	43
4.1.3	Results.....	44
4.1.4	Discussion.....	47
4.2	The dynamics of an impact event.....	51
4.2.1	Introduction.....	51
4.2.2	Method	52
4.2.3	Results.....	53
4.2.3.1	Hammer impact.....	53
4.2.3.2	The device impact.....	58
4.2.4	Discussion.....	63
	Chapter conclusions	64
CHAPTER FIVE: ANGLE OF IMPACT CONSIDERATIONS.....		65
5.1	The method used to fit an ellipse to a bloodstain when determining the angle of impact.....	66
5.1.1	Introduction.....	66
5.1.2	Method	68
5.1.2.1	Microsoft® Excel 2000.....	69
5.1.2.2	Microsoft® Office Visio® Professional 2003	70
5.1.2.3	BackTrack™/Images	72
5.1.2.4	STABS	74
5.1.3	Results.....	76
5.1.4	Discussion and conclusion.....	77

5.2	<i>The effect of target surface</i>	81
5.2.1	The effect of different target surfaces on the angle of impact estimation	81
5.2.1.1	Introduction	81
5.2.1.2	Method	81
5.2.1.3	Results	82
5.2.1.3.1	Student's t test results	84
5.2.1.4	Discussion	85
5.2.1.5	Conclusions	87
5.3	<i>Surface wettability</i>	89
5.3.1	Introduction	89
5.3.2	Method	92
5.3.3	Results	92
5.3.4	Discussion and conclusion	96
5.4	<i>High-speed photography of blood drops impacting different target surfaces</i>	99
5.4.1	Introduction	99
5.4.2	Method	99
5.4.3	Results and discussion	101
5.4.3.1	Cardboard	102
5.4.3.2	Vinyl	104
5.4.3.3	Wallpaper	106
5.4.3.4	Wood	108
5.4.4	Conclusion	111
5.5	<i>The effect of different velocities on the angle of impact calculation</i>	112
5.5.1	Introduction	112
5.5.2	Method	112
5.5.2.1	Generation of bloodstains	112
5.5.2.2	Measurement of bloodstains	113
5.5.2.3	Determination the angle of impact	113
5.5.3	Results	113
5.5.4	Discussion	114
5.5.5	Conclusions	115
5.6	<i>Was there an underestimation of the angle of impact at acute angles?</i>	116
5.6.1	Introduction	116
5.6.2	Method	116
5.6.3	Results	116
5.6.3.1	Surface experiment (section 5.2)	116
5.6.3.2	Velocity experiment (section 5.5)	117
5.6.4	Discussion and conclusion	118
CHAPTER SIX: BLOODSTAIN SELECTION SURVEY		121
6.1	<i>Introduction</i>	121
6.2	<i>Method</i>	121
6.3	<i>Results</i>	123
6.3.1	Participants	123
6.3.2	Selection of bloodstains	123
6.3.3	Question 1: Briefly explain why you selected these particular bloodstains.	125

6.3.4	Question 2: Can you give any other details of the strategy you use at scenes when selecting bloodstains for region of origin calculations?	126
	Responses included:.....	126
6.3.5	Question 3: If you were to go on to determine the region of origin which method would you use?.....	127
6.3.6	Question 4: If you were presenting a region of origin you had determined in a statement or likewise, would you include any indication that it could involve an element of error? If so how would you state this?	127
	Table 6.5 shows the responses to this question.....	127
6.4	<i>Discussion</i>	128
6.4.1	Selection of bloodstains	128
6.4.2	Question 1	129
6.4.3	Question 2	129
6.4.4	Question 3	130
6.4.5	Question 4	131
6.5	<i>Conclusion</i>	131

CHAPTER SEVEN: BLOODSTAIN SELECTION132

7.1	<i>Ability of individual bloodstains to predict the region of origin</i>	132
7.1.1	Introduction.....	132
7.1.2	Method	133
7.1.2.1	Generation of impact spatter patterns	133
7.1.2.2	Stain selection and recording procedure	134
7.1.2.3	Analysis of bloodstains	135
7.1.2.4	Quantifying the ability of individual bloodstains to determine the region of origin	135
7.1.3	Results.....	137
7.1.3.1	Graphs of d versus length, width, alpha, gamma Y and Z position for impact A.	139
7.1.3.2	Graphs of d versus length, width, alpha, gamma Y and Z position for impact B.	141
7.1.3.3	Graphs of d versus length, width, alpha, gamma Y and Z position for impact C.	143
7.1.3.4	Graphs of d versus length, width, alpha, gamma Y and Z position for impact D.	145
7.1.4	Discussion	147
7.1.5	Conclusion	148
7.2	<i>The time of flight of blood drops</i>	150
7.2.1	Introduction.....	150
7.2.2	Method	150
7.2.3	Results.....	153
7.2.4	Discussion	156
7.2.5	Conclusion	157
7.3	<i>Investigation of stain selection theories</i>	158
7.3.1	Well-formed bloodstains.....	158
7.3.2	The effect of selecting an equal number of bloodstains from an impact pattern when using a manual method to determine the region of origin	160
7.3.2.1	Introduction.....	160
7.3.2.2	Method	160

7.3.2.3	Results.....	161
7.3.2.4	Discussion.....	163
7.3.3	Assessing whether the accuracy of a region of origin estimate improves as the number of bloodstains selected for the analysis increases.....	163
7.3.3.1	Introduction.....	163
7.3.3.2	Method	164
7.3.3.3	Results.....	165
7.3.3.4	Discussion.....	168
7.3.3.5	Conclusions.....	169
7.4	<i>Bloodstain selection criteria.....</i>	171
7.4	<i>Selection strategies identified in bloodstain pattern analyst survey.....</i>	173
CHAPTER EIGHT: FUTURE DIRECTIONS.....		176
APPENDIX 1: HEALTH AND SAFETY PROCEDURES		177
APPENDIX 2: RESULTS TABLES AND DATA.....		180
REFERENCES.....		184

LIST OF TABLES

Table 2.1 The average difference between the determined and known region of origin coordinate for single-blow targets using different methods.	27
Table 3.1 Specifications of the cameras used during the research.	38
Table 4.1 The width and length of bloodstains formed at various angles of impact.	49
Table 5.1 Summary of the different target surfaces.....	68
Table 5.2 Student's t-test results for the angle of impact of bloodstains created on different surfaces at 20 degrees.....	84
Table 5.3 Student's t-test results for the angle of impact of bloodstains created on different surfaces at 30 degrees.....	84
Table 5.4 Student's t-test results for the angle of impact of bloodstains created on different surfaces at 40 degrees.....	84
Table 5.5 Student's t-test results for the angle of impact of bloodstains created on different surfaces at 60 degrees.....	85
Table 5.6 Student's t-test results for the angle of impact of bloodstains created on different surfaces at 80 degrees.....	85
Table 5.7 Summary of the different surfaces used in the experiment.	92
Table 5.8: The contact angle of a single droplet of blood on different surfaces.....	96
Table 5.9 Summary of the different target surfaces.....	100
Table 5.10 The width and length measurements and the calculated angle of impact of three bloodstains made on a cardboard surface.	103
Table 5.11 The width and length measurements and the calculated angle of impact of three bloodstains made on a vinyl surface	105
Table 5.12 The width and length measurements and the calculated angle of impact of three bloodstains made on a wallpaper surface.....	107
Table 5.13 The width and length measurements and the calculated angle of impact of three bloodstains made on a wood surface.	109
Table 5.14 The time taken for bloodstains to form on different surfaces.....	111
Table 6.1 The number of participants from each country.....	123
Table 6.2 The total number of bloodstains selected by each analyst and the grid number they were selected from.	124
Table 6.3 The analysts reasons for selecting bloodstains.	125
Table 6.4 The method(s) used by the 14 analysts to determine the region of origin...	127
Table 6.5 Whether each of the 14 analysts would include a statement of error in a statement of likewise and if so how they would state it.	128
Table 7.1 The method of generation and position of impacts A – D.....	134

LIST OF FIGURES

Figure 1.1 Directionality of bloodstains. Bloodstain impacting a surface at 10°, direction observed (a), a 90° stain that has no direction (b).....	4
Figure 1.2 The gamma angle is determined by drawing a vertical line next to the bloodstain, drawing a line through the long axis of the bloodstain and then measuring the angle of the long axis in a clockwise direction from the vertical line.....	5
Figure 1.3 The area of convergence is determined by drawing lines through the major axis of a number of bloodstains along their direction of travel and looking for an area where the majority of these lines intersect.....	6
Figure 1.4 A droplet impacting as a sphere and the trigonometric relationship of the resultant ellipse with that sphere (Formula 1.1). Where ab is the width of the ellipse and bc is the length of the ellipse.	7
Figure 1.5 A bloodstain showing wave cast-off with a best-fit ellipse superimposed. .	8
Figure 1.6 A three-dimensional representation of the X, Y and Z coordinate system used when determining the region of origin.	9
Figure 1.7 When the tangent method is used the convergence point (B) is determined first, followed by the angle of impact (α) and the distance from each bloodstain to the convergence point (D). Using this information the distance from the convergence point to the region of origin can be calculated using $X = D \tan \alpha$. A is the position of the bloodstain.	10
Figure 1.8 Top view from BackTrack™/Win where virtual strings represent the trajectories of blood droplets.	11
Figure 1.9 Side view from BackTrack™/Win where virtual strings represent the trajectories of blood droplets.	12
Figure 1.10 The beta angle is the acute angle between the flight path and the wall when observing the top view.	13
Figure 1.11 As the angle of impact approached 90°, the variance of the estimated angle of impact grew without limit (experimental). The derived equation accurately predicts the variance up to an angle of impact of 60° and predicts that the variance increases rapidly as the angle of impact approaches 90° (calculated).....	15
Figure 2.1 An ellipse fitted to the bloodstain resulting in an underestimation of the angle of impact (incorrect fit) and the ellipse that should be measured (correct fit). The differences in the ellipses include the length and how well they fit the bloodstain at the back edge.	21
Figure 2.2 Graph of the average observed minus expected angles (20 degrees) for bloodstains measured manually and by the computer method.	22
Figure 2.3 The expected angle plotted against the observed minus expected angle. The data was collected from the Collaborative Testing Service tests.	23
Figure 2.4 Graph of the difference between observed and expected angles, against expected angle for different stain sizes.	24
Figure 2.5 The flight path of a blood droplet is concave downward. This results in the Z-axis coordinate often being overestimated.	26
Figure 3.1 Front view of the angle board showing the positioning of the target surface and the bulldog clips.....	31

Figure 3.2 Side view of the angle board showing the protractor used in conjunction with an angle finder to set the angle	32
Figure 3.3 Johnson magnetic angle locator	32
Figure 3.4 A 200 μ l Gilson pipette clamped to a 2 m clamp stand positioned above the angle board	33
Figure 3.5 Parafilm covered wooden block with blood pool.....	34
Figure 3.6 Hammer used to make impacts.....	34
Figure 3.7 Impact device.....	36
Figure 3.8 Chamfer on the dropping weight.....	36
Figure 4.1 Parameters of importance during drop impact.	40
Figure 4.2 Impact of a drop on a solid surface: bouncing, spreading and splashing	41
Figure 4.3 Blood droplet with satellite spatter.....	41
Figure 4.4 A series of photographs taken as a blood drop impacts an angled surface .	42
Figure 4.5 The resulting bloodstain	43
Figure 4.6 Mirror set-up.....	43
Figure 4.7 Blood droplet impacting a cardboard surface at 10°.....	44
Figure 4.8 Blood droplet impacting a cardboard surface at 20°.....	45
Figure 4.9 Blood droplet impacting a cardboard surface at 30°.....	46
Figure 4.10 Blood droplet impacting a cardboard surface at 40°.....	47
Figure 4.11 Wave cast-off at 30° (left hand side) and 20° (right hand side)	48
Figure 4.12 Measurement of the length of the bloodstain	49
Figure 4.13 The width of the bloodstain at different angles of impact.....	50
Figure 4.14 The length of the bloodstain at different angles of impact.....	50
Figure 4.15 Bevel and Gardner propose that the majority of droplets are created during the shaded period and that this results in a preponderant stain size.	52
Figure 4.16 Overview of the hammer impact event	54
Figure 4.17 Position of hammer when it struck a 2 ml pool of blood	55
Figure 4.18 The left hand side of this image shows the horizontal sheet	55
Figure 4.19 The right hand side of this image shows the wave coming up around hammer.	56
Figure 4.20 The sheet.....	56
Figure 4.21 The sheet breaking up into filaments.....	57
Figure 4.22 The filaments breaking up into drops.....	57
Figure 4.23 Overview of the hammer impact event	59
Figure 4.24 The horizontal layer after device impact.....	60
Figure 4.25 Misting effect shown on the resulting bloodstain pattern	60
Figure 4.26 Layer travelling upwards.....	61
Figure 4.27 Sheet breaking into filaments	61
Figure 4.28 Filaments	62
Figure 4.29 Droplets	62
Figure 5.1 The method for fitting an ellipse to a bloodstain.....	66
Figure 5.2 In a survey to determine how accurately bloodstain pattern analysts measured the angle of impact, it was found that the accuracy of the measurements was above 50% in only four of the drops.....	67
Figure 5.3 Fitting an ellipse to a bloodstain in Microsoft® Excel 2000.....	70
Figure 5.4 Fitting of an ellipse to a bloodstain in Microsoft® Office Visio® Professional 2003.....	71
Figure 5.5 Size and position table in Microsoft® Office Visio® Professional 2003.	72
Figure 5.6 Pulling the mouse across the bloodstains width at the approximate mid-length in BackTrack™/Images.	73

Figure 5.7 Clicking the mouse at the leading edge of the bloodstain reveals a dotted ellipse in BackTrack™/Images.....	73
Figure 5.8 Manual ellipse editing function in BackTrack™/Images.....	74
Figure 5.9 The main screen of STABS with a bloodstain loaded and ready for an ellipse to be fitted.....	75
Figure 5.10 The main screen of STABS showing an ellipse fitted to a bloodstain and the slide bars and arrows that allow the ellipse to be adjusted.	75
Figure 5.11 The observed minus expected angle of impact calculated using four different methods plotted against the angle of impact at 20°, 30°, 40°, 60° and 80 °for bloodstains formed on wood. The standard deviation is also plotted on the graph.	76
Figure 5.12 The observed minus expected angle of impact calculated using four different methods plotted against the angle of impact at 20°, 30°, 40°, 60° and 80 °for bloodstains formed on cardboard. The standard deviation is also plotted on the graph.	77
Figure 5.13 The error in the angle of impact calculation at varying impact angles (actual). Results were determined using Microsoft ® Office Visio ® Professional 2003.....	83
Figure 5.14 The standard deviation of the calculated angle of impact increased with the angle of impact.....	83
Figure 5.15 The contact angle (Θ).	89
Figure 5.16 Normal view of the impact of a 2 mm diameter water droplet at 1 m/s onto a 45° stainless steel incline over a 20 ms period.	90
Figure 5.17 Liquid-solid contact angle (θ) measurement from a photograph of a droplet of pure water 8.2 ms after impacting a stainless steel surface.....	91
Figure 5.18 Photograph of a single blood droplet on cardboard.....	93
Figure 5.19 Diameter of a blood droplet on cardboard.....	93
Figure 5.20 Photograph of a single blood droplet on paper.	93
Figure 5.21 Diameter of a blood droplet on paper.	93
Figure 5.22 Photograph of a single blood droplet on tile.	94
Figure 5.23 Diameter of a blood droplet on tile.....	94
Figure 5.24 Photograph of a single blood droplet on wood.....	94
Figure 5.25 Diameter of a blood droplet on wood.....	94
Figure 5.26 Photograph of a single blood droplet on vinyl.	95
Figure 5.27 Diameter of a blood droplet on vinyl.	95
Figure 5.28 Photograph of a single blood droplet on glass.....	95
Figure 5.29 Diameter of a blood droplet on glass.....	95
Figure 5.30 The observed minus expected angle of impact (determined using Microsoft Office Visio) versus the contact angle for five different surfaces (the impact angle was 30 degrees).	97
Figure 5.31 The observed minus expected angle of impact (determined using Microsoft Office Visio) versus the contact angle for five different surfaces (the impact angle was 80 degrees).	98
Figure 5.32 High-speed camera set-up.	100
Figure 5.33 The width of a blood drop prior to impacting the target surface was 4 mm.	101
Figure 5.34 Still images taken from a high-speed video of a blood drop impacting a piece of cardboard at 30 degrees – front view.	102
Figure 5.35 Still images taken from a high-speed video of a blood drop impacting a piece of cardboard at 30 degrees – side view.	102
Figure 5.36 The resulting bloodstain – cardboard.	103

Figure 5.37 Still images taken from a high-speed video of a blood drop impacting a piece of vinyl at 30 degrees – front view.	104
Figure 5.38 Still images taken from a high-speed video of a blood drop impacting a piece of vinyl at 30 degrees – side view.	104
Figure 5.39 The resulting bloodstain – vinyl.	105
Figure 5.40 Still images taken from a high-speed video of a blood drop impacting a piece of wallpaper bound to cardboard at 30 degrees – front view.	106
Figure 5.41 Still images taken from a high-speed video of a blood drop impacting a piece of wallpaper bound to cardboard at 30 degrees – side view.	106
Figure 5.42 The resulting bloodstain – wallpaper.	107
Figure 5.43 Still images taken from a high-speed video of a blood drop impacting a piece of wood at 30 degrees – front view.	108
Figure 5.44 Still images taken from a high-speed video of a blood drop impacting a piece of wood at 30 degrees – side view.	108
Figure 5.45 The resulting bloodstain – wood.	109
Figure 5.46 The observed minus expected angle of impact determined for bloodstains generated at different angles from different heights.	113
Figure 5.47 The error in the angle of impact calculation at varying impact angles (actual). Results were determined using Microsoft ® Office Visio ® Professional 2003.	117
Figure 5.48 The angle of impact determined for bloodstains generated at different angles from different heights.	118
Figure 6.1 Image of the entire impact pattern and the position of each of the grids. ..	122
Figure 6.2 Image of the entire impact pattern and the number of bloodstains selected from each grid.	124
Figure 6.3 The method used by analysts for determining the region of origin. Some analysts indicated that they would use more than one method.	130
Figure 7.1 Diagram representing the position of a bloodstain on a wall (P_0), the region of origin (P_i) and the virtual string drawn along the flight path of the bloodstain.	136
Figure 7.2: Graph of d versus bloodstain length 2D.	139
Figure 7.3: Graph of d versus bloodstain length 3D.	139
Figure 7.4: Graph of d versus bloodstain width 2D.	139
Figure 7.5: Graph of d versus bloodstain width 3D.	139
Figure 7.6: Graph of d versus alpha 2D.	139
Figure 7.7: Graph of d versus alpha 3D.	139
Figure 7.8: Graph of d versus gamma 2D.	140
Figure 7.9: Graph of d versus gamma 3D.	140
Figure 7.10: Graph of d versus Y position 2D.	140
Figure 7.11: Graph of d versus Y position 3D.	140
Figure 7.12: Graph of d versus Z position 2D.	140
Figure 7.13: Graph of d versus Z position 3D.	140
Figure 7.14: Graph of d versus bloodstain length 2D.	141
Figure 7.15: Graph of d versus bloodstain length 3D.	141
Figure 7.16: Graph of d versus bloodstain width 2D.	141
Figure 7.17: Graph of d versus bloodstain width 3D.	141
Figure 7.18: Graph of d versus alpha 2D.	141
Figure 7.19: Graph of d versus alpha 3D.	141
Figure 7.20: Graph of d versus gamma 2D.	142
Figure 7.21: Graph of d versus gamma 3D.	142
Figure 7.22: Graph of d versus Y position 2D.	142
Figure 7.23: Graph of d versus Y position 3D.	142

Figure 7.24: Graph of d versus Z position 2D	142
Figure 7.25: Graph of d versus Z position 3D.	142
Figure 7.26: Graph of d versus bloodstain length 2D.....	143
Figure 7.27: Graph of d versus bloodstain length 3D.....	143
Figure 7.28: Graph of d versus bloodstain width 2D.....	143
Figure 7.29: Graph of d versus bloodstain width 3D.....	143
Figure 7.30: Graph of d versus alpha 2D.....	143
Figure 7.31: Graph of d versus alpha 3D.....	143
Figure 7.32: Graph of d versus gamma 2D.....	144
Figure 7.33: Graph of d versus gamma 3D.....	144
Figure 7.34: Graph of d versus Y position 2D.....	144
Figure 7.35: Graph of d versus Y position 3D.....	144
Figure 7.36: Graph of d versus Z position 2D.	144
Figure 7.37: Graph of d versus Z position 3D.	144
Figure 7.38: Graph of d versus bloodstain length 2D.....	145
Figure 7.39: Graph of d versus bloodstain length 3D.....	145
Figure 7.40: Graph of d versus bloodstain width 2D.....	145
Figure 7.41: Graph of d versus bloodstain width 3D.....	145
Figure 7.42: Graph of d versus alpha 2D.....	145
Figure 7.43: Graph of d versus alpha 3D.....	145
Figure 7.44: Graph of d versus gamma 2D.....	146
Figure 7.45: Graph of d versus gamma 3D.....	146
Figure 7.46: Graph of d versus Y position 2D.....	146
Figure 7.47: Graph of d versus Y position 3D.....	146
Figure 7.48: Graph of d versus Z position 2D.	146
Figure 7.49: Graph of d versus Z position 3D.	146
Figure 7.50 The horizontal and vertical components of the flight path of a blood drop.	151
Figure 7.51 Diagram showing point f, Vfy, Vfz, Zf, Yf and i.....	152
Figure 7.52 The time a bloodstain travelled through the air (t^2) before impacting a wall versus the amount of 3D error in the region of origin estimation (d) for Impact A.....	154
Figure 7.53 The time a bloodstain travelled through the air (t^2) before impacting a wall versus the amount of 3D error in the region of origin estimation (d) for Impact B.....	154
Figure 7.54 The time a bloodstain travelled through the air (t^2) before impacting a wall versus the amount of 3D error in the region of origin estimation (d) for Impact C.....	155
Figure 7.55 The time a bloodstain travelled through the air (t^2) before impacting a wall versus the amount of 3D error in the region of origin estimation (d) for Impact D.....	155
Figure 7.56 The concept of a well-formed bloodstain. If the bloodstain is divided along it's major axis, the opposite halves would be equal to each other.	158
Figure 7.57 Examples of bloodstains that are not well-formed.	159
Figure 7.58 Examples of bloodstains that are well-formed.	159
Figure 7.59 Examples of bloodstains with ellipses fitted to them. Bloodstain b is a well-formed stain and a and c are not.	159
Figure 7.60 The area of convergence when an equal number of bloodstains were selected from each side of the impact pattern.....	162
Figure 7.61 The area of convergence when an equal number of bloodstains were selected from each side of the impact pattern.	162

Figure 7.62 MATLAB® editor showing the number of combinations and bloodstains selected.....	165
Figure 7.63 The X distribution when 10000 groups of 10 bloodstains were randomly selected from Impact C.....	166
Figure 7.64 The X distribution when 10000 groups of 20 bloodstains were randomly selected from Impact C.	166
Figure 7.65 The X distribution when 10000 groups of 30 bloodstains were randomly selected from Impact C.	166
Figure 7.66 The X distribution when 10000 groups of 40 bloodstains were randomly selected from Impact C.	166
Figure 7.67 The Y distribution when 10000 groups of 10 bloodstains were randomly selected from Impact C.....	167
Figure 7.68 The Y distribution when 10000 groups of 20 bloodstains were randomly selected from Impact C.	167
Figure 7.69 The Y distribution when 10000 groups of 30 bloodstains were randomly selected from Impact C.	167
Figure 7.70 The Y distribution when 10000 groups of 40 bloodstains were randomly selected from Impact C.....	167
Figure 7.71 As the number of bloodstains randomly selected increased from 10 – 40 the spread of the X and Y-axis distribution decreased.	168

LIST OF ABBREVIATIONS

g	grams
ml	millilitre
EDTA	ethylenediaminetetraacetic acid
BPA	bloodstain Pattern Analysis
°	degrees
°C	degrees Celsius
gsm	grams per square metre
s	second
ms	millisecond
mm	millimetre
%	percent
2D	two-dimensional
3D	three-dimensional
pos	position
CD	compact disc
AVI	audio video file
m	metre
df	degrees of freedom
p	probability

SUMMARY OF RESEARCH FINDINGS

Blood dynamics

- When a blood drop impacts a surface at different angles the blood behaves very differently.
 - The width of the resulting bloodstain increases as the angle of impact increases.
 - The length of the resulting bloodstain increases as the angle of impact increases.
 - A combination of both 'spreading' and 'splashing' occurs.
- When an object strikes a blood source there are many different dynamic process that occur.
 - Blood is 'squeezed' out between the object and surface on which the blood source is and it travels horizontally at a high velocity.
 - This appears as misting on the target surface.
 - The blood travels in a sheet-like formation before separating into droplets.
 - This means that the true impact site is different to the position in three-dimensional space that the blood separates into droplets.
 - This means that the actual point of origin is likely to be slightly different to the region of origin calculated by analysts at a crime scene. This difference is unavoidable.
- When a blood drop impacts different surfaces the dynamics are very different
 - On textured/non-glossy surfaces blood 'skims' over the grains of the surface forming a bloodstain with voids where the blood hasn't touched the surface.
 - Bloodstains on textured/non-glossy surfaces were longer than those on smooth/glossy, even though the volume of the blood drop was the same in each situation.

Angle of impact

- Microsoft® Excel 2000, Microsoft® Office Visio® Professional 2003, BackTrack™ and STABS are computer programs that can be used to fit an ellipse to a bloodstain to determine the angle of impact.
 - They all performed as well as each other so the method an analyst uses should be based on the specific features of each program.
 - Microsoft® Excel 2000 is time consuming but allows work to be saved and accessed later.
 - Microsoft® Office Visio® Professional 2003 is the best program to use for experimental work because the angle of impact must be calculated manually.
 - BackTrack™/Images is best when going on to determine a region of origin.
 - STABS is the fastest program to use and it calculates the angle of impact.

- The target surface has a significant effect on the angle of impact result.
 - On textured/non-glossy surfaces the angle of impact result has a greater amount of error than on smooth/glossy surfaces.
 - Textured/non-glossy surfaces have a greater contact angle than that of smooth/glossy surfaces.
 - The greater the contact angle, the greater the error in the angle of impact calculation.
- The greater the velocity of a blood drop impacting a target surface vertically, the more accurate the angle of impact calculation.
- About 63 % of the time the angle of impact was calculated at acute angles of impact it was underestimated.
 - Due to measurement errors made due to the incorrect fitting of an ellipse to the bloodstain (ellipse is longer than it should be).

Selection of bloodstains

- The factors that were identified in this research as important when selecting bloodstains from an impact pattern for a region of origin analysis are:
 - How well the bloodstain has formed on the target surface.
 - The directionality of the bloodstain (gamma)
 - The size of the bloodstain
 - The position of the bloodstain relative to the area of convergence.
 - The number of bloodstains that are selected.
 - Whether an equal number of bloodstains are selected from each side of the impact pattern.
- If a manual method is used for the analysis the following criteria should be applied:
 - Well-formed bloodstains should be selected.
 - Upward moving bloodstains should be selected.
 - The gamma value of the bloodstains should be $> 280^\circ$ or $< 80^\circ$.
 - If using a manual method to measure the width and length of the bloodstain, larger bloodstains should be selected.
 - If small bloodstains are included in the analysis, a computer-based method should be used to fit an ellipse for measuring the width and length.
 - In the Y-axis, bloodstains that are within about 50 % of the distance to the furthest out stain should be selected.
 - An equal number of bloodstains from each side of the pattern should be selected.
 - Approximately 20 bloodstains should be considered in the analysis.
 - Elliptical bloodstains with an angle of impact less than 60° .
- When using directional analysis the following criteria should be applied:
 - Well-formed bloodstains should be selected.
 - Upward moving bloodstains should be selected.
 - The gamma value of the bloodstains should be $> 280^\circ$ or $< 80^\circ$.
 - In the Y-axis, bloodstains that are within about 50 % of the distance to the furthest out stain should be selected.
 - Approximately 20 bloodstains should be considered in the analysis.
 - Elliptical bloodstains with an angle of impact less than 60° .

CHAPTER ONE: INTRODUCTION

1.1 Introduction

Bloodstain pattern analysis (BPA) is defined as the examination of the shapes, locations and distribution patterns of bloodstains, in order to provide an interpretation of the physical events that gave rise to their origin [1]. The objective of this type of analysis is to apply concepts of biology, biochemistry, physics and mathematics to define and reconstruct events associated with the ‘static aftermath’ of a violent crime [2].

If blood is transferred to a crime scene it results in a *bloodstain pattern*. There are a number of types of bloodstain patterns that can be observed at a crime scene and these are discussed in the following section.

1.1.1 *Classification of bloodstain patterns*

Bloodstains are classified based on their appearance and mechanism of transfer onto a surface. Categories of bloodstains include:

- Passive stains – transfer caused by the force of gravity. These can be further subdivided into:
 - Drops
 - Flows
 - Splashed
 - Saturated, pooling
- Contact transfer stains – created when a bloodied object comes into contact with a surface. These bloodstains can be further subdivided into:
 - Pattern transfer
 - Wipes
 - Swipes
 - Absorbed
 - Miscellaneous contact transfer

- Projected stains – created when a blood source is subjected to an external force greater than gravity. Examples include:
 - Cast-off
 - Expired blood
 - Arterial spurt
 - ***Impact spatter***

Impact spatter patterns will be studied in this research and are described in detail in the following section. For details on any other type of bloodstain pattern the reader is directed to [3-5].

1.1.2 Impact patterns

Impact spatter is generated by the application of some force to a blood source resulting in the random dispersion of smaller drops of blood [6]. The blood source may be on the skin's surface, as in the case of a beating, or it may be exposed at the moment of impact, as in the case of a gunshot injury [7]. The resulting impact pattern may consist of thousands of bloodstains.

All spatter patterns have common class characteristics of [7]:

- Some force was applied to a blood source.
- A blood source was separated into drops.
- Separated drops were distributed over flight paths.

Impact patterns can be more specifically identified by observing the following [7]:

- Radiation of blood spatter out from an area of convergence/origin.
- Alignment of individual spatter stains with respect to each other.
- A spatter density and size range decrease the further away from the origin.

1.1.3 Information from an impact pattern

A good estimate of the locations of victims and suspects when bloodletting blows were struck may assist the investigator in refuting or corroborating the testimony of a witness, victim or suspect [8]. The determinations made from studying an impact spatter pattern at a crime scene may be used to estimate the force involved in the impact and to reconstruct the crime scene allowing the position of the blood source at the time of impact to be approximated.

This thesis will focus on the latter of these two determinations – the position of the blood source at the time of impact or the ***region of origin*** of impact spatter. This is defined as the common point (area) in three-dimensional space to which the trajectories of several blood drops can be retraced [6].

1.2 Background to the region of origin

When blood is struck droplets are formed. These follow physical laws, travelling along an approximately parabolic flight path until they impact a surface, the target surface. At a crime scene the target surface could be anything, but if it is an immovable wall or surface that can easily be studied, a region of origin may be determined.

The traditional procedure for determining the region of origin begins when an analyst selects a number of elliptically shaped bloodstains to analyse. The selection of these bloodstains is based on the analyst's experience and the few guidelines for bloodstain selection that currently exist. For a region of origin analysis, the flight path of the blood drop is always assumed to be a **straight line**. The effect of this assumption on the region of origin estimation is discussed in Section 2.1.3.

There are various important concepts on which the method for determining the region of origin is based and each of these are discussed in Sections 1.2.1 – 1.2.4. The methods used to determine the region of origin are discussed in Section 1.2.5.

1.2.1 Directionality of bloodstains

The first important concept is the directionality of a bloodstain. When a spherical drop of blood strikes a surface at any angle other than 90° , it will produce an elliptical bloodstain – elongated relative to the angle of impact [3] (Fig. 1.1 (a)). The elliptical shape, the ‘tail’ and other edge characteristics allow the direction of travel to be inferred. If a spherical blood droplet impacts a target surface at 90° , it will produce a circular bloodstain exhibiting no indication of direction (Fig. 1.1 (b)).

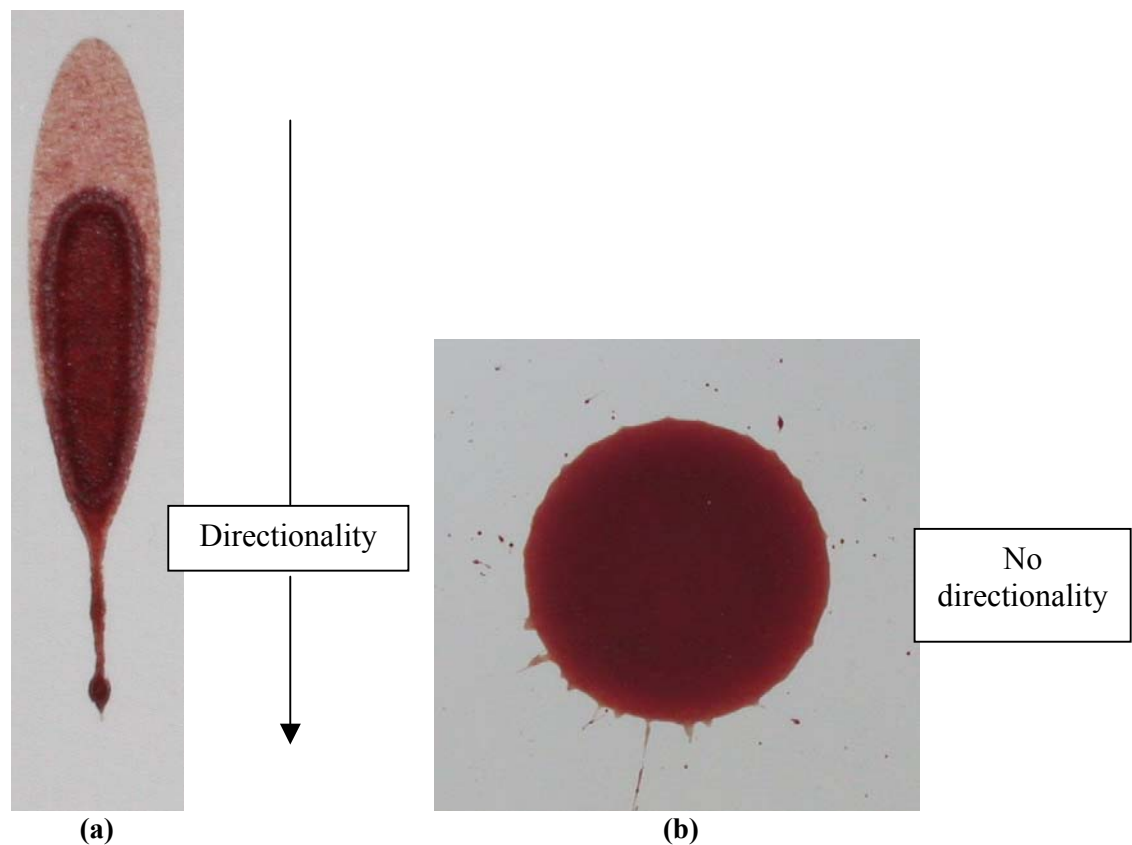


Figure 1.1 Directionality of bloodstains. Bloodstain impacting a surface at 10° , direction observed (a), a 90° stain that has no direction (b).

The directionality of a bloodstain can be used to determine its glancing angle (γ). This is the angle in the plane of the wall (or surface on which the bloodstain is) measured between the long axis of the stain and the vertical. The gamma angle is determined by drawing a vertical line next to the bloodstain, drawing a line through the long axis of the bloodstain and then measuring the angle of the long axis in a clockwise direction from the vertical line (Fig. 1.2).

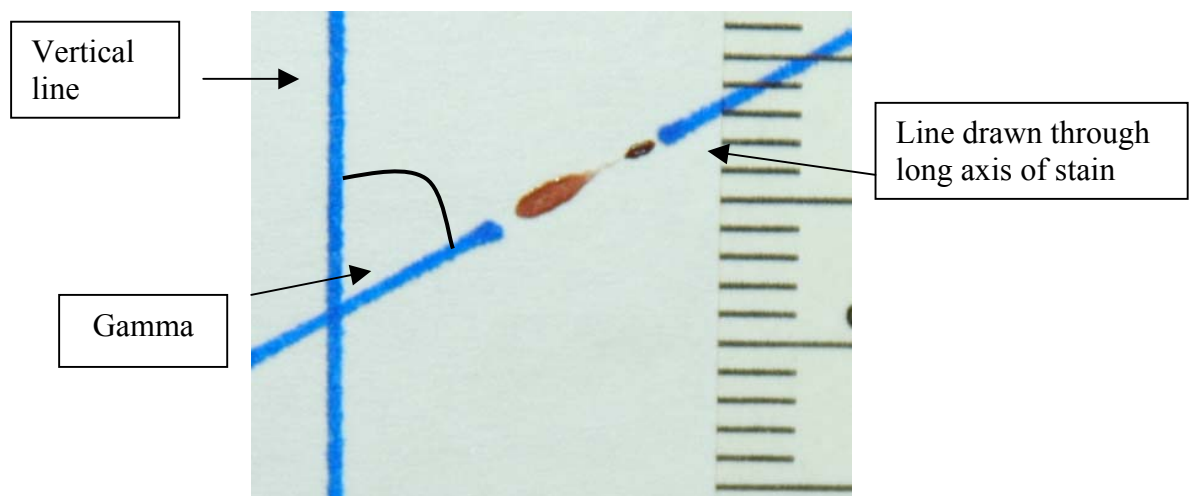


Figure 1.2 The gamma angle is determined by drawing a vertical line next to the bloodstain, drawing a line through the long axis of the bloodstain and then measuring the angle of the long axis in a clockwise direction from the vertical line.

1.2.2 2D Area of convergence

Once the directionality of a number of bloodstains has been established, the area of convergence can be determined. This is defined as the common point (area), on a two-dimensional surface, over which the directionality of several blood drops can be retraced [6].

In practice, a reverse azimuth (a line which extends backwards along the path the droplet was following) is drawn onto the target surface and an area of convergence can be deduced by looking for an area in which a majority of the lines intersect (Fig. 1.3). It is claimed that as the number of evaluated stains increases, so too does the level of accuracy of the area of convergence [4].

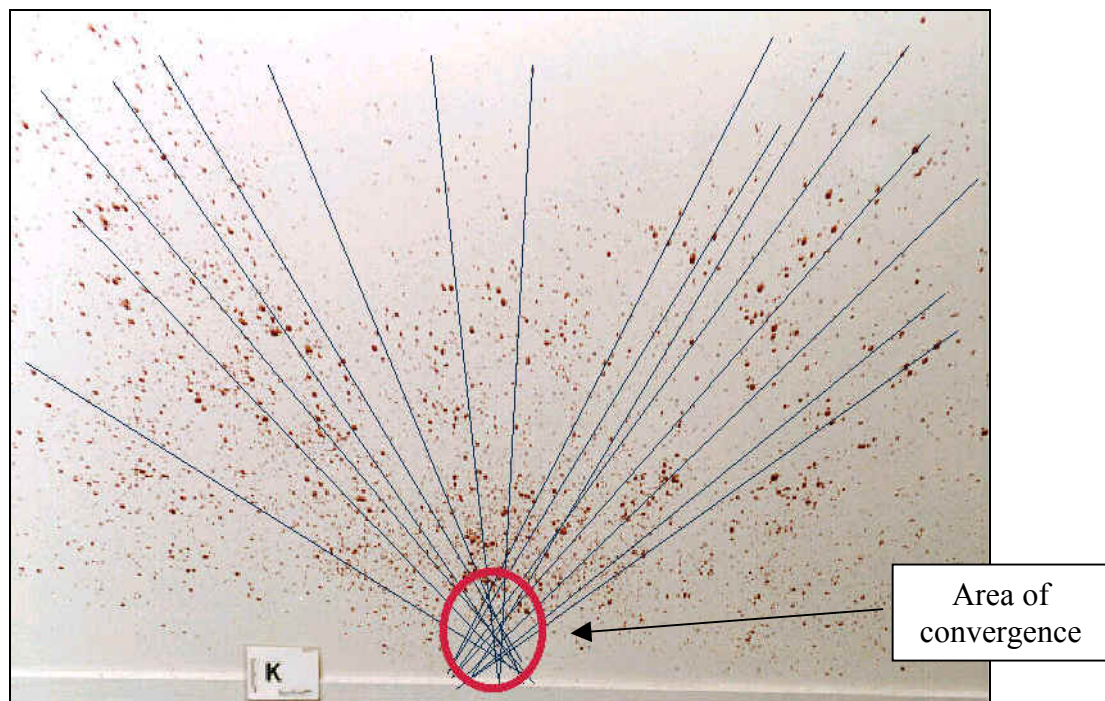


Figure 1.3 The area of convergence is determined by drawing lines through the major axis of a number of bloodstains along their direction of travel and looking for an area where the majority of these lines intersect [9].

1.2.3 Angle of impact

The next step in the traditional method of determining the region origin is determining the angle of impact for the bloodstains that were selected. Rizer introduced the use of a sine equation (Equation 1.1) in 1960 to allow the angle of impact (α) to be determined [10]. He stated that the ratio of the shortest or minor diameter of the elliptical pattern to the longest or major diameter is equal to the trigonometric sine function of the angle between the receiving surface and the tangent to the drop's trajectory at its meeting with the receiving surface (Fig. 1.4). In other words, the angle of impact is the acute or internal angle formed between the direction of a blood drop and the plane of the surface it strikes and it can be determined by using the width and length of the bloodstain [6].

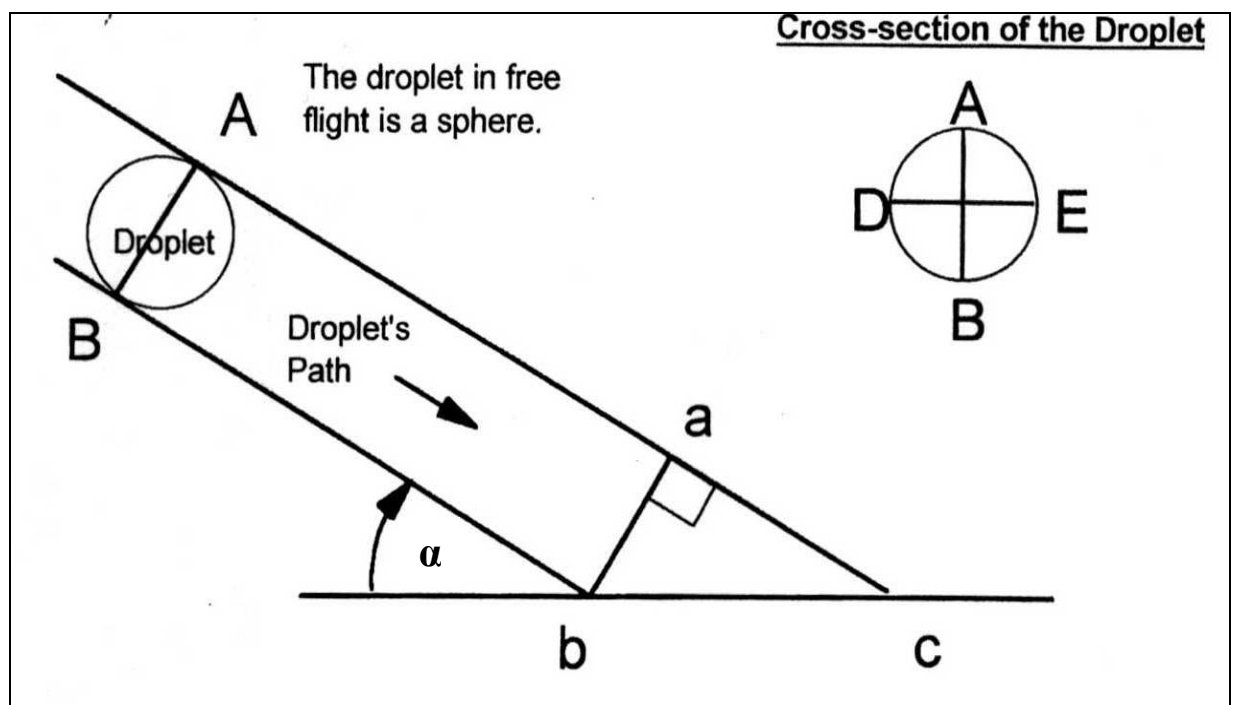


Figure 1.4 A droplet impacting as a sphere and the trigonometric relationship of the resultant ellipse with that sphere (Formula 1.1). Where ab is the width of the ellipse and bc is the length of the ellipse [4].

$$\sin \alpha = \frac{W}{L} \quad [1.1]$$

1.2.4 *Ellipse fitted to a bloodstain*

The required measurements for an angle of impact calculation are the length and width of the best-fit *ellipse* of a bloodstain. This will in most cases not mean measuring the actual length and width of the bloodstain because in most instances bloodstains are not perfectly elliptical. This is due to the way in which they impact a surface and is especially true at acute angles of impact. The non-elliptical end of a bloodstain is often described as exhibiting a ‘tail’. The correct terminology for this tail-like feature is wave cast-off.

Wave cast-off is a small amount of blood that originates from a parent drop of blood due to the wave-like action of the blood in conjunction with striking a surface [6]. Figure 1.5 illustrates this feature. Figure 1.5 also illustrates a bloodstain with a best-fit ellipse superimposed.

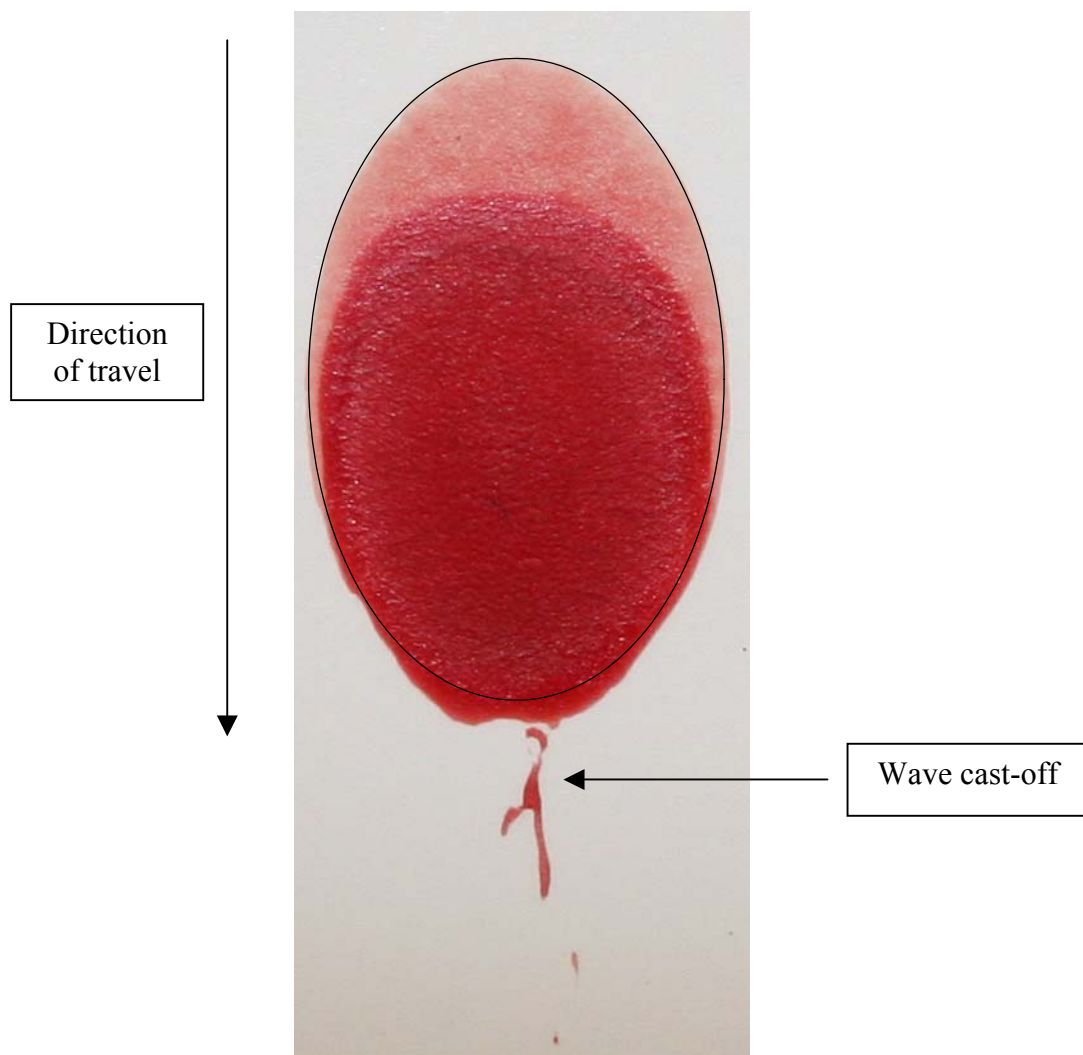


Figure 1.5 A bloodstain showing wave cast-off with a best-fit ellipse superimposed.

1.2.5 Determination of the region of origin

As described in previous sections, one important consideration in BPA is the three-dimensional region of origin of bloodstains. Also known as the ‘area’ or ‘point’ of origin and defined as the three-dimensional space to which the trajectories of several blood drops can be retraced [6].

After a number of bloodstains from either side of an impact pattern have been selected and the directionality, area of convergence and angle of impact determined, it is possible to calculate the region of origin.

A region of origin analysis can be accomplished by three different methodologies; the string method, the tangent method and directional analysis [11]. These are described in sections 1.2.5.1 – 1.2.5.3.

For a region of origin analysis, Z represents the height from the ground, Y represents the distance from the left hand wall or a reference point to the left and X represents the distance out from the front wall (Fig. 1.6).

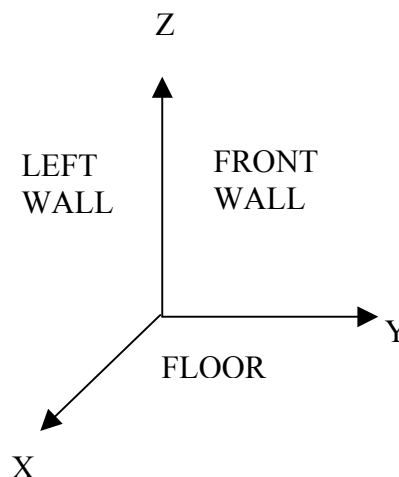


Figure 1.6 A three-dimensional representation of the X, Y and Z coordinate system used when determining the region of origin.

1.2.5.1 Stringing

The traditional method used to determine the region of origin is so-called ‘stringing’, as it involves the use of strings that are pulled back in the direction of travel of a

bloodstain at its angle of impact. This is repeated for each of the selected bloodstains and the outcome is an X, Y and Z coordinate, which together represent the region of origin.

Stringing is useful as it can be carried out by an analyst at a crime scene to visually indicate the position a blood source was impacted. It is however a cumbersome technique which has some theoretical and practical limitations.

1.2.5.2 Tangent method

The tangent method is another manual method that can be used to determine the region of origin. When using this method, the Y and Z coordinates for the blood source location are estimated by approximating the 2D area of convergence on the surface upon which the bloodstains are (Fig. 1.4). The angle of impact (α) is then determined for each stain and the flight path of the blood drop is assumed to be a straight line that will be the hypotenuse of a right angled triangle with one angle equal to alpha [11]. The X coordinate can then be determined by calculating the tangent of the alpha angle for each bloodstain ($X = D \tan(\alpha)$), where D is the distance from the bloodstain to the convergence point (Fig. 1.7). The X values determined for each bloodstain are then averaged to give the X coordinate of the region of origin.

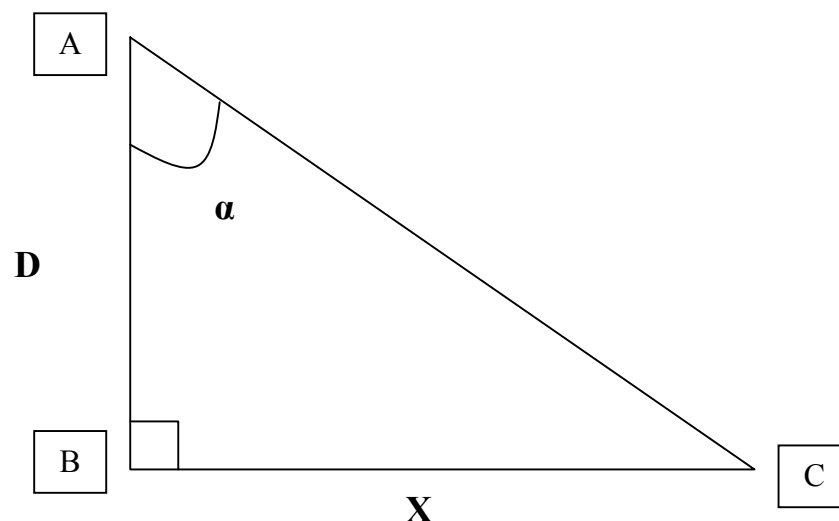


Figure 1.7 When the tangent method is used, the convergence point (B) is determined first, followed by the angle of impact (α) and the distance from each bloodstain to the convergence point (D). Using this information the distance from the convergence point to the region of origin can be calculated using $X = D \tan \alpha$. A is the position of the bloodstain.

1.2.5.3 Directional analysis

The directional analysis of a bloodstain pattern is a mathematical procedure for finding the directions in space that point from the bloodstains to a spot directly above the location of the blood source [12].

Because of its mathematical complexity, directional analysis requires a computer in order for the analysis to be carried out. Specific software, BackTrack™, has been developed in order to allow the analysis to be carried out by computer and it is discussed in section 1.2.5.3.1.

The theory upon which directional analysis is based relies on the well-known physical laws of motion plus the resolution of the velocity into its 3 components and simple trigonometry [13]. This produces what is essentially an area of convergence in the horizontal XY plane (Fig 1.8). Once the horizontal convergence has been established, the Z coordinate is determined manually by viewing the convergence from the side (Fig. 1.9). Unlike stringing, both upward and downward moving bloodstains can be included in this type of analysis because the computer solves for XY first, then Z.

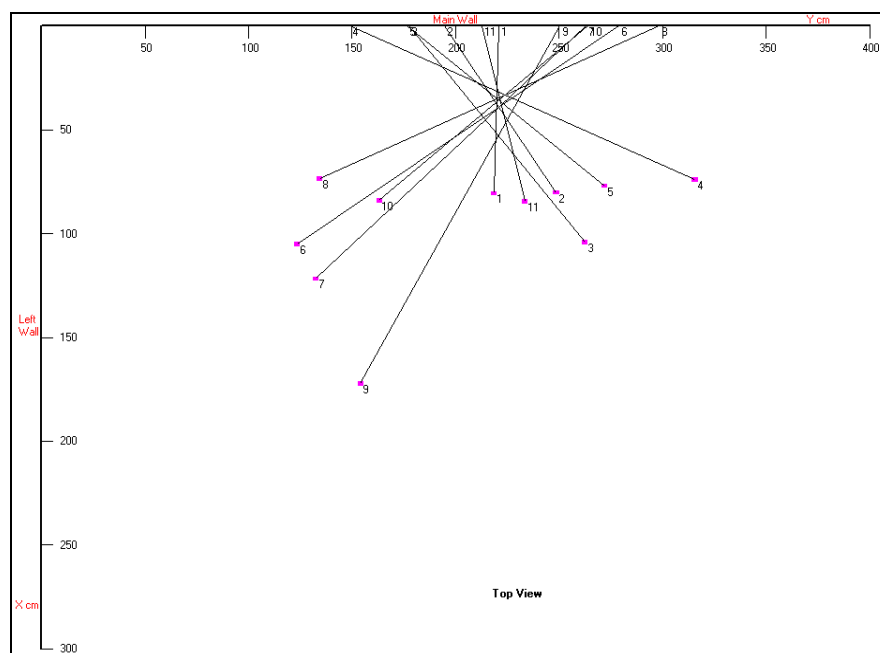


Figure 1.8 Top view from BackTrack™/Win where virtual strings represent the trajectories of blood droplets.

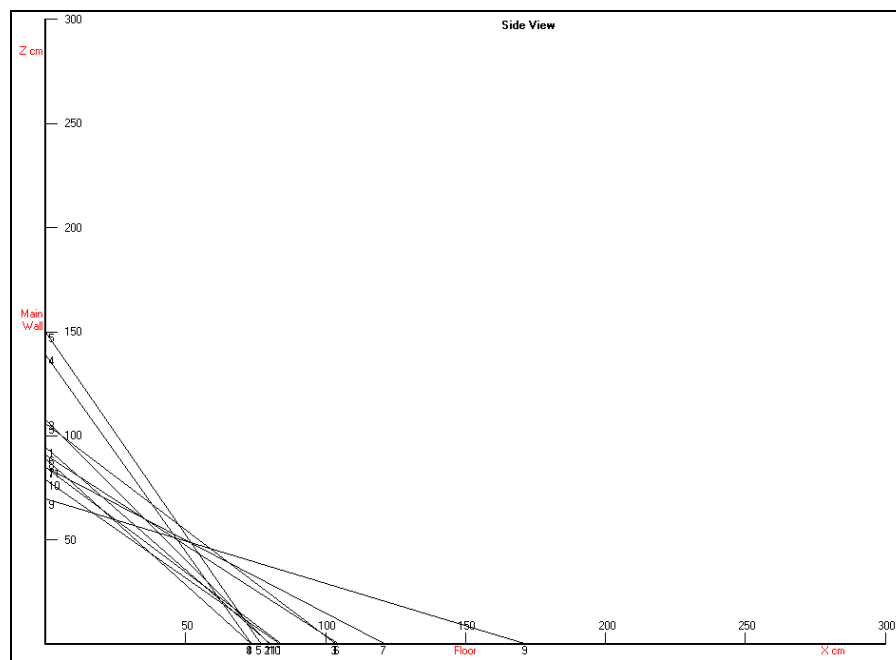


Figure 1.9 Side view from BackTrack™/Win where virtual strings represent the trajectories of blood droplets.

1.2.5.1.1 BackTrack™

BackTrack™ is a computer program that was developed in 1992 for the purpose of region of origin determinations in BPA. To use the program, bloodstains must first be selected and then labelled with a scale and a vertical line. Digital close-up images of the stains are then taken and loaded into the first part of the software program – BackTrack™/Images. The analyst enters the coordinates for each bloodstain (the XYZ position of the bloodstain on the target surface) and using the scale, the images are calibrated. The program then uses the gamma and alpha angles to determine the angle beta. This is the acute angle between the flight path and the wall when observing the top view (Fig. 1.10) and it is determined using Equation 1.2 [12]. The complementary software program BackTrack™/Win is subsequently used to determine the three-dimensional region of origin [11, 12, 14, 15]. The results can be visualised in the top and side view of BackTrack™/Win where virtual strings (lines) represent the trajectories of blood droplets (Fig. 1.8 and 1.9).

$$\tan \beta = \frac{\tan \alpha}{\sin \gamma} \quad [1.2]$$

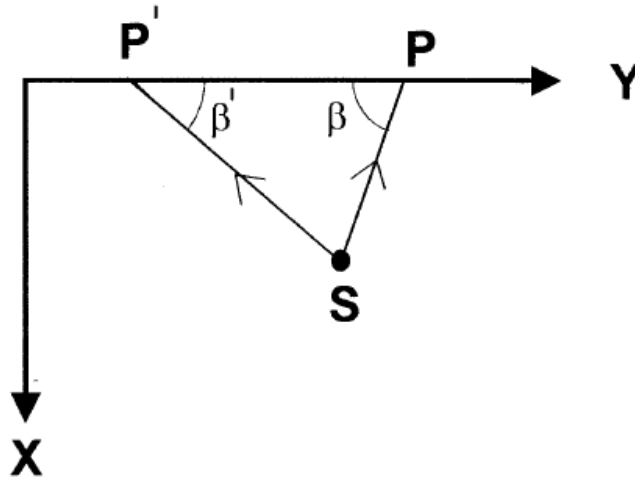


Figure 1.10 The beta angle is the acute angle between the flight path and the wall when observing the top view.

1.2.6 The result

Regardless of the method used, the result is a three dimensional region of origin representing the approximate position of the blood source at the time of impact. This may be used to corroborate or refute a statement given by someone involved with a crime.

It has been established that the region of origin determination involves an amount of uncertainty. This is often stated as being equivalent to the volume of a grapefruit or basketball [16]. There are many factors that may contribute to this uncertainty and these factors along with how they may be overcome are described in detail in chapter 2.

Preceding this is a discussion of the current procedures and criteria used by analysts to select bloodstains from an impact pattern when determining the region of origin. Various methods to estimate the potential error involved in the determination are also presented.

1.3 Stain selection criteria and estimation of error

In the 1993 Daubert decision, the United States Supreme Court set out some criteria for courts to consider when determining whether or not a testimony is scientifically sound [17]. Among the criteria was the known or potential error rate. In terms of the region of origin in BPA this is the potential error in the determined region of origin in three-dimensional space. As a result of this decision, the potential error rate relating to the region of origin has come into focus and various papers have been published investigating it [18-21].

Liesegang [22] published a method which considered two bloodstains from an impact pattern, O and A. Elementary calculus was applied allowing the calculation of quotable uncertainties or errors in X and Y. For the set of equations the reader is directed to [22].

The results presented in the paper led to the following conclusions with respect to the selection of bloodstains during a region of origin determination:

- Care is necessary when selecting the plan or horizontal separation between stains and their position with respect to the suspected position of the blood source.
- This choice may not always be easily available and so care needs to be taken to evaluate the possible uncertainty in source coordinates using equations for individual stain pairs.

Willis *et al.* [18] presented derived equations for the estimation of the variances in the estimated angle of impact of blood droplets. The derived equation for the variance in the estimated angle of impact showed that as the angle of impact approached 90°, the variance grew without limit. Figure 1.11 shows that the derived equation accurately predicted the variance up to an angle of impact of 60° and a rapid increase in the variance as the angle of impact approached 90°. The authors also showed that the uncertainties in the angle of impact are determined primarily by the errors in the width and length measurements of the bloodstain.

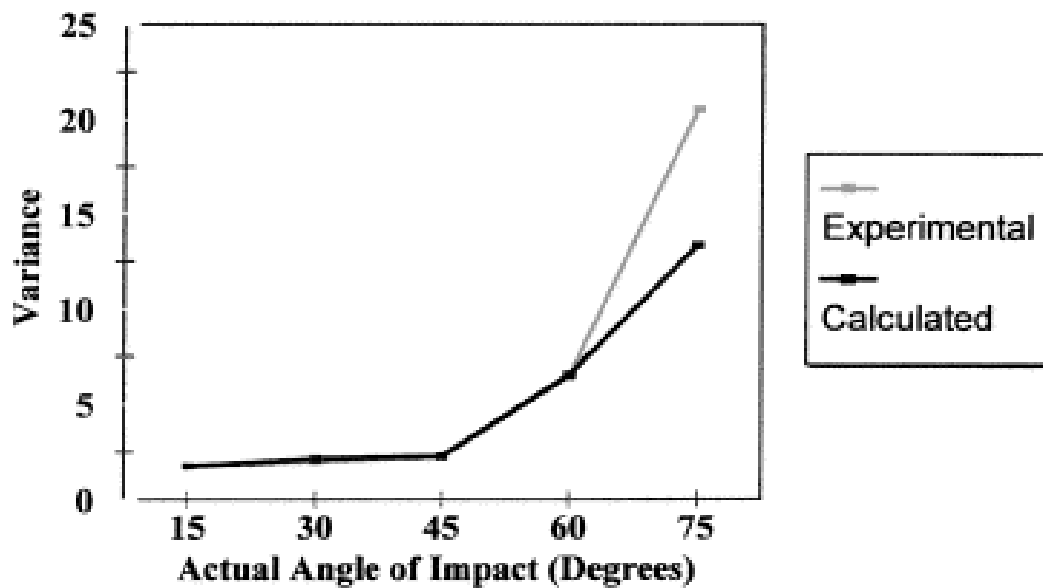


Figure 1.11 As the angle of impact approached 90°, the variance of the estimated angle of impact grew without limit (experimental). The derived equation accurately predicts the variance up to an angle of impact of 60° and predicts that the variance increases rapidly as the angle of impact approaches 90° (calculated) [18].

The results of the study led to the following conclusions with respect to the selection of bloodstains during a region of origin determination:

- When attempts are made to locate the region of origin of an impact pattern, the greatest weight should be placed on bloodstains that impacted the target surface at an acute angle. This is because the angles of impact for these stains can be estimated with the greatest confidence.
- Less weight should be placed on estimates of angles of impact when the angles are close to perpendicular.

The calculated impact angle is based on the fact that a droplet impacts a surface in the shape of a sphere. However if a blood droplet was oscillating at the time of impact with a target surface, the width and length ratio of that bloodstain could be altered such that the calculated impact angle would be inaccurate. Raymond *et al.* [23] presented a paper exploring the effects of oscillations on the shape of blood droplets. High-speed photography was used to photograph falling drops and measurements were made of the drop width and length frame by frame. They determined that oscillations were negligible after travelling 40 cm for free-falling droplets and 1 metre for impacted or projected droplets.

The results presented in the paper led to the following conclusion with respect to the selection of bloodstains during a region of origin determination:

- Bloodstains furthest from the site of an impact would provide the most accurate results when determining the angle of impact because these droplets would have been less likely to have been affected by the effect of the oscillations.

Rowe [20] commented that at high angles of impact, the error in the length and width measurements is dependent mainly on the measuring instrument, where as for oblique angles of impact, the error in the length measurement increases due to the presence of irregularities at one end of the bloodstain (termed scalloping and/or spines). A number of equations were presented for the uncertainties in the coordinates of the area of origin.

The equations presented in the paper led to the following conclusion with respect to the selection of bloodstains during a region of origin determination:

- In order to minimise the uncertainty in the X coordinate, an analyst should select bloodstains such that the area of origin lies approximately midway between the bloodstains.

Other criteria that have been presented include:

- Well-formed, undistorted bloodstains should be selected in order to eliminate errors when measuring the bloodstain [24].
- Bloodstains that could be satellite spatter or the result of droplet ricochet should be excluded [4].
- Bloodstains that are separated horizontally by a distance of approximately 1 m should be selected [25].
- Elliptical, low-impact angle stains rather than those having a nearly-circular shape should be selected [24].

The stain selection criteria that have previously been published and methods for quantifying potential error in region of origin calculations have been presented above.

Because of the need for accuracy when determining the region of origin a general procedure is followed by the analyst analysing the impact pattern. This procedure however is not defined and varies from analyst to analyst.

1.4 Scope and layout of this thesis

The objectives of this thesis are to:

- Investigate the dynamics of blood in relation to:
 - The formation of blood drops on different surfaces.
 - The formation of blood drops on an angled surface.
 - Impact spatter generation.
- Investigate the angle of impact calculation to determine the effect of target surface on the accuracy of the calculation and to determine if there is an underestimation of the angle of impact at acute angles (as cited in previous research) and if so why this may be.
- Finally to establish the conditions that result in the most accurate region of origin result and present the findings as a set of criteria that bloodstain pattern analysts could use to produce optimal results.
 - These criteria would standardise the methodology used throughout the world for this type of analysis, make sure optimal results are obtained and ensure stain selection for a region of origin determination is based on scientific research.

The thesis is therefore focused around three separate investigations. First the investigation of blood dynamics. Second, the investigation of factors that may affect the angle of impact calculation and finally research about bloodstain selection for region of origin determinations including a survey carried out to establish the methods and criteria used by analysts currently when determining the region of origin.

Chapter 2 describes the factors that may contribute to the uncertainty present in region of origin determinations, along with how it may be overcome.

Chapter 3 describes the methods used in the experiments as an overview and each chapter describes specific details of the methodology used in the particular experiment.

Chapter 4 describes the use of high-speed photography to investigate the dynamics of blood.

Chapter 5 describes the experiments carried out to investigate various aspects of the angle of impact calculation.

Chapter 6 details the results of a survey to establish the methods used by bloodstain pattern analysts worldwide to select bloodstains from an impact pattern and chapter 7 describes the experiments carried out to determine bloodstain selection criteria.

Finally, a summary of the main findings of the work and suggestions for future research may be found in chapter 8.

CHAPTER TWO: FACTORS THAT MAY CONTRIBUTE TO UNCERTAINTIES IN THE REGION OF ORIGIN

This chapter describes the errors that may affect region of origin calculations. Broadly speaking these can be divided into two groups:

- Errors relating to the flight path calculation.
- Errors relating to the method of convergence.

There are a number of factors that may contribute to the uncertainty in each of these groups and these will be discussed in detail in the following section.

2.1 Errors relating to the flight path calculation

Factors that may affect the accuracy of the flight path calculation include the accuracy of the angle of impact and direction determinations, gravity, air resistance and the suitability of the sine relationship for predicting the angle of impact. These factors are described in sections 2.1.1 – 2.1.4. Sections 2.3 and 2.4 contain a discussion of the effects of these errors and how they are overcome (if they are).

2.1.1 *Determination of the angle of impact*

2.1.1.1 'Normal' measurement errors

As with any type of measurement, normal measurement uncertainties will arise for angle of impact calculations. At acute angles, measurement errors have less of an effect on the angle of impact calculation than measurement error made for angles approaching 90° (see Fig. 1.11) [18]. This is because as W/L approaches 1 (the bloodstain becomes more circular), the effect of measurement errors increases. Measurement errors of this type will usually be random. This effect can be shown mathematically (Equation 2.1 – 2.3).

$$\sin \alpha = \frac{W}{L} \quad [2.1]$$

$$\frac{d\alpha}{d(W/L)} = \cos \alpha \quad [2.2]$$

$$d(\alpha) = \frac{d(W/L)}{\cos \alpha} \quad [2.3]$$

Inaccurate when $\cos \alpha$ approaches zero because α approaches 90° .

2.1.1.2 Asymmetric nature of a bloodstain

It is assumed by bloodstain pattern analysts that the angle of impact of a blood droplet can be calculated using the equation $\alpha = \sin^{-1} (W/L)$, where the length and width relates to that of an ellipse fitted to a bloodstain. One of the critical skills of bloodstain pattern analysis therefore is to make proper measurements of the bloodstain's width and length in order to accurately calculate this angle. One of the difficulties in measuring a bloodstain is that it is often asymmetric. Most analysts estimate the length and width of a bloodstain using a ruler or callipers and in recent years digital methods have become available allowing more accurate measurements to be made. Regardless of the method used it is difficult to fit an ellipse to an asymmetric bloodstain and systematic length measurement errors may result. This is especially so as α approaches 0° (the bloodstain gets longer).

Laternus carried out a study to investigate the rate of error in bloodstain measurement [21]. Twenty-seven members of the International Association of Bloodstain Pattern Analysts (I.A.B.P.A) were sent a photocopy of 10 drops of human blood. The stains were created by setting targets at various known angles and the recipients were asked to provide length and width measurements and comment on the method used to measure the ellipse of the bloodstain.

The methods used by analysts included using callipers or a ruler and in about 40% of the cases, some form of magnification was used enabling the analyst to better visualise the bloodstain.

The results showed that the width measurement that was made was very accurate; however the length measurements were in most cases inaccurate. This was because the majority of analysts were measuring to the tail of the drop, instead of the best-fit ellipse length. A bloodstain with a well fitting ellipse and one with a poorly fitted (elongated) ellipse are shown in Figure 2.1.

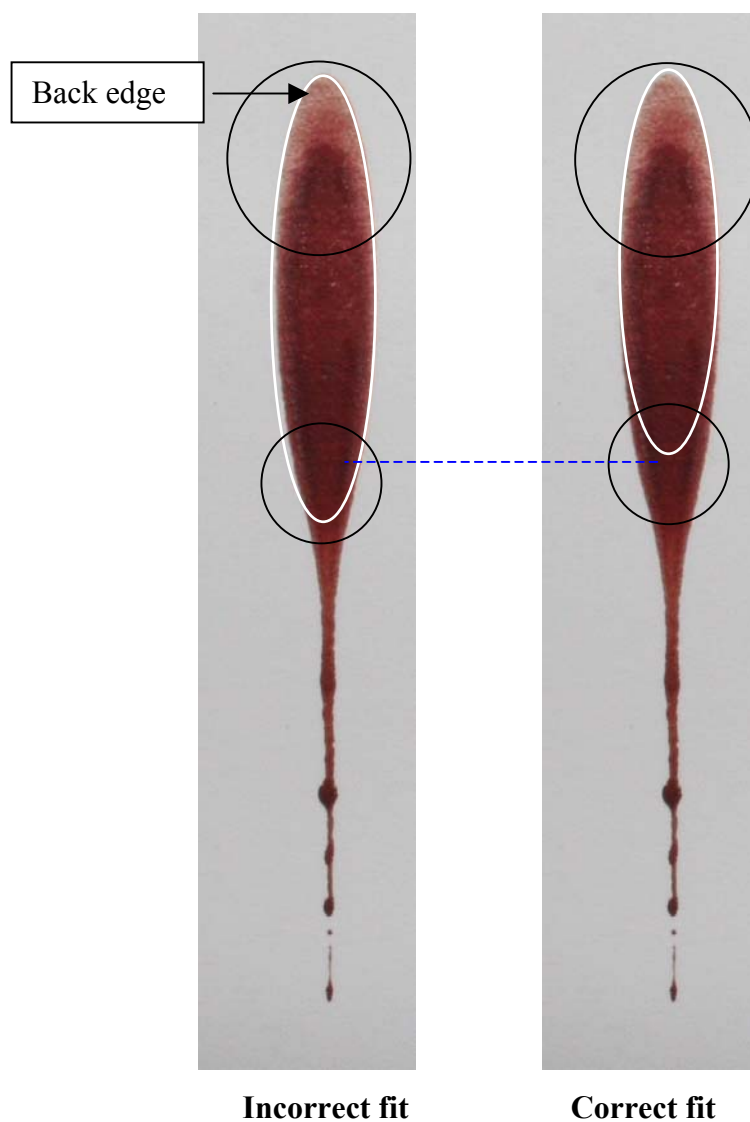


Figure 2.1 An ellipse fitted to the bloodstain resulting in an underestimation of the angle of impact (incorrect fit) and the ellipse that should be measured (correct fit). The differences in the ellipses include the length and how well they fit the bloodstain at the back edge.

2.1.1.3 Additional systematic error

Additional systematic error in the angle of impact calculation has been noted [26]. Janes found that the angle of impact was generally underestimated when the actual

angle of impact was below 50° [26]. Even the use of a computer program to fit the ellipse did not eliminate this problem (Fig. 2.2).

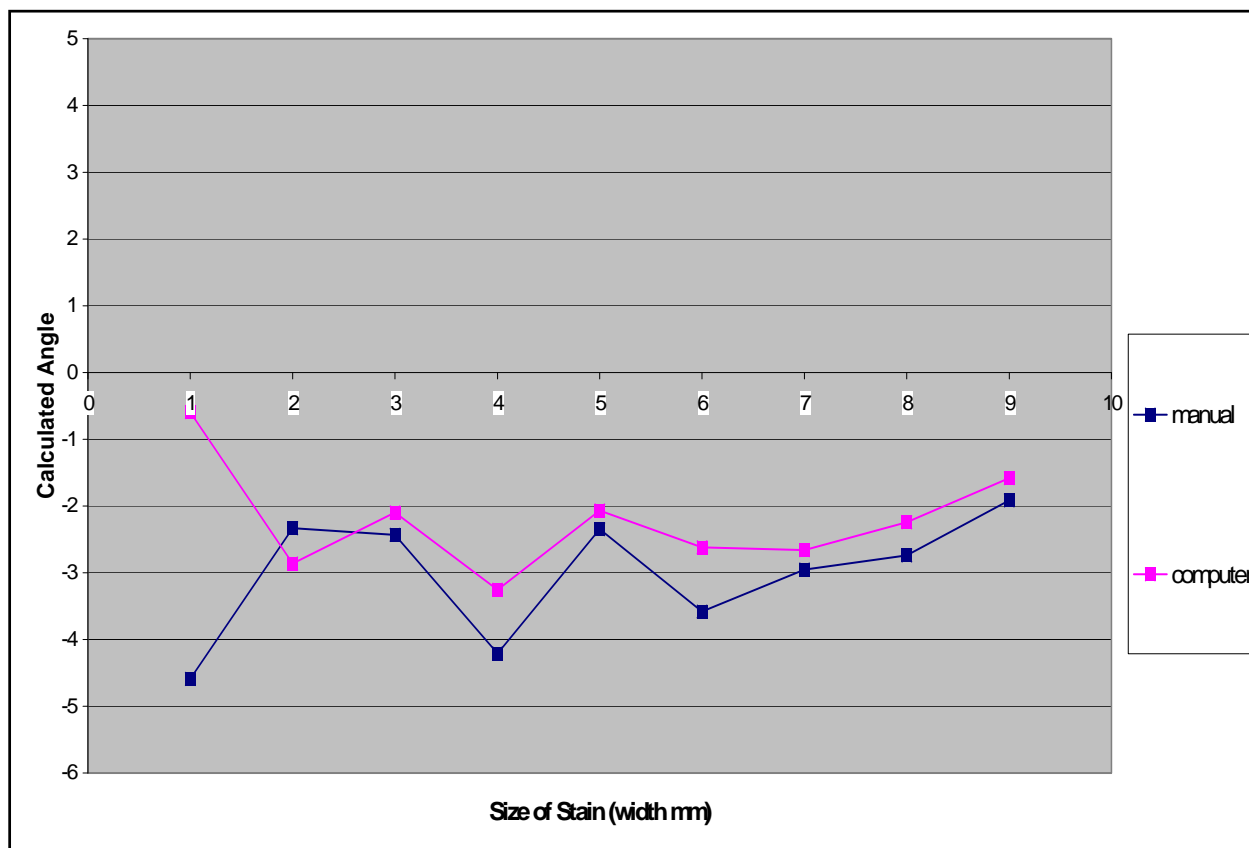


Figure 2.2 Graph of the average observed minus expected angles (20°) for bloodstains measured manually and by the computer method [26].

Figure 2.3 shows the results of a yearly quality assurance test provided by the Collaborative Testing Services¹ (CTS). The reported average impact angle was compared to the actual angle of impact and the results were plotted. It can be seen that at acute angles, (especially between $20^\circ - 40^\circ$), the angle of impact was often underestimated (black circle).

¹ Collaborative Testing Services Inc. PO Box 1049, Herndon VA 20170, USA

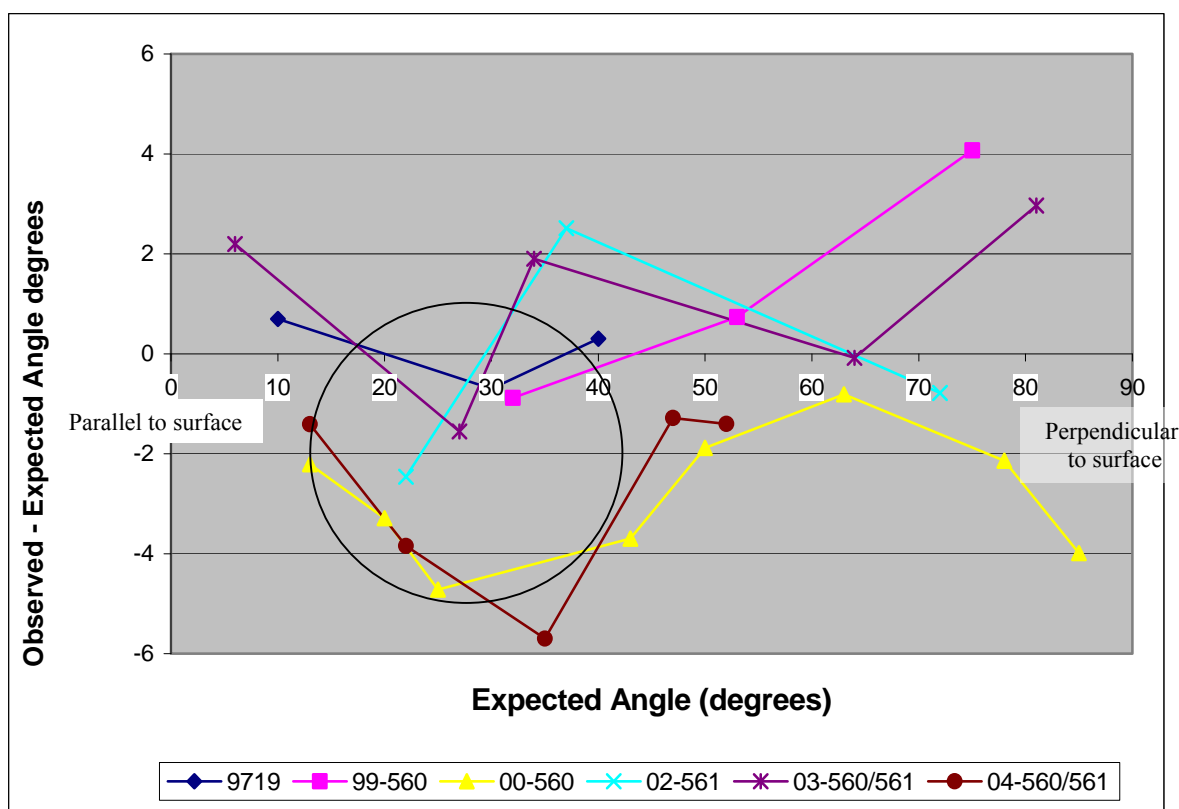


Figure 2.3 The expected angle plotted against the observed minus expected angle. The data was collected from the Collaborative Testing Service tests.

The stains were created by:

9719 – Releasing a single drop of horse blood onto a white poster board target.

99-560 – Releasing a single drop of horse blood onto a white poster board target.

00-560 – Releasing a single drop of human blood onto white-coated coverstock.

02-561 – Releasing a single drop of human blood onto white-coated coverstock.

03-560/561 – Releasing a single drop of human blood onto white poster board.

04-560/561 – Releasing a single drop of human blood onto white poster board.

Janes tested the proposition that errors in the angle of impact calculation could be due to some unknown interaction occurring at the target surface. This parameter was tested for angles of 20°, 30° and 90° using eight different surfaces [26]. It was found that the angle of impact was underestimated for all but one surface (cardboard). The stain size was also looked at and it was found that at stain sizes of 0.1 – 10 mm there was still an underestimation of alpha at acute angles of impact (Fig. 2.4).

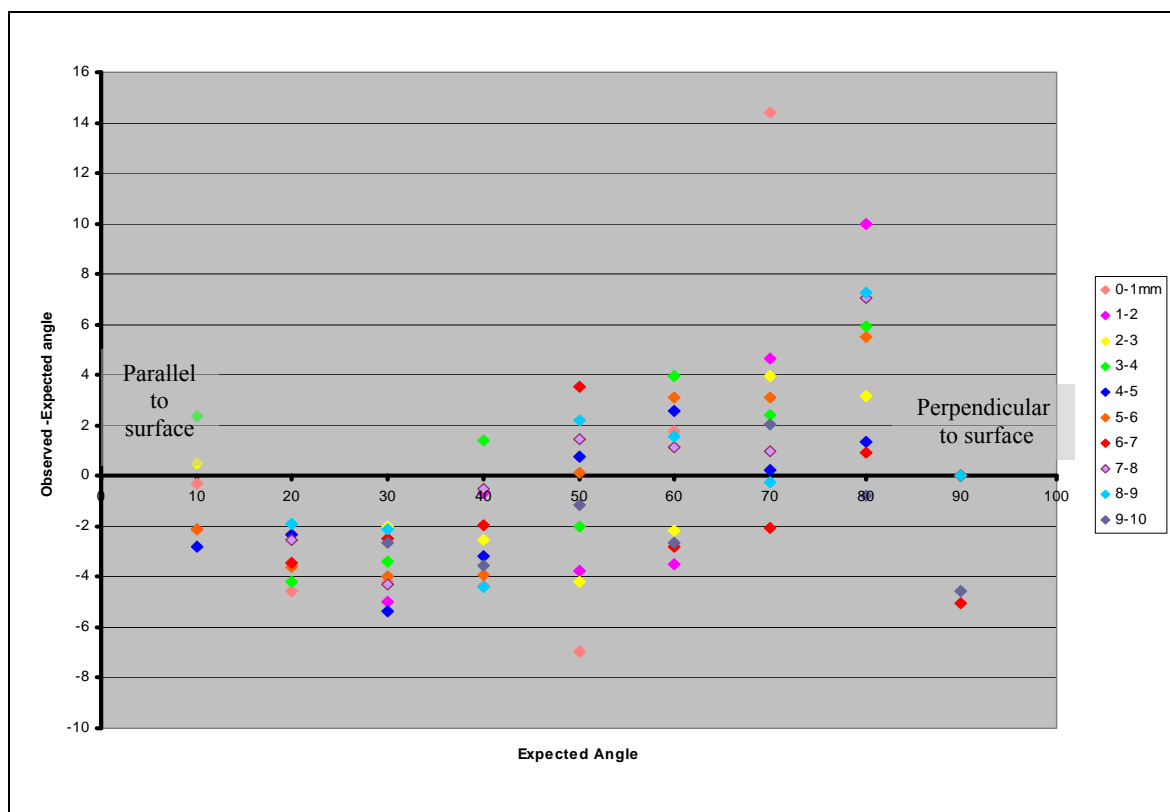


Figure 2.4 Graph of the difference between observed and expected angles, against expected angle for different stain sizes [26].

This unexplained, additional error has been found to be greatest when the angle of impact is below 50° [19, 27].

Reasons for this systematic error may include:

- The effect of the target surface upon which the blood drop forms.
- The sine function may not be suitable for calculating the angle of impact in different situations such as on different target surfaces and at different angles of impact.
- The ellipse may not be fitted to the bloodstain correctly.
- The dynamics of a blood droplet as it impacts a target surface.

While these may be reasons for the additional error, the authors that noted it did not explain it. This finding will therefore be further investigated in this research (Chapter 5).

2.1.1.4 Oscillations

Oscillations may affect the accuracy of an angle of impact calculation especially for bloodstains that have travelled short distances. The analysis of bloodstains on surfaces relies on the assumption that blood droplets are spherical when they strike

the surface. However in some situations this assumption is unreliable. Raymond, Smith and Liesegang [23] studied this phenomenon and a discussion of the results were presented in section 1.3.

2.1.2 Determination of direction

2.1.2.1 'Normal' measurement error

Generally upwardly moving bloodstains are selected for a region of origin analysis. The implication of this is that these bloodstains are more likely to have travelled fast and therefore in a straight line (fulfilling one of the main assumptions made in a region of origin determination). Droplets that exhibit downward directionality may have passed the peak of the parabola of their flight path and hence would be travelling in a downward direction due to gravity. Selecting stains with a downward direction could therefore introduce additional error into the Z coordinate of the region of origin determination. Although there is regard paid to the direction of a bloodstain, there is no published data to show the effect of it on the region of origin calculation. This research investigates the impact of the directionality of a bloodstain on a region of origin estimate (Chapter 7).

2.1.3 The effect of gravity and air resistance

All flight paths have a curvature that can be described as concave downward because the direction of the force of gravity is always downward. The flight paths of faster moving droplets have less curvature (flatter trajectories). The Z coordinate is therefore always overestimated.

The only effect of air resistance on blood droplets is to reduce speed thereby increasing the curvature of the flight paths of smaller droplets. This effect can be visualised in Figure 2.5, where the blue dotted line shows the path a blood droplet would travel if air resistance and gravity were negated. The plain line shows the actual path the blood droplet travels. The double-headed arrow shows the position of the Z coordinate that would be determined by pulling a string back at the angle of impact.

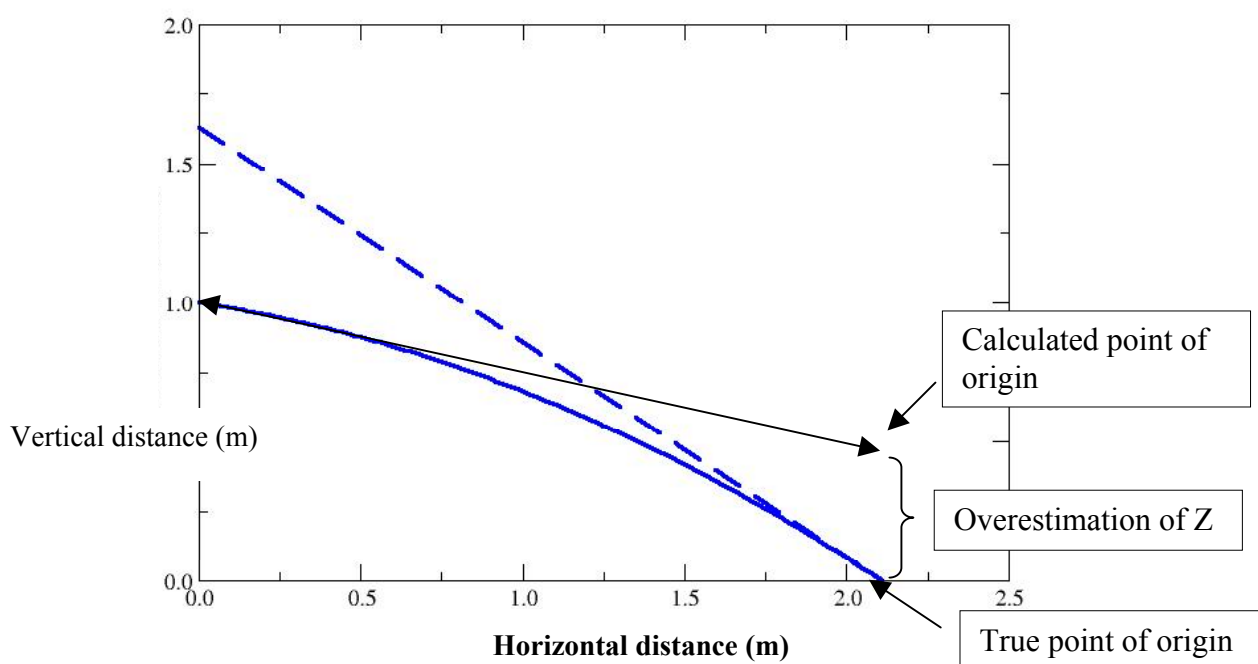


Figure 2.5 The flight path of a blood droplet is concave downward. This results in the Z-axis coordinate often being overestimated.

2.1.4 Secondary effects

Secondary effects can result in bloodstains called ricochet and satellite spatter. Ricochet is defined as the deflection of blood after impact with a target surface that results in staining of a second target surface. Satellite spatter is defined as small droplets of blood that are distributed around a drop or pool of blood as a result of the blood impacting the target surface [6]. These bloodstains, if they are selected for a region of origin analysis result in a region of origin determination that is erroneous.

2.2 Errors relating to the method of convergence

There are various methods available to an analyst for determining the region of origin. Stringing, the tangent method and directional analysis were described in section 1.2.5.

Typically, stringing at a scene can be cumbersome, especially where more than one blow has been struck and where strings must be woven between one and other [11]. Uncertainties can be introduced when measuring both the direction and angle of impact as well as when the string is moved unintentionally when it is being pulled

back. In a study assessing the accuracy of the string method it was found that an error of 10 – 20 cm in any direction was typical [11] (Table 2.1). Overall the study showed that directional analysis using BackTrack™ software was found to be the most accurate method for determining the region of origin, followed by the tangent method and then stringing.

Table 2.1 The average difference between the determined and known region of origin coordinate for single-blow targets using different methods [11].

	X (cm)	Y (cm)	Z (cm)
BackTrack™	3.88	2.96	6.64
Tangent method	3.91	2.05	7.90
Stringing	10 - 20	10 - 20	10 - 20

2.3 The effect of errors on the region of origin

2.3.1 Systematic errors

2.3.1.1 Errors in alpha

Overestimating the length of an ellipse results in an underestimation of the angle of impact. This results in an underestimation of the average value of the X coordinate of the region of origin [3]. The Y coordinate is not as sensitive as the X coordinate to the choice of the length of ellipses [3].

2.3.1.2 Gravity and air resistance

Traditional methods to determine the region of origin involve pulling a string back at the angle of impact to a three-dimensional point. Figure 2.5 showed that pulling a string back at the angle of impact from a blood droplet affected by gravity and air resistance (all blood drops) results in an overestimation in the Z-axis, the height. The use of directional analysis can help to minimise this overestimation because the convergence is found in the XY plane before the Z coordinate is determined. However even when directional analysis is used the estimation in the Z-axis should be interpreted as an indication of the *maximum* height of the blood source.

2.3.1.3 Different methods of convergence

Depending on the method used to determine the region of origin, the amount of uncertainty is different. When stringing is used there is usually an overestimation in the Z-axis because a 2D convergence is found in the YZ plane before strings are pulled back to determine the X coordinate. This is the same when the tangent method is used. As stated previously directional analysis is the most accurate method to use for determining the region of origin because convergence is found in the XY plane before the Z coordinate is established.

2.3.2 *Random errors*

2.3.2.1 Errors in gamma

If the direction of travel of a bloodstain is not measured accurately the result may be an error in the Y coordinate of the region of origin. There is however currently no published information on the effect of errors in gamma on the region of origin and research is therefore required to determine this effect.

2.4 **Avoiding errors**

Angle of impact

- Angle of impact errors can be minimised by ensuring an ellipse is fitted properly to a bloodstain before the length and width of that ellipse are measured. Computer programs including BackTrack™, Microsoft ® Office Visio ® Professional and Microsoft Excel can all be used for this purpose.
- Bloodstain selection is also important to avoid such errors because if a poorly formed bloodstain is selected for analysis, the outline may be hard to distinguish, resulting in an ellipse that is not well-fitted to the bloodstain and hence errors in the width and length measurements.
- The measurement errors observed as alpha approaches 90° may be overcome by proper stain selection and replication of measurements.
- The additional systematic error discussed in section 2.1.1.3 has not yet been investigated in enough detail to confirm that it is real and therefore the cause cannot yet be speculated. Further research is required to confirm and investigate this observation.

Gamma

- Because there is currently no information on the effect of errors in gamma on the region of origin, the way in which to avoid errors is not properly established.
- Generally speaking, gamma errors may be avoided by replication of measurements and proper stain selection.
- Stain selection should be carried out to ensure that bloodstains with defined directionality are selected for the region of origin analysis and replication may reduce the amount of error involved in the calculation.

Air resistance and gravity

- In a paper presented by Dr Alfred Carter (2001) it was concluded that the best one can do when determining a region of origin is 'estimate the upper limit for the height of the source' [12].
- While this is true, stain selection may allow the overestimation in the Z-axis to be minimised.
- There have not been any studies carried out to determine how to minimise this overestimation and thus research is required to investigate this.

Method of convergence

- The primary way to avoid errors from the method of convergence is to use directional analysis instead of stringing or the tangent method to determine the region of origin.
- The most common method used by bloodstain pattern analysts to determine the region of origin (i.e. stringing, tangent method or directional analysis) is not known and research is therefore required to establish this.

Other errors

- Bloodstains that appear to be secondary spatter should not be selected for analysis.

CHAPTER THREE: GENERAL METHODS AND MATERIALS

3.1 Laboratories

The experiments in this project were carried out in two laboratories, both of which were designed for the purposes of BPA research. The laboratory that was predominantly used was equipped with an adjustable t-grid ceiling, moveable wall panels, two paper dispensers containing 80 gsm Bleach Kraft white paper, in both 900 mm and 1800 mm widths, a fridge, a water bath and a foot activated sink.

The second laboratory had 900 mm movable wall panels, which were also lined with 80 gsm Bleach Kraft white paper, 900 mm or 1800 mm width prior to experimentation.

3.2 Blood

The blood used in the experiments was that of white pigs and it was obtained weekly from Alliance Group Limited². It was collected directly into a 500 ml large mouthed glass bottle containing 3.5 g EDTA (Sigma Chemical Co.).

Each bottle was given a batch number and stored in a refrigerator at 4°C and all blood was used within one week of collection. Prior to use, the blood was warmed to 37°C \pm 1°C for a minimum of 30 minutes in a water bath.

² Alliance Group Limited, Sockburn Plant, Christchurch, New Zealand.

3.3 Angle board and dropping pipette

An angle board was used to drop blood onto a target surface at a known angle (Fig. 3.1). The angle board was designed and constructed as described by Janes [26]. It was constructed of a steel plate base and a movable top plate and it had a protractor attached to allow the angle to be altered (Fig. 3.2). A Johnson magnetic angle locator was used in conjunction with the protractor to set the board at the required angle (Fig. 3.3). The target surface was secured with bulldog clips to the top plate to ensure it was completely flat at all times (Fig. 3.1).

A 200 μ l Gilson pipette (22 μ l blood per drop) was clamped to a 2 m clamp stand so that blood could be released from any height above the angle board (Fig. 3.4).

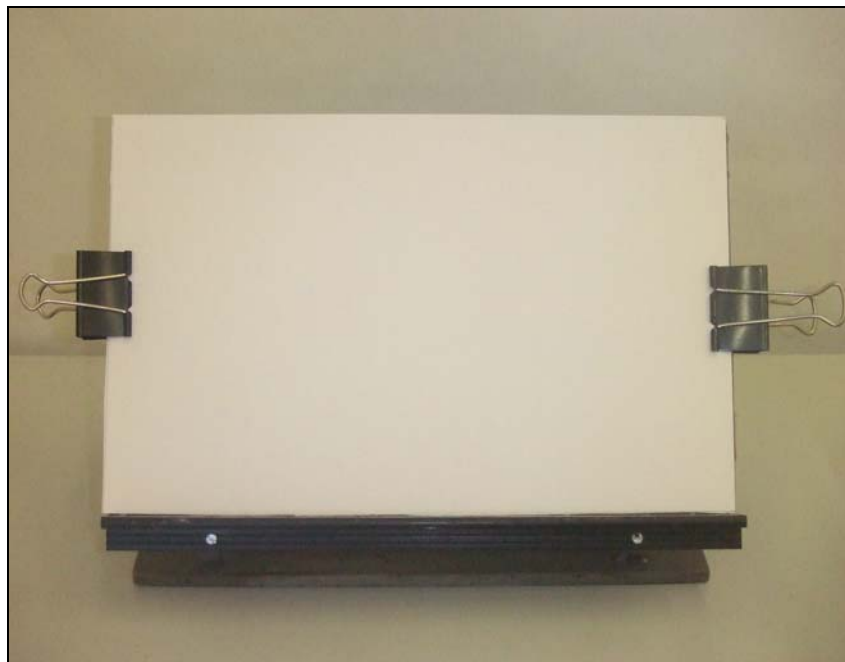


Figure 3.1 Front view of the angle board showing the positioning of the target surface and the bulldog clips.

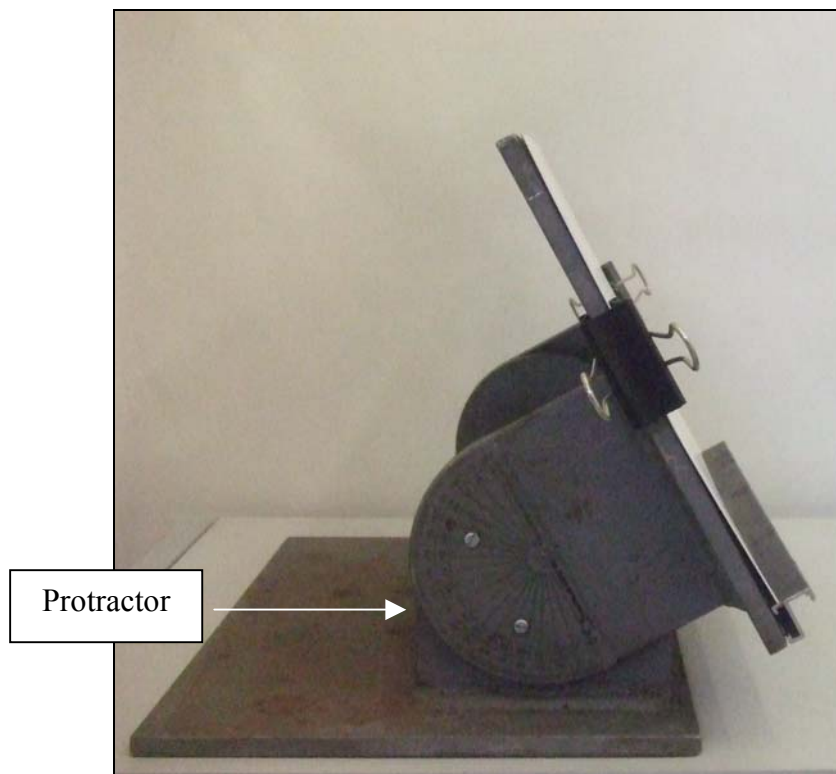


Figure 3.2 Side view of the angle board showing the protractor used in conjunction with an angle finder to set the angle.



Figure 3.3 Johnson magnetic angle locator.

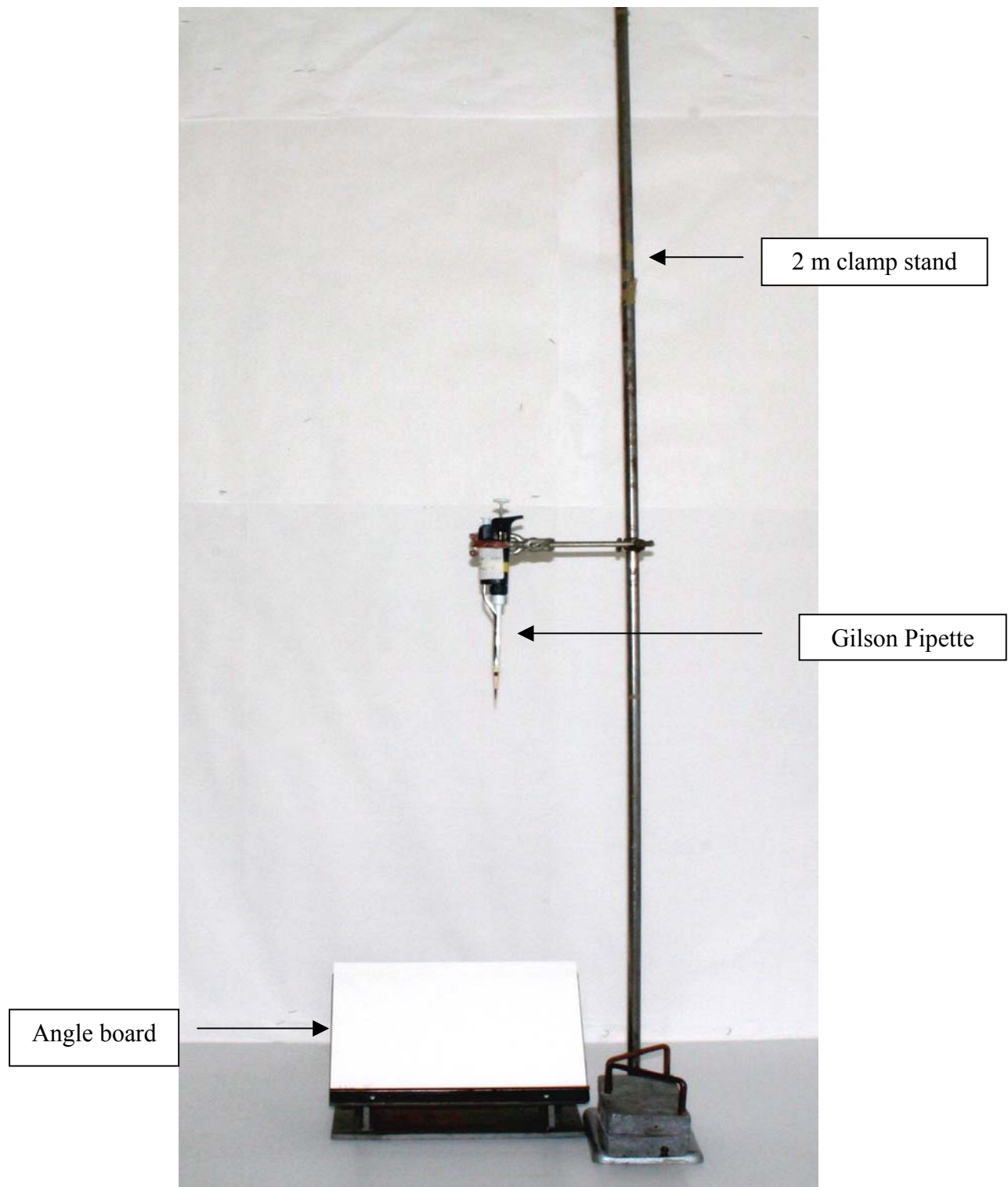


Figure 3.4 A 200 µl Gilson pipette clamped to a 2 m clamp stand positioned above the angle board.

3.4 Generation of impact spatter patterns

This research required that a number of impact spatter patterns were generated on a wall. This was achieved by either manually striking a pool of blood with a hammer or using an impact device, constructed for the purpose of this project. These methods are described in sections 3.4.1 and 3.4.2.

3.4.1 *Hammer and wooden block method*

A piece of Parafilm was stretched over one end of a wooden block and a pool of blood was placed in the centre (Fig. 3.5). A hammer was then used to strike the blood pool resulting in an impact spatter pattern on the nearby wall/walls (Fig. 3.6). The quantity of blood used and the number of times it was struck was varied and is stated in the relevant experiments.



Figure 3.5 Parafilm covered wooden block with blood pool.



Figure 3.6 Hammer used to make impacts.

3.4.2 *Impact device*

An impact device was constructed by Nicolas Oliver of the Chemistry Department, University of Canterbury (Fig. 3.7). A 980 mm long stainless steel rod was fixed to the centre of a steel base with a diameter of 315 mm and a thickness of 20 mm. Also fixed to the base was a 16 mm thick by 120 mm diameter disc of stainless steel to act as a platform for the blood sample. This disc had a 25 mm hole bored through the centre to allow the steel rod to pass through it. A 50 mm long spacer was placed between the base and the disk to avoid shielding of the impact spatter by the larger base. The total weight of the static apparatus of the device was 16 kg making it a stable foundation for impact events.

A 100 mm diameter, 3 kg sliding weight with a central hole was also constructed from stainless steel this was placed onto the steel rod so that it could freely slide up and down. A chamfer was added to the contact face of the weight to allow an unimpeded path for blood to travel vertically immediately after impact (Fig. 3.8). The opposite face of the sliding weight had two pieces of 10 mm by 80 mm long threaded rod fixed to it, allowing the securing of any additional weights. These additional weights consisted of 3 x 1 kg discs which could be attached to the 3 kg weight with 10 mm wing nuts. Therefore the sliding weight could be weighted to a total of 6 kg.

Finally, the base of the device was secured to a solid wooden stool to allow an easy working height, portability and a good degree of rigidity to be maintained.

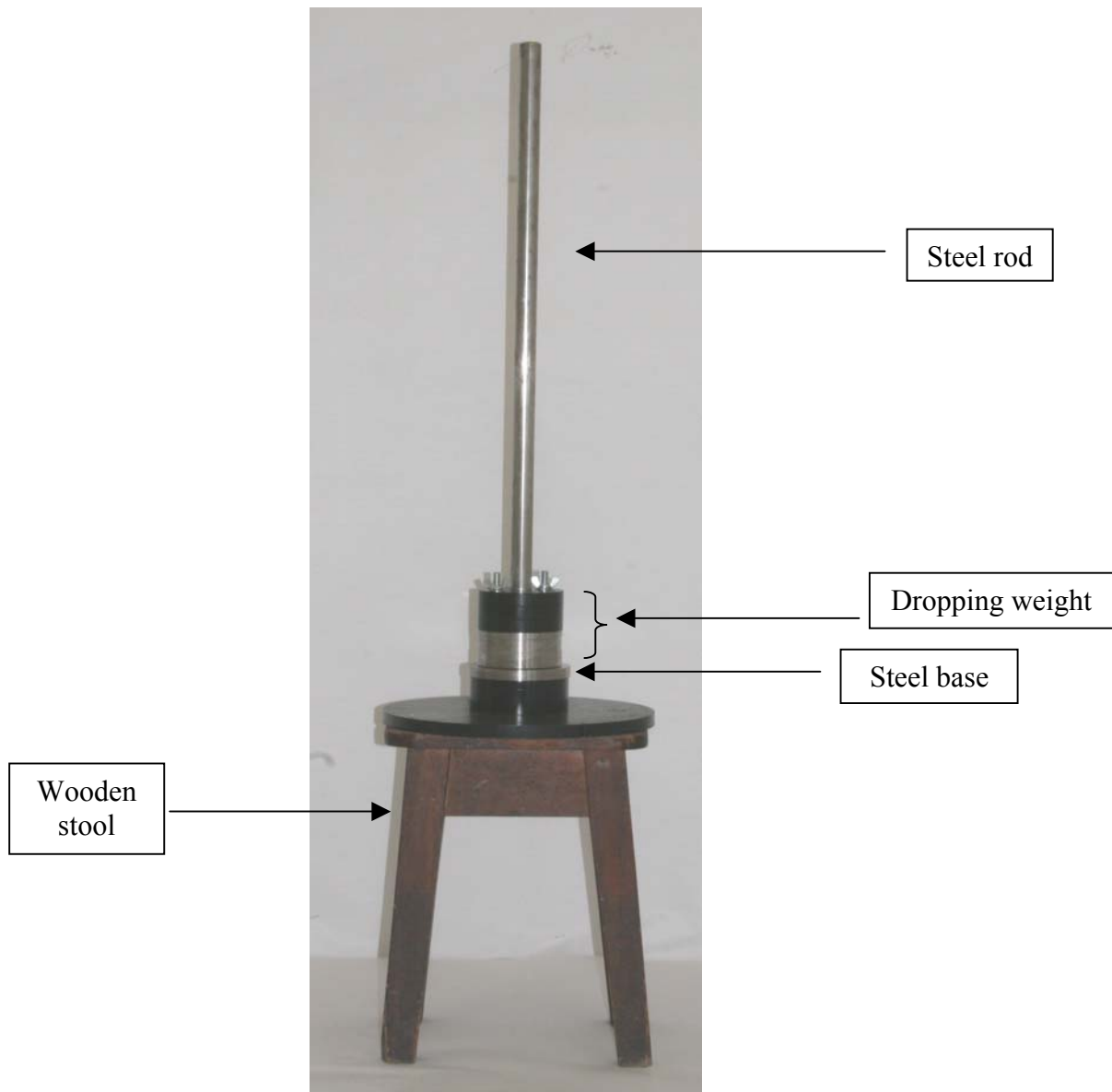


Figure 3.7 Impact device.



Figure 3.8 Chamfer on the dropping weight.

The device was designed to:

- Produce an impact with a sufficient number of bloodstains such that a detailed analysis could be carried out.
- Allow an impact to be generated at a well-defined location.
- Allow portability.
- Allow reproducibility.

It was necessary for the position of the impact site to be known precisely for the results to have significant meaning because the trajectories of individual bloodstains and the region of origin for groups of bloodstains were going to be compared with the known region of origin.

3.5 Photography

Four cameras were used throughout this research (Table 3.1). Three of these were digital cameras and one was a High-Speed B/W CMOS Camera, model #MS50K which was borrowed from the University of Canterbury Chemical and Process Engineering Department. This camera was capable of saving files as both AVI and bitmap files. These were then burnt onto CDs for analysis. The capture settings used in each experiment are given in the relevant chapter.

Table 3.1 Specifications of the cameras used during the research.

Camera	Maximum Resolution	Effective Pixels/ Frames per second	Format, sensor type and shutter speed
Nikon D100	3008 x 2000	6 MP	SLR format CCD sensor Shutter speed: 250 μ s – 30 s
Fuji Finepix Z3	2592 x 1944	5.1 MP	SLR format CCD sensor Shutter speed: - 1ms – 4 s
High- Speed CMOS	1280 x 1020	< 50,000 fps	Shutter speed: 2 μ s – 30 ms (image size dependent) 8-bit AD converter Mega Pixel CMOS sensor
Canon EOS-1Ds, Mark 2	4992 x 3328	16.6 MP	SLR format CMOS sensor Shutter speed: 250 μ s – 30 s

3.6 Health and safety procedures

A detailed description of the health and safety procedures followed during this research can be found in Appendix 1, however a broad description follows:

- At all times while carrying out experiments with blood in the bloodstain pattern analysis laboratory, disposable overalls, over-shoes and latex gloves were worn.
- The equipment used in the BPA labs was washed with detergent between use or if disposable was disposed of into the medical waste bin in the laboratory.
- Excess blood was washed down the sink with a large amount of water, and bleach was added if necessary.
- The blood used in experiments was stored in the refrigerator in the laboratory and no substance other than blood was permitted in this refrigerator.
- Appropriate first aid was applied or sought in the event of an incident. All accidents or injuries, no matter how minor - including blood splashed onto skin, face, eyes, or mouth - was reported to the Health & Safety Officers.

CHAPTER FOUR: BLOOD DYNAMICS

The knowledge of the fluid dynamics of blood flight and collisions are important in the interpretation of impact spatter patterns at crime scenes. Much of the early research on fluid dynamics was focused on properties of water, not blood and as a result this section includes a discussion of studies examining both water and blood. This chapter is divided into two parts. The first part investigates droplet impact with a target surface and the second looks at the dynamics of an impact event.

4.1 Droplet impact with a target surface

4.1.1 Introduction

When a droplet impacts a surface it behaves according to a number of parameters. Figure 4.1 provides an overview of different parameters that are of importance during drop impact. This shows that for blood drop impact, the drop type, impact angle and target surface composition are all parameters that will affect the appearance and therefore the properties of the resulting bloodstain.

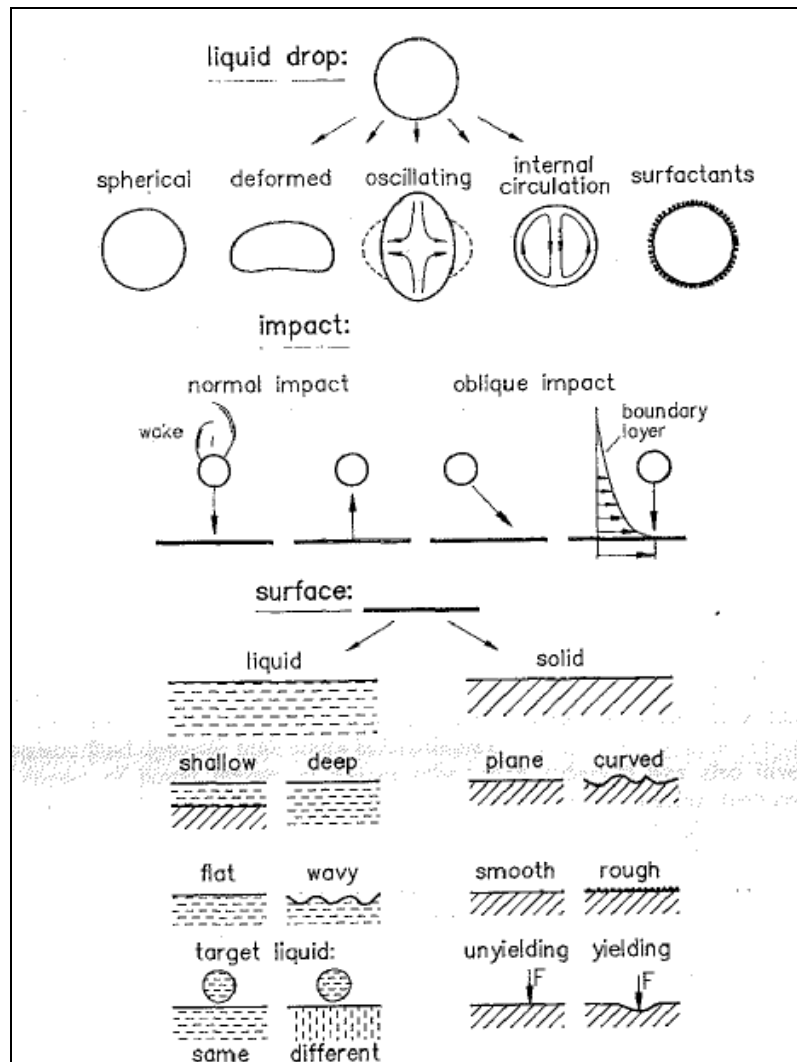


Figure 4.1 Parameters of importance during drop impact [28].

When a liquid drop impacts a solid surface the result can be ‘bouncing’, ‘spreading’ or ‘splashing’ (Fig. 4.2) [28]. Once again, this behaviour will depend on the drop type, impact angle and target surface, and it will affect the appearance and properties of the resulting bloodstain.

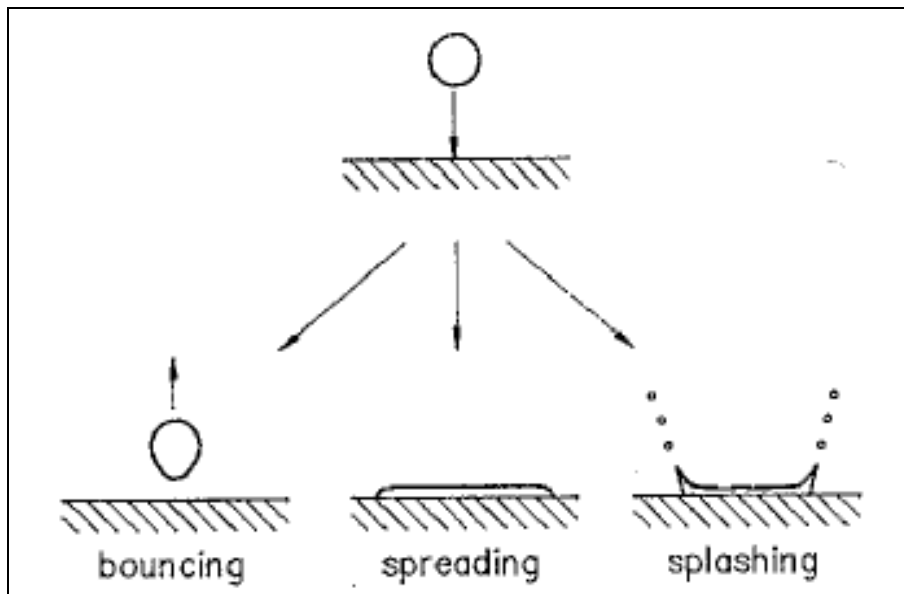


Figure 4.2 Impact of a drop on a solid surface: bouncing, spreading and splashing [28].

After the drop contacts the solid surface the liquid usually starts spreading out. An exception is when the kinetic energy of the drop is extremely small and the process of spreading is dominated by intermolecular forces [28]. A drop is said to ‘splash’ whenever it disintegrates into two or more secondary droplets after colliding with a solid surface [28]. In bloodstain pattern analysis, these secondary droplets are referred to as satellite spatter (Fig. 4.3).



Figure 4.3 Blood droplet with satellite spatter.

In a study carried out by Pizzola *et al.* [29], a series of high-speed photographs were taken as blood was released from a Pasteur pipette onto a stationary surface positioned at a set angle. The dynamics of the impact event were described as follows and can be visualised in Figure 4.4:

- Distortion of the drops is limited to the lower area in contact with the surface (1-3).
- As the drop continues to travel, it gradually collapses downward (toward the target surface) (4 – 8).
- The top of the upper hemisphere falls further while fluid displaced during the drop collapse is forced out radially forming a rim at the circumference (8 & 9).
- Shortly after the collapse, the centre region is significantly depressed (9).
- Following this the fluid forced to the rim retracts, collapses and progresses forward into a somewhat prolate form at the leading edge (10 – 14).
- The lower portion of the prolate area adheres to the impact surface while the upper portion grows or forms a droplet as it rises away from the impact surface (10 – 14).
- At this impact angle (used in experiments, but not stated by Pizzola) and dropping height the kinetic energy of the moving blood initially overcomes the surface tension and pulls away from the main body of blood to form a droplet which becomes approximately spherical, drawing out a fine filament in the process (10 – 14). The resulting blood drop shows this wave cast off [4].

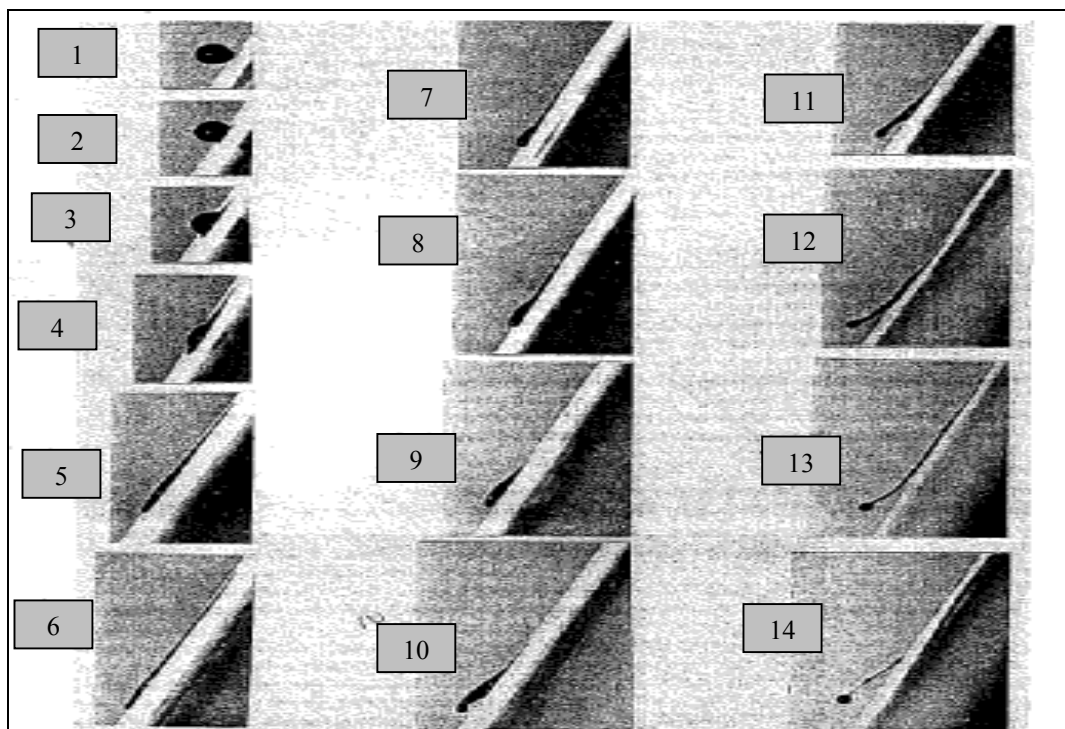


Figure 4.4 A series of photographs taken as a blood drop impacts an angled surface [29].



Figure 4.5 The resulting bloodstain.

4.1.2 Method

In this study, high-speed photography was used to allow the dynamics of droplet impact on an angled surface to be observed. This section describes the experimental set-up and the observations made from the high-speed photography.

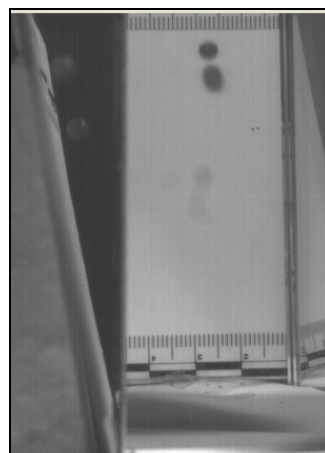
One drop of blood was released from a plastic pipette onto a 10 cm long x 5 cm wide piece of cardboard, which was set at an angle of 10, 20, 30 or 40 degrees from the vertical (Fig. 4.6). The blood was released onto each piece of cardboard and this was repeated so that in total there were two videos for each angle. The volume of the drops released from the pipette was approximately 0.04 ml. The cardboard had an adhesive scale stuck to it so that the bloodstain could be measured from the images. Two mirrors were set up so that the high-speed camera could capture the impact of the blood droplet on the surface from two different views – a side view and a front view (Fig. 4.6). The event was recorded at 1037 frames per second with an exposure time of 960 μ s.



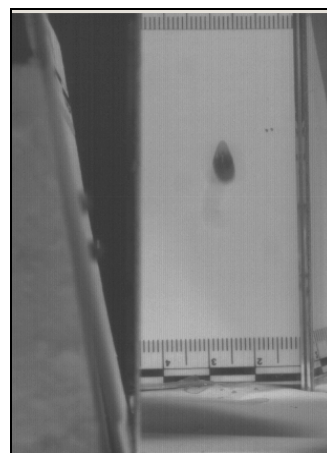
Figure 4.6 Mirror set-up.

4.1.3 Results

Figures 4.7 – 4.10 show still images of four different stages of droplet impact on an inclined surface taken from the high-speed videos. The dynamics are slightly different at each angle and are discussed in section 4.1.4. Note that in the first image of each figure it appears as if there are two blood drops present. This is because a shadow is cast *below* the actual blood drop.



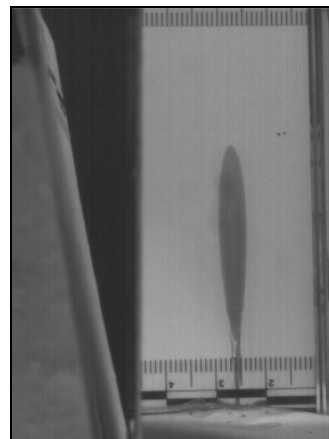
Frame 12/59



Frame 21/59



Frame 26/59

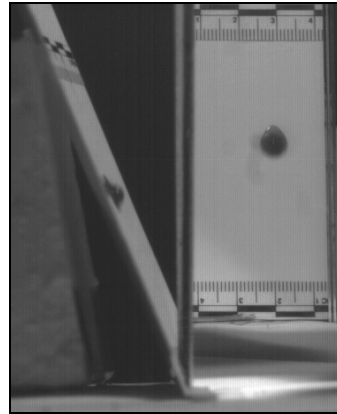


Frame 59/59

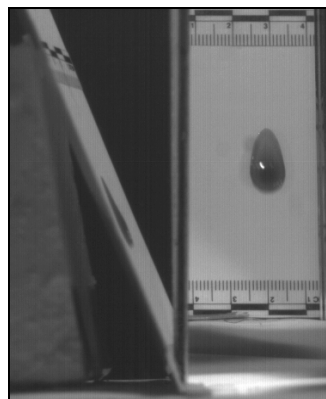
Figure 4.7 Blood droplet impacting a cardboard surface at 10°.



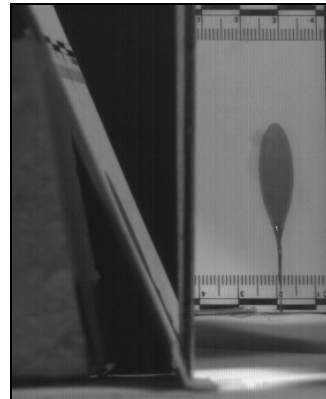
Frame 7/40



Frame 15/40



Frame 18/40



Frame 40/40

Figure 4.8 Blood droplet impacting a cardboard surface at 20°.



Frame 11/49



Frame 14/49



Frame 17/49



Frame 49/49

Figure 4.9 Blood droplet impacting a cardboard surface at 30°.

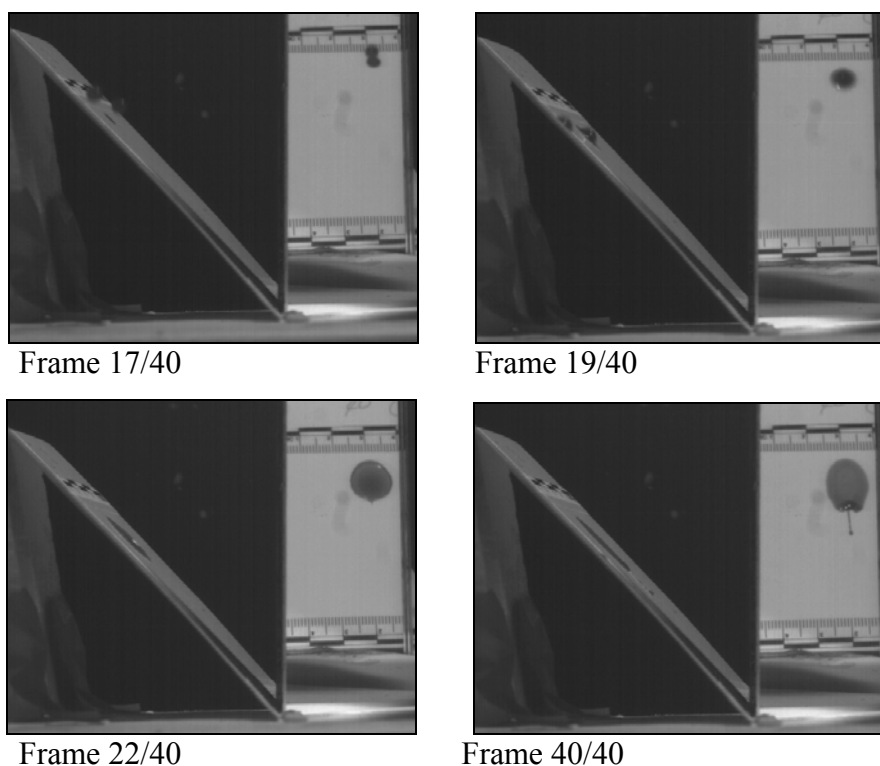


Figure 4.10 Blood droplet impacting a cardboard surface at 40°.

4.1.4 Discussion

When the blood droplets impacted the cardboard surface at the four different angles the bloodstain formed quite differently at each angle. At the most acute angle, (10°), the width of the resulting bloodstain was closest to the width of the blood drop from which it was formed. As the angle increased from 10° to 40°, the width of the resulting bloodstain increased. The angle of impact therefore affects the amount the bloodstain spreads out on the surface upon which it lands.

When the blood drop impacted the cardboard surface, the shape of the forming bloodstain differed at each angle. At 10°, it was teardrop shaped and as it approached 40° it got more circular. This resulted in the bloodstains travelling very differently over the surfaces at different angles. At 10° the blood travelled predominantly in a downward direction with very little spreading resulting in a long, thin bloodstain. As

the angle of impact increased, the blood began to be pushed out as well as down resulting in bloodstains with a greater width and a shorter length.

At each of the four angles observed in this study, wave cast-off formed. The length of the cast-off increased as the angle of impact became more acute. This was because at the more acute angles component of the velocity perpendicular to the surface is less than at greater angles of impact meaning the cast-off travelled at a greater velocity and therefore landed further away from the bloodstain (Fig. 4.11). The blue lines allow the distance of the wave cast-off to be compared at two different angles of impact. At 20° , it was longer than that at 30° .

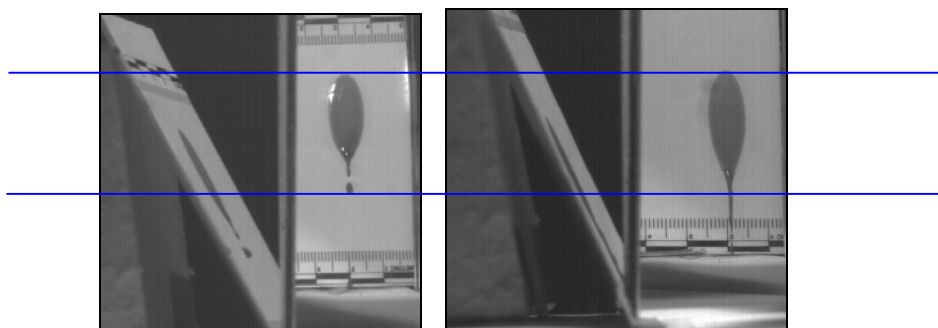


Figure 4.11 Wave cast-off at 30° (left hand side) and 20° (right hand side).

The diameter of the blood drop prior to impacting the cardboard was 4 mm. As discussed earlier the width and length of the resulting bloodstain varied depending on the angle of impact. These measurements were determined using the scale in the images and are given in Table 4.1. The length was measured from the leading edge of the bloodstain to the position at which it tapered off (excluding the wave cast-off) (Fig. 4.12). The width and length were plotted in Excel for each angle of impact and are shown in Figures 4.13 and 4.14. A trend line was fitted to each graph in Excel. Figure 4.13 has a logarithmic trend line and Figure 4.14 has a linear trend line fitted.

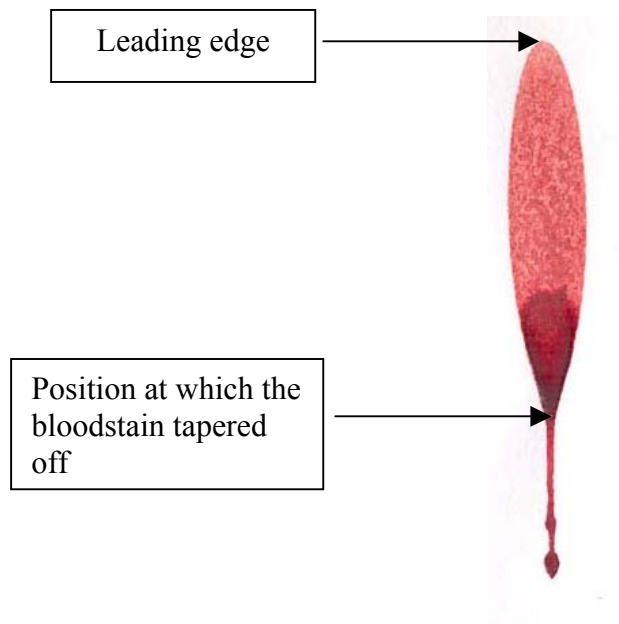


Figure 4.12 Measurement of the length of the bloodstain.

Table 4.1 The width and length of bloodstains formed at various angles of impact.

Angle of incline	Diameter of drop (d)	Width of stain (w)	d/w	Length to end of taper (l)	l/d
10°	4 mm	6 mm	0.66	35 mm	8.75
20°	4 mm	9 mm	0.44	31 mm	7.75
30°	4 mm	11 mm	0.36	27 mm	6.75
40°	4 mm	12 mm	0.33	17 mm	4.25

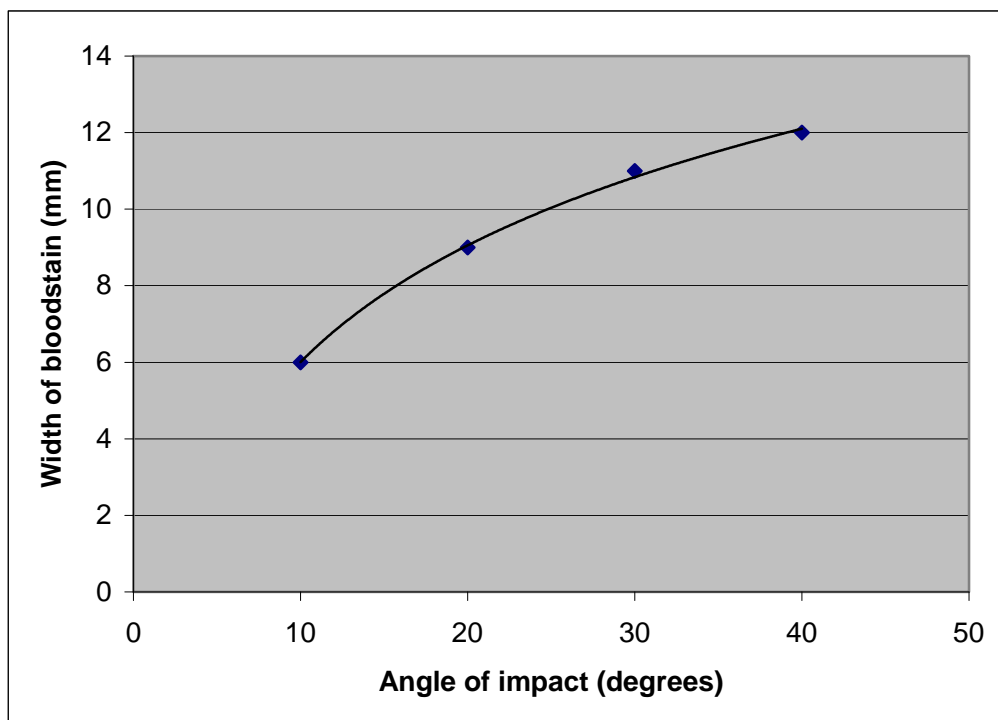


Figure 4.13 The width of the bloodstain at different angles of impact.

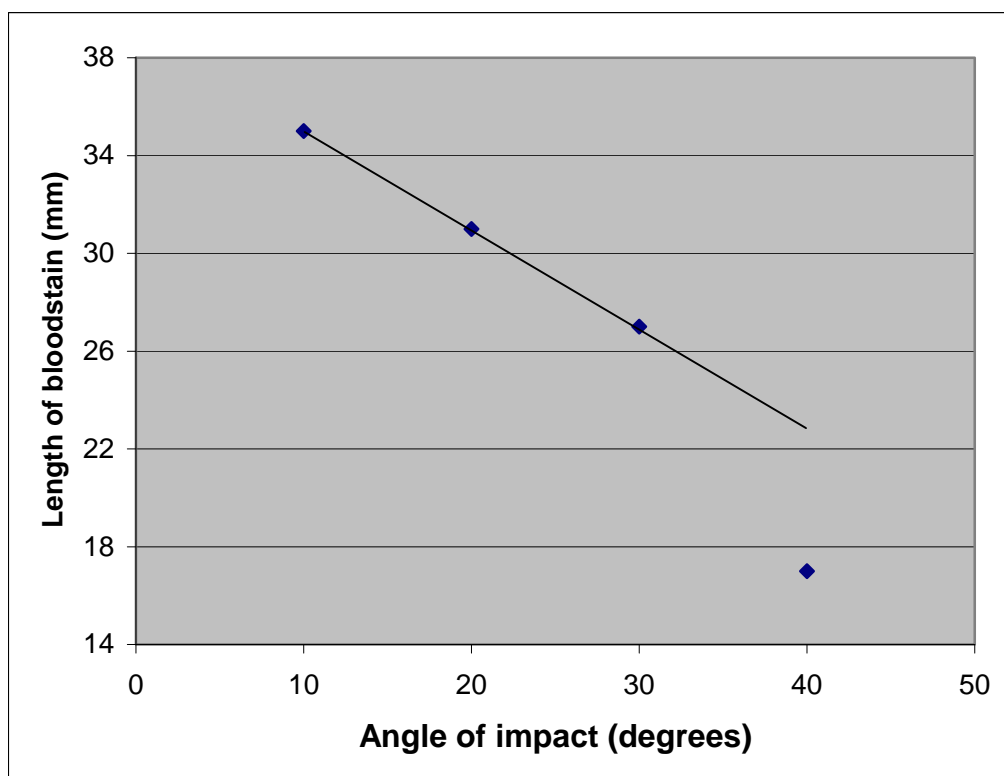


Figure 4.14 The length of the bloodstain at different angles of impact.

Figure 4.13 shows that at the most acute angle, 10° , the width was the least out of all the bloodstains, (6 mm). As the angle of impact increased so too did the width of the resulting bloodstain. This increase was not however linear and it can be seen that the graph flattened out as the angle of impact increased.

Figure 4.14 shows that the length of the bloodstains began to decrease for $10^\circ - 20^\circ$ and $20^\circ - 30^\circ$ (4 mm) however for $30^\circ - 40^\circ$ the difference decreased significantly (10 mm). The bloodstain that resulted when the blood drop impacted the surface at 40° did not taper as the bloodstains at the more acute angles had (Fig. 4.10). Instead it was quite circular and explains why there was such a significant decrease in bloodstain length at this angle (see the last frame of Fig. 4.10).

The observations made in this study show that a combination of both ‘spreading’ and ‘splashing’ occur when a blood drop is released onto an angled surface and that the extent to which these affect the appearance of the resulting bloodstain is based on the angle of impact.

4.2 The dynamics of an impact event

4.2.1 Introduction

An impact event is a dynamic process. It is made up of a number of different stages each of which is highly variable depending on the conditions at the time. The result is a unique impact spatter pattern.

Although every impact pattern is different, they are sometimes categorised. Analysts base one approach to categorising spatter on impact velocities [30]. These categories are based on the velocity at which the blood source was impacted and include low, medium and high velocity. The categorisation can be carried out by looking at the size of the bloodstains that make up the impact pattern. Bevel and Gardner state that to properly categorise a pattern, an analyst must look at the ‘preponderant stain size’ and that this spatter is generated during a certain stage of the impact event (Fig. 4.15) [30]. The ‘preponderant stain size’ is the droplet size that is most commonly seen in the impact pattern.

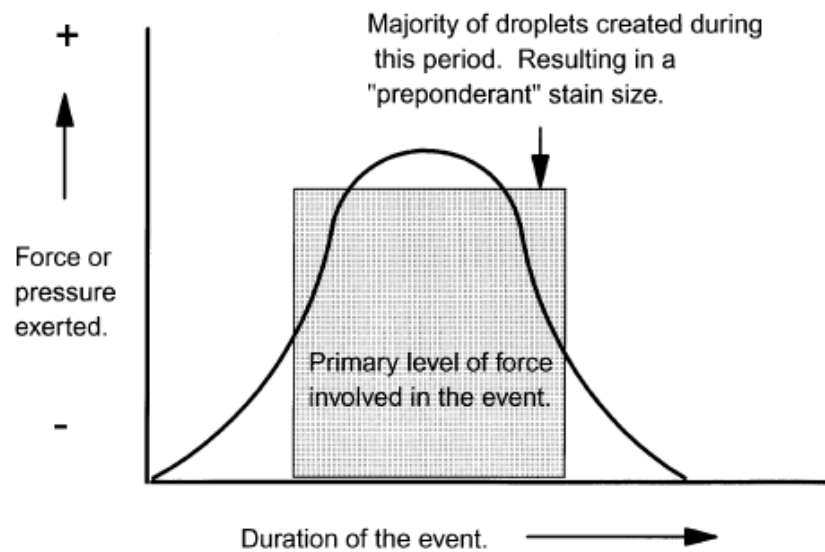


Figure 4.15 Bevel and Gardner propose that the majority of droplets are created during the shaded period and that this results in a preponderant stain size [30].

This method of categorisation of impact patterns is not an accurate way of describing such an event, as it is often misinterpreted as being a description of the ferocity of the event – not the velocity at which a blood source was impacted. For this reason many analysts avoid classifying spatter as low, medium or high velocity.

What can however be deduced from the stain sizes in an impact pattern is a relative estimate of the amount of energy applied to the blood source. In general as the energy applied to a blood source increases, the spatter size in an impact pattern decreases.

In order to further investigate the dynamics of an impact event, two impacts were recorded with a high-speed camera. This section describes the experimental set-up and the observations made from the high-speed photography.

4.2.2 Method

2 ml of blood was placed on a Parafilm covered wooden block (10 cm² surface). This was struck with a hammer and the event recorded with the high-speed camera, which was set perpendicular to the surface of the wood. The event was recorded at 1037 frames per second with an exposure time of 600 μs.

Following this, the impact device was dropped from a height of 60 cm with a 3 kg weight onto 3 ml of blood. This event was recorded at 2066 frames per second with an exposure time of 480 μ s.

4.2.3 *Results*

For each impact, a high-speed video was recorded and from these videos, a number of still frames were extracted. An overview containing these frames is given in Figures 4.16 and 4.23 for each impact and following these are larger images showing more detail. Alongside the overview images, is the time at which each frame occurred.

4.2.3.1 Hammer impact

The hammer hit the wooden block slightly off the centre of the 2 ml blood pool (Fig. 4.17). The surface of the hammer was not completely perpendicular to the surface of the wooden block (Fig 4.17). As soon as it touched/impacted the blood pool, the blood began to travel out from the pool. Because the hammer was not centred, the blood behaved differently on the leading and trailing edges of the hammer head. On the trailing edge it was ‘squashed’ and it came out horizontally in a flat sheet (Fig. 4.18). On the other side, the blood was projected upwards around the hammer like a wave (Fig. 4.19). It then formed a sheet, in the shape of the hammer’s round edge and this travelled vertically for approximately 15 ms (Fig. 4.20). The sheet then broke up into filaments, which subsequently broke up into droplets of varying size (Fig. 4.21 and 4.22). The entire event took approximately 120 ms.

1. The hammer before it impacted the blood pool
 $t = 0$



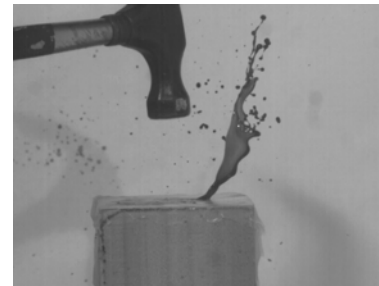
2. The left hand side of this image shows the horizontal sheet, the right hand side shows the wave coming up around the hammer
 $t + 4.83 \text{ ms}$



3. The sheet
 $t + 19.29 \text{ ms}$



4. The sheet breaking up into filaments
 $t + 55.93 \text{ ms}$



5. The filaments breaking up into drops
 $t + 121.5 \text{ ms}$

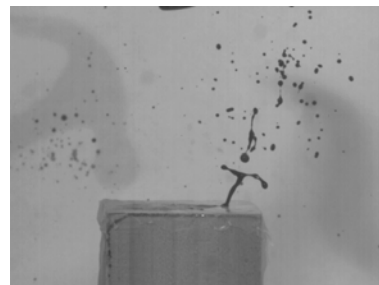


Figure 4.16 Overview of the hammer impact event.



Figure 4.17 Position of hammer when it struck a 2 ml pool of blood.



Figure 4.18 The left hand side of this image shows the horizontal sheet.



Figure 4.19 The right hand side of this image shows the wave coming up around the hammer.



Figure 4.20 The sheet.

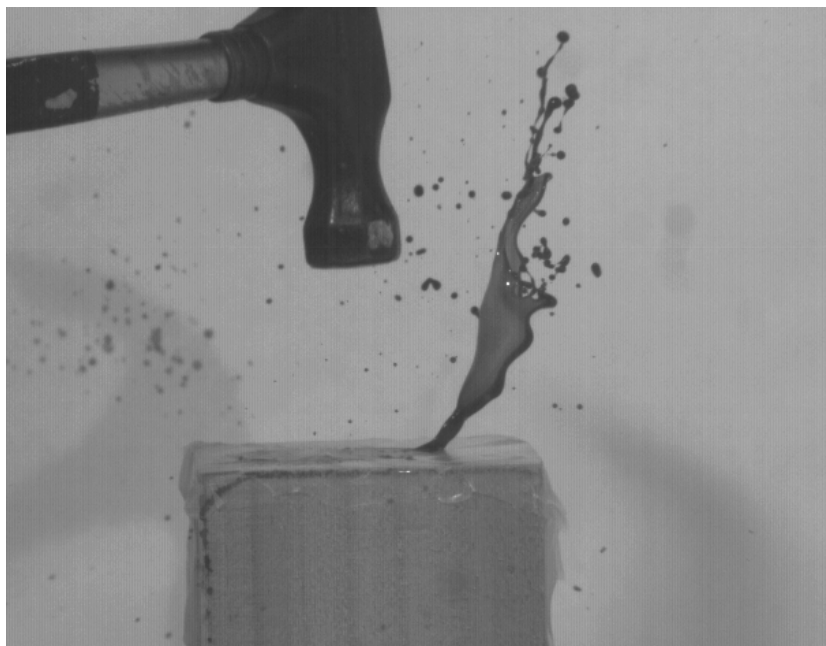


Figure 4.21 The sheet breaking up into filaments.

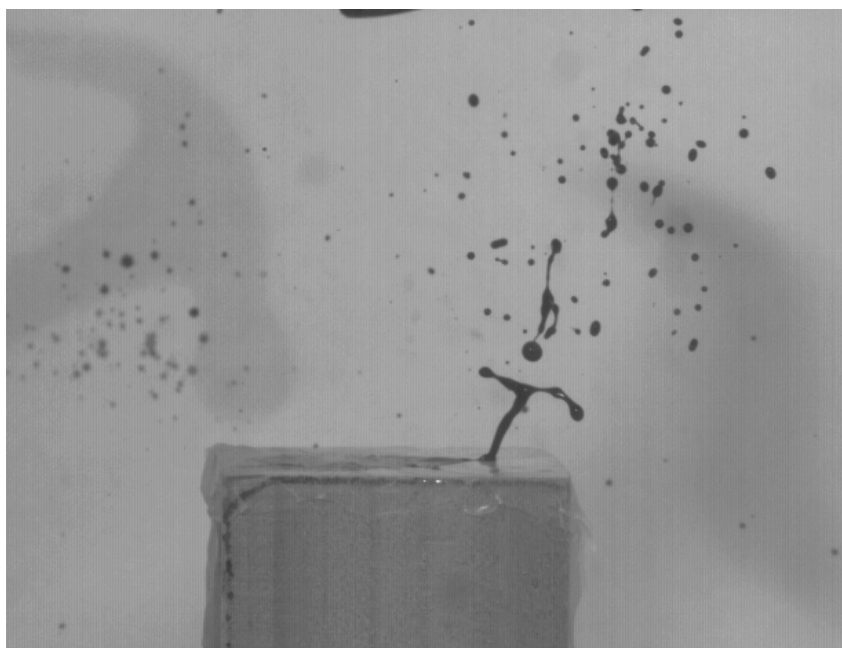
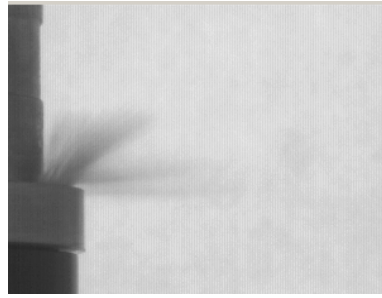


Figure 4.22 The filaments breaking up into drops.

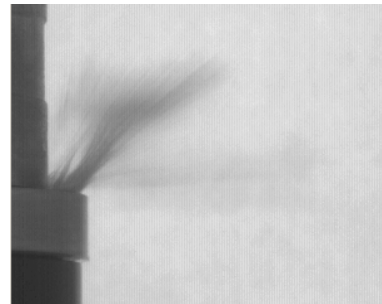
4.2.3.2 The device impact

When the device impacted the blood it began to travel in two ‘layers’, each of which was coming out from the device at a different angle. The bottom layer was travelling horizontally and was the fastest (Fig. 4.24). This resulted in a misting effect on the wall (Figure 4.25). The layer that was travelling upwards (Fig. 4.26) was projected towards the wall and it consisted of a sheet (Fig. 4.27), which broke into filaments then droplets of varying size (Fig. 4.28 and 4.29). The reason for the layering effect was that the edge of the dropping weight had a chamfer on it allowing the blood to travel upwards as well as outwards (see Fig 3.8). The entire event took less than 20 ms to occur.

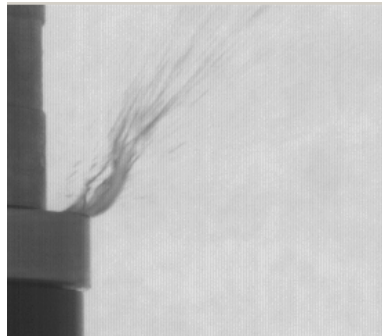
1. The horizontal, fast travelling sheet that results in misting
 $t = 0$



2. The second layer that results in the majority of the drops in the impact pattern
 $t + 0.49 \text{ ms}$



3. The sheet
 $t + 3.86 \text{ ms}$



4. The sheet breaking into filaments
 $t + 6.78 \text{ ms}$



5. Blood drops
 $t + 16.46 \text{ ms}$



Figure 4.23 Overview of the hammer impact event.

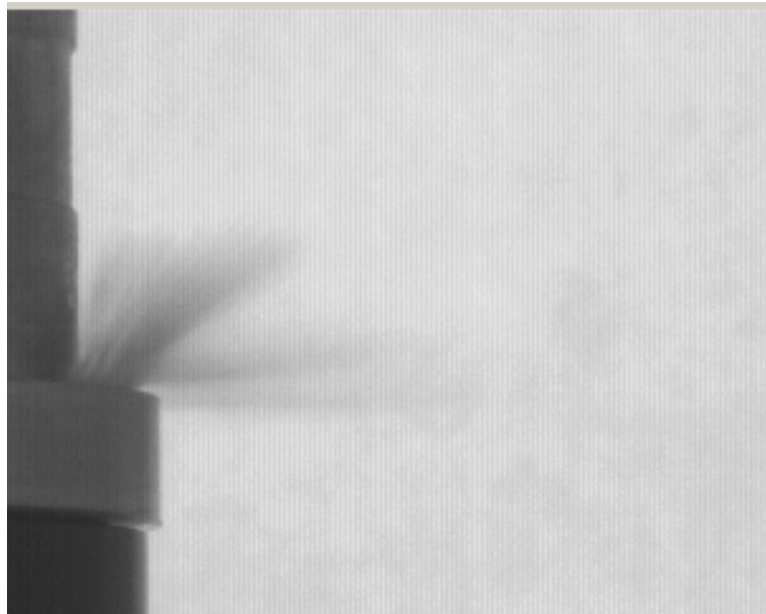


Figure 4.24 The horizontal layer after device impact.

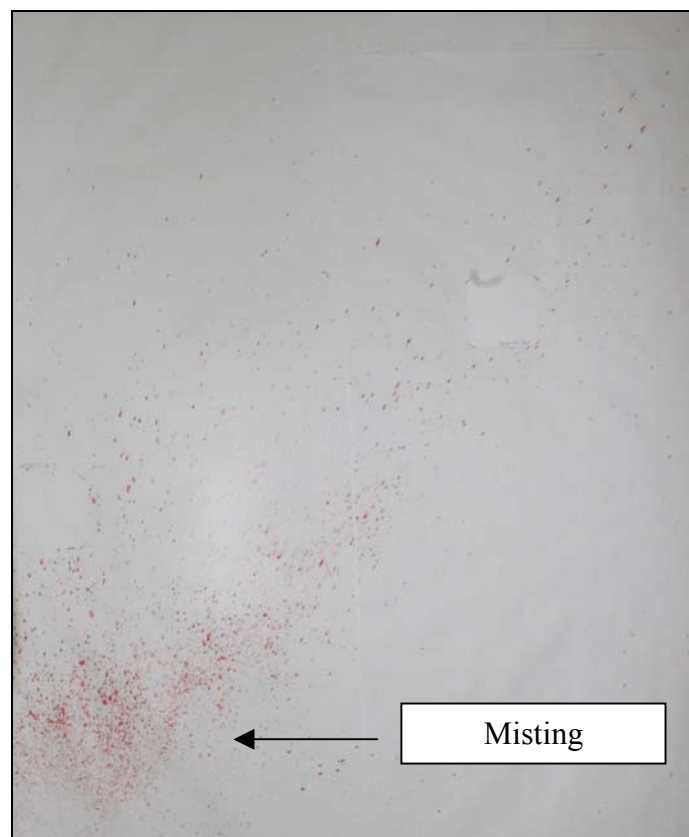


Figure 4.25 Misting effect shown on the resulting bloodstain pattern.

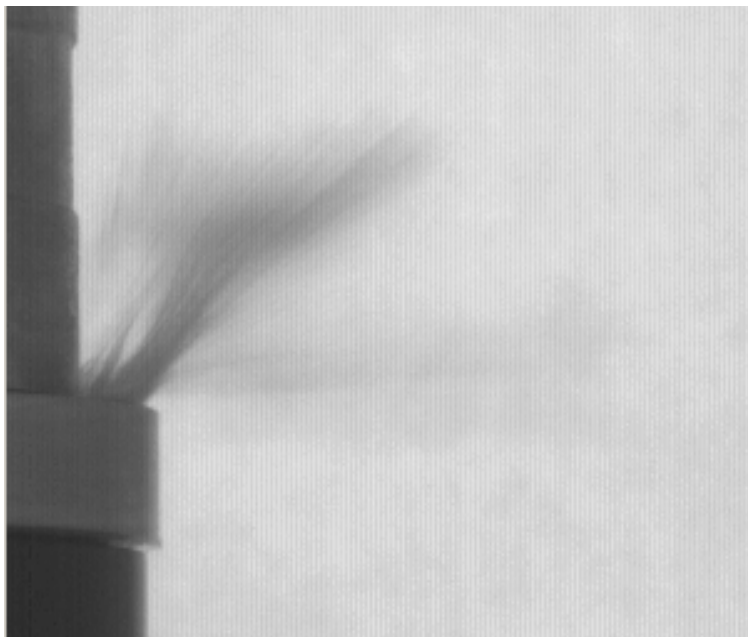


Figure 4.26 Layer travelling upwards.

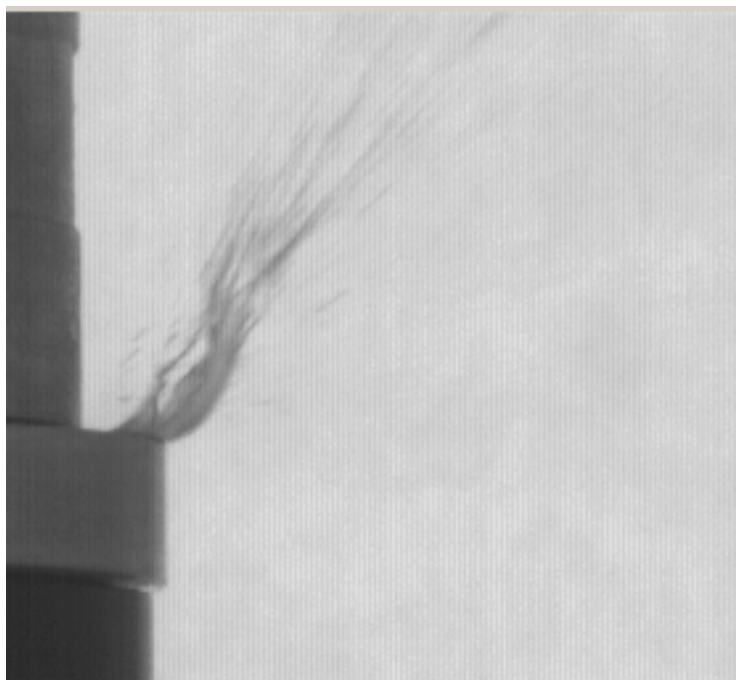


Figure 4.27 Sheet breaking into filaments.

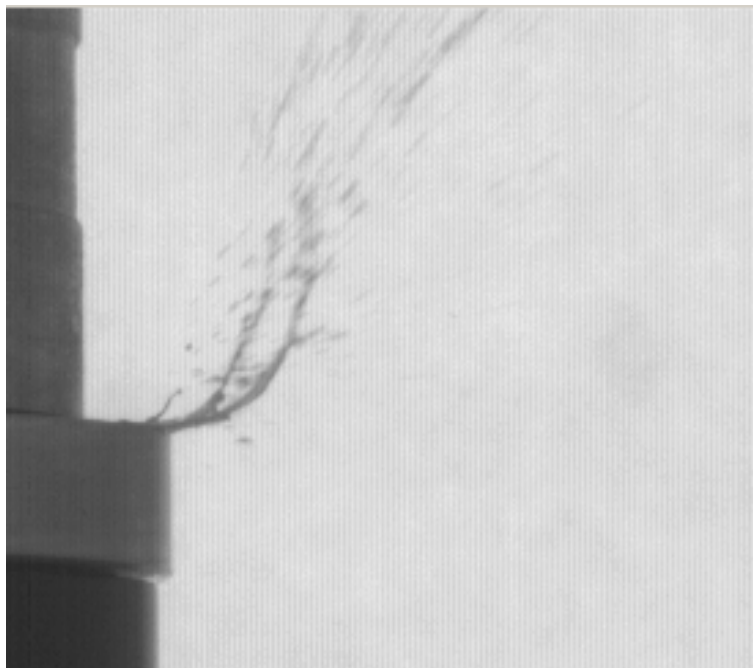


Figure 4.28 Filaments.



Figure 4.29 Droplets.

4.2.4 Discussion

The high-speed videos show that there are many different dynamic processes that occur when blood is struck and an impact pattern is formed. The process begins when an object touches a blood source and the blood begins to move because of the forces acting on it.

In the case of the hammer impact, the blood went through many stages, each of which could be visualised on the high-speed videos. The blood that impacted the wall first following the impact appeared as ‘misting’ and travelled out horizontally from the impact site. The blood formed a ‘sheet’ before breaking into filaments and finally droplets, which then travelled towards the wall. The sheet travelled out from the hammer towards the wall approximately 3 cm before breaking into filaments, which travelled approximately a further 3 cm before the drops began to break off.

In BPA when determining a region of origin it is assumed that blood drops travel in a straight line. For this to be true, there can be no forces acting on a blood drop. The data presented in this chapter prove that this is not the case. The fact that a sheet is seen means that there are forces acting on the blood after it is struck preventing it from splitting instantly into droplets and travelling in a straight line.

The implication of this finding is that a region of origin estimate will never be completely accurate. In the case of experimental work the implication is that when a impact pattern is generated from a measured point of origin, the bloodstains may indicate a slightly different region of origin – the position in 3D space that the sheet of blood broke into blood drops.

The high-speed videos have provided an insight of the events that occur when blood impacts a target surface and when an object strikes a blood pool. Every impact is unique and it is important that blood dynamics are considered when a pattern is analysed to determine the region of origin.

Chapter conclusions

- When a blood drop impacts a surface at different angles the blood behaves very differently.
 - The width of the resulting bloodstain increases as the angle of impact increases.
 - The length of the resulting bloodstain increases as the angle of impact increases.
 - A combination of both ‘spreading’ and ‘splashing’ occurs.
- When an object strikes a blood source there are many different dynamic process that occur.
 - Blood is ‘squeezed’ out between the object and surface on which the blood source is and travels horizontally at a high velocity.
 - This appears as misting on the target surface.
 - The blood travels in a sheet-like formation before separating into droplets.
 - This means that the true impact site is different to the position in three-dimensional space that the blood separates into droplets.
 - This means that the actual point of origin is likely to be slightly different to the region of origin calculated by analysts at a crime scene. This difference is unavoidable.
- When a blood drop impacts different surfaces the dynamics are very different
 - On rough/textured surfaces blood ‘skims’ over the grains of the surface forming a bloodstain with voids where the blood hasn’t touched the surface.
 - Bloodstains on rough/textured surfaces were longer than those on smooth/non-textured surfaces, even though the volume of the blood drop was the same in each situation.

CHAPTER FIVE: ANGLE OF IMPACT CONSIDERATIONS

This chapter will outline the analysis conducted to investigate the effect that various factors have of the angle of impact calculation.

5.1 Computer programs that can be used to calculate the angle of impact are compared.

5.2 Determination of the effect the target surface has on the formation of bloodstains.

5.3 Investigation into the effect of the target surface through assessment of the contact angle of blood on different surfaces.

5.4 Discussion the use of high-speed photography in the investigation blood dynamics on different surfaces.

5.5 The fifth section details an experiment carried out to determine the effect of velocity on estimates of the angle of impact.

5.6 The final section assesses whether there is a systematic underestimation of the angle of impact using results from the experiments carried out in this chapter.

5.1 The method used to fit an ellipse to a bloodstain when determining the angle of impact

5.1.1 Introduction

The method used to fit an ellipse to a bloodstain varies between analysts. It may be a matter of the equipment available at the time. A poorly fitted ellipse can result in an inaccurate angle of impact calculation and this can affect the accuracy of the region of origin determination. It is therefore important that an ellipse is fitted properly to a bloodstain.

A number of methods can be used to fit an ellipse to a bloodstain. These include both computer based and manual methods. The general procedure involves fitting the ellipse to the width of the bloodstain but not to its length (Fig. 5.1). The critical skill is deciding on the length of the ellipse and this is often overestimated, especially at acute angles of impact where the bloodstain exhibits an elongated shape [21]. An overestimation of the length of the ellipse results in an underestimation of the angle of impact.

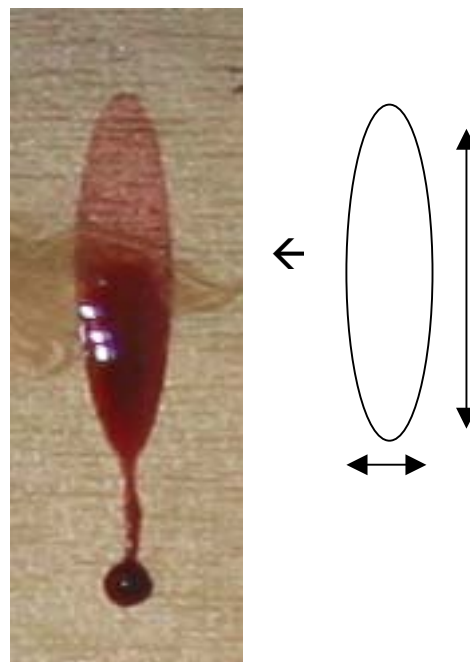


Figure 5.1 The method for fitting an ellipse to a bloodstain.

As discussed in section 2.1.1.2 a study was carried out in 1991 both to establish the methods used by bloodstain pattern analysts to determine the angle of impact and to find out how accurately the angle of impact measurements made by these analysts were. The methods used were all manual methods including using callipers or a ruler.

It was found that the analysts often overestimated the lengths of the bloodstains resulting in an inaccurate angle of impact result. Figure 5.2 shows how accurate the angle of impact determinations were. The Y-axis shows the accuracy of the measurements for each of the 10 drops. It can be seen that the accuracy of the measurement was above 50% in only four of the drops. The reason given in the study for this finding was that the majority of analysts were measuring to the tail of the drop.

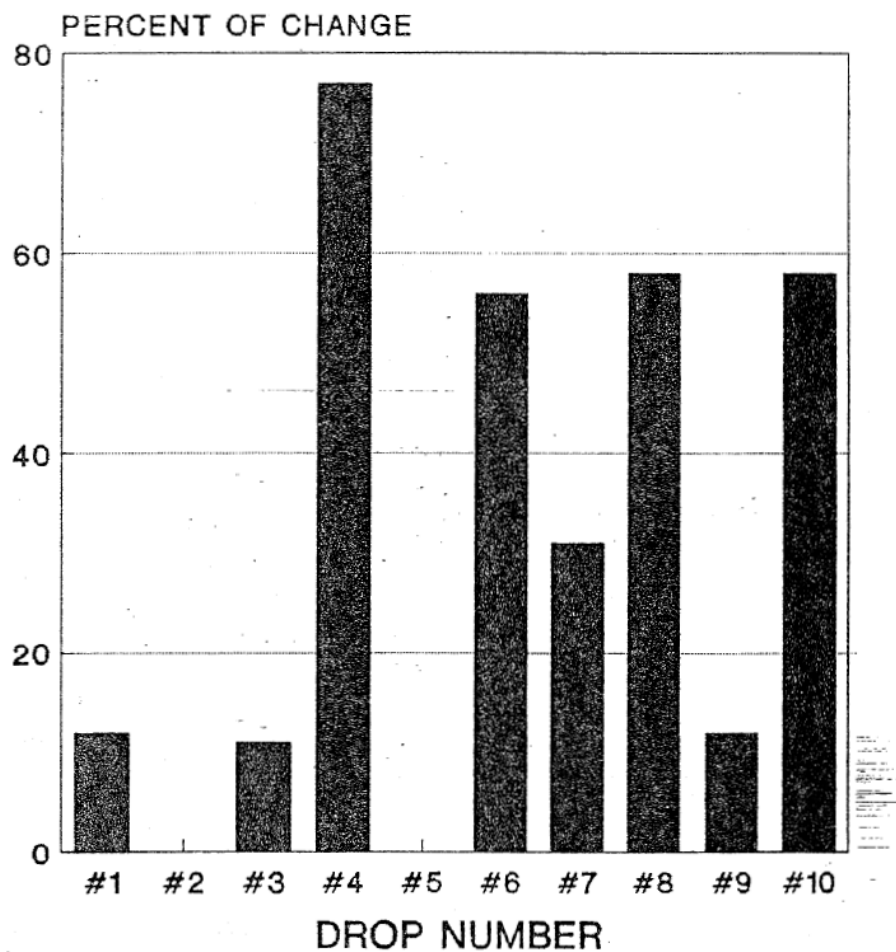


Figure 5.2 In a survey to determine how accurately bloodstain pattern analysts measured the angle of impact, it was found that the accuracy of the measurements was above 50% in only four of the drops [21].

Several computer programs for measuring the width and length of bloodstains were compared. The objective was to determine the most accurate computer-based method for fitting an ellipse to a bloodstain.

5.1.2 Method

Four different computer programmes were used to fit ellipses to bloodstains formed at different angles on six different surfaces. These programmes included Microsoft® Excel 2000, Microsoft® Office Visio® Professional 2003, BackTrack™/Images and System for Trigonometric Analysis of Blood Spatter (STABS).

An angle board, set at the desired angle was placed exactly 1 m below a 200 µL Gilson pipette which was secured to a 2 m clamp stand (as described in chapter 3). Six target surfaces were used during the experiment. They are described in Table 5.1 and images of each surface can be seen in Appendix 2.

Table 5.1 Summary of the different target surfaces.

Target Surface	Description	Texture
Cardboard	A4 chlorine free cardboard (225gsm, Klippan Kaskad Boards)	Smooth Glossy surface
Vinyl	20 cm ² piece of lightly coloured vinyl	Smooth Glossy surface A small number of indentations
Wallpaper	Textured, brown and gold wallpaper	Rough Matt surface Textured
Wood	10 cm ² oak	Rough Matt surface Many large and distinct vesicles making it very textured
Glass	20 cm ² clear plate of glass	Smooth Glossy surface
Tile	10 cm ² white tile	Smooth Glossy surface

The target surface was secured to the angle board. The pipette was filled with 200 μL of blood and sufficient pressure applied that one droplet would form and be released. Seven blood drops were released onto each of the six target surfaces.

The vinyl, glass and tile samples were cleaned with soapy water, dried and then wiped with a 70% ethanol solution before being reused.

Every bloodstain was photographed and transferred to a computer for analysis. The angle of impact was determined from the ellipses fitted using the different computer programmes and the difference between the actual and calculated angle of impact (termed observed – expected angle) was calculated. This value was then plotted against the actual angle of impact for different surfaces and the graphs are given in Figures 5.11 and 5.12. Instead of plotting a graph for every surface, the results were plotted for wood and cardboard because of the greater spread of data. All of the data however can be found in Appendix 2. The standard deviation is also shown on the graphs. The time taken to analyse each bloodstain and the ease of doing so was also considered while using each of the computer programs and is discussed in Section 5.1.4.

A description of the four different methods used follows.

5.1.2.1 Microsoft® Excel 2000

When Microsoft® Excel 2000 was used, a photograph of a bloodstain was pasted onto a new worksheet and the drawing functions were used initially to draw a vertical line on either side of the bloodstain such that only a small portion of the bloodstain touched the line [31] (Fig. 5.3).

- It was important that the vertical lines were aligned with the directionality of the bloodstain. If the bloodstain was on a slight angle (primarily due to the angle at which the photograph was taken) the parallel lines were drawn on at the same angle. A line was then drawn horizontally through the two points at which the bloodstain began to curve and stop touching the vertical line.
- A line was then drawn through the centre of these two lines to determine the mid-length of the ellipse that was to be fitted to the bloodstain.

- An ellipse was then fitted by positioning it initially at the centre line and then extending it both ways at the same time by holding down the Ctrl key. The ellipse was fitted closely to the actual width of the bloodstain.

The result of this procedure is given in Figure 5.3. The parameters of the ellipse were double clicked and the size (length and width) of the ellipse was shown by clicking on the size tab. These values were input to the sine formula ($\alpha = \arcsin(w/l)$) to determine the angle of impact.

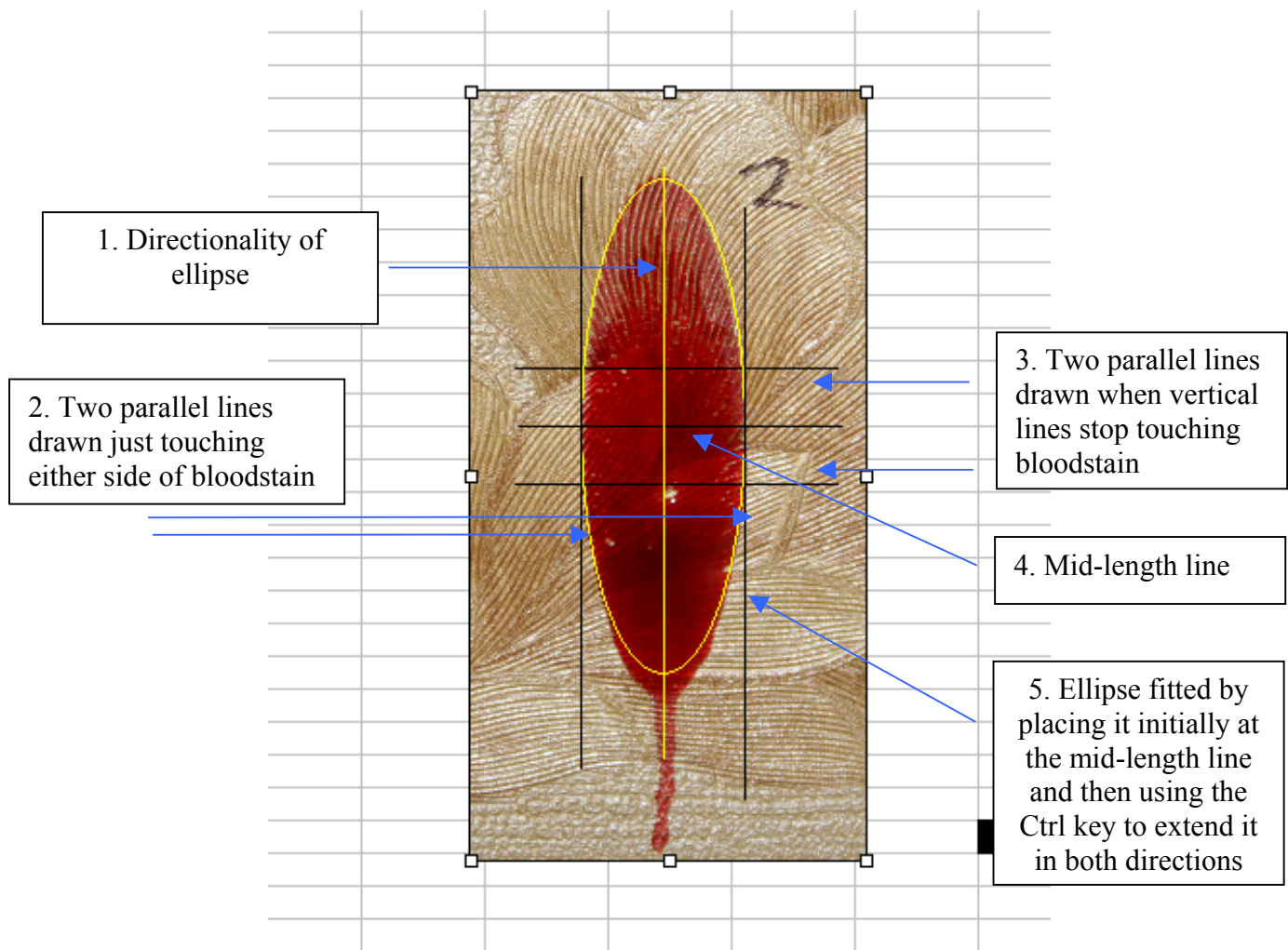


Figure 5.3 Fitting an ellipse to a bloodstain in Microsoft® Excel 2000.

5.1.2.2 Microsoft® Office Visio® Professional 2003

When using Microsoft® Office Visio® Professional 2003, a photograph was pasted into a 'blank drawing' without altering any of the proportions of the bloodstain (Fig. 5.4).

- An ellipse was then fitted to the bloodstain so that it fitted well around the leading end of the bloodstain (approximately the front third) and the fit around the other end was just left as it was.
- The angle of impact was subsequently calculated from the 'size and position' table shown on the drawing page (Fig. 5.5).

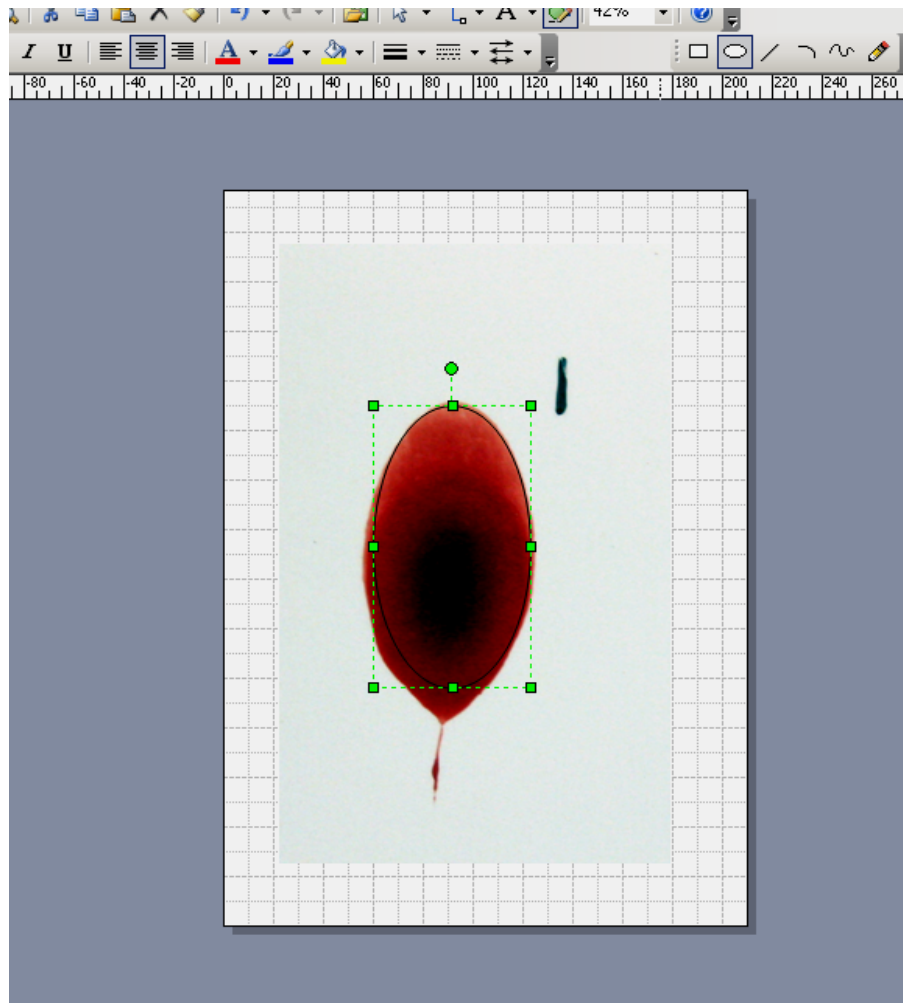


Figure 5.4 Fitting of an ellipse to a bloodstain in Microsoft® Office Visio® Professional 2003.

Size & Positi...	X	91.5 mm
	Y	155.5 mm
	Width	63 mm
	Height	109 mm
	Angle	0 deg
X	Pin Pos	Center-Cent

Figure 5.5 Size and position table in Microsoft® Office Visio® Professional 2003.

5.1.2.3 BackTrack™/Images

When using BackTrack™/Images, a photograph is opened and the initial step is to calibrate it. This meant that a scale had to be included in the image.

- After calibration had been carried out and various details such as the position of the bloodstain on the surface has been input, the gamma and alpha angles were calculated.
- The gamma angle is simply determined by indicating the direction of a vertical line (included in image) and the directionality of the bloodstain.
- Alpha was then determined by pulling the mouse along the bloodstains width at approximately the mid-length (Fig. 5.6). The mouse was then clicked at the leading edge of the bloodstain resulting in the appearance of a dotted ellipse (Fig. 5.7).
- The ellipse could then be edited manually using the 'fitting the ellipse' box or it could be accepted and the alpha value produced (Fig. 5.8). The ellipse was manually edited if it was deemed necessary due to an ellipse being fitted poorly. An ellipse was said to be a good fit when it fit the leading edge of the bloodstain well.

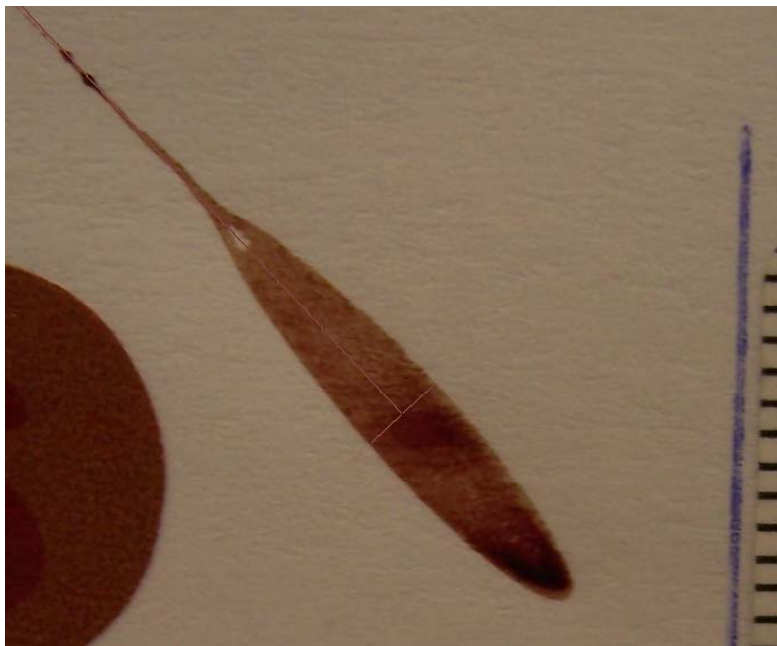
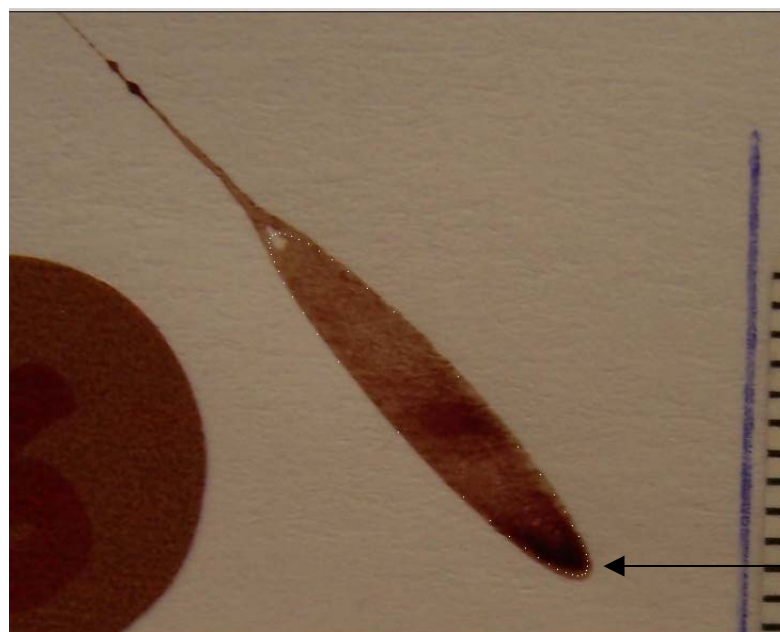


Figure 5.6 Pulling the mouse across the bloodstains width at the approximate mid-length in BackTrack™/Images.



Mouse is
clicked here

Figure 5.7 Clicking the mouse at the leading edge of the bloodstain reveals a dotted ellipse in BackTrack™/Images.

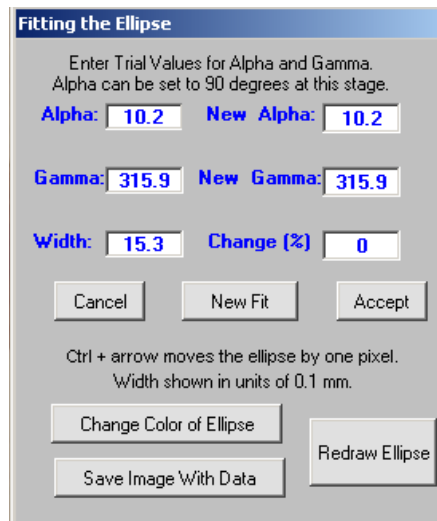


Figure 5.8 Manual ellipse editing function in BackTrack™/Images.

5.1.2.4 STABS

STABS is a computer programme developed at the Institute for Environmental Research and Science Limited³ (ESR).

- When using STABS to calculate the angle of impact a photograph of the bloodstain was opened in the main screen and an ellipse fitted to the bloodstain by clicking on the draw ellipse function and dragging the mouse along the long axis (Figures 5.9 and 5.10).
- An ellipse was then shown on the bloodstain and it could be adjusted using the slide bars and arrows. The angle of impact value was shown on the main screen and was recorded for each bloodstain.

The requirements that were needed to get STABS to the stage that it was capable of performing these functions were reported to the software developers within ESR and the changes were made.

³ ESR Ltd, 27 Creyke Road, Ilam, Christchurch, New Zealand

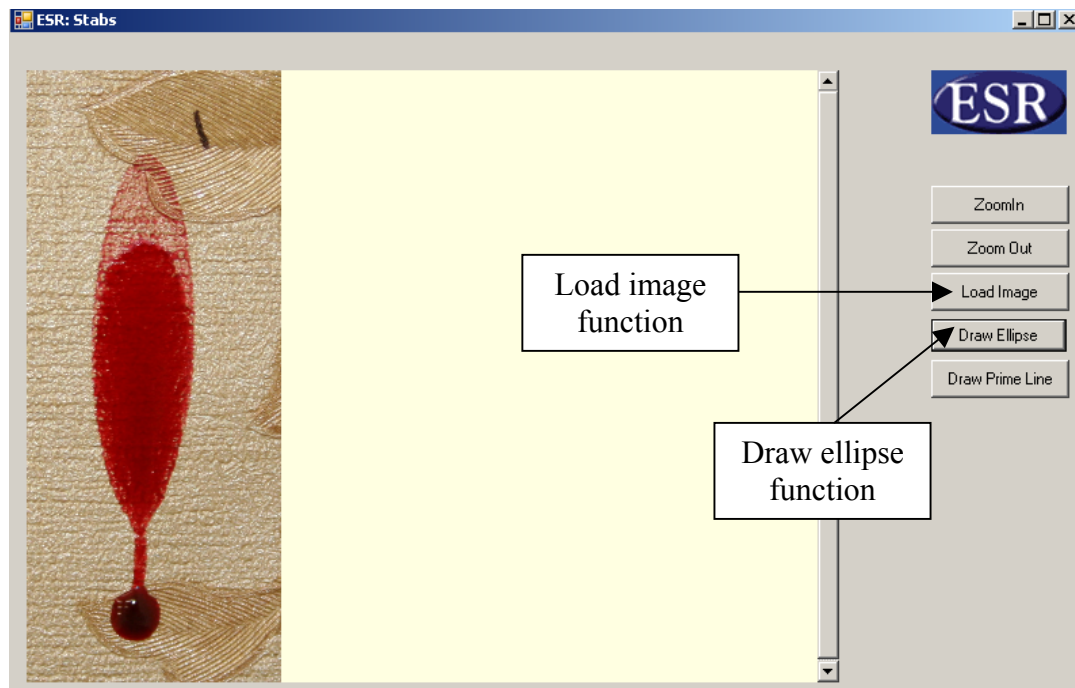


Figure 5.9 The main screen of STABS with a bloodstain loaded and ready for an ellipse to be fitted.

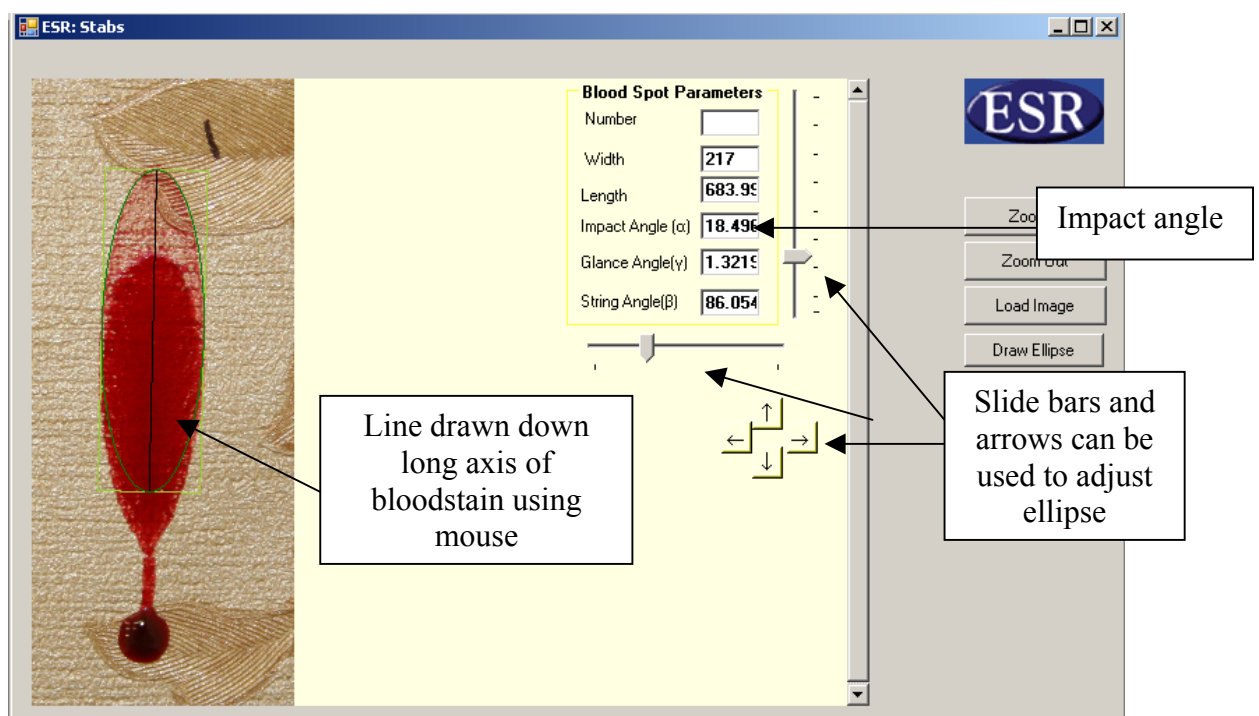


Figure 5.10 The main screen of STABS showing an ellipse fitted to a bloodstain and the slide bars and arrows that allow the ellipse to be adjusted.

5.1.3 Results

Figures 5.11 and 5.12 show the observed minus expected value, calculated using the four different methods, plotted against the actual angle of impact at 20°, 30°, 40°, 60° and 80 ° for wood and cardboard. The standard deviation is also plotted on the graphs.

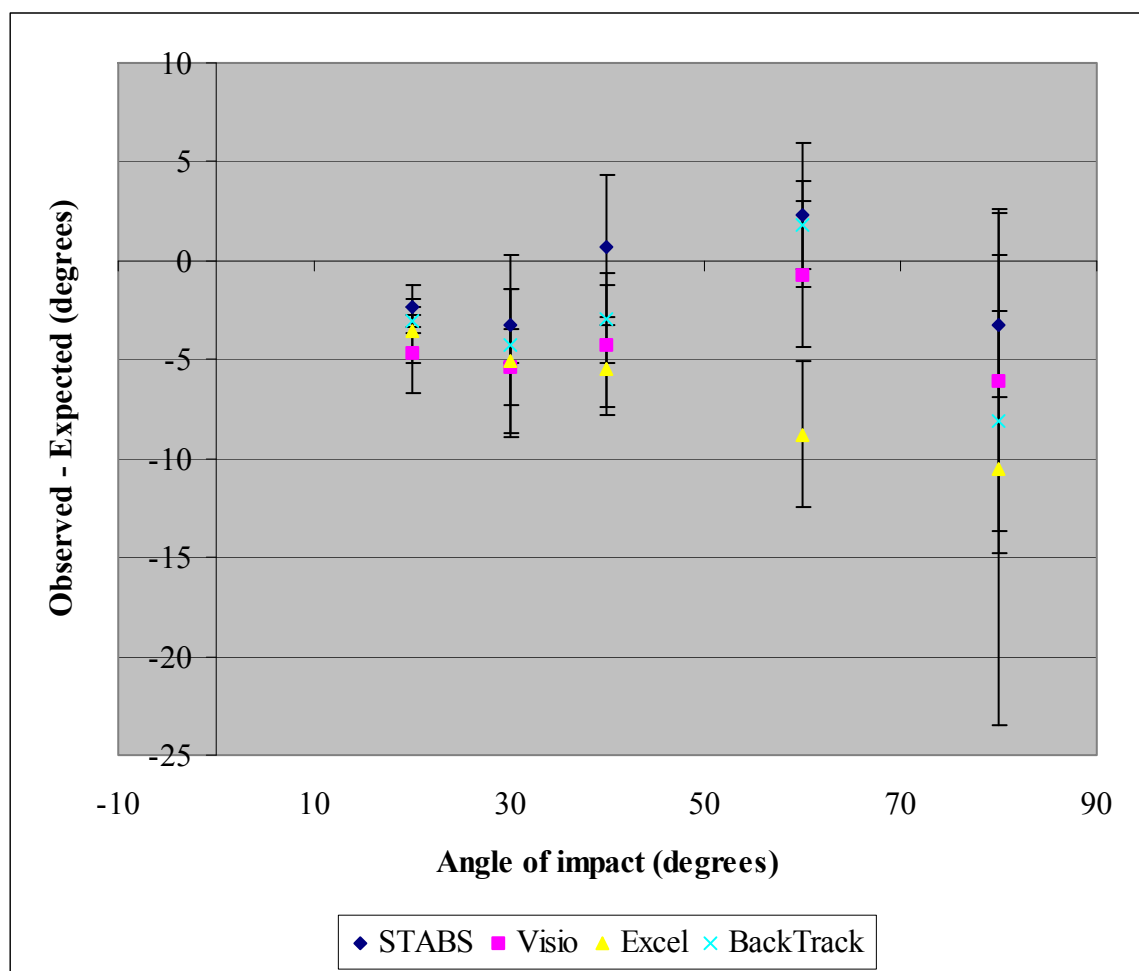


Figure 5.11 The observed minus expected angle of impact calculated using four different methods plotted against the angle of impact at 20°, 30°, 40°, 60° and 80 ° for bloodstains formed on wood. The standard deviation is also plotted on the graph.

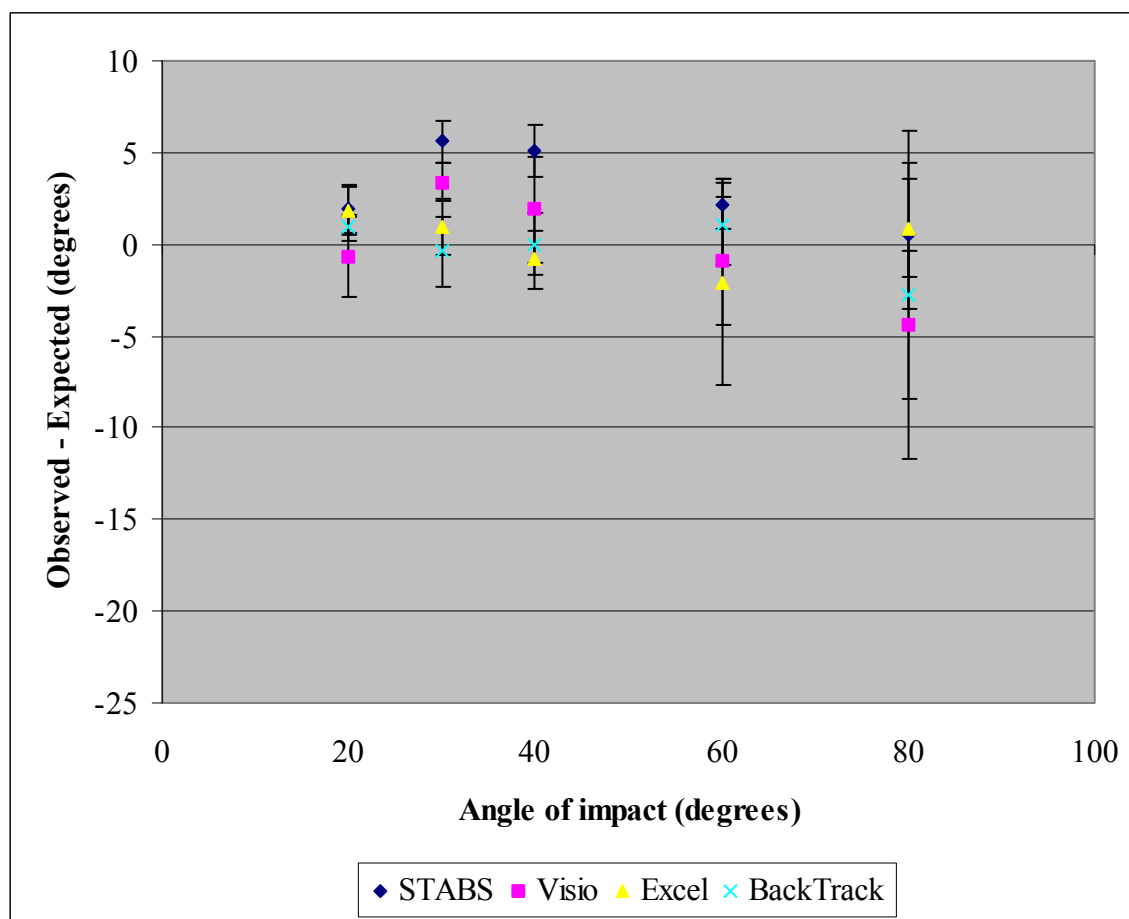


Figure 5.12 The observed minus expected angle of impact calculated using four different methods plotted against the angle of impact at 20°, 30°, 40°, 60° and 80 °for bloodstains formed on cardboard. The standard deviation is also plotted on the graph.

5.1.4 Discussion and conclusion

Microsoft® Excel 2000 was a time consuming method to use for fitting an ellipse to a bloodstain. One of the major problems was that the ellipse could not be fitted on an angle meaning that if the bloodstain was not completely straight in the photograph, the ellipse would be on a slight angle. This made it difficult to fit the ellipse well to the perimeters of the bloodstain.

The only times an ellipse needed to be manually adjusted was when the width was overestimated and when the angle of impact was close to 90°. In these cases the ellipse was made larger or smaller so it fitted the bloodstain as required. One of the advantages of using Microsoft® Excel 2000 was that all ellipses could be saved so that they could be accessed later. This could be useful when an analyst is unable to analyse all of the data at one time.

Microsoft® Office Visio® Professional 2003 was a very efficient method to use. An ellipse could be drawn with a mouse onto a bloodstain and the angle of the ellipse altered to suit the directionality of the bloodstain. The width and length of the ellipse were given in a 'size and position' table meaning that the angle of impact had to be calculated by the user. This is particularly useful however when experiments are being carried out involving the determination of the angle of impact when the actual angle is known. It means that the results are non-biased.

BackTrack™/Images was quite a time consuming method to use for fitting an ellipse to a bloodstain. The reason for this is that the program is designed to be used for determining a region of origin, not just determining an angle of impact. It requires a calibration step to be carried out before the ellipse fitting procedure can begin. As calibration is not required for the angle of impact determination (as this is just a ratio of the width and length of the bloodstain) this is a unnecessary step. The gamma angle is then specified in a 2-step process. This angle could be calculated from the ellipse that is fitted to the bloodstain instead of adding this extra step. The program also requires that XY and Z coordinates are input prior to beginning the ellipse fitting procedure. This is good if BackTrack™ is going to be used for the entire region of origin analysis however if the analyst is just determining the angle of impact of bloodstains these initial steps waste a lot of time. Overall the ellipse fitting process is easy to do however because BackTrack™ is designed to be used for a region of origin analysis it is not the best method to use for simply determining the angle of impact.

STABS was the quickest method for fitting an ellipse out of the four tested in this experiment. It simply involved opening an image of a bloodstain and very easily fitting an ellipse. The angle of impact was then displayed on the screen. The program did not involve any unnecessary steps such as putting in coordinates or determining gamma, making it the easiest to use.

The average observed minus expected value was always within $+9^\circ$ and -11° when Microsoft® Excel 2000 was used to fit an ellipse to a bloodstain. At acute angles this value was much smaller, within about $\pm 6^\circ$ and as the angle of impact increased so did the observed minus expected value. The standard deviation increased as the angle of impact increased.

The average observed minus expected value was always within $+ 4^{\circ}$ and $- 8^{\circ}$ when Microsoft® Office Visio® Professional 2003 was used to fit an ellipse to a bloodstain. At acute angles this value was much smaller, within about $\pm 6^{\circ}$ and as the angle of impact increased so did the observed minus expected value. The standard deviation increased as the angle of impact increased.

The average observed minus expected value was always within $+ 3^{\circ}$ and $- 8^{\circ}$ when BackTrack™/Images was used to fit an ellipse to a bloodstain. At acute angles this value was much smaller, within about $+ 2^{\circ}$ and $- 5^{\circ}$ and as the angle of impact increased so did the observed minus expected value. The standard deviation increased as the angle of impact increased.

The average observed minus expected value was always within $+ 7^{\circ}$ and $- 3^{\circ}$ when STABS was used to fit an ellipse to a bloodstain. At acute angles this value was much smaller, within about $+ 6^{\circ}$ and $- 2^{\circ}$ and as the angle of impact increased so did the observed minus expected value. The standard deviation increased as the angle of impact increased.

Overall all of the methods used in this experiment produced an average observed minus expected value within the range of about $\pm 10^{\circ}$. At acute angles this range was much smaller, within $\pm 6^{\circ}$. All of the methods produced relatively similar results showing that any computer based method for calculating the angle of impact will produce approximately the same result. Bevel and Gardner state that ‘as a general rule the angle indicated is probably accurate to within 5° to 7° ’ [30]. The results from this study are consistent with this range.

STABS was the easiest program to use as it did not require unnecessary steps to be carried out before the angle of impact analysis could begin, as was the case with BackTrack™/Images. Microsoft® Office Visio® Professional 2003 was easy to use and was identified as being particularly useful for studies involving the calculation of the angle of impact when the actual angle was known. Microsoft® Excel was the most time consuming method to use and considering the results were no more accurate than those of the other programs it would not be recommended for use when determining the angle of impact.

In conclusion every method used in this experiment had both positive and negative aspects that made more or less suited for determining the angle of impact. The results were relatively similar for each program meaning that the best method to use should be based on the requirements of the analyst. STABS and BackTrack™ are both packages designed for calculating the angle of impact and while Microsoft® Office Visio® Professional 2003 and Microsoft® Excel 2000 are not. This study shows that any of the methods is acceptable for calculating the angle of impact and the easily available Microsoft programs could be used to calculate the angle of impact even when a manual method is being used to determine the region of origin.

Based on the results of this study, Microsoft® Office Visio® Professional 2003 will be used for subsequent experiments that require the angle of impact to be calculated when the true angle is known. This will ensure that the results are non-biased.

5.2 The effect of target surface

5.2.1 *The effect of different target surfaces on the angle of impact estimation*

5.2.1.1 Introduction

The influence of surface type on the formation of bloodstains is an important consideration when investigating reasons for errors in region of origin calculations.

There are a vast number of surfaces that an impact pattern may be found on at a crime scene and it is imperative any effect that the surface type has on the impact angle estimation is known. If the surface type does however influence this calculation it is important that this can be accounted for when carrying out a region of origin analysis.

It is expected that there will always be some random measurement error involved with an angle of impact estimation. This is because the estimation involves both the fitting of an ellipse to a bloodstain and the measurement of the width and length of that ellipse. The angle of impact determined by an analyst can therefore never be expected to be completely precise. It is however important to ensure that particular variables, such as target surface, do not systematically affect the accuracy of this calculation.

Janes [26] investigated the effect of different target surfaces on the calculation of impact angle in an attempt to explain a consistent underestimation of the calculated angle of impact found in experimental results. The underestimation of the angle of impact was found to be independent of the surface type. The difference in angle of impact results between different target surfaces was not compared in the study.

The objective of this experiment was to determine whether the surface upon which an impact pattern exists affects the amount of error involved in an angle of impact calculation.

5.2.1.2 Method

The data from the bloodstains generated in section 5.1 was used in this section. The details of how the bloodstains were generated can be found in Section 5.1.2. The data

was analysed in Microsoft® Office Visio® Professional 2003 and the average difference between the observed and expected angle was calculated for each target surface and the results plotted on individual graphs.

Finally Student's t-test was carried out to determine if the means of the angle of impact results were statistically different from each other for different surfaces at each angle of impact.

5.2.1.3 Results

Examples of the photographs that were taken of the bloodstains on each of the six different surfaces are found in Figures A2-1 – A2-5 of Appendix 2 for 20° – 80° respectively.

The average impact angle was calculated Microsoft ® Office Visio ® Professional 2003 for each angle and surface and the results can be found in Tables A2-1 – A2-5 of Appendix 2 (the raw data is also given in Appendix 2).

The observed minus expected impact angles were calculated for every bloodstain on every surface. Figure 5.13 illustrates the average of these values and the actual angle of impact for each surface.

The angle of impact results for surfaces including cardboard, glass, tile and vinyl were closer to the actual angle of impact while the results for surfaces including wood and wallpaper were less accurate.

Figure 5.14 illustrates the standard deviations at each angle of impact for each surface for results generated Microsoft ® Office Visio ® Professional 2003. The standard deviation increased as the angle of impact increased.

Tables 5.2 – 5.6 show the results of Student's t-test carried out to determine if there was a significant difference in the angle of impact results for different surfaces.

The t-test shows that at impact angles of 20°, 30° and 40° there was a systematic significant difference between angle of impact results for a number of surfaces. This systematic difference is not however seen at impact angles of 60° and 80°.

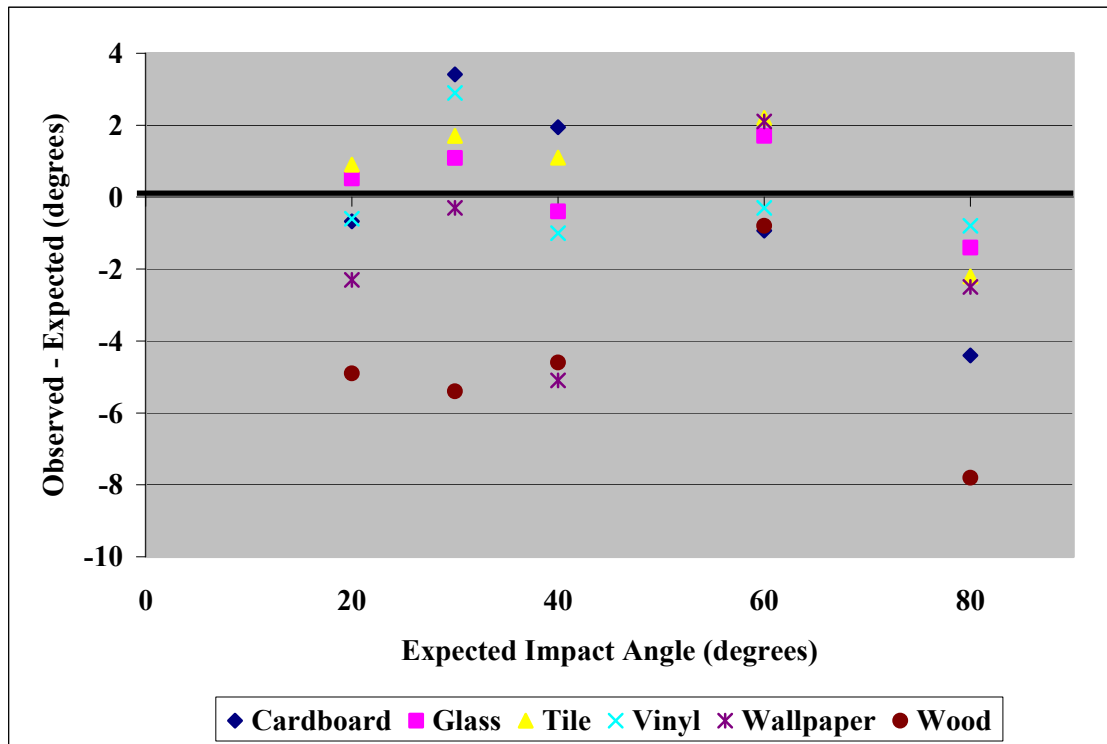


Figure 5.13 The error in the angle of impact calculation at varying impact angles. Results were determined using Microsoft® Office Visio® Professional 2003.

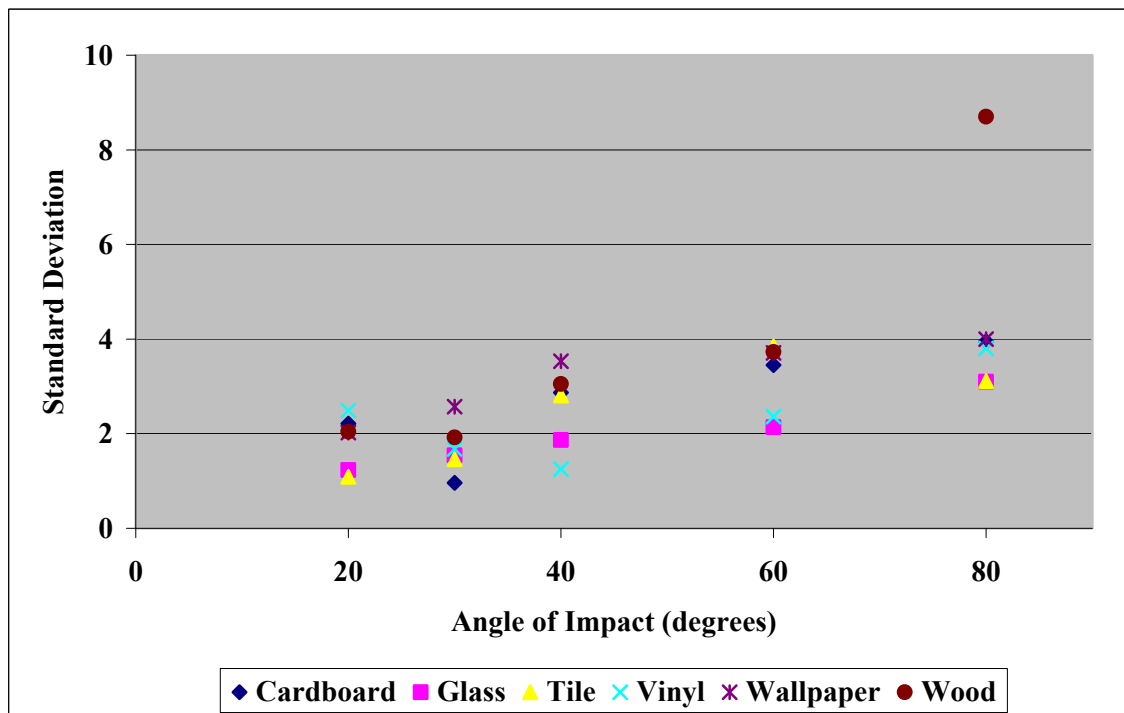


Figure 5.14 The standard deviation of the calculated angle of impact increased with the angle of impact.

5.2.1.3.1 Student's *t* test results

In Tables 5.2 – 5.6, the bold cells represent $P < 0.05$ (there is a significant difference between the results of the two surfaces). All values given here were calculated in Microsoft® Excel 2000 from data generated in Microsoft® Office Visio® Professional 2003. The results of the *t*-test are given to 4 decimal places unless the value was less than 0.0001. In this situation the number is given as < 0.0001 .

Table 5.2 Student's *t*-test results for the angle of impact of bloodstains created on different surfaces at 20 degrees.

	Cardboard	Glass	Tile	Vinyl	Wallpaper	Wood
Cardboard	X	X	X	X	X	X
Glass	0.1468	X	X	X	X	X
Tile	0.0675	0.4580	X	X	X	X
Vinyl	0.8727	0.4408	0.1309	X	X	X
Wallpaper	0.2215	0.0359	0.0045	0.1322	X	X
Wood	0.0010	0.0005	0.0005	0.0342	0.0926	X

Table 5.3 Student's *t*-test results for the angle of impact of bloodstains created on different surfaces at 30 degrees.

	Cardboard	Glass	Tile	Vinyl	Wallpaper	Wood
Cardboard	X	X	X	X	X	X
Glass	0.0736	X	X	X	X	X
Tile	0.0476	0.5264	X	X	X	X
Vinyl	0.3790	0.0273	0.1737	X	X	X
Wallpaper	0.0231	0.3964	0.0150	0.0405	X	X
Wood	< 0.0001	< 0.0001	0.0003	< 0.0001	0.0110	X

Table 5.4 Student's *t*-test results for the angle of impact of bloodstains created on different surfaces at 40 degrees.

	Cardboard	Glass	Tile	Vinyl	Wallpaper	Wood
Cardboard	X	X	X	X	X	X
Glass	0.0736	X	X	X	X	X
Tile	0.7547	0.0637	X	X	X	X
Vinyl	0.0511	0.1929	0.0348	X	X	X
Wallpaper	0.0292	0.0348	0.0179	0.0432	X	X
Wood	0.0015	0.0213	0.0051	0.0503	0.9817	X

Table 5.5 Student's t-test results for the angle of impact of bloodstains created on different surfaces at 60 degrees.

	Cardboard	Glass	Tile	Vinyl	Wallpaper	Wood
Cardboard	X	X	X	X	X	X
Glass	0.1427	X	X	X	X	X
Tile	0.2386	0.9377	X	X	X	X
Vinyl	0.4640	0.2810	0.2974	X	X	X
Wallpaper	0.1216	0.6521	0.6868	0.3356	X	X
Wood	0.9144	0.2193	0.4065	0.5659	0.2704	X

Table 5.6 Student's t-test results for the angle of impact of bloodstains created on different surfaces at 80 degrees.

	Cardboard	Glass	Tile	Vinyl	Wallpaper	Wood
Cardboard	X	X	X	X	X	X
Glass	0.0380	X	X	X	X	X
Tile	0.2293	0.2959	X	X	X	X
Vinyl	0.1105	0.8263	0.3766	X	X	X
Wallpaper	0.2556	0.4272	0.8200	0.4130	X	X
Wood	0.6506	0.0321	0.3888	0.0503	0.2980	X

5.2.1.4 Discussion

Figure 5.13 shows that the angle of impact value for surfaces including cardboard, glass, tile and vinyl was closer to the actual angle of impact compared to the results for surfaces including wood and wallpaper.

Based on the general description of these surfaces given in Table 5.1 the surfaces that produced the most accurate results have similar characteristics and the surfaces that produced the more inaccurate results have similar characteristics. The surfaces that produced the most accurate results were smooth and had relatively glossy surfaces. The surfaces that produced the least accurate results were rough (textured) and did not have glossy surfaces. Where necessary in the discussions that follow about the difference in angle of impact results for different surfaces, the surfaces that produced the most accurate results (cardboard, glass, tile and vinyl) will be referred to as smooth/glossy and the surfaces that produced the least accurate results (wood and wallpaper) will be referred to as textured/non-glossy. These terms do not take into account all of the characteristics that may be responsible for the results seen in this study and a recommendation for the characterisation of different surfaces will be

made in the future directions chapter (Chapter 8). The reason for the results may for example be a result of the absorptivity of the surfaces. The smooth and glossy surfaces would be less absorptive than the textured and non-glossy surfaces.

The two-sample Student t -test is used to compare the means of small samples as a means of determining confidence intervals related to the whole data populations. T -test values are calculated according to independent variables p , or probability, and df , degrees of freedom. For this experimentation, the standard p value of 5% was used. Student's t -test showed that at impact angles of 20, 30 and 40 degrees, there was a systematically significant difference between angle of impact results for smooth/glossy and textured/non-glossy surfaces. This systematic difference was not seen at impact angles of 60 and 80 degrees or within smooth/glossy and textured/non-glossy surfaces alike.

When fitting ellipses to bloodstains on wood and cardboard, the perimeters of the bloodstain were hard to see making it hard to fit an ellipse accurately. Fitting an ellipse to a bloodstain on a smooth/glossy surface was much easier because the perimeter of the bloodstain was well defined. This may be a factor that is contributing to the significant difference between the angle of impact calculated for smooth/glossy and textured/non-glossy surfaces.

This difference could also be due to the way in which the blood interacts with the target surface. Similar surfaces such as glass and tile gave similar angle of impact results. Surfaces that were dissimilar, (such as the smooth/glossy cardboard and the grainy wood) gave very different angle of impact results. There was up to 26% difference in the angle of impact calculation for these two surfaces. The way in which the blood collapses onto the surface may be influenced by the surface texture. This theory required further research and is investigated using high-speed camera photography in Section 5.4.

The standard deviation increased as the angle of impact increased (Fig. 5.14). It has been shown that bloodstains that impacted a surface at an angle greater than 60° have a large uncertainty involved with them [18]. This is primarily because of the uncertainties in the width and length measurements. The increase in standard deviation was therefore consistent with past studies.

In a study carried out investigating difficulties in the determination of the angle of impact of blood droplets on fabric, it was found that bloodstains observed on highly absorbent materials exhibited the greatest degree of distortion and would not be suitable for angle of impact determinations [32]. These fabrics included 100 % silk, 100 % polyester and 60 % rayon/ 40 % polyester.

Another observation was that bloodstains that impacted 100 % acrylic fabrics at an acute angle were near circular in appearance. That type of bloodstain could be misinterpreted as impacting the fabric near to perpendicular. Fabrics with poor absorbency properties were also found to cause this effect. This was due to a 'rolling effect', which occurred when the blood initially contacted the fabric. A final observation that was made in the study, relevant to the results of this study was the fact that the greater the coarseness of the texture of the fabric, the greater the distortion of the bloodstain. The blood droplet was found to conform to the prominent grain of the fabric.

The results of the aforementioned study are consistent with the results of this study. The more 'coarse' the surface, the more distorted the bloodstain was.

When a region of origin determination is made at a crime scene, a number of bloodstains are analysed from the wall or surface upon which the impact pattern exists. If the impact pattern is on a textured/non-glossy surface such as a wall covered with textured wallpaper, the angle of impact calculations may involve an uncertainty. This uncertainty has not yet been quantified for different surfaces and is not usually considered when making such calculations. The errors introduced in the angle of impact calculations may have a significant effect on the overall accuracy of the region of origin determination. It is therefore important that the uncertainties introduced when calculating the angle of impact on various surface types are determined so that the analyst can take this into consideration when presenting region of origin results.

5.2.1.5 Conclusions

It has been shown in this study that there is a significant error in an angle of impact calculation for surfaces that for the purposes of this research have been described as 'textured/non-glossy'. This may be due to a unique surface interaction occurring at the time the bloodstain forms on the surface, or it may simply be due to measurement

errors introduced because of the difficulties in deciphering the perimeters of the bloodstain.

Either way, errors in the calculation of the angle of impact will result in greater uncertainties in the region of origin determination than that of a determination made on a surface such as white cardboard. Future experiments may allow this uncertainty to be quantified permitting analysts to alter the region of origin uncertainty accordingly.

The interaction that occurs when blood impacts various target surfaces at different angles will be investigated with high-speed photography in section 5.4.

5.3 Surface wettability

5.3.1 Introduction

To further investigate the effect of different target surfaces on the formation of bloodstains, the contact angle of blood on different surfaces was determined.

It is given by the angle between the interface of the droplet and the horizontal surface (Fig. 5.15).

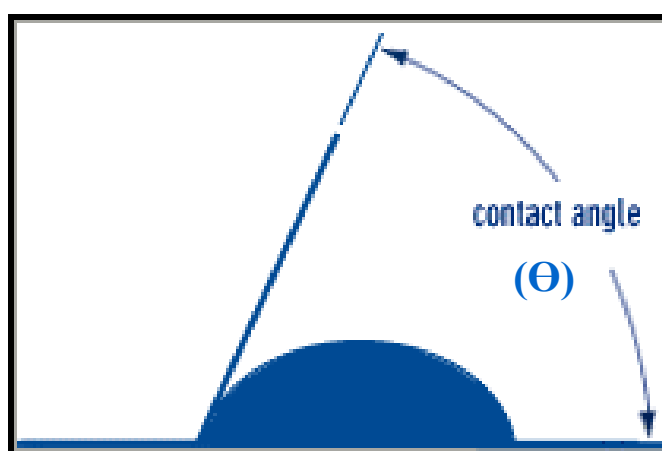


Figure 5.15 The contact angle (Θ) [33].

The interaction that occurs between blood and any surface is unique for that particular surface. It was seen in section 5.2 that textured/non-glossy surfaces exhibited a larger error in the angle of impact calculation compared to smooth/glossy surfaces. Determining the contact angle for blood on different surfaces may help to explain the difference in angle of impact results obtained with different surfaces.

Wetting studies have been carried about in order to investigate the solid-liquid relationship of various solids/liquids. These studies usually involve the measurement of the solid-liquid contact angle. The contact angle indicates the degree of wetting when a solid and liquid interact [34]. The smaller the contact angle the greater the wetting.

Bussmann *et al.* [35] presented the results of 2 scenarios: the impact of a 2 mm water droplet at 1 m/sec onto a 45° incline and of a similar impact of a droplet onto a sharp edge. It was found that what happens when a droplet strikes a surface is dependent on

a variety of factors including droplet size, impact velocity, the type of fluid and surface properties. In one of the scenarios, single droplets were formed by slowly pumping distilled water through a hypodermic needle until they detached under their own weight. The droplets were uniformly 2 mm in diameter. The velocity of the droplets was so low that they did not shatter upon impact. A photo was then taken of the impact event (Fig. 5.16). The contact angles and contact diameters were measured manually from enlarged photographs.

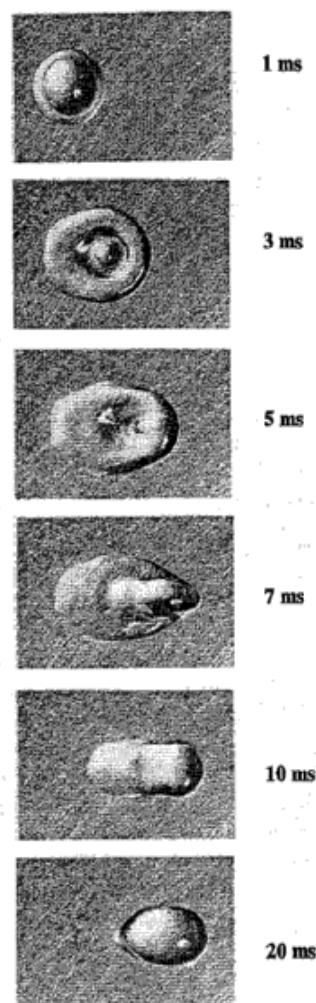


Figure 5.16 Normal view of the impact of a 2 mm diameter water droplet at 1 m/s onto a 45° stainless steel incline over a 20 ms period [35].

In a study carried out by Pasandideh-Fard *et al.* [36], water droplets were impacted at low velocity (so that they did not shatter on impact) on a flat, solid surface (stainless steel). The liquid-solid contact angle was then measured from a photograph of the droplet. A photograph with the measured contact angle is given in Figure 5.17.



Figure 5.17 Liquid-solid contact angle (θ) measurement from a photograph of a droplet of pure water 8.2 ms after impacting a stainless steel surface [36].

Ford *et al.* [37], looked at wetting in relation to the foliar spray applications of pesticides, which is governed by a number of factors including the extent to which the liquid wets and covers the foliage surface. It was found that when a drop impacts on a surface with negligible impact energy it will spread to an equilibrium position, which will be governed by the following equation (Formula 5.1). However when the impact energy is high, disintegration of the drop may occur (drop will “splash”).

$$F = R/r = \frac{[4\sin^3 \theta]^{1/3}}{(1 - \cos \theta)^2 (2 + \cos \theta)}$$

Where: R = radius of wetted area
 r = radius of initial drop
 θ = contact angle at the liquid/solid/air boundary

Formula 5.1 Impaction theory – spread factor.

The contact angle of blood on different surfaces has never been explored in relation to the formation of bloodstains and it is hoped that this research may assist in explaining why there is a larger error in the angle of impact calculation on some surfaces.

The objective of this experiment is to determine the contact angle of blood on a number of different surfaces and relate this angle to the results from section 5.2.

5.3.2 Method

A single drop of blood was released from a 3 ml plastic pipette onto a horizontal target surface. The blood was dropped from a vertical height of 1 cm to ensure that the droplet formed on the surface at minimum velocity. A photograph was taken of the droplet on the surface perpendicular to the vertical plane using a Canon EOS-1Ds digital camera (see Table 3.1 for specifications). Each photograph was transferred to a computer and Microsoft® Office Visio® Professional 2003 was used to determine the contact angle and diameter of the blood droplet. A description of the surfaces used in the experiment is given in Table 5.7.

Table 5.7 Summary of the different surfaces used in the experiment.

Surface	Description
Cardboard	A4 chlorine free cardboard (225gsm, Klippan Kaskad Boards)
Vinyl	Lightly coloured vinyl
Paper*	A4 tinted multi-functional board, 225gsm, Olympic, white
Wood	Oak with many large vesicles making it very rough
Glass	Clear plate of glass
Tile	White tile

*Different to the wallpaper used in the previous experiment (Section 5.2)

5.3.3 Results

Figures 5.18 to 5.29 show the blood droplets that were measured. A millimetre scale is shown in the images. Table 5.8 shows the contact angle and diameter of each blood droplet.



Figure 5.18 Photograph of a single blood droplet on cardboard.

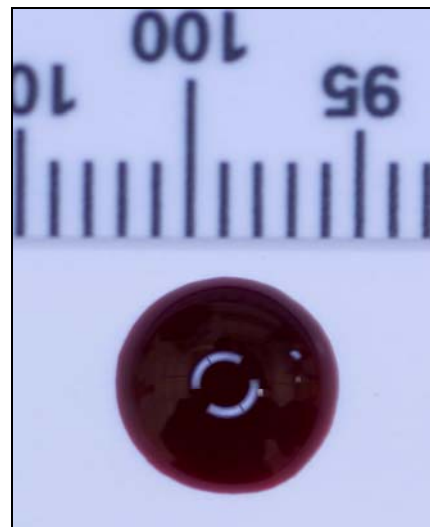


Figure 5.19 Diameter of a blood droplet on cardboard.

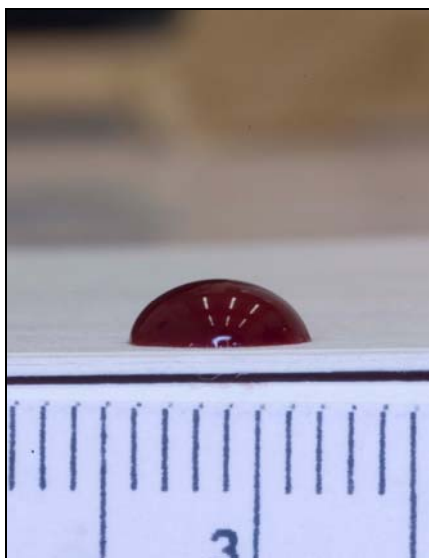


Figure 5.20 Photograph of a single blood droplet on paper.

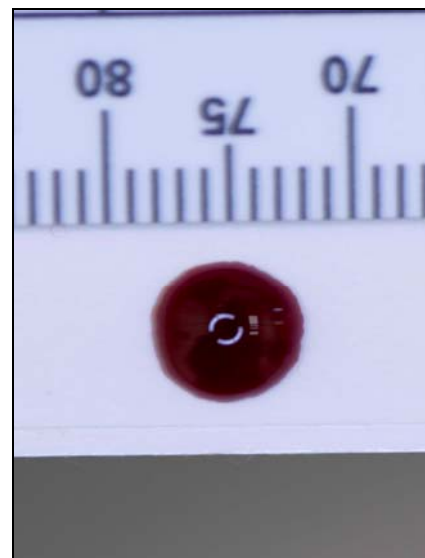


Figure 5.21 Diameter of a blood droplet on paper.

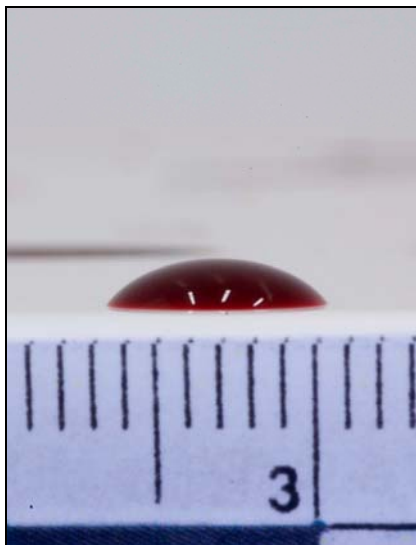


Figure 5.22 Photograph of a single blood droplet on tile.

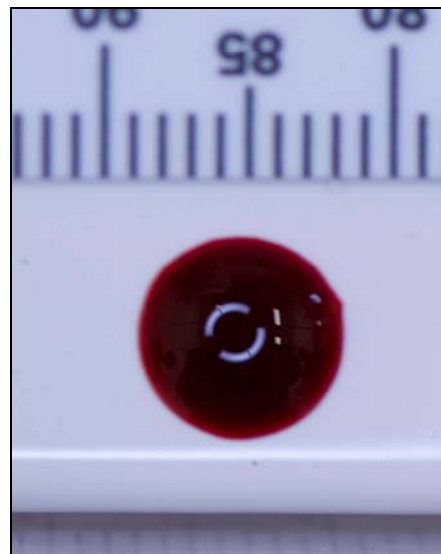


Figure 5.23 Diameter of a blood droplet on tile.

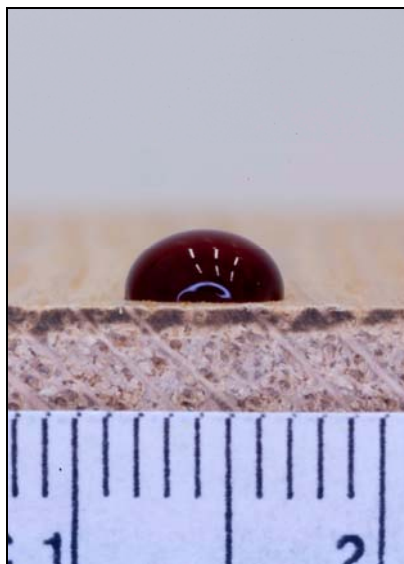


Figure 5.24 Photograph of a single blood droplet on wood.



Figure 5.25 Diameter of a blood droplet on wood.

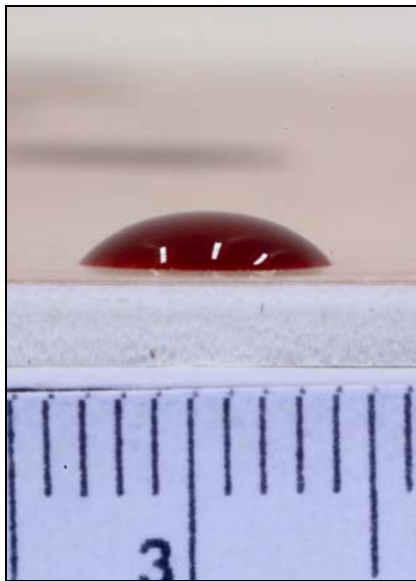


Figure 5.26 Photograph of a single blood droplet on vinyl.

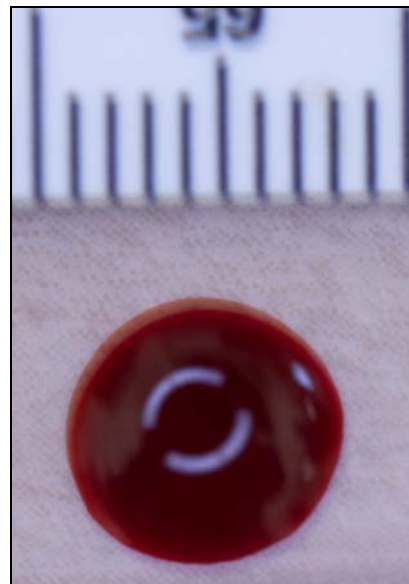


Figure 5.27 Diameter of a blood droplet on vinyl.

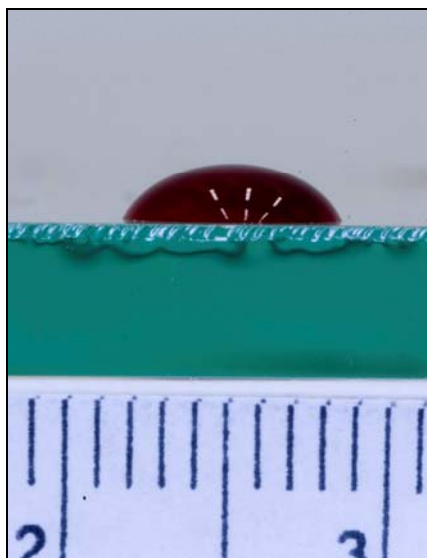


Figure 5.28 Photograph of a single blood droplet on glass.

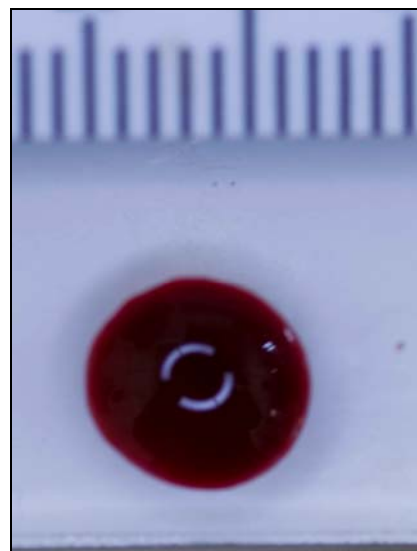


Figure 5.29 Diameter of a blood droplet on glass.

Table 5.8: The contact angle of a single droplet of blood on different surfaces.

	Contact angle	Diameter (mm)
Wood	87°	5.5
Paper	84°	6.0
Cardboard	72°	5.0
Glass	53°	6.5
Tile	44°	7.0
Vinyl	42°	7.0

5.3.4 Discussion and conclusion

On surfaces including the oak and paper the profile of the blood drop was a semi-circular shape resulting in a relatively large contact angle for these surfaces (Figures. 5.24 & 5.20). On tile, vinyl and glass the blood spread out more to form a semi-oval shape consequently producing a smaller contact angle (Figures 5.22, 5.26 & 5.28).

The results of the experiment carried out in Section 5.2 indicate that at acute angles, the angle of impact calculation is more accurate when blood impacts a smooth/glossy surface as opposed to a textured/non-glossy surface.

This study showed that when a blood drop impacted a smooth/glossy, non-absorbent surface, even at minimal velocity, it spread out immediately. The same did not happen for textured/non-glossy, absorbent surfaces. On the more absorbent surfaces the blood spread out less producing a greater contact angle. This shows that the type of surface a blood drop lands on affects the way in which the bloodstain forms. The results from experiment 5.2 therefore may have been due to the difference in the way a blood droplet spreads on different surfaces.

The trend found in this experiment was the smoother and less absorbent the surface the smaller the contact angle (i.e. the blood spread out more). In order to determine whether these results related to those in Section 5.2 a graph was plotted of the contact angle versus the observed minus expected angle of impact (O-E) calculated in this experiment. The observed minus expected angle of impact was calculated at 20, 30, 40, 60 and 80 degrees, however for this experiment the graphs were plotted using only

the results from the 30 and 80 degree impacts because at these angles there was a large spread of data (Figures 5.30 & 5.31). Because white paper was used in this experiment, instead of wallpaper, the results for these two surfaces were not plotted.

The graphs both show that as the contact angle decreases, O - E approaches zero, meaning the angle of impact estimation becomes more accurate. Overall the less textured, non-absorbent surfaces including glass, tile and vinyl all had a contact angle within about 10° of each other and they all gave relatively accurate angle of impact results (O - E was close to zero). Wood had the largest contact angle and the least accurate angle of impact result.

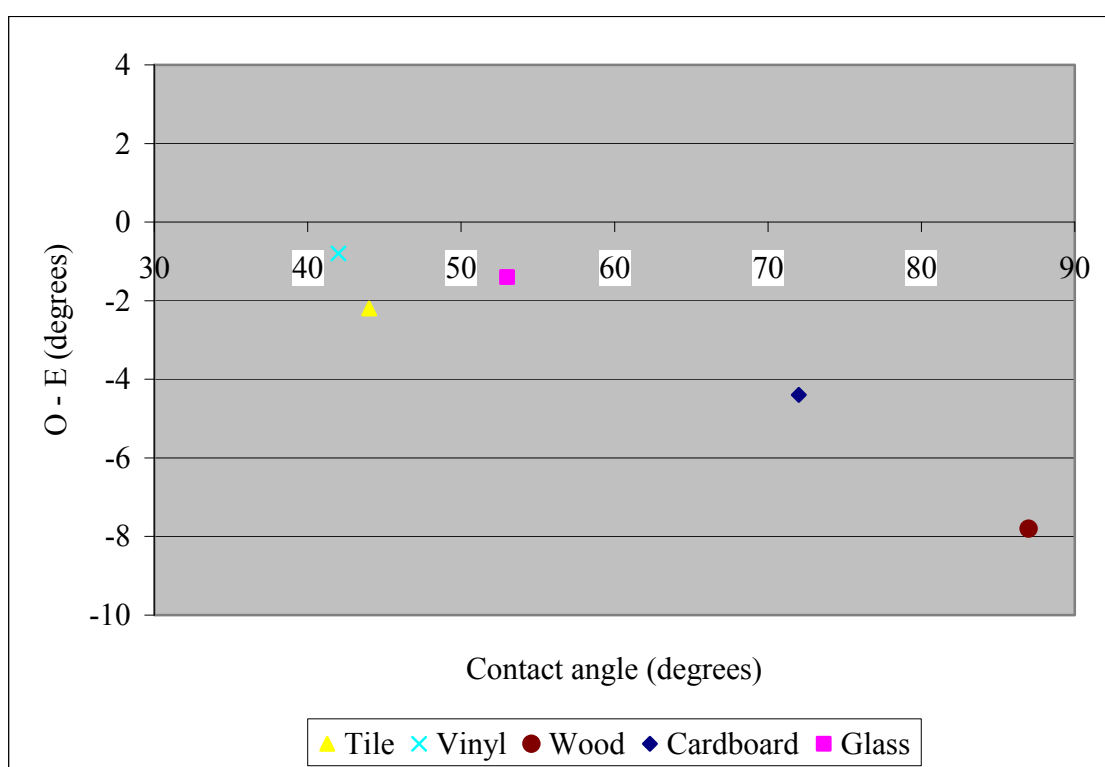


Figure 5.30 The observed minus expected angle of impact (determined using Microsoft Office Visio) versus the contact angle for five different surfaces (the impact angle was 30 degrees).

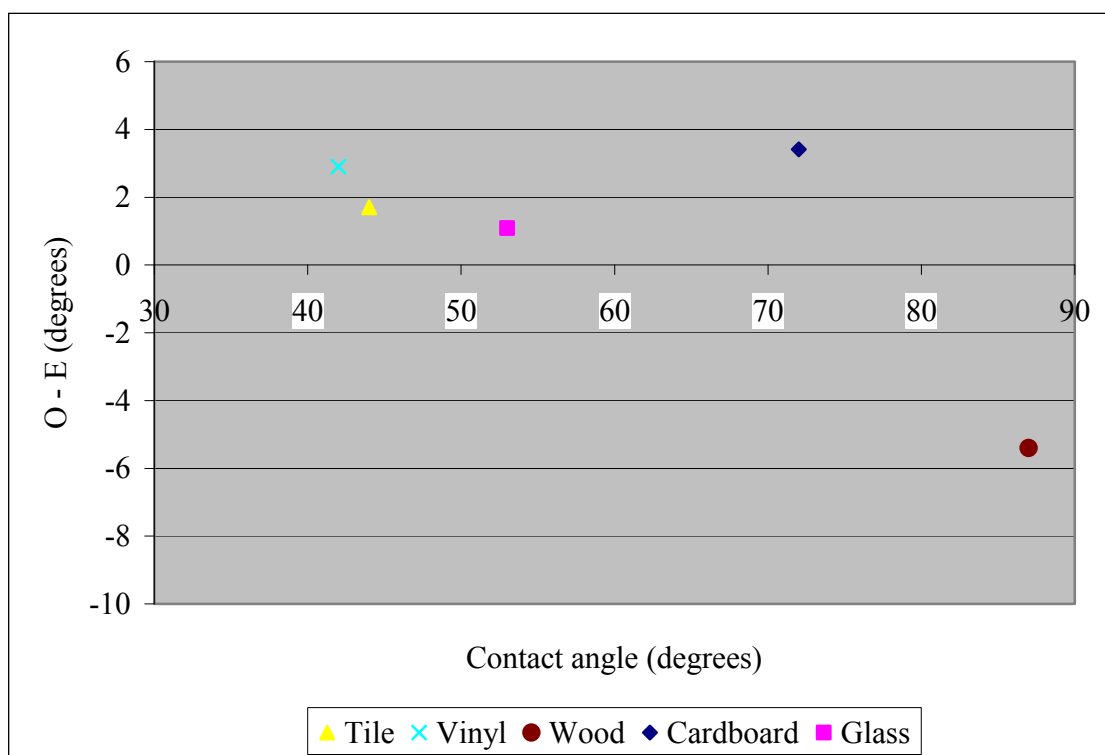


Figure 5.31 The observed minus expected angle of impact (determined using Microsoft Office Visio) versus the contact angle for five different surfaces (the impact angle was 80 degrees).

In conclusion the results of this study showed that when a single blood drop is released onto different surfaces at minimal velocity, the contact angle varies. Textured and more absorbent surfaces had a greater contact angle than that of smoother, non-absorbent surfaces. This indicates that the way in which blood interacts with these different surfaces is different. The use of high-speed photography may help to determine whether the unique surface interaction that occurs when a blood droplet impacts a surface is the cause of errors in the angle of impact calculation.

5.4 High-speed photography of blood drops impacting different target surfaces

5.4.1 Introduction

The results of the experiment carried out in section 5.1 showed that textured/non-glossy surfaces exhibited the greatest amount of error in the angle of impact calculation compared to smooth/glossy surfaces. At acute angles (20°, 30°, 40°) wood was the most inaccurate surface followed by wallpaper. This may be due to the way in which the bloodstains formed on the different surfaces and this experiment was carried out to allow a slow motion view of the formation bloodstains on various surfaces.

The objective of this experiment is to determine whether there is a difference in the way in which bloodstains form on smooth/glossy and textured/non-glossy surfaces and to document these differences.

5.4.2 Method

Two mirrors were set up so that the surface upon which the blood drop was being released onto could be viewed in two ways – front on and side on (See Fig. 4.6). A high-speed camera was then set up so that it was perpendicular to the surface (Fig. 5.32). One drop of blood was released from a plastic pipette, which was clamped 40 cm above the target surface, onto the surface, which was set at 30° to the vertical. The high-speed camera was used to record the blood drop impacting each surface at 1037 frames per second with an exposure time of 960 μ s. This process was repeated three times for each surface. The surfaces used in the experiment are given in Table 5.9. The width and length of the resulting bloodstains was measured for each surface.

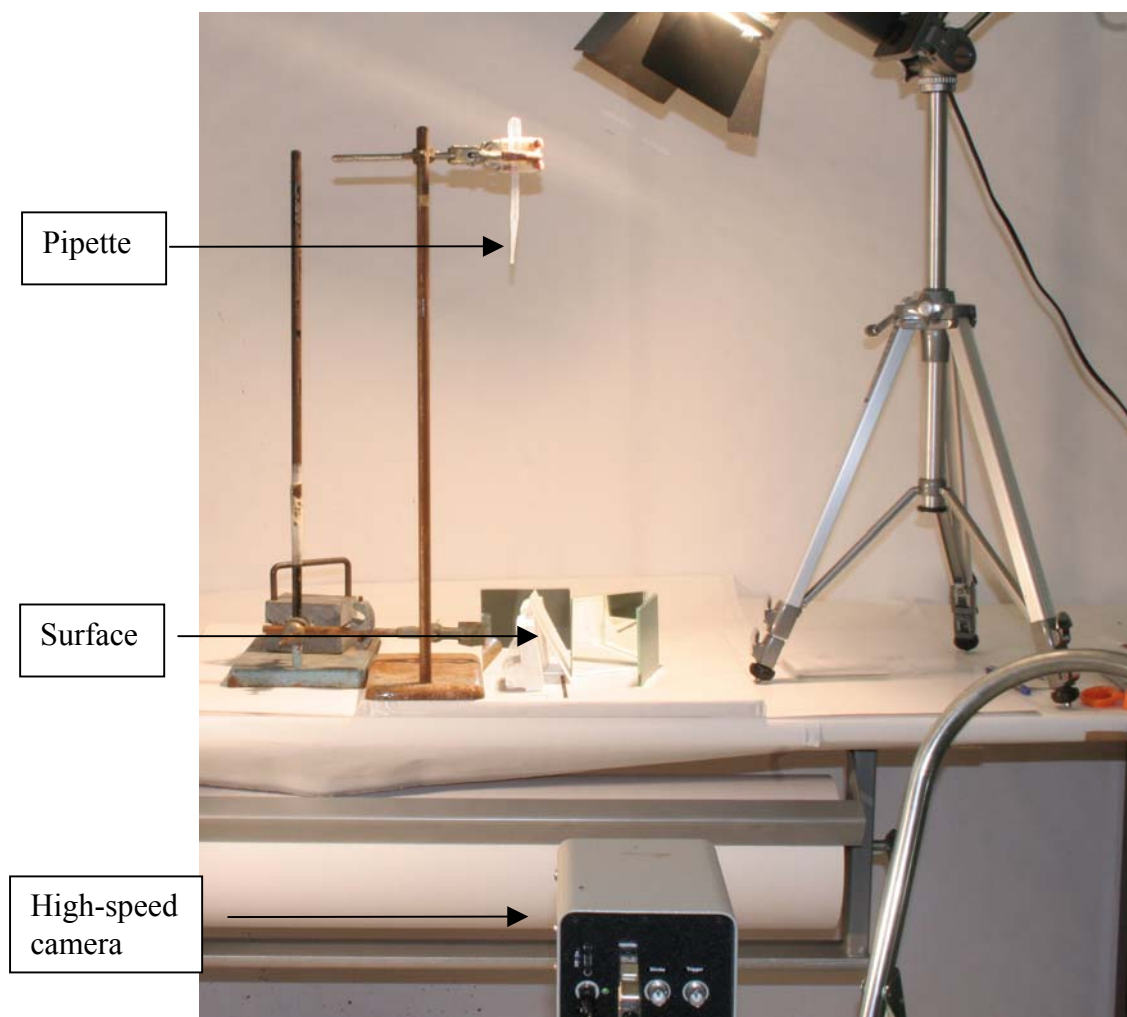


Figure 5.32 High-speed camera set-up.

Table 5.9 Summary of the different target surfaces.

Target Surface	Description
Cardboard	10 cm long x 5 cm wide A4 chlorine free cardboard (225gsm, Klippan Kaskad Boards)
Vinyl	10 cm long x 5 cm wide lightly coloured vinyl
Wallpaper	10 cm long x 5 cm wide textured, brown and gold wallpaper
Wood	10 cm ² oak

5.4.3 Results and discussion

Still images of a single blood drop impacting each target surface taken from high-speed videos are shown in Figures 5.34 – 5.45. Following these is a series of observations made from the videos along with a table showing the average width and length of the resulting bloodstains. The diameter of a blood drop prior to impacting the target surface was $4\text{ mm} \pm 0.5\text{ mm}$ (Fig. 5.33).

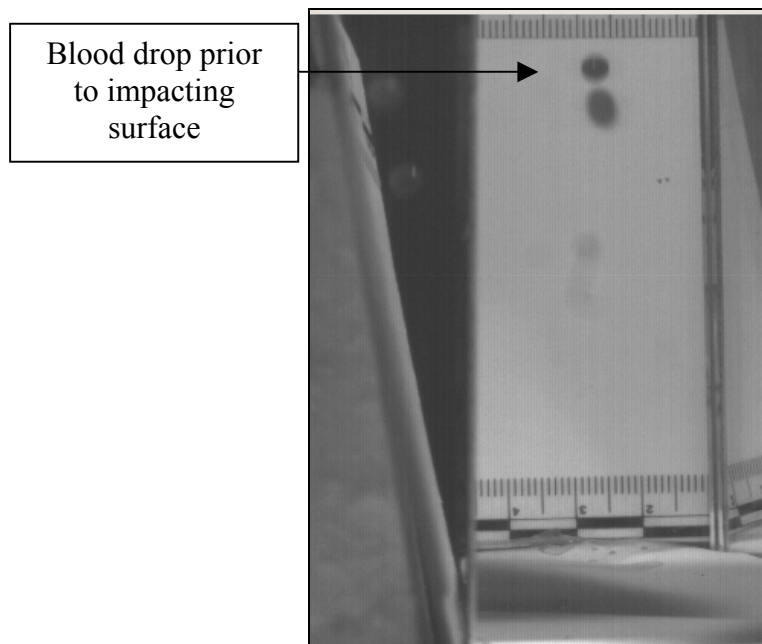


Figure 5.33 The width of a blood drop prior to impacting the target surface was 4 mm.

5.4.3.1 Cardboard

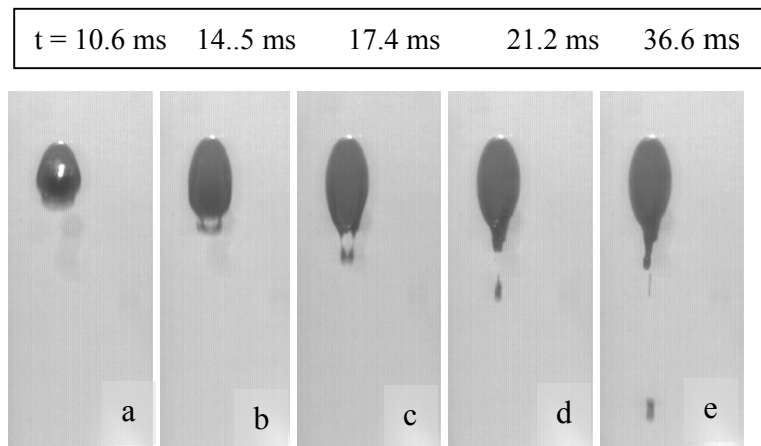


Figure 5.34 Still images taken from a high-speed video of a blood drop impacting a piece of cardboard at 30 degrees – front view.

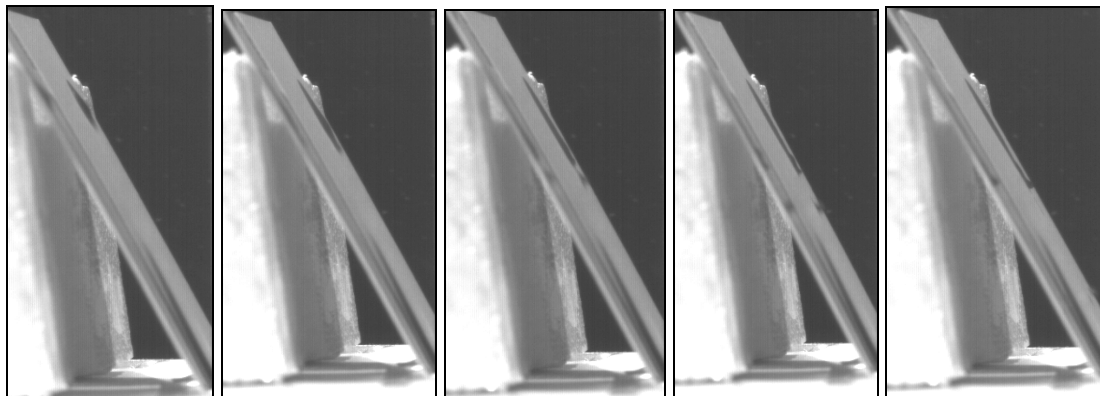


Figure 5.35 Still images taken from a high-speed video of a blood drop impacting a piece of cardboard at 30 degrees – side view.

- When the blood drop impacted the cardboard it began to flow over the surface (a).
- When the bloodstain was about half of its final size, wave cast-off began to form from both sides (b).
- These continued to be pushed out from the bloodstain and eventually merged to form a single wave cast-off (c,d).
- This finally landed on the cardboard surface below the bloodstain at a distance about the length of the bloodstain (e).
- There was a small pool of blood that sat at the bottom of the bloodstain, above the wave cast-off. A small amount of this blood ran down into the wave cast-off, elongating it and the resulting bloodstain appeared to have one ‘tail’ below the elliptical body (Fig. 5.30).

- The blood was continuously flowing in a downward direction.



Figure 5.36 The resulting bloodstain – cardboard.

Table 5.10 The width and length measurements and the calculated angle of impact of three bloodstains made on a cardboard surface. The actual impact angle was 30°.

Cardboard	1	2	3	Average
Width	10	10	9	9.7
Length	22	22	20	21.3
Calculated angle of impact (degrees)	27.0	27.0	26.7	27°

5.4.3.2 Vinyl

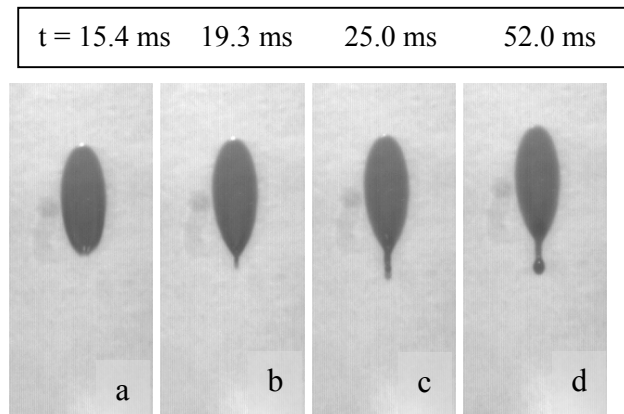


Figure 5.37 Still images taken from a high-speed video of a blood drop impacting a piece of vinyl at 30 degrees – front view.

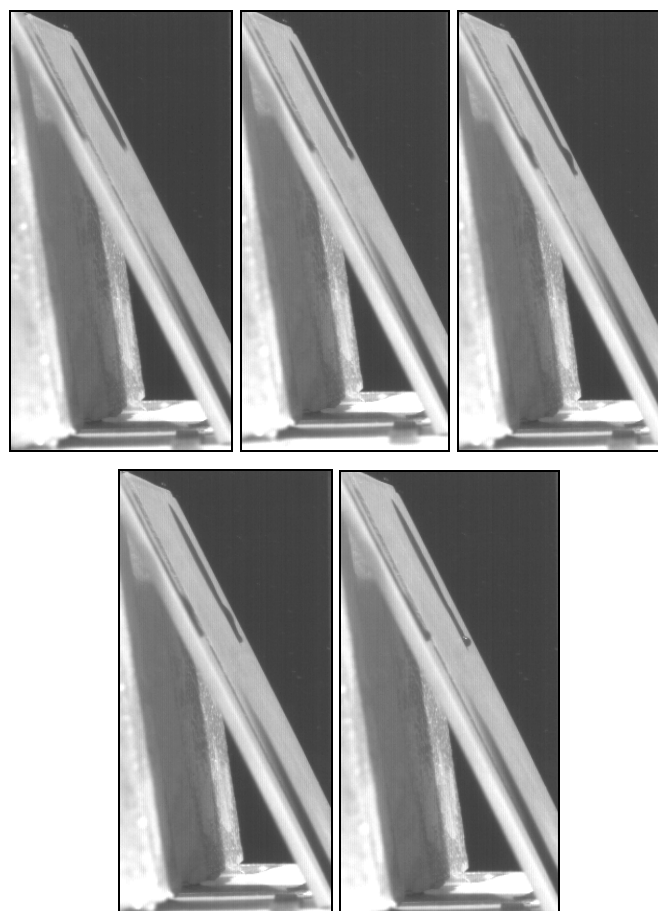


Figure 5.38 Still images taken from a high-speed video of a blood drop impacting a piece of vinyl at 30 degrees – side view.

- When the blood drop impacted the vinyl it began to flow over the surface (a).
- The blood continuously flowed downwards resulting in cast-off forming from the bottom of the bloodstain (c,d).
- The wave cast-off had a circular blood drop at the end of it (d).

- After the bloodstain formed, the blood from this drop began to run downwards, elongating the cast-off.
- The final bloodstain appeared very dilute and throughout the bloodstain and wave cast-off, there was a 'channel' through which the blood had travelled in a downward direction.

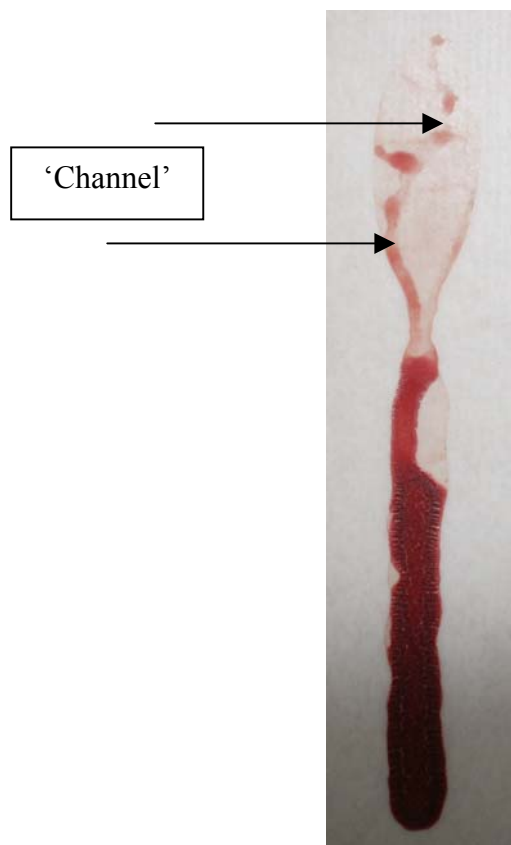


Figure 5.39 The resulting bloodstain – vinyl.

Table 5.11 The width and length measurements and the calculated angle of impact of three bloodstains made on a vinyl surface. The actual impact angle was 30°.

Vinyl	1	2	3	Average
Width	10	10	10	10
Length	22	23	23	22.7
Calculated angle of impact (degrees)	27.0	25.8	25.8	26°

5.4.3.3 Wallpaper

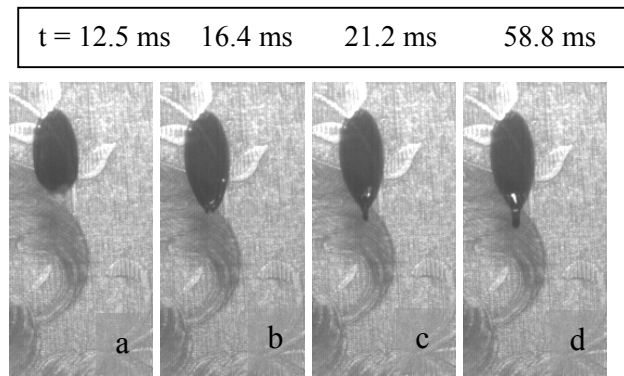


Figure 5.40 Still images taken from a high-speed video of a blood drop impacting a piece of wallpaper bound to cardboard at 30 degrees – front view.

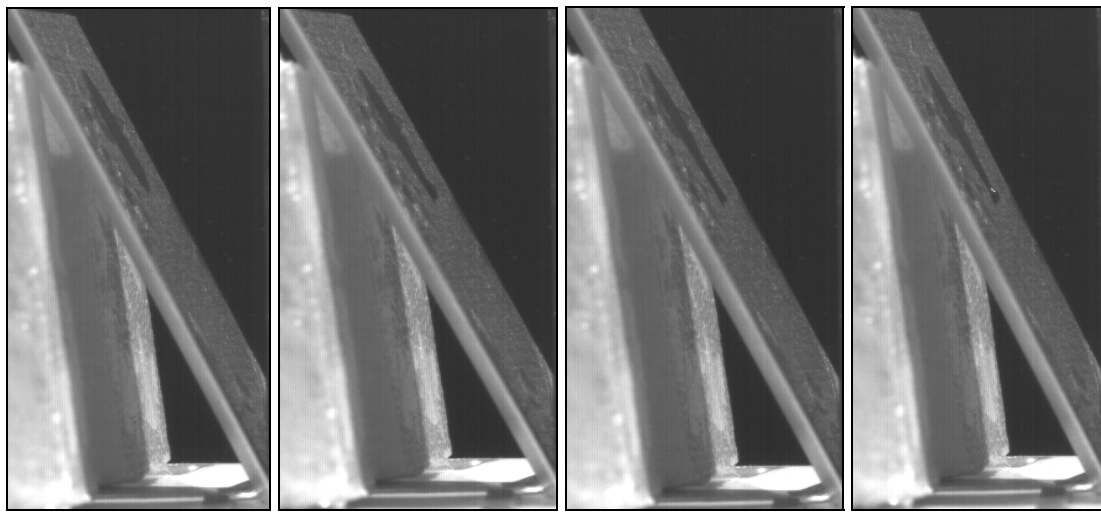


Figure 5.41 Still images taken from a high-speed video of a blood drop impacting a piece of wallpaper bound to cardboard at 30 degrees – side view.

- The blood drop moved over the surface of the wallpaper forming an elliptical shape with a small amount of wave cast-off (c,d).
- After the bloodstain had formed, a small blood pool formed just above the wave cast-off (d).
- This pool of blood was pushed upwards towards the leading edge of the bloodstain and then moved down toward the wave cast-off.
- This occurred a number of times before the blood began to run down the wave cast-off.
- After about one minute the bloodstain began to crack and flake off from the wallpaper.



Figure 5.42 The resulting bloodstain – wallpaper.

Table 5.12 The width and length measurements and the calculated angle of impact of three bloodstains made on a wallpaper surface. The actual impact angle was 30°.

Wallpaper	1	2	3	Average
Width	9	10	10	9.7
Length	23	23	23	23
Calculated angle of impact (degrees)	23.0	25.8	25.8	25°

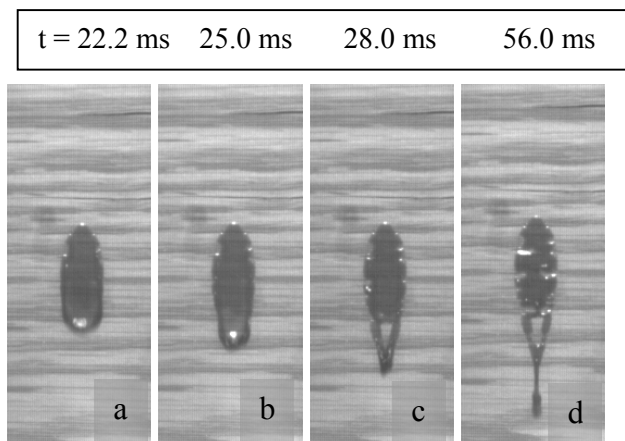
5.4.3.4 Wood

Figure 5.43 Still images taken from a high-speed video of a blood drop impacting a piece of wood at 30 degrees – front view.

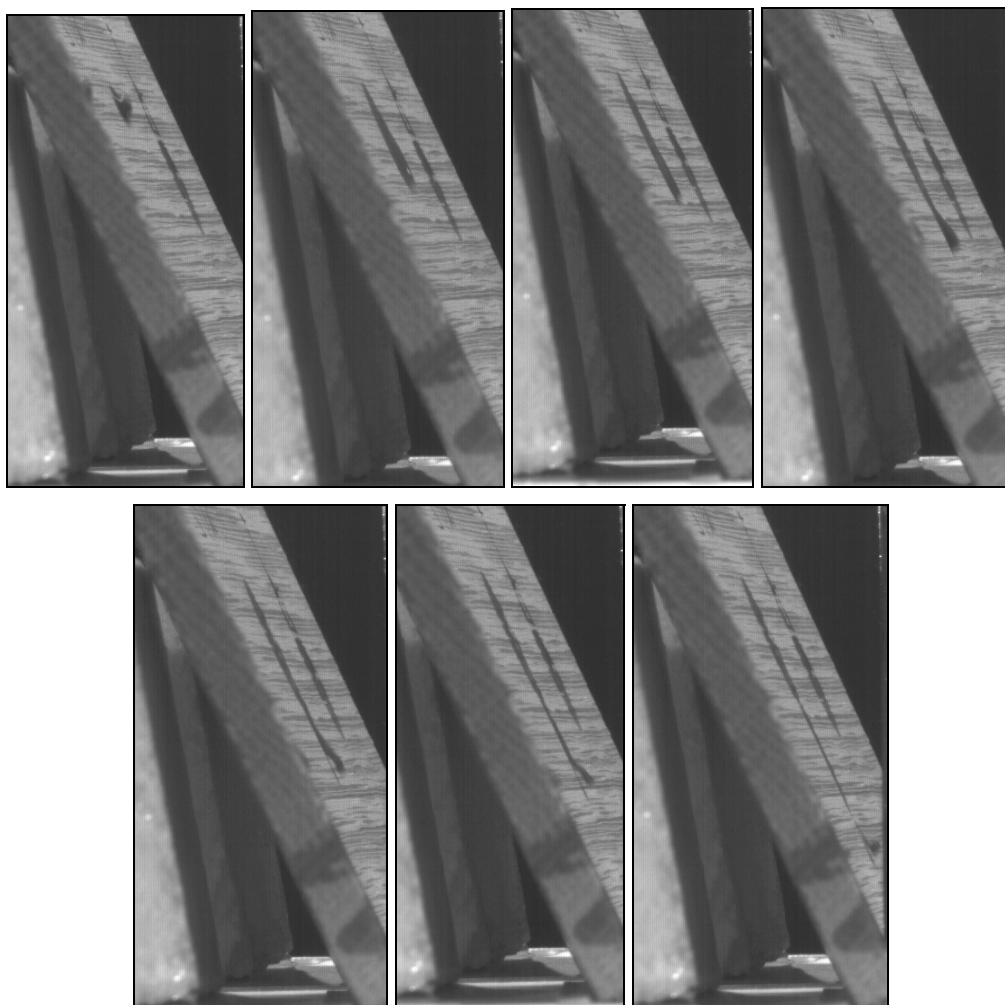


Figure 5.44 Still images taken from a high-speed video of a blood drop impacting a piece of wood at 30 degrees – side view.

- The blood drop travelled over the grainy wood surface and as the wave cast-off began to form, it lifted off the surface of the wood leaving a space without blood directly above the wave cast-off (a-d).

- The bloodstains that formed on the wood surface had areas that had no blood because of the grains on the surface.



Figure 5.45 The resulting bloodstain – wood.

Table 5.13 The width and length measurements and the calculated angle of impact of three bloodstains made on a wood surface. The actual impact angle was 30°.

Wood	1	2	3	Average
Width	11	9	9	9.7
Length	28	27	29	28
Calculated angle of impact (degrees)	23.1	19.5	18	20°

The blood formed differently on all of the surfaces examined in this experiment. On surfaces including the wood and wallpaper, the blood ‘skimmed’ over the grains and the bloodstain that formed on the wood had voids where the blood had not touched the surface. The blood glided smoothly over the vinyl and cardboard resulting in a bloodstain with more defined perimeters compared to those that formed on wood and wallpaper.

The widths of the resulting bloodstains were very similar for each different surface ($10^{\circ} \pm 1^{\circ}$). The length however was very different for each different surface. The resulting bloodstain was longer for wood and wallpaper compared to that of cardboard and vinyl. This may be due to the fact that on these more textured surfaces the blood

moved over the grains in the surface leaving voids where blood had not touched the surface. Because the blood drops consisted of the same volume of blood, it may have been that because the blood ‘skimmed’ the surface it could travel further down the surface as opposed to when it formed on a surface such as cardboard where it covered the entire surface. Elongation of blood drop may account for the underestimation of the angle of impact at acute angles that was found in Section 5.2.

The time taken for a bloodstain to form on cardboard and wallpaper was different by about 24 ms, the bloodstain forming on cardboard much more quickly than on wallpaper (Table 5.14). The bloodstain on wood however only took 39.7 ms to form, which was similar to the time taken for a bloodstain to form on vinyl. It could be seen in the high-speed videos that the blood glided over the cardboard surface without any blood moving back up the bloodstain (all the blood moved in a downwards direction forming a long wave cast-off). This was however not the case for wallpaper where the blood could be seen moving up and down the bloodstain before finally forming the bloodstain. This may have been due to the amount of friction the blood encountered when moving along the surface – there would not have been much friction force in the case of the cardboard, however on the wallpaper, because it is a textured surface, there would have been a greater friction force. Given this finding, it would have been expected that the time taken for a bloodstain to form on the wood surface would have taken approximately the same time as the time taken for a bloodstain to form on wallpaper. This was however not the case, with the bloodstain forming in only 39.6 ms on wood. It was seen in the high-speed video of a bloodstain forming on wood that the blood travelled continuously in a downward direction meaning no extra time was spent with blood moving up and down the bloodstain. The bloodstains that took the shortest amount of time to form had the longest wave cast-off. Therefore in general perhaps the longer that the wave cast-off is, the less time that was taken to form a bloodstain.

Table 5.14 The time taken for bloodstains to form on different surfaces

Surface	Time at which blood touched surface (ms)	Time at which bloodstain had formed (ms)	Time to form bloodstain (ms)
Cardboard	8.7	36.6	27.9
Wood	16.4	56.0	39.6
Vinyl	11.5	52.0	40.5
Wallpaper	6.7	58.8	52.1

5.4.4 Conclusion

The high-speed photography used in this study showed that blood drops behave differently on different surfaces. An impact spatter pattern can be found on a number of different surfaces at a crime scene. Regardless of the surface type, if it is necessary, a region of origin determination may be carried out. The experiments carried out in this chapter have shown that the surface type can affect the accuracy of the angle of impact calculation, which may consequently affect the accuracy of the region of origin determination. Surfaces including wood and wallpaper produced less accurate angle of impact results compared to surfaces including cardboard, tile glass and vinyl.

This study has shown that the way in which bloodstains form on a surface is unique for that particular surface. It is therefore important for forensic analysts to be aware that the surface upon which an impact spatter pattern is can affect the accuracy of the angle of impact calculation. While the exact amount of uncertainty in the result may not be able to be quantified, it should at least be recognised that the surface type might affect the overall region of origin result.

5.5 The effect of different velocities on the angle of impact calculation

5.5.1 Introduction

This section will outline an experiment carried out to determine the effect, if any, of different falling velocities on the angle of impact calculation of bloodstains at acute angles of impact.

Every bloodstain that makes up an impact pattern is different because of a number of factors. These factors include:

- The velocity at which a droplet impacted the target surface.
- The angle at which a droplet impacted the target surface.
- The distance a droplet travelled through the air.
- The blood drop volume.
- The composition of the target surface.

There are many other factors that may affect the appearance of a bloodstain in an impact pattern however they are beyond the scope of this discussion. This section focuses on the velocity at which a blood droplet has travelled through the air at before it impacts a surface.

5.5.2 Method

5.5.2.1 Generation of bloodstains

Eight different impact angles were investigated including 10°, 15°, 20°, 25°, 30°, 35°, 40°, and 45°. Blood was released from three different falling heights; 0.5 m, 1 m, and 1.5 m, from a pipette, which was secured to a clamp stand secured at the required height above the target surface (height was measured from the pipette tip to the target surface). The blood was released from a 200 µL Gilson pipette onto A4, 225 gsm, Olympic, white board. Five blood drops were released onto the target surface at every impact angle at each of the three heights. The board was left at the given angle to dry for 24 hours before being placed horizontally for photographing. A photograph was taken of every bloodstain and these were transferred to a computer for analysis.

5.5.2.2 Measurement of bloodstains

An ellipse was fitted to every bloodstain using Microsoft ® Office Visio ® Professional 2003. The width and length of the ellipse was recorded for subsequent angle of impact calculations.

5.5.2.3 Determination the angle of impact

The angle of impact was calculated in Microsoft Excel using Formula 1.1. The expected angle of impact was subtracted from the observed angle of impact to give a single value representing the accuracy of the results (Fig. 5.46).

5.5.3 *Results*

As the falling distance increased so did the accuracy of the angle of impact calculation. The results for a falling height of 1.5 m were on average 81% more accurate than the results for a falling height of 0.5 m.

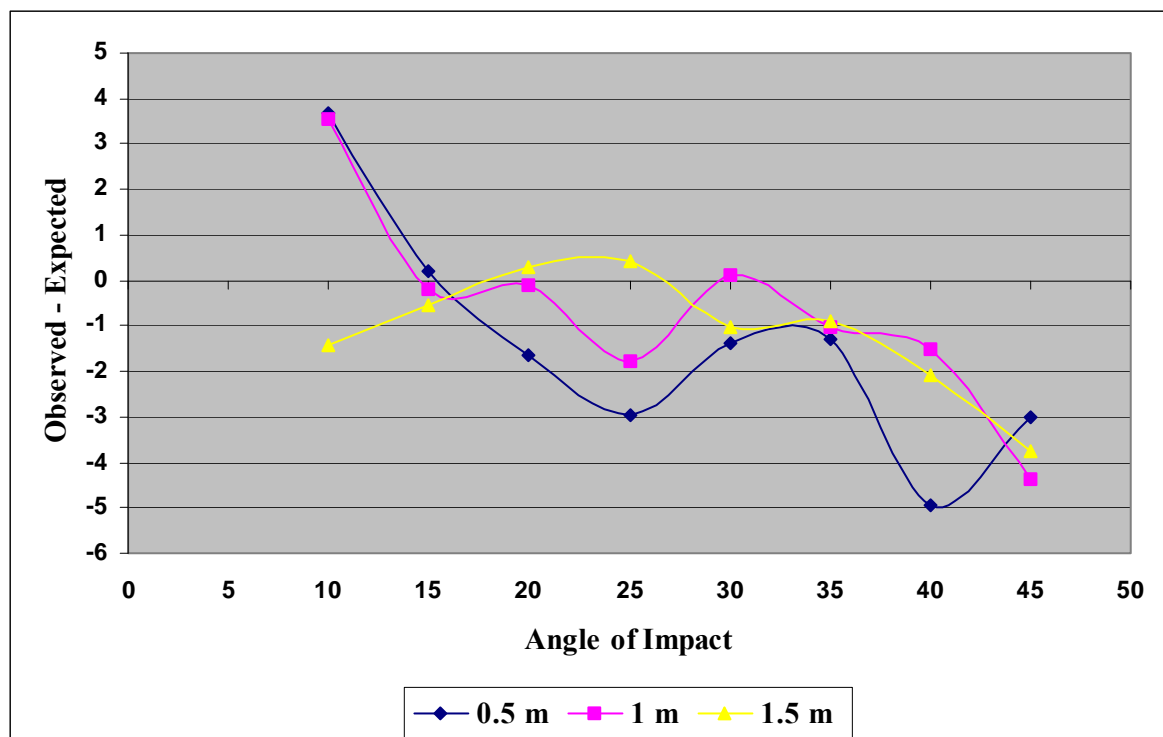


Figure 5.46 The observed minus expected angle of impact determined for bloodstains generated at different angles from different heights.

5.5.4 Discussion

It is known that oscillations can affect the shape of a bloodstain after it impacts a surface. This is only so if the droplet contacts the surface while still in an oscillating state. The shortest distance travelled by the blood droplets in this experiment was 0.5 m. In a previous study it was found that after a blood droplet had travelled vertically 0.4 m, oscillations had completely dampened [23]. This means that oscillations are unlikely to be the cause of the results observed in this study.

The increase in accuracy of the angle of impact results as the vertical distance increased may be due to the increase in the velocity at which the blood droplets impacted the target surface. This increase in velocity may result in the blood drops forming on the surface in a way that the resulting bloodstain conforms well to the sine equation used to calculate the angle of impact.

It was noticed that the overall size of the resulting bloodstain increased as the falling distance increased. This was predominantly in length when the angle of impact was between 10 and 20° and was noticeable in both the length and width when the angle of impact was between 25 and 45°.

The fact that greater accuracy was found when the bloodstains were generated from a greater height may have implications for bloodstain selection when determining a region of origin. It is often stated that ‘fast travelling’ bloodstains should be selected from an impact pattern for analysis. The reason for this is that fast moving bloodstains have a trajectory closer to a straight line. The problem is that there is no way to identify ‘fast travelling’ bloodstains from an impact pattern.

The results of this study show that as the distance travelled vertically by a bloodstain increases, the angle of impact results become more accurate and as the distance travelled increases, so too does the size of the resultant bloodstain. Therefore, the size of a bloodstain may be an indication of how fast it was travelling and by selecting the larger bloodstains for a region of origin determination, the results may be more accurate.

The major limitation of this finding is that when a bloodstain pattern is studied for a region of origin determination, it is usually on a vertical surface such as a wall and the blood drops have travelled horizontally before impacting it. This study involved investigating bloodstains travelling vertically onto an angled surface and because of gravity and air resistance the results may not be able to be inferred to impact spatter patterns on vertical surfaces.

It has previously been shown that bloodstains created by drops falling vertically onto a sloped surface are comparable to those produced when blood drops are projected out at angles and impact horizontal or vertical surfaces [29]. If this is true then the two situations may be able to be compared with each other. This would mean that larger bloodstains might be indicative of bloodstains that have travelled faster in an impact pattern. This concept will be further investigated in the bloodstain selection chapter (Chapter 7).

5.5.5 Conclusions

As the falling distance increased so did the accuracy of the angle of impact calculation. A possible reason for this is that as the vertical distance travelled by the blood droplet increases, so too does the velocity at which it impacts the target surface. This increased velocity may cause the bloodstain to form in a way that better conforms to the angle of impact formula therefore producing a more accurate result.

Because the bloodstain increased in size as the dropping distance was increased, the size of a bloodstain may be an important factor to consider when selecting bloodstains for a region of origin determination. It will therefore be considered in chapter 7.

5.6 Was there an underestimation of the angle of impact at acute angles?

5.6.1 Introduction

In a number of studies and data collected involving the angle of impact calculation, an underestimation of the angle at acute angles has been noted. Section 2.1.2.3 of chapter 2 discusses this observed error. Whether this observation is real and reasons for it have not yet been explored.

Throughout this chapter, various experiments have been carried out which have involved calculating the angle of impact. The results from these experiments will be analysed to determine whether there is a systematic underestimation of the angle of impact.

5.6.2 Method

The results of the experiments carried out in sections 5.2 and 5.5 were analysed to determine if the angle of impact was systematically underestimated for acute angles of impact.

5.6.3 Results

5.6.3.1 Surface experiment (section 5.2)

The average difference between the observed and expected angle of impact was calculated for each target surface using Microsoft® Office Visio® Professional 2003 and the results were plotted on a graphs. The angle of impact was calculated 210 times for the purpose of the surface experiment (7 replicates x 6 surfaces x 5 angles). The graph is given in Figure 5.48.

Out of the 126 times that the angle of impact was calculated in the surface experiment (acute angles only), when the analysis was carried out the angle of impact was underestimated 56 % of the time.

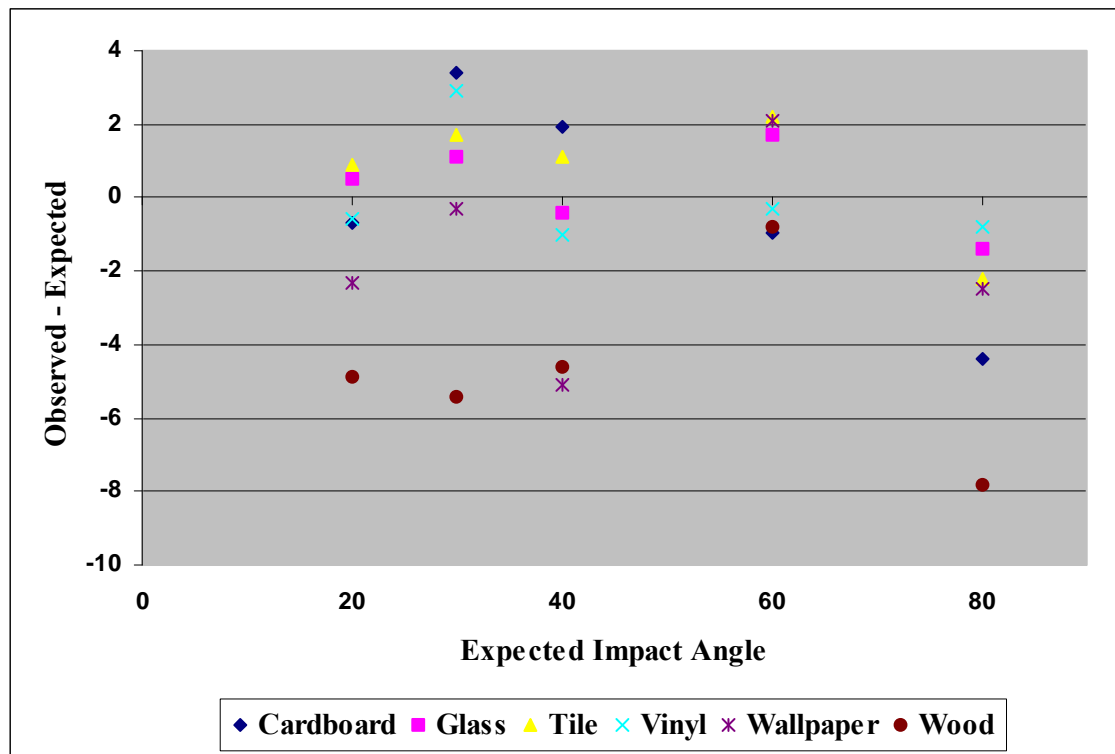


Figure 5.47 The error in the angle of impact calculation at varying impact angles (actual). Results were determined using Microsoft ® Office Visio ® Professional 2003.

5.6.3.2 Velocity experiment (section 5.5)

The angle of impact was calculated 120 times in this experiment, five times at each angle for each of the three heights. This was calculated using Microsoft ® Office Visio ® Professional 2003 and the observed minus the expected angle of impact was calculated for the average of the five calculations and plotted on a graph (Fig. 5.48).

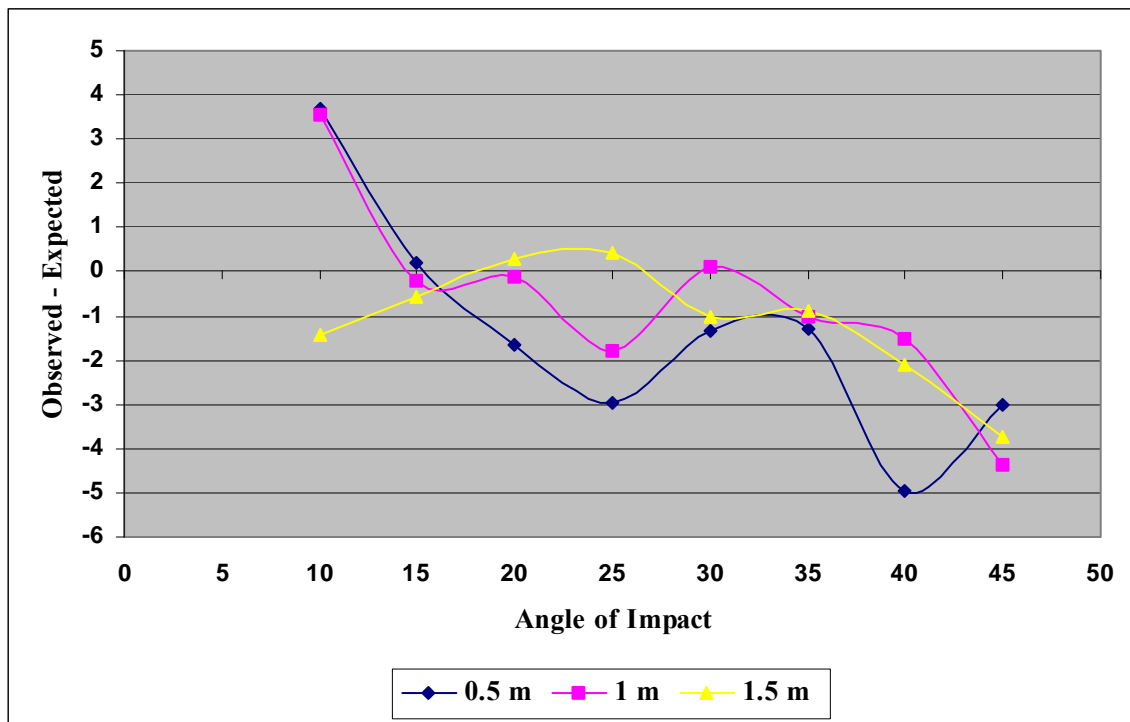


Figure 5.48 The angle of impact determined for bloodstains generated at different angles from different heights.

There were 26 values plotted on the graph. Out of these 18 were less than zero. This means that the angle of impact was underestimated about 70 % of the time. This underestimation was not regionalised – it was evenly spread out over the graph (10 – 45 degrees).

5.6.4 Discussion and conclusion

It has previously been noted that the angle of impact is often underestimated at acute angles and the objective of this study was to analyse the results of the work carried out in the previous experiments to determine whether there was a systematic underestimation of this angle.

Overall the results show that about 63 % of the time the angle of impact was underestimated at acute angles. Reasons for this underestimation include the method used to determine the angle of impact, the equation used, the dynamics that occur when a blood drop impacts a surface and the way in which an analyst fits an ellipse to a bloodstain.

Another possible reason for this underestimation at acute angles of impact may involve the sine equation used to determine the angle of impact. The equation may not accurately determine the angle of impact resulting in this systematic error.

This error may be the way in which the analyst fits the ellipse to the bloodstain. One person carried out all of the analysis in these experiments. A systematic error in fitting an ellipse would have resulted in a systematic error in the angle of impact results. At acute angles, the bloodstains were very elongated exhibiting wave cast-off. The ellipse must be fitted to the bloodstain such that the wave cast-off is excluded and a symmetrical shape is formed. This is often difficult to achieve and it has been found in a previous study assessing the way in which analysts fit ellipses to bloodstains that the ellipse is often fitted at a length exceeding that which it should be [21]. During the experiments carried out in this chapter it was found that on the wood and wallpaper surfaces the angle of impact calculations were often underestimated. The high-speed photography revealed that bloodstains formed from the same volume of blood on these surfaces were longer than bloodstains that formed on cardboard, glass, tile and vinyl. The underestimation of the angle of impact for these surfaces may have therefore been because of the extra length seen in these bloodstains, which would have resulted in the ellipse being fitted to the length of the bloodstain resulting in an underestimation of the angle of impact.

In conclusion an underestimation of the angle of impact was found at acute angles of impact 63 % of the time throughout the two experiments carried out in this chapter. The reason for this has not been established but may be a result of several factors, which in future work, could be investigated.

Chapter conclusions

- Microsoft® Excel 2000, Microsoft® Office Visio® Professional 2003, BackTrack™/Images and STABS are computer programs that can be used to fit an ellipse to a bloodstain.
 - They all performed as well as each other so the method an analyst uses may be based on the specific features of each program.
 - Microsoft® Excel 2000 is time consuming but allows work to be saved and accessed later.

- Microsoft® Office Visio® Professional 2003 is the best program to use for experimental work because the angle of impact must be calculated manually.
 - BackTrack™/Images is best when going on to determine a region of origin.
 - STABS is the fastest program to use and it calculates the angle of impact.
- The target surface has a significant effect on the angle of impact result
 - On rough/textured surfaces the angle of impact result has a greater amount of error than on smooth/glossy/non-textured surfaces.
 - Identified cause as either surface interaction of measurement error.
 - Rough/textured surfaces have a smaller contact angle than that of smooth/glossy/non-textured surfaces.
 - The smaller the contact angle, the greater the error in the angle of impact calculation.
 - The greater the velocity of a blood drop impacting a target surface vertically, the more accurate the angle of impact calculation.
 - Possible due to the way in which a bloodstain forms making it conform better to the angle of impact formula.
 - About 63 % of the time the angle of impact was calculated at acute angles of impact it was underestimated.

This is probably due to measurement errors made due to the incorrect fitting of an ellipse to the bloodstain (ellipse is longer than it should be).

CHAPTER SIX: BLOODSTAIN SELECTION SURVEY

6.1 Introduction

While doing some background research on the methods used by analysts to select bloodstains from an impact pattern for a region of origin analysis it became apparent that in the literature there was no information on this topic. One of the objectives of this research was to establish the methods currently used by analysts to select bloodstains from an impact pattern. A survey was carried out in order to ascertain this information.

6.2 Method

The survey was sent to 15 practising bloodstain pattern analysts, 14 of who responded. Each survey was assigned a letter so that the analysts remained anonymous (A - N).

An impact pattern was generated for the purposes of the survey. It was made by dropping the impact device from a height of 95 cm onto a 7 ml pool of blood, twice.

The survey consisted of:

- Photographs of the impact pattern;
 - One image of the entire pattern (Fig. 6.1).
 - 16 close-up images (grids labelled 1 – 16).
- A series of questions.

The analysts were asked to use the image of the entire pattern to put together the close-up images to give a close-up view of the entire pattern. They were then asked to select any number of bloodstains from the impact pattern as they would if they were going to determine the region of origin and circle these bloodstains on the close-up images. The questions that followed were:

1. Briefly explain why you selected these particular bloodstains.
 1. Can you give any other details of the strategy you use at scenes when selecting bloodstains for region of origin calculations?

3. If you were to go on to determine the region of origin which method would you use?

- Strings
- Tangent method
- Computer program (please specify) _____
- Other (please specify) _____

4. If you were presenting a region of origin you had determined in a statement or likewise, would you include any indication that it could involve an element of error? If so how would you state this?



Figure 6.1 Image of the entire impact pattern and the position of each of the grids.

6.3 Results

6.3.1 Participants

There were 14 participants in the survey (A – N). Table 6.1 shows the number of participants from each country.

Table 6.1 The number of participants from each country.

Country	Number of participants
New Zealand	4
Canada	5
Australia	2
United Kingdom	1
USA	2

6.3.2 Selection of bloodstains

Each analyst selected a number of bloodstains from the impact pattern and circled them on the close up images. The total number of bloodstains selected by each analyst and the grid they were from is shown in Table 6.2. Figure 6.2 shows an image of the entire impact pattern and the number of bloodstains selected from each grid. The number on the bottom right hand corner of each grid is the grid number and the number in the centre of each grid is the total number of bloodstains selected by the 14 analysts.

Table 6.2 The total number of bloodstains selected by each analyst and the grid number they were selected from.

Analyst	Total No. of stains selected	1	2	3	4	5	6	7	8	9	10	11	12	13	14	15	16
A	8										4	4					
B	20										4	5			4	7	
C	15										4	4			3	4	
D	16										4	4			4	4	
E	24						3	2			9	10					
F	14						3		3		4	4					
G	14						2	1			5	6					
H	10						1				4	4	1				
I	10						1		1		1	1		1	2	2	1
J	10						1				4	4	1				
K	8						2		2		2	2					
L	12						2			1	4	4		1			
M	12						4	2	2		2	2					
N	13						5				1	5	2				

0	0	0	0
1	2	3	4
5	6	7	8
9	10	11	12
13	14	15	16

Figure 6.2 Image of the entire impact pattern and the number of bloodstains selected from each grid.

6.3.3 Question 1: Briefly explain why you selected these particular bloodstains.

The reasons for selecting bloodstains were assigned to one of ten categories based on the analyst's responses. Table 6.3 shows these categories and the selection each analyst made. The reasons that make up the 'other' category are listed below the table. The table is ordered such that the most popular reason for selecting the bloodstains is at the top and the least popular is at the bottom.

Table 6.3 The analysts reasons for selecting bloodstains.

Analyst	A	B	C	D	E	F	G	H	I	J	K	L	M	N
Upward moving	✓		✓	✓	✓	✓	✓	✓	✓			✓		
Well-formed				✓	✓		✓	✓	✓	✓	✓		✓	✓
Elliptical				✓	✓	✓			✓	✓		✓	✓	
Larger stains	✓	✓	✓			✓				✓	✓			✓
Dispersed across pattern				✓			✓	✓	✓	✓	✓		✓	
Core of pattern			✓	✓				✓				✓		
Not affected by gravity		✓								✓	✓			
Point to probable convergence	✓	✓							✓					
Balanced	✓					✓		✓						
'Other'					✓						✓	✓	✓	✓

'Other' reasons included:

- Long tail (fast moving)
- Select a suitable number of bloodstains
- 'Fast' moving x 2
- Medium sized relative to the rest of the spatter
- 6-10 stains
- Decide on the number of impacts based on convergence
- Distance from source to ensure no effect from oscillations

6.3.4 *Question 2: Can you give any other details of the strategy you use at scenes when selecting bloodstains for region of origin calculations?*

Responses included:

- Look at the overall pattern and distribution of stains. Misting occurs at the likely point of origin.
- Consider all staining before diving into the analysis.
- Draw back to find the area of convergence and use bloodstains that point to this area.
- Take an overall photo of the impact pattern then put a measurement grid onto the pattern and take another photo.
- Estimate the area of convergence by looking for circular stains and then select elliptical stains that are to the left and right of this area.
- Use a string to find 2D area of convergence (and the number of convergences there are)
- When selecting individual stains, take into consideration the general shape and clarity to measure the length and width.
- Take into account the directionality of bloodstains.
- Select about 7 bloodstains from each side of the impact pattern.
- First establish that the pattern is a spatter pattern, second determine the area of convergence (with a string), thirdly select fast upwardly moving stains, fourthly select bloodstains not too far from the area of convergence.
- Represent the distribution of stains in the pattern.
- Stains chosen are oriented so that they are likely to have a common area of origin.
- Consider the surface type (as may affect readings) and consider if the surface is flat or on an angle.
- Consider the number of patterns, the types of patterns, select well shaped stains from the centre of the impact spatter.
- Ensure $W/L \sim 0.5$ to minimise error.
- If using string method select larger stains.
- Select well-shaped stains.

6.3.5 *Question 3: If you were to go on to determine the region of origin which method would you use?*

Table 6.4 shows the responses to this question.

Table 6.4 The method(s) used by the 14 analysts to determine the region of origin.

Analyst	Method
A	Strings or BackTrack™
B	Calculate tangent to do strings
C	Tangent or strings
D	Tangent or BackTrack™
E	BackTrack™
F	Strings or BackTrack™
G	Strings, BackTrack™
H	Strings or tangent
I	Tangent
J	Tangent
K	Eye, string or BackTrack™
L	Tangent
M	String
N	BackTrack™

6.3.6 *Question 4: If you were presenting a region of origin you had determined in a statement or likewise, would you include any indication that it could involve an element of error? If so how would you state this?*

Table 6.5 shows the responses to this question.

Table 6.5 Whether each of the 14 analysts would include a statement of error in a statement of likewise and if so how they would state it.

Analyst	Statement
A	Approximately
B	Approximately
C	Approximately area and whether person was sitting/ stinging/lying on ground
D	Verify results w another analyst doing it
E	Not in report but as witness. Uses most recent literature. Includes larger origin than the known error rate.
F	General area the size of a volleyball
G	No
H	Yes
I	No
J	Approximately located
K	Approximately area, laying on ground etc
L	Approximately only (especially height)
M	State source was X cm or closer from wall and X cm or closer to ground
N	Point of origin \pm 10 cm

6.4 Discussion

6.4.1 Selection of bloodstains

Each analyst was asked to circle the bloodstains they would select for a region of origin analysis on the close up images of the impact pattern. The information that was obtained from this exercise was the total number of bloodstains that the analyst would select, the position that they would select them from and whether they would select an equal number from each side of the pattern.

The number of bloodstains selected ranged from 8 to 24; the average number selected being about 13. The most bloodstains were selected from grid number 11, followed by number 10. Overall the most bloodstains were selected from an area that formed a v-shape around the area of convergence (Fig. 6.2).

Nine out of the 14 analysts surveyed selected an equal number of bloodstains from each side of the impact pattern. Selecting an equal number of bloodstains may be

important when determining the region of origin using a manual method and this is further investigated in Chapter 7.

6.4.2 Question 1

The reasons given by analysts for selecting the bloodstains they did are given in Table 6.3 and in the bullet points following the table. The most common reason given for selecting the particular bloodstains was that they were upward moving and well formed. Following these reasons were larger bloodstains, elliptical and dispersed across the impact pattern.

By selecting bloodstains that are upward moving, the overestimation in the Z-axis may be minimised. This may therefore improve the accuracy of the region of origin determination.

A well-formed bloodstain means that if a bloodstain was divided along its major axis, the opposite halves would be equal to each other [30]. A well-formed bloodstain may be chosen for a region of origin determination because the width and length measurements are easier to make for a bloodstain with a clear perimeter. Well-formed bloodstains are also unlikely to be secondary spatter such as satellite spatter or cast-off. The selection of well-formed bloodstains is further investigated in chapter 7.

Other reasons that were given included 'fast' moving bloodstains. This may be because a bloodstain travelling at a relatively high velocity may have been travelling in the air for less time and therefore would have had less time to be affected by gravity, therefore more closely representing the straight line trajectory that is assumed in region of origin estimations. Currently there is however no way for an analyst to determine which bloodstains were 'fast' moving in an impact pattern making it difficult to understand what they are basing this selection on. This finding will be further investigated in chapter 7.

6.4.3 Question 2

Other details of the strategy used by analysts at scenes when selecting bloodstains for region of origin calculations were listed in section 6.3.4. Several analysts pointed out

that it is important to look carefully at the impact pattern before beginning the analysis.

In this case the impact pattern was made by dropping the impact device from a height of 95 cm onto a 7 ml pool of blood, twice. Two analysts pointed out that there was more than one distinct area of convergence meaning the stain selection process would be a lot more complicated. This was because stains would be required to be selected for determining two points of origin. The rest of the analysts failed to establish that there were two areas of convergence.

6.4.4 Question 3

The 14 analysts indicated that they used one of four different methods for determining the region of origin. Some stated that they would use a combination of two or more methods where required. For example one analyst used the tangent method to calculate the tangent before using the string method to determine the region of origin. Figure 6.3 shows the number of analysts that used each of the four different methods. Eight analysts indicated that they would use more than one method or either one method or another therefore for each analyst there may have been more than one selection.

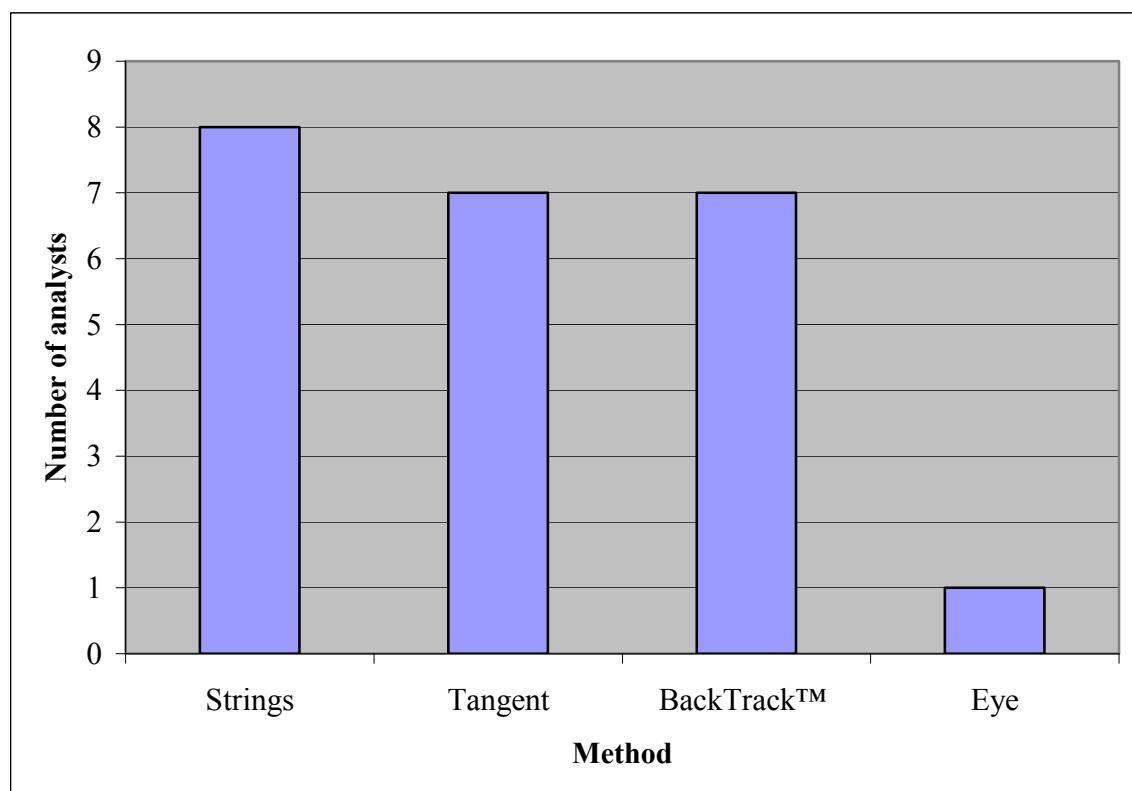


Figure 6.3 The method used by analysts for determining the region of origin. Some analysts indicated that they would use more than one method.

The stringing method was the most commonly used method for determining the region of origin closely followed by the tangent method and BackTrack™. One analyst stated that they would use their eye to judge the position of the impact site and use stringing or BackTrack™ to calculate the area if necessary.

6.4.5 Question 4

Twelve analysts stated that they would include an indication that the region of origin determined could involve an element of error. Most of the analysts dealt with this by stating that the calculation was an approximation. Two analysts said that they would give an estimation of whether a person was sitting, standing or lying down at the time of impact as opposed to stating a specific point of origin.

6.5 Conclusion

The survey has indicated the strategies used by analysts to select bloodstains from an impact pattern for a region of origin analysis. Chapter 7 will look at some of the strategies indicated by analysts to determine if they have a scientific basis and if they actually improve the accuracy of the region of origin estimate. Chapter 7 will further discuss the strategies these analysts have indicated they use for selecting bloodstains in light of the criteria that have been determined to be important in this research.

CHAPTER SEVEN: BLOODSTAIN SELECTION

This chapter discusses the generation and analysis of four impact spatter patterns for research into bloodstain selection criteria. The first section of the chapter outlines the experiments carried out to determine the ability of individual bloodstains to predict the region of origin. The second section discusses how the equations of motion were used to determine the time that individual bloodstains were in the air and how this time was compared to the results from section 7.1. The third section looks at a number of different stain selection variables in order to determine which are important when selecting bloodstains and the final section concludes the chapter by setting out some stain selection criteria.

7.1 Ability of individual bloodstains to predict the region of origin

7.1.1 Introduction

At a crime scene involving a vicious attack, blood is commonly spattered onto a surface or a number of surfaces resulting in the production of a distinctive ‘impact pattern’. An impact pattern is a bloodstain pattern created when blood receives a blow or force resulting in the random dispersion of smaller drops of blood [6]. The bloodstains that make up an impact pattern can be studied and may reveal various facts about the events that caused it, including the position in three dimensional space that the blood source was impacted – the region of origin.

An impact pattern can consist of a large number of bloodstains, however only a limited number can be selected for a region of origin analysis because of time limitations. A detailed literature review revealed that when bloodstain selection criteria are stated, and often they are not, it is generally in a very broad statement such as ‘fast’, ‘upwardly moving’ bloodstains. Because these criteria are not tightly defined the selection of stains is left up to the subjective judgement of the analyst. In order to remove the subjective element and improve the accuracy of region of origin determination, a more specific set of criteria is required.

Section 1.3 of the introduction described criteria that have been presented in literature prior to this research project. The research that led to the development of these criteria was, in most cases, investigating only one parameter in relation to the region of origin determination and as a result a comprehensive set of criteria has not yet been presented.

Regardless of the method used, computer based or manual, it is necessary to select bloodstains for a region of origin determination and until an automated method is developed this will remain so. Bloodstain selection criteria could improve the accuracy of a region of origin determination, save analysis time and standardise the way in which an impact pattern is analysed by bloodstain pattern analysts worldwide.

The objective of this research is to determine whether bloodstain selection criteria can be implemented when determining a region of origin and if so, what criteria should be used to ensure the result is as accurate as possible.

This study is focused only on practical criteria only. A bloodstain pattern analyst should be able to implement the criteria at a crime scene to ensure the most accurate results are obtained without making the process any more time consuming than it already is.

7.1.2 Method

7.1.2.1 Generation of impact spatter patterns

Four impact spatter patterns were generated and labelled Impact A, B, C and D. Their method of creation is described in Table 7.1. Impacts A and B were created on a target surface that had a grid system drawn onto it (30 cm high by 45 cm wide). There were a total of 12 grids for impact A and 9 for impact B. A grid system was placed onto impacts C and D after they were generated. This was done using string and was 45 cm high by 83 cm wide for impact C and 35 high x 67 cm wide for impact D. The impact patterns were left to dry for 24 hours before taking measurements and photographs. The position in 3D space at which the impact was made was recorded. X was measured out from the wall to the blood pool, Y was measured from the left-hand wall, or a reference line marked onto the wall on the left-

hand side of the impact pattern, and Z was measured from the ground to the blood pool. Because of the nature of the impacts, the impact position may have been ± 2 cm of the point measured in the X, Y and Z-axis.

Table 7.1 The method of generation and position of impacts A – D.

	Method of generation	Quantity of blood	Impact position (cm)
Impact A	Hammer striking a pool of blood once on a Parafilm covered wooden block	3 ml	X = 22 ± 2 cm Y = 99 ± 2 cm Z = 57 ± 2 cm
Impact B	Impact device dropped from 70 cm, once	4 ml	X = 25.5 ± 2 cm Y = 115 ± 2 cm Z = 50 ± 2 cm
Impact C	Hammer impacting a wooden block three times	10 ml	X = 25 ± 2 cm Y = 146 ± 2 cm Z = 50 ± 2 cm
Impact D	Impact device dropped from 95 cm, twice	7 ml	X = 25 ± 2 cm Y = 138 ± 2 cm Z = 50 ± 2 cm

7.1.2.2 Stain selection and recording procedure

Approximately four bloodstains were selected from each grid for Impacts A – D. These bloodstains were selected so that overall there was a range of different sizes and gamma angles. A vertical line was drawn next to each stain with a level and the X, Y and Z positions were measured. An adhesive scale and number were both placed alongside the bloodstain. The stains were then photographed and transferred into Microsoft® Office Visio® Professional 2003 for analysis.

7.1.2.3 Analysis of bloodstains

The length, width and glancing angle (γ) of each bloodstain was measured in Microsoft® Office Visio® Professional 2003. The impact angle (α) was calculated using equation 1.1.

7.1.2.4 Quantifying the ability of individual bloodstains to determine the region of origin

In order to quantify the ability of each individual bloodstain to predict the region of origin, basic mathematics was applied to determine the closest perpendicular distance from the ‘virtual string’ of a bloodstain to the known region of origin (Fig. 7.1). A virtual string is a line that approximates the trajectory of a bloodstain assuming no gravity and air resistance and it is calculated using alpha, gamma, the position of the bloodstain on the wall and the known point of origin.

This analysis was carried out both two and three dimensionally and the equations used are given and explained below. The reason for carrying out both a two-dimensional and three-dimensional analysis was that a three dimensional analysis includes the effects of gravity because the Z-axis was included in the analysis. It is known that the Z-axis introduces the most error into the region of origin estimate and therefore the two dimensional analysis was included because it negates the effect of gravity allowing the error in the X and Y-axes to be considered separately. Figure 7.1 shows a bloodstain on a wall represented by the YZ plane. Also shown is the impact velocity vector, V .

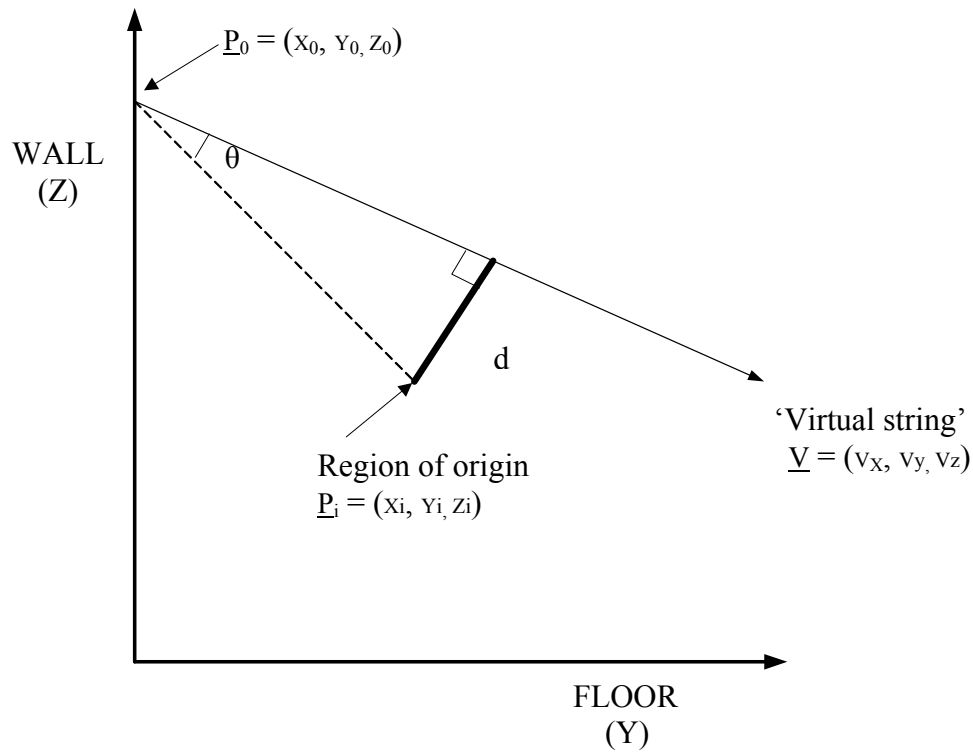


Figure 7.1 Diagram representing the position of a bloodstain on a wall (P_0), the region of origin (P_i) and the virtual string drawn along the flight path of the bloodstain.

The analysis:

1. Calculating the angle between two vectors using vector dot products:

Vector 1: V_x, V_y, V_z , determined using γ (glancing angle) and α (angle of impact)

Vector 2: $X_i - X_0, Y_i - Y_0, Z_i - Z_0$, determined using the position of the bloodstain on the wall (P_0) and the known region of origin (P_i).

$$\cos \theta = \frac{a \cdot b}{|a| \cdot |b|}$$

Two-dimensional:

$$= \frac{v_x(x_i - x_0) + v_y(y_i - y_0) + v_z(z_i - z_0)}{\sqrt{v_x^2 + v_y^2 + v_z^2} \cdot \sqrt{(x_i - x_0)^2 + (y_i - y_0)^2 + (z_i - z_0)^2}} \quad [7.1]$$

Three-dimensional:

$$= \frac{v_x(x_i - x_0) + v_y(y_i - y_0) + v_z(z_i - z_0)}{\sqrt{v_x^2 + v_y^2 + v_z^2} \cdot \sqrt{(x_i - x_0)^2 + (y_i - y_0)^2 + (z_i - z_0)^2}} \quad [7.2]$$

2. Determining d, using trigonometry:

Two-dimensional:

$$\sin \theta = \frac{d}{\sqrt{(x_i - x_0)^2 + (y_i - y_0)^2}} \quad [7.3]$$

Three-dimensional:

$$\sin \theta = \frac{d}{\sqrt{(x_i - x_0)^2 + (y_i - y_0)^2 + (z_i - z_0)^2}} \quad [7.4]$$

The assumptions made were:

$$\tan \gamma = \frac{v_y}{v_z}$$

$$v_z = \sqrt{v_y^2 + v_z^2} \tan \gamma$$

These equations were put into a Microsoft Excel spreadsheet to allow d to be determined for every documented bloodstain from impacts A - D. The length, width, α , γ , Y, and Z position of each bloodstain was plotted against d in Excel and a linear or polynomial trend line was added to the graphs that appeared to show a trend. On the graphs of Y and Z and gamma versus d, the true coordinate values and the region of downward moving bloodstains are indicated. Values of d that are large represent a bloodstain that is a poor stain choice that would introduce error into a region of origin determination.

7.1.3 Results

For every bloodstain selected from Impacts A - D, the closest perpendicular distance from the bloodstains virtual string to the known point of origin was calculated both two and three dimensionally. The graphs of d versus length, width, α , γ , Y, and Z position of the same bloodstain are shown in Figures 7.2 – 7.49.

The most obvious trend is that seen on the gamma versus d graphs (Figures 7.8, 7.9, 7.20, 7.21, 7.32, 7.33, 7.44 and 7.45). As gamma approached 0 and 360 degrees, d decreased forming a 'n' shaped curve. This trend is observed for each impact (A-D) however it is more pronounced in the 3D analysis.

The graphs of length, width and alpha versus d show no trend for both the two and three-dimensional analysis.

Some of the graphs of y and z position versus d appear to show a trend (Figures 7.11, 7.23, 7.25 and 7.47). This is usually a 'u' shaped graph where one point has a small d value (towards the centre of the graph) and the y and z positions on either side of this point have greater d values forming a 'u' shape. In all cases this trend was more pronounced in the 3D analysis.

The 3D calculation produced d values greater than that of the 2D calculation in every situation. This is because the 3D calculation took into account the error from the X, Y and Z coordinates, where the 2D calculation only took into account the error from the X and Y coordinates. For a parameter like gamma, where there is significant error introduced from the Z-axis, the difference between the 2D and the 3D calculation was quite large.

The d values for Impact C were the greatest. This impact was generated by striking a 10 ml pool of blood three times with a hammer. The graphs are given below and the results are discussed in section 7.1.4.

7.1.3.1 Graphs of d versus length, width, alpha, gamma Y and Z position for impact A.

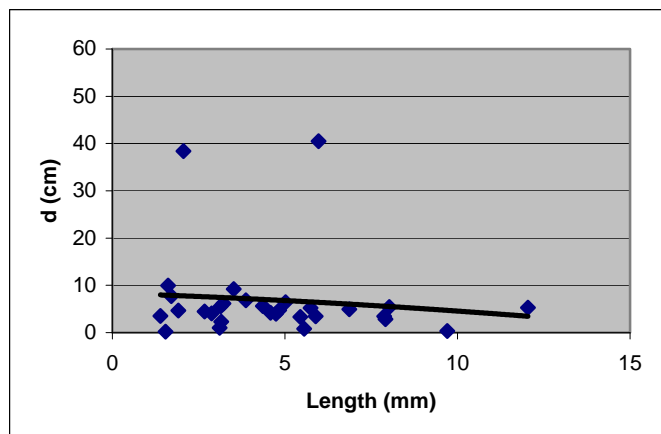


Figure 7.2: Graph of d versus bloodstain length 2D

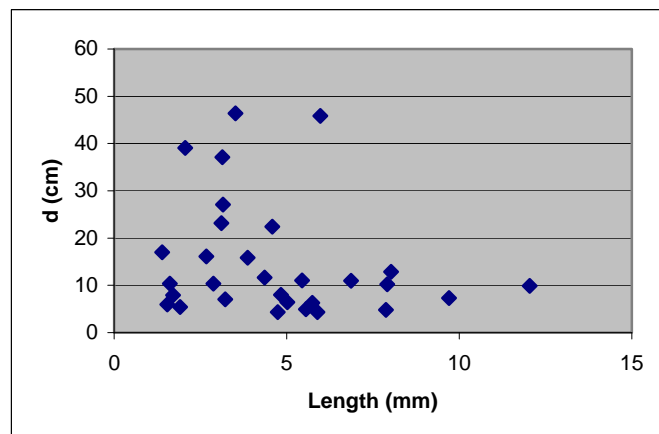


Figure 7.3: Graph of d versus bloodstain length 3D

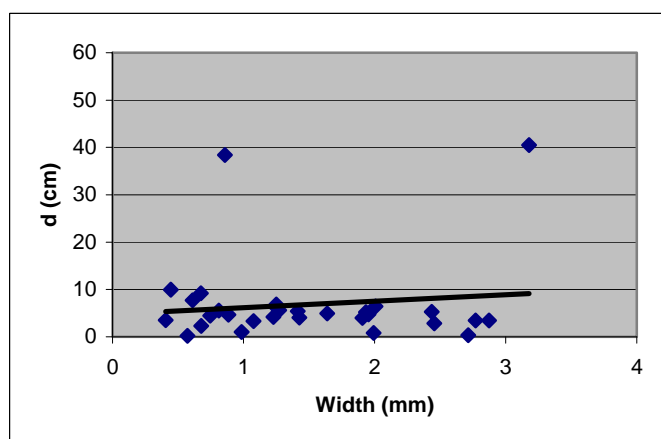


Figure 7.4: Graph of d versus bloodstain width 2D

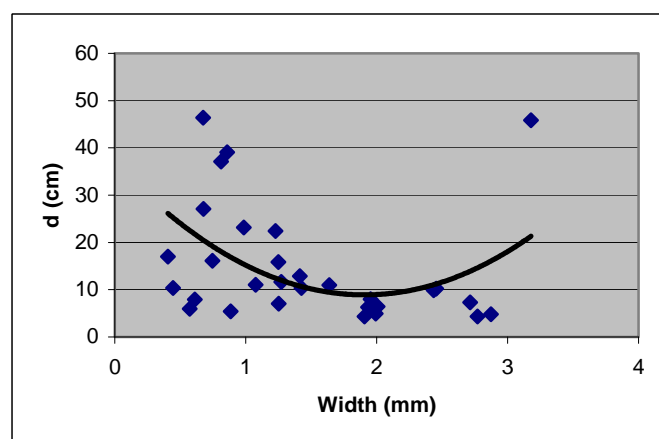


Figure 7.5: Graph of d versus bloodstain width 3D

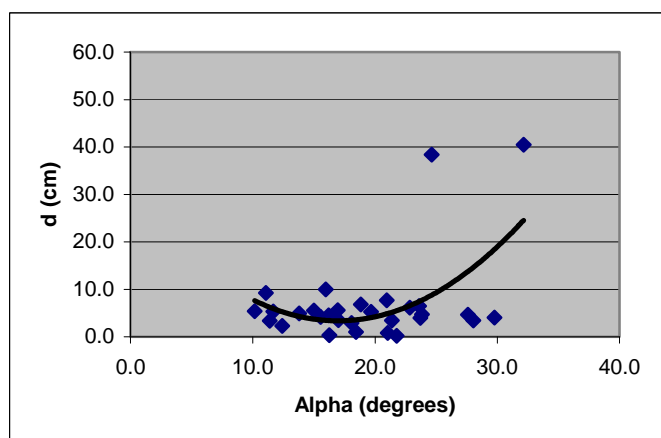


Figure 7.6: Graph of d versus alpha 2D

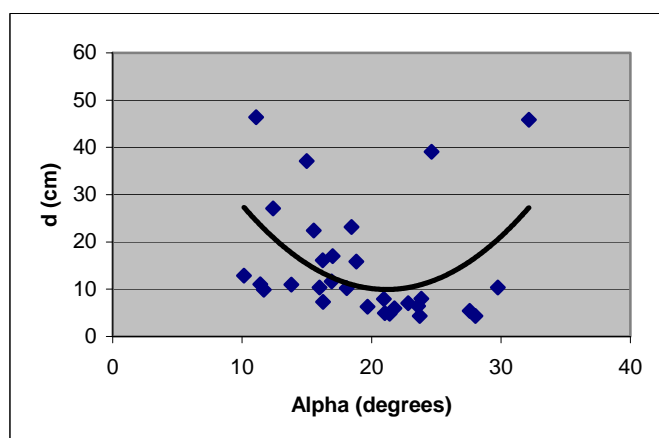


Figure 7.7: Graph of d versus alpha 3D

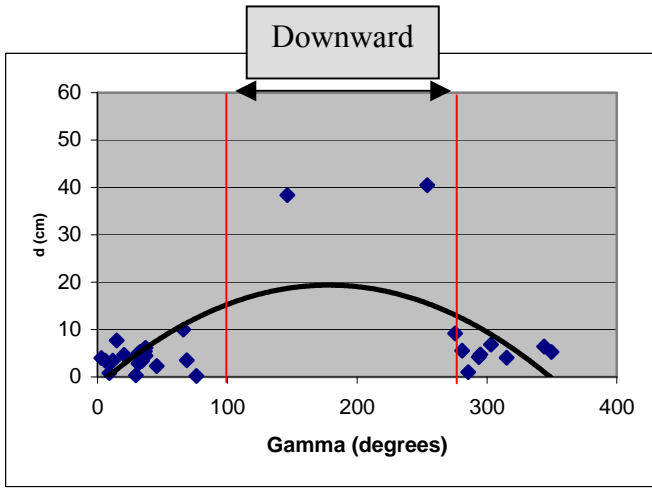


Figure 7.8: Graph of d versus gamma 2D

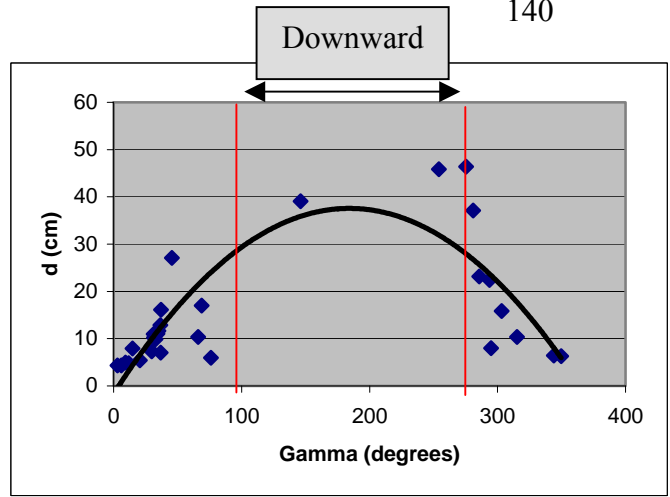


Figure 7.9: Graph of d versus gamma 3D

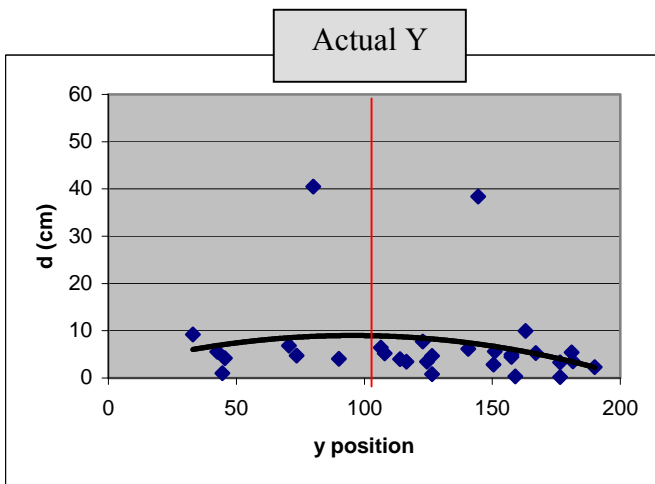


Figure 7.10: Graph of d versus Y position 2D

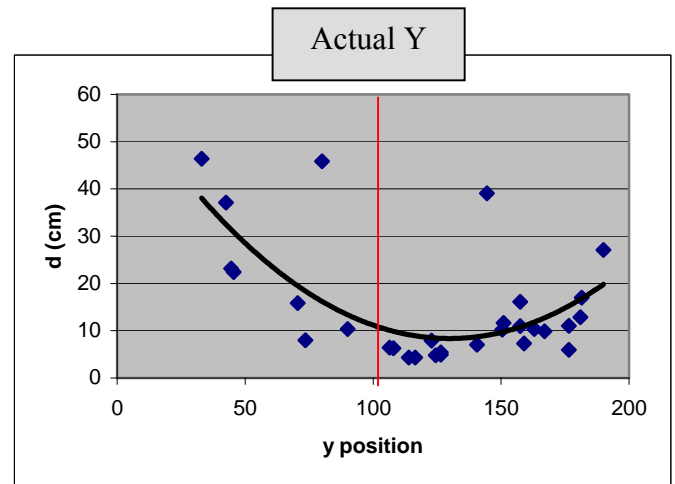


Figure 7.11: Graph of d versus Y position 3D

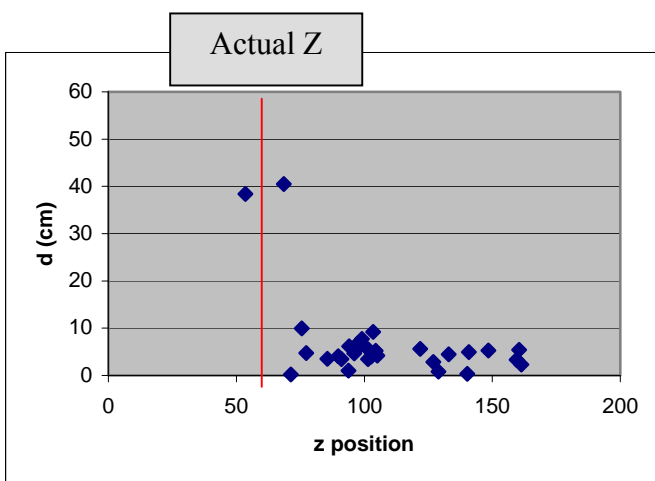


Figure 7.12: Graph of d versus Z position 2D

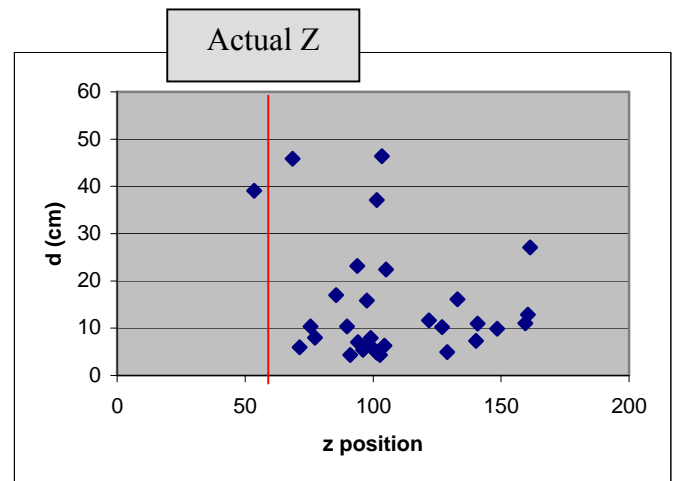


Figure 7.13: Graph of d versus Z position 3D

7.1.3.2 Graphs of d versus length, width, alpha, gamma Y and Z position for impact B.

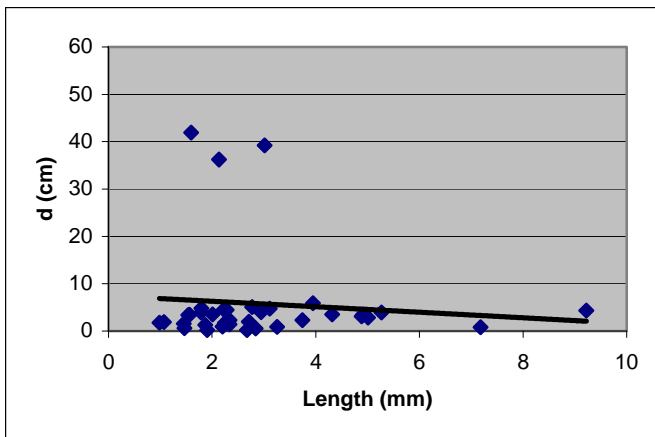


Figure 7.14: Graph of d versus bloodstain length 2D

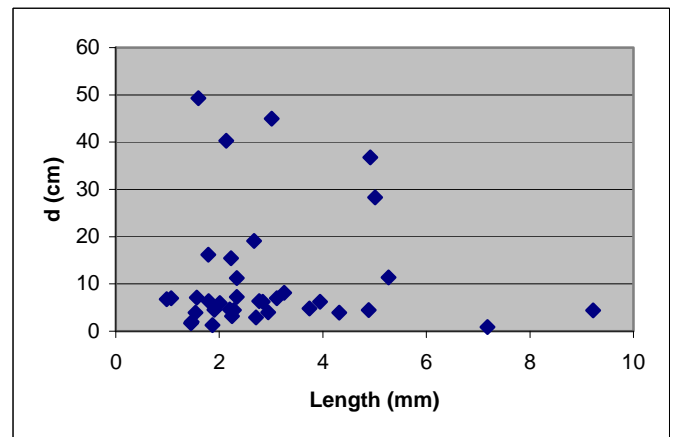


Figure 7.15: Graph of d versus bloodstain length 3D

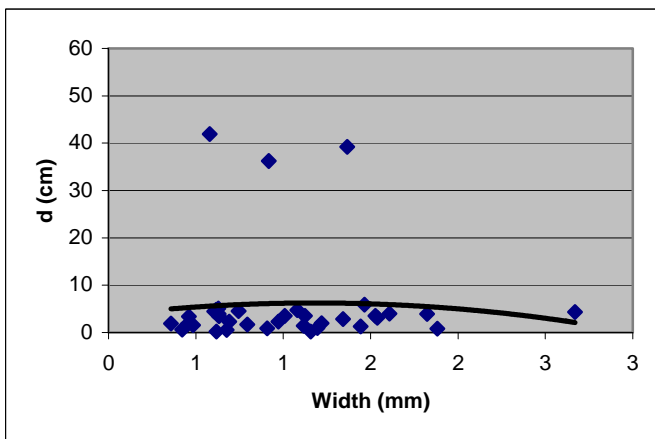


Figure 7.16: Graph of d versus bloodstain width 2D

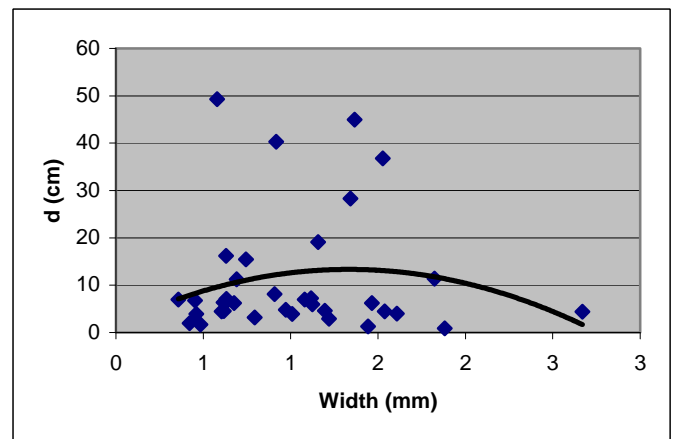


Figure 7.17: Graph of d versus bloodstain width 3D

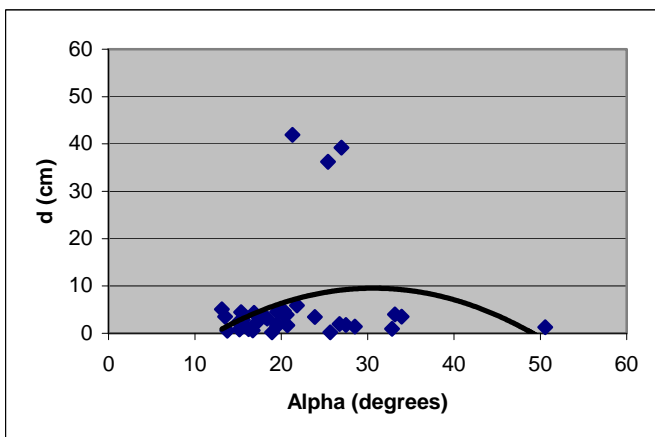


Figure 7.18: Graph of d versus alpha 2D

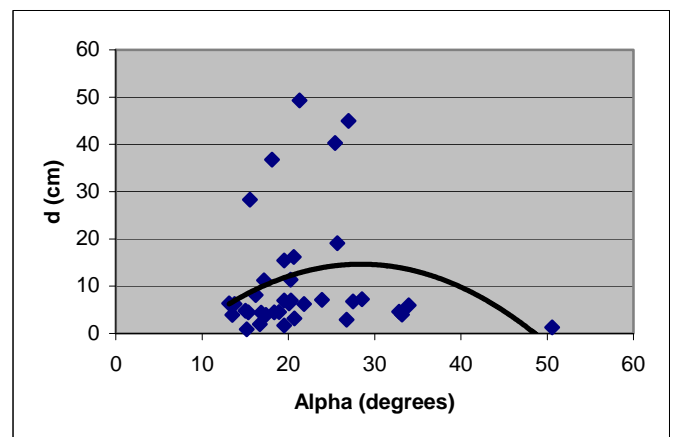


Figure 7.19: Graph of d versus alpha 3D

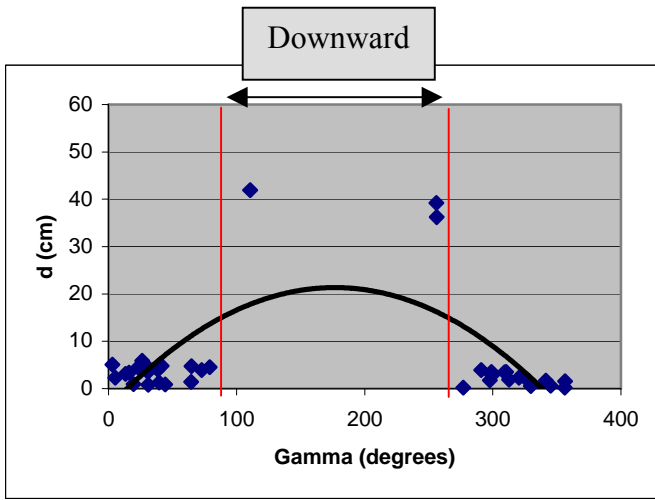


Figure 7.20: Graph of d versus gamma 2D

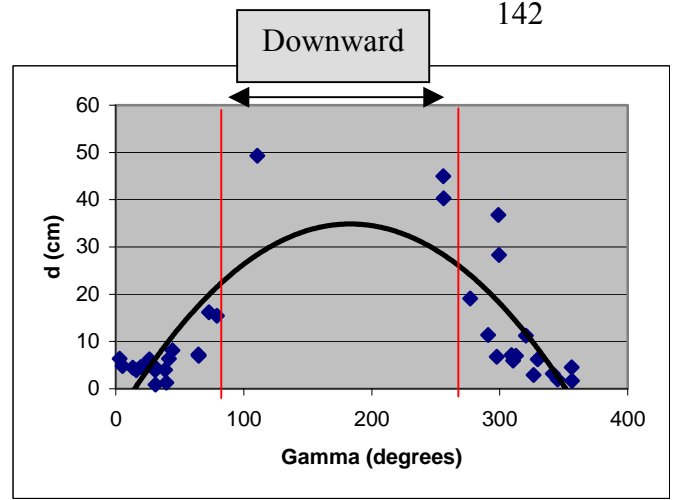


Figure 7.21: Graph of d versus gamma 3D

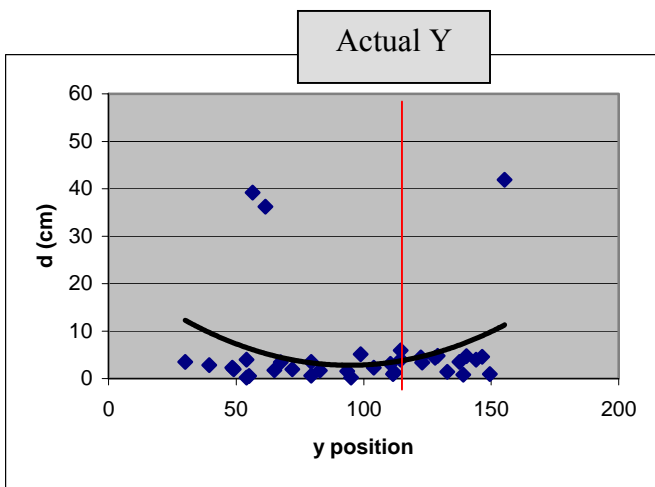


Figure 7.22: Graph of d versus Y position 2D

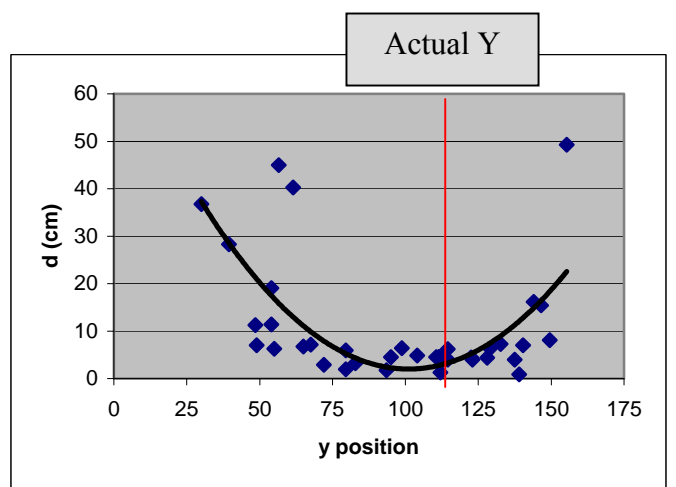


Figure 7.23: Graph of d versus Y position 3D

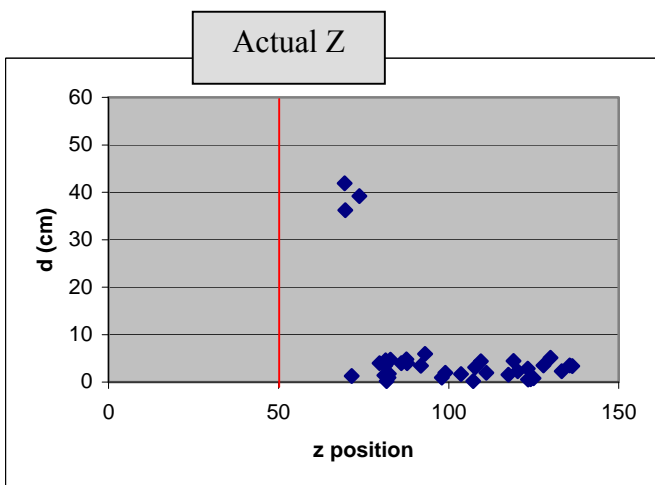


Figure 7.24: Graph of d versus Z position 2D

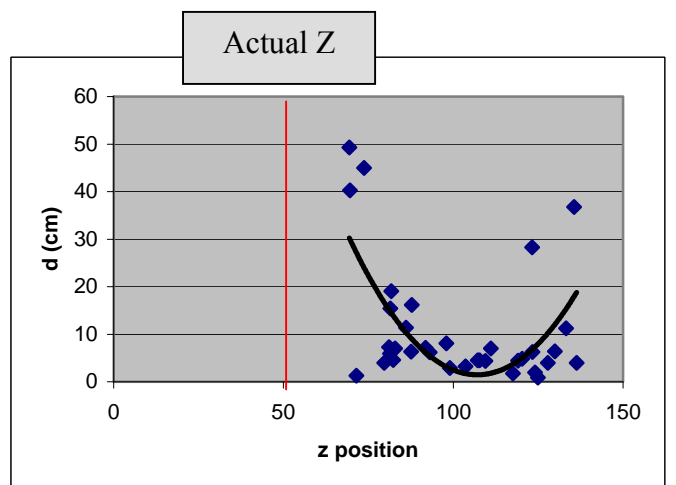


Figure 7.25: Graph of d versus Z position 3D

7.1.3.3 Graphs of d versus length, width, alpha, gamma Y and Z position for impact C.

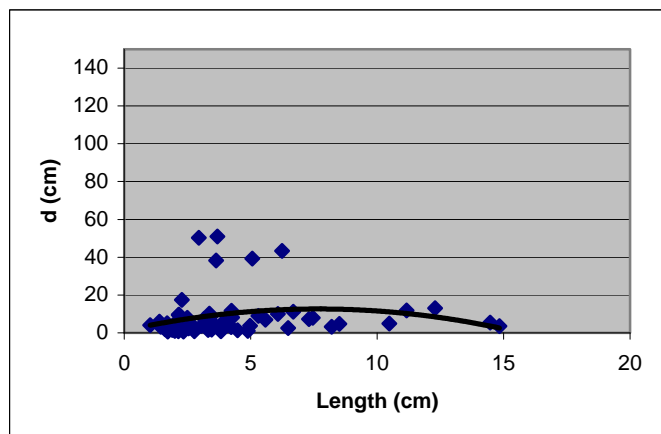


Figure 7.26: Graph of d versus bloodstain length 2D

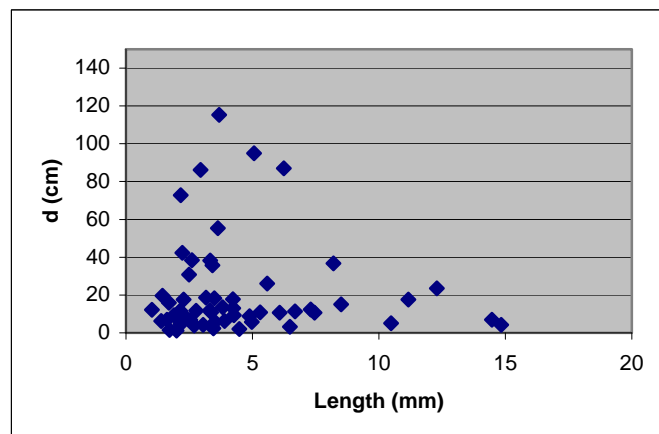


Figure 7.27: Graph of d versus bloodstain length 3D

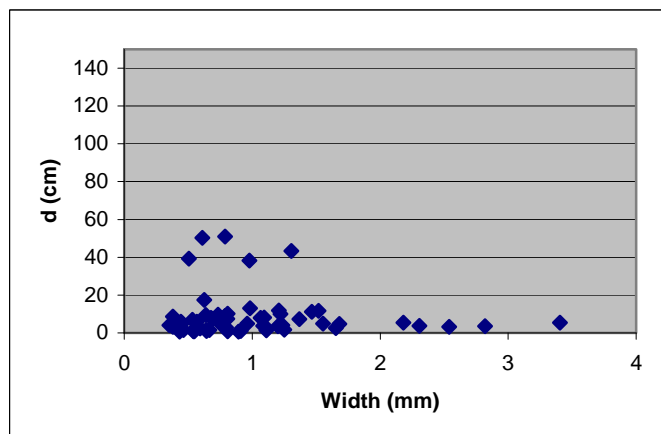


Figure 7.28: Graph of d versus bloodstain width 2D

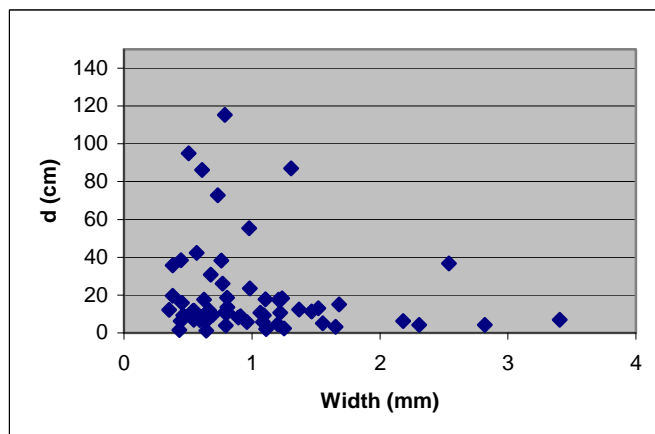


Figure 7.29: Graph of d versus bloodstain width 3D

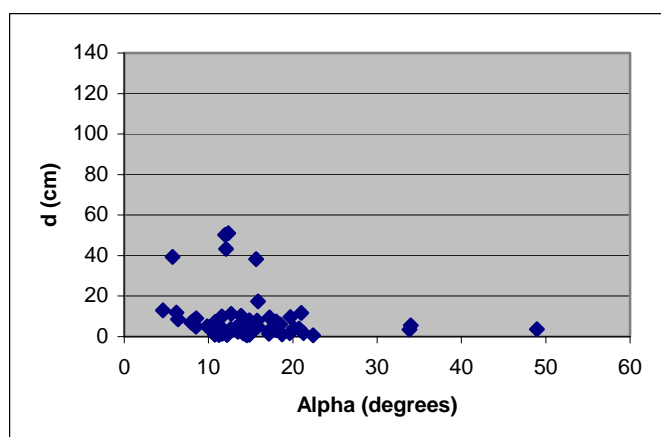


Figure 7.30: Graph of d versus alpha 2D

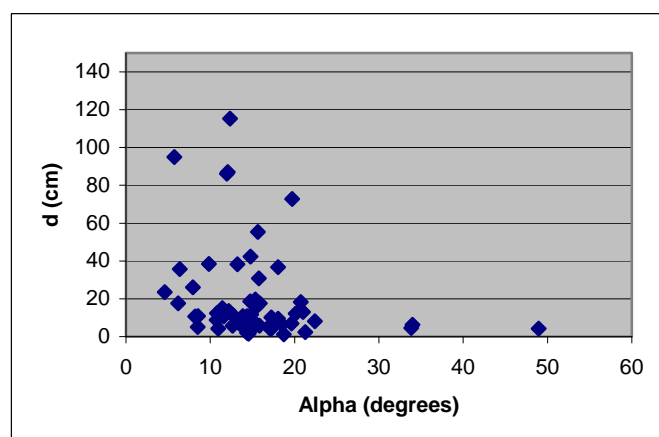


Figure 7.31: Graph of d versus alpha 3D

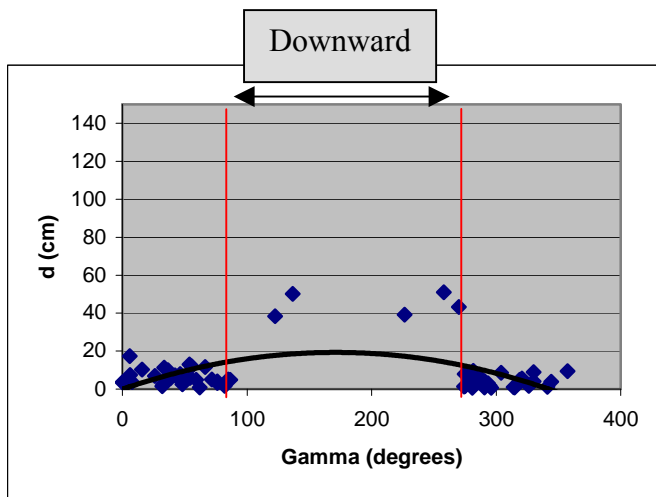


Figure 7.32: Graph of d versus gamma 2D

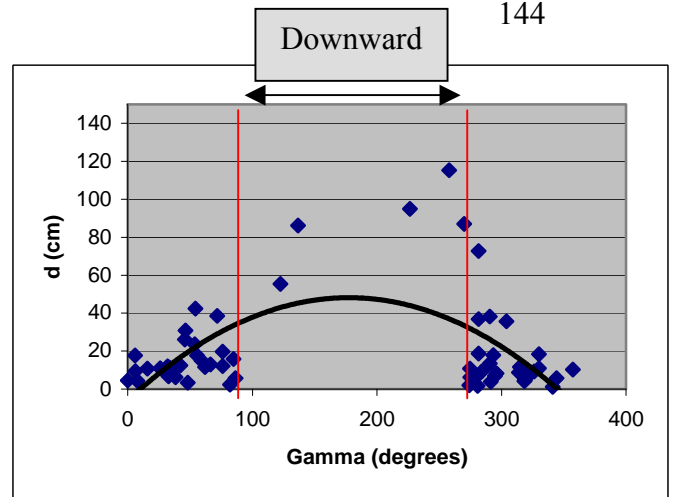


Figure 7.33: Graph of d versus gamma 3D

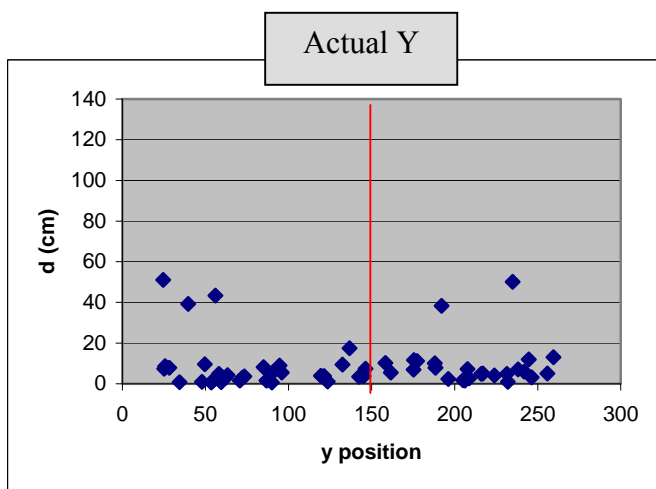


Figure 7.34: Graph of d versus Y position 2D

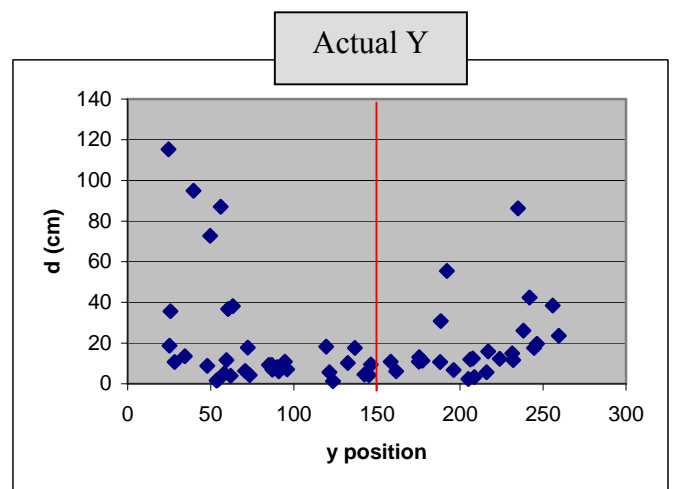


Figure 7.35: Graph of d versus Y position 3D

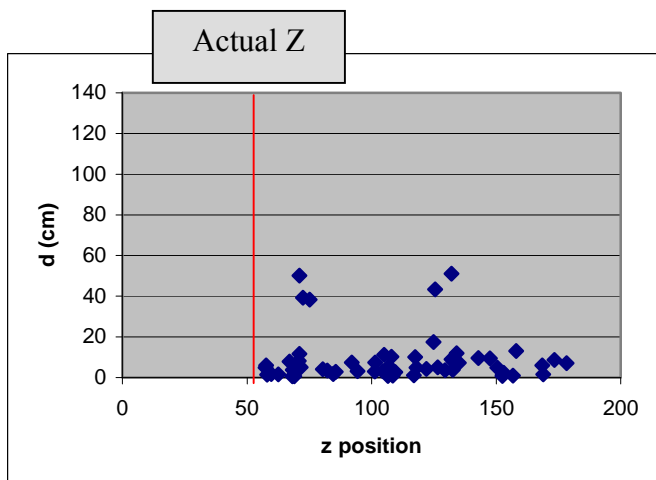


Figure 7.36: Graph of d versus Z position 2D

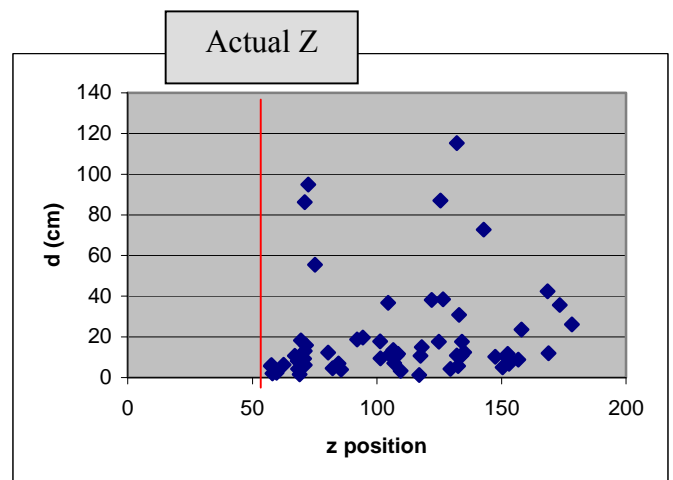


Figure 7.37: Graph of d versus Z position 3D

7.1.3.4 Graphs of d versus length, width, alpha, gamma Y and Z position for impact D.

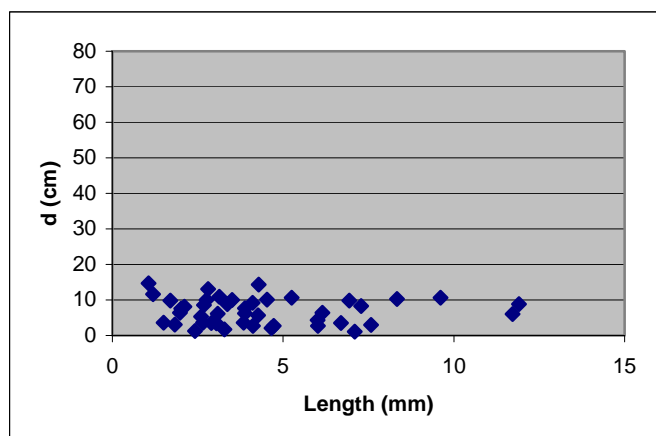


Figure 7.38: Graph of d versus bloodstain length 2D

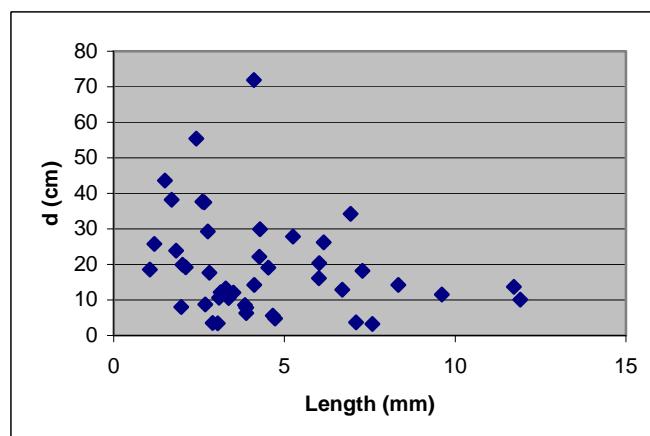


Figure 7.39: Graph of d versus bloodstain length 3D

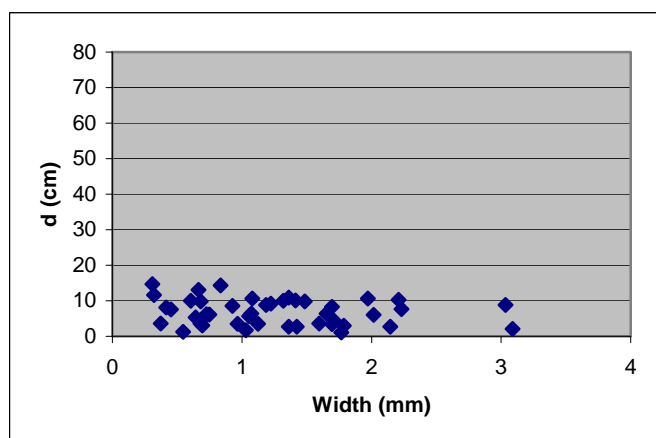


Figure 7.40: Graph of d versus bloodstain width 2D

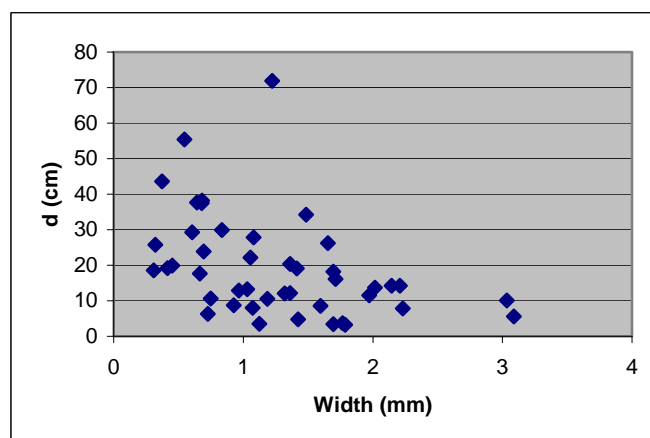


Figure 7.41: Graph of d versus bloodstain width 3D

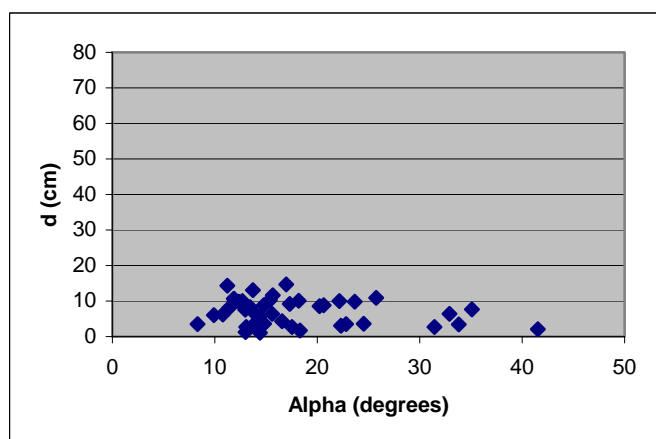


Figure 7.42: Graph of d versus alpha 2D

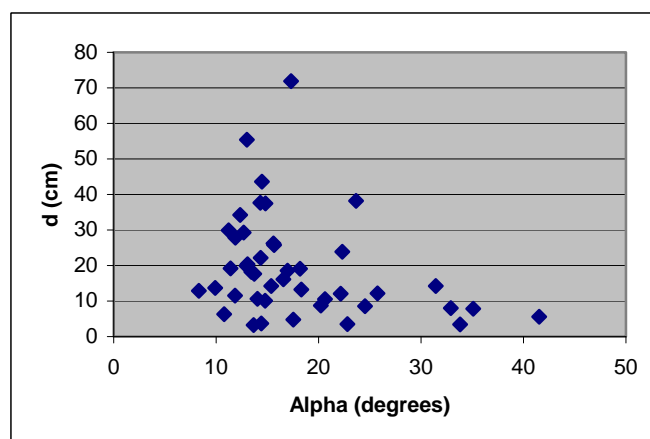


Figure 7.43: Graph of d versus alpha 3D

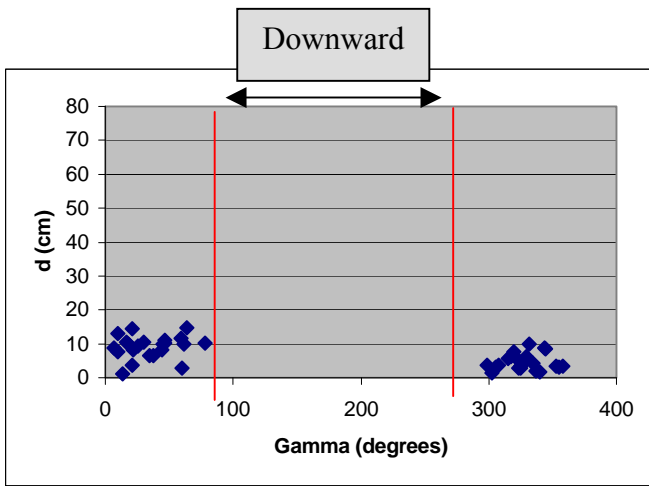


Figure 7.44: Graph of d versus gamma 2D

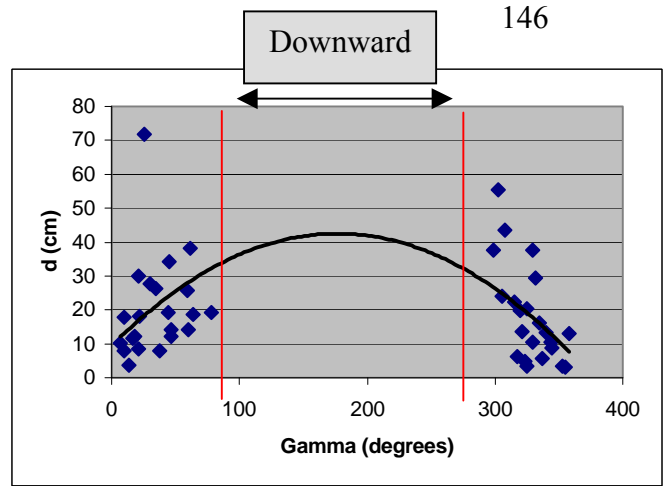


Figure 7.45: Graph of d versus gamma 3D

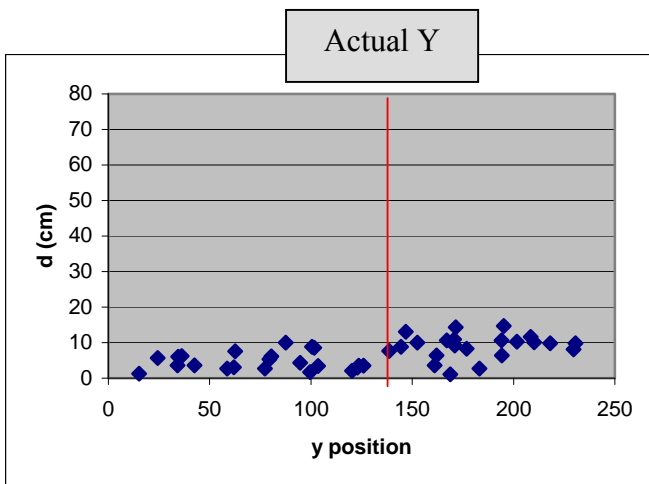


Figure 7.46: Graph of d versus Y position 2D

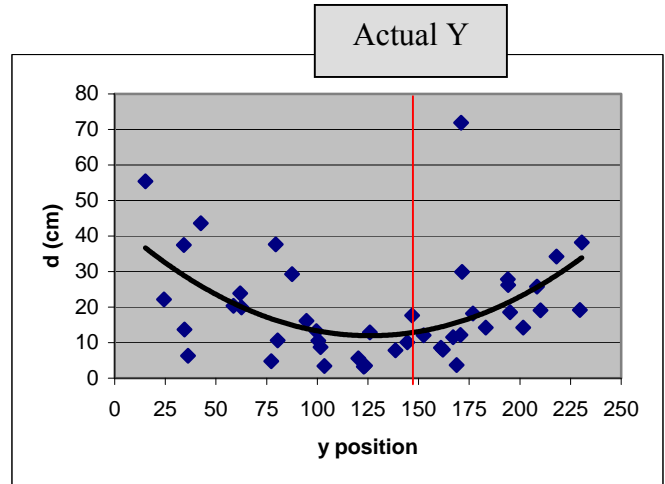


Figure 7.47: Graph of d versus Y position 3D

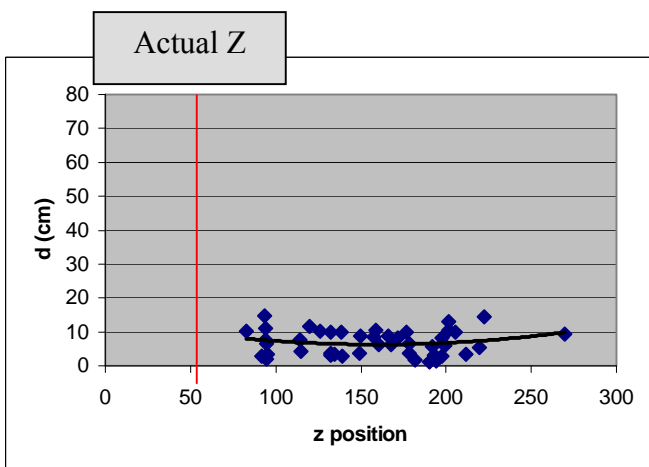


Figure 7.48: Graph of d versus Z position 2D

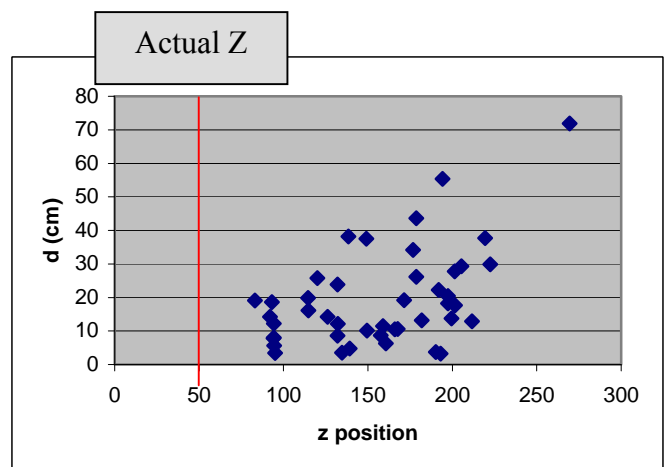


Figure 7.49: Graph of d versus Z position 3D

7.1.4 Discussion

When a bloodstain pattern analyst begins the process of determining the region of origin, a number of bloodstains are first selected for analysis. This experiment was carried out to determine the bloodstain parameters that are of importance in ensuring an accurate region of origin calculation. Only parameters that could be easily considered at a crime scene were included in the analysis.

The most prominent trend was observed when d was plotted against gamma. For gamma values close to 0 and 360°, d was small and for gamma values approaching 180° d was large. The trend was more pronounced for the 3D calculation of d than for the 2D. The reason for this observation is that a bloodstain travels in a parabolic flight path; however it is traced back to the point of origin with a virtual string that has a straight trajectory. The result is an overestimation in the Z-axis. This explains why d was greater in the 3D calculation, which took into consideration error from the X, Y and Z-axes. The gamma values that gave the most accurate result were those greater than 280° and those less than 80°.

The graphs of length, width and alpha versus d showed no trend for both the two and three-dimensional analysis. Alpha is calculated using the equation $\alpha = \sin^{-1} (W/L)$. It is therefore directly related to the length and width of a bloodstain and considering these two parameters do not show any trend when plotted against d , alpha would not be expected to. A computer-based method was used to fit an ellipse to the bloodstains for measuring their width and length and in this experiment both small and large bloodstains produced similar results when determining how accurately they predict the region of origin. Bloodstains that are large or small should therefore not be discounted from an analysis however if small bloodstains are considered in the analysis, a computer-based method should be used to fit the ellipse.

The preponderant stain theory, proposed by Bevel and Gardner and introduced in chapter 4, section 4.2.1, states that when an impact spatter pattern is generated the time at which the most common sized bloodstain is formed is when the maximum force is being applied to the blood source. If this theory is true, it may also be true that by selecting bloodstains that are the size of the most common size in the impact pattern the bloodstains will produce the most accurate results as they were generated

at the time the maximum amount of force was applied and therefore travelled with the flattest trajectory. So while the size of a bloodstain did not affect d in this experiment, it cannot be discounted as a parameter that may affect the accuracy of a region of origin determination.

Some of the graphs of Y position versus d show a trend (Figures 7.13, 7.25 and 7.49). This is a 'u' shaped graph where one point has a small d value (towards the centre of the graph) and the y position on either side of this point have greater d values forming a u shape. In all cases this trend was more pronounced in the 3D analysis. The point at which the d value was the smallest was when the Y position was approximately the same as the actual Y position of the point of origin. This suggests that by selecting bloodstains close to the point of convergence, the region of origin determination will be more accurate. Bloodstains at Y positions greater than about 50 % of the distance to the furthest out bloodstains had greater d values than bloodstains that were closer to the area of convergence. This suggests that by measuring the distance to the furthest out bloodstain in the Y -axis and dividing this distance by 2 then selecting bloodstains within this calculated distance from the area of convergence, the results will be the most accurate.

No obvious correlation was seen on the Z position versus d graphs for each of the four impacts. This may mean that there is no relationship between the height of a bloodstain on a surface (in this case a wall) and how accurately it predicts the region of origin. This finding is further investigated in Section 7.2.

The d values for Impact C were the greatest. This impact was generated by striking a 10 ml pool of blood three times with a hammer. Out of all of the four impacts generated, it is likely that this impact was generated with the greatest variability (most strikes, largest quantity of blood and a comparatively low velocity impact compared to that made with the impact device) therefore the results are consistent with the type of impact.

7.1.5 Conclusion

This experiment quantified the ability of individual bloodstains to determine the point of origin and related the ability, quantified as d , to various parameters of that

bloodstain. The six parameters that were studied included the width and length of the bloodstain, the angle of impact, the glancing angle and the Y and Z position of the bloodstain on the wall. Of all of these parameters the glancing angle, gamma was found to have the most significant effect on d.

Gamma values close to 0 and 360° resulted in the most accurate point of origin estimate so bloodstains with these glancing angles should be selected when determining the region of origin.

The length and width of a bloodstain, when individually studied, did not have an effect on the accuracy of the point of origin determination.

When the Y position was plotted against d, a trend was observed in the graphs for all of the impacts. The d value was generally the smallest when the Y position was approximately equal to the actual position of the bloodstain on the wall. This suggests that bloodstains close to the point of convergence in the Y-axis would be the most useful for a region of origin determination.

Some of the findings of this experiment will be further investigated in section 7.2.

7.2 The time of flight of blood drops

7.2.1 Introduction

The survey carried out in chapter 6 revealed that analysts often select bloodstains that they believe impacted a target surface at a high velocity when determining the region of origin. The reason for this is that bloodstains travelling at a relatively high velocity may have been travelling in the air for less time and therefore would have had less time to be affected by gravity. This means that the trajectory would more closely represent a straight line rather than a parabola. When determining the region of origin in BPA the main assumption that is made is that the blood drops that land on the target surface travelled in a straight line. This is in most cases not true and results in the Z coordinate of the region of origin being overestimated.

The objective of this experiment was to use the equation of motion to determine the velocity at which a number of blood drops from four impact patterns impacted a target surface and to establish if there is a relationship between the time the blood drops are in the air for and the d value calculated in Section 7.1 (the error in the region of origin estimation).

7.2.2 Method

Ignoring the effects of air resistance, a blood drop with an initial velocity, V_i accelerating at a rate a has a velocity at time t given by:

$$V_f = V_i + at \quad [7.5]$$

There are two components to the parabolic flight path of a blood drop, the horizontal component and the vertical component (Fig. 7.50). Because the plane of the wall on which the bloodstains land is the YZ plane, these letters will be used for the equations. The horizontal component is Y and the vertical component is Z. Equation 7.5 can therefore be written relating to these two components:

$$\text{Horizontal component (Y): } V_{fy} = V_{iy} + a_xt \quad [7.6]$$

$$\text{Vertical component (Z): } V_{fz} = V_{iz} + a_zt \quad [7.7]$$

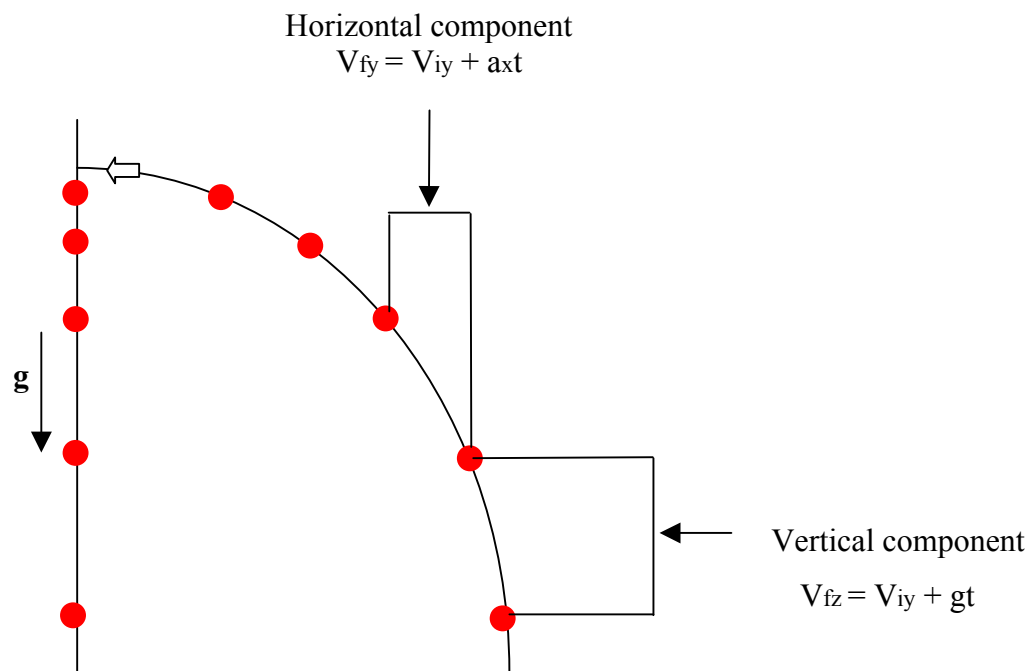


Figure 7.50 The horizontal and vertical components of the flight path of a blood drop.

For horizontal motion, $a_x = 0$ therefore $V_{fy} = V_{ix}$. For vertical motion $a_z = \mathbf{g}$. This means that the equations can be rewritten as:

$$\text{Horizontal component (Y): } V_{fy} = V_{iy} \quad [7.8]$$

$$\text{Vertical component (Z): } V_{fz} = V_{iz} + gt \quad [7.9]$$

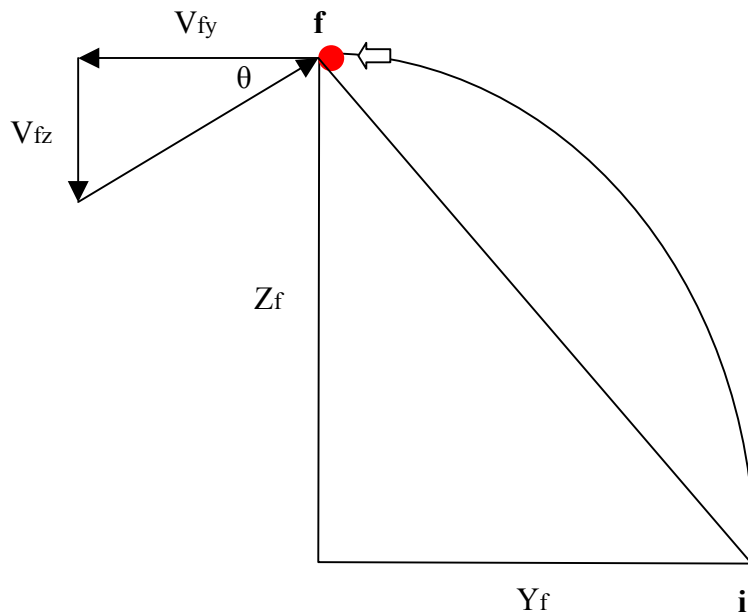


Figure 7.51 Diagram showing point f, V_{fy} , V_{fz} , Z_f , Y_f and i.

At a point f in the parabolic flight path (Fig. 7.51):

$$\tan \theta = \frac{V_{fz}}{V_{fy}} \quad [7.10]$$

$$\text{Given: } Z_f = V_{iz} \cdot t$$

$$Y_f = V_{iy} \cdot t \quad [7.11]$$

$$Z_f = V_{iz} \cdot t + \frac{1}{2}gt^2 \quad [7.12]$$

$$\tan \theta = \frac{V_{fz}}{V_{fy}} = \frac{V_{iz} + gt}{V_{iy}} \quad [7.13]$$

Substitute for V_{iz} from [7.12] and V_{iy} from [7.11]:

$$= \frac{\frac{Z_f - \frac{1}{2}gt^2}{t} + gt}{Y_f / t}$$

Therefore:

$$\tan \theta = \frac{Z_f + \frac{1}{2}gt^2}{Y_f}$$

Finally:

$$\boxed{t^2 = \frac{2(Y_f \tan \theta - Z_f)}{g}} \quad [7.14]$$

Equation 7.14 allows the time that a blood drop is travelling through the air, after an impact has occurred until it touches the wall, to be calculated.

The data from four impact patterns was input to a Microsoft ® Excel 2000 spreadsheet. This data included:

- The d value (3D),
- Gamma,
- Y position of the bloodstain on the wall,
- Z position of the bloodstain on the wall.

The impact patterns that were used were the impacts made in Section 7.1 and details of the method of generation of these impacts can be found in Table 7.1.

The t^2 value was calculated using equation 7.14 and a graph was plotted for each impact pattern of t^2 versus d. A linear trend line was fitted to each graph in Excel.

7.2.3 Results

t^2 was successfully calculated using equation 10. The time the blood droplets were in the air for ranged from less than 30 ms to about 600 ms. This time range is consistent with results observed using the high-speed camera.

Graphs were plotted for each impact pattern (A-D) of t^2 versus d (Figures 7.52 – 7.55).

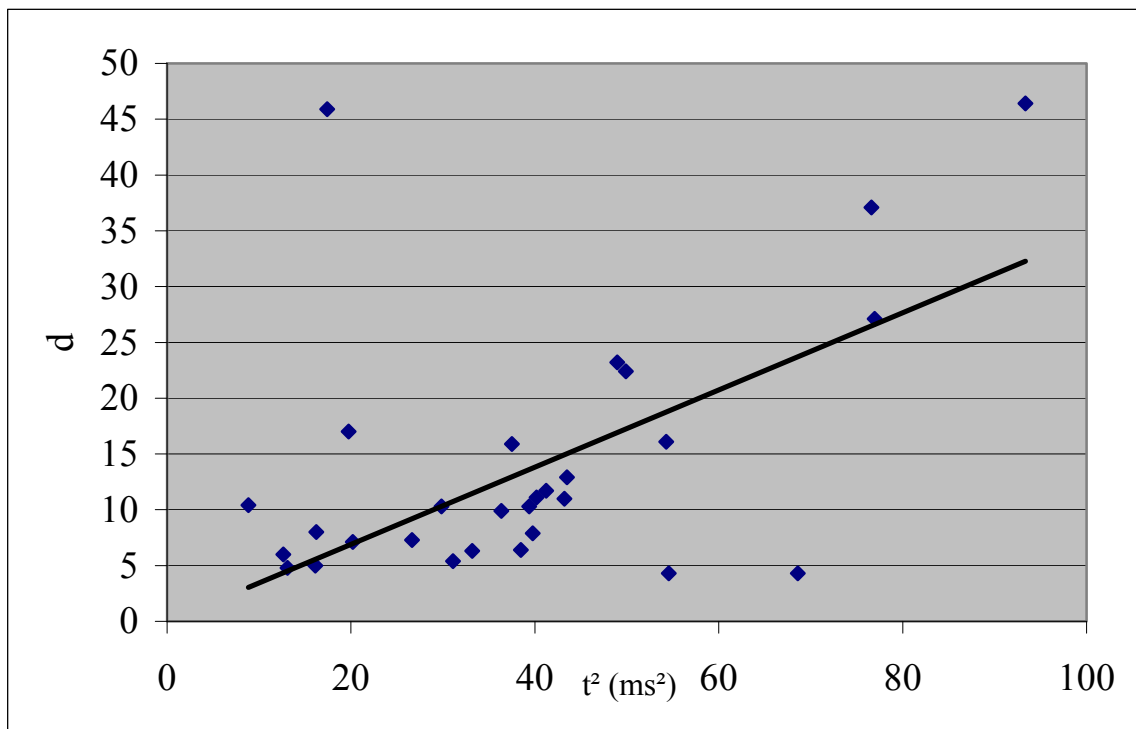


Figure 7.52 The time a bloodstain travelled through the air (t^2) before impacting a wall versus the amount of 3D error in the region of origin estimation (d) for Impact A.

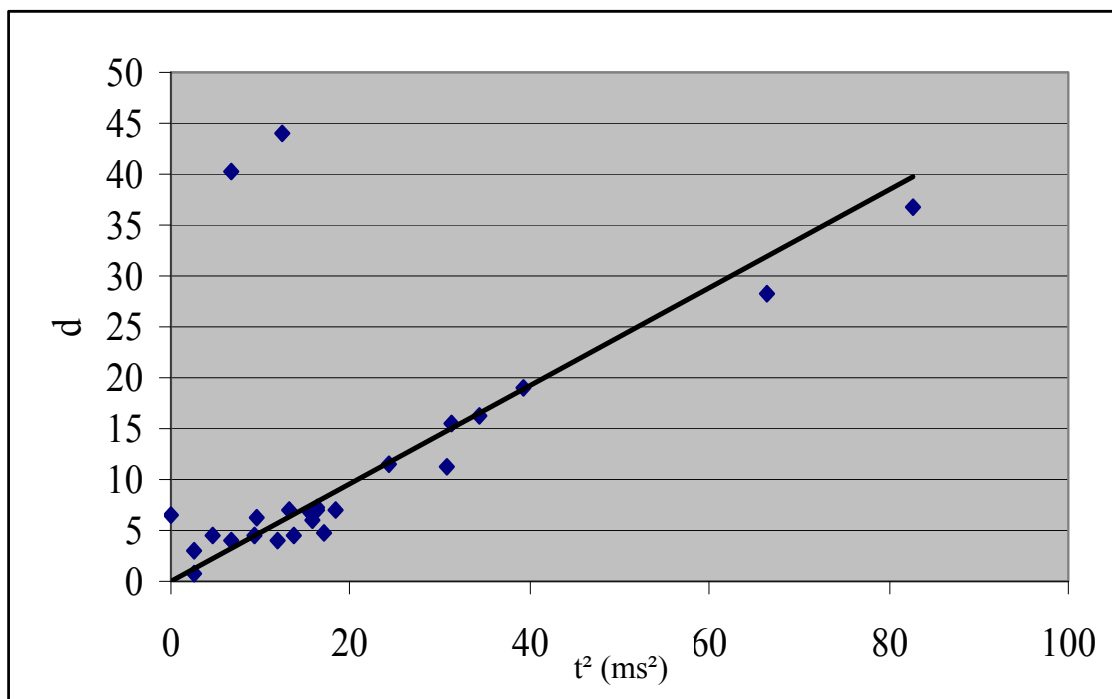


Figure 7.53 The time a bloodstain travelled through the air (t^2) before impacting a wall versus the amount of 3D error in the region of origin estimation (d) for Impact B.

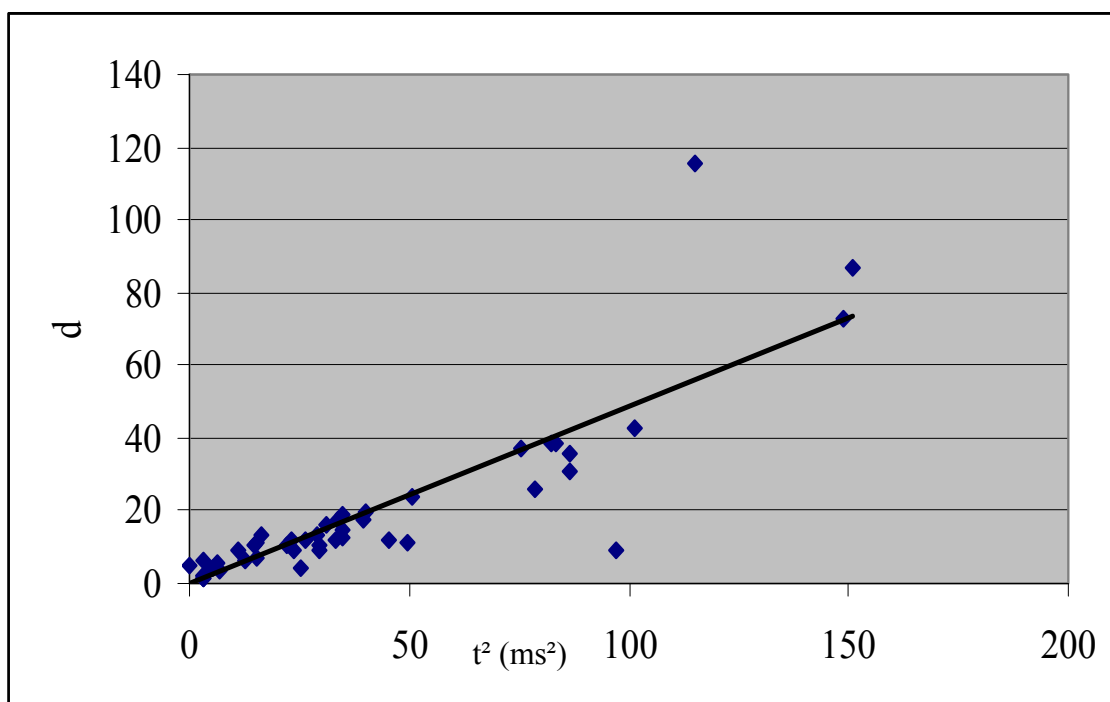


Figure 7.54 The time a bloodstain travelled through the air (t^2) before impacting a wall versus the amount of 3D error in the region of origin estimation (d) for Impact C.

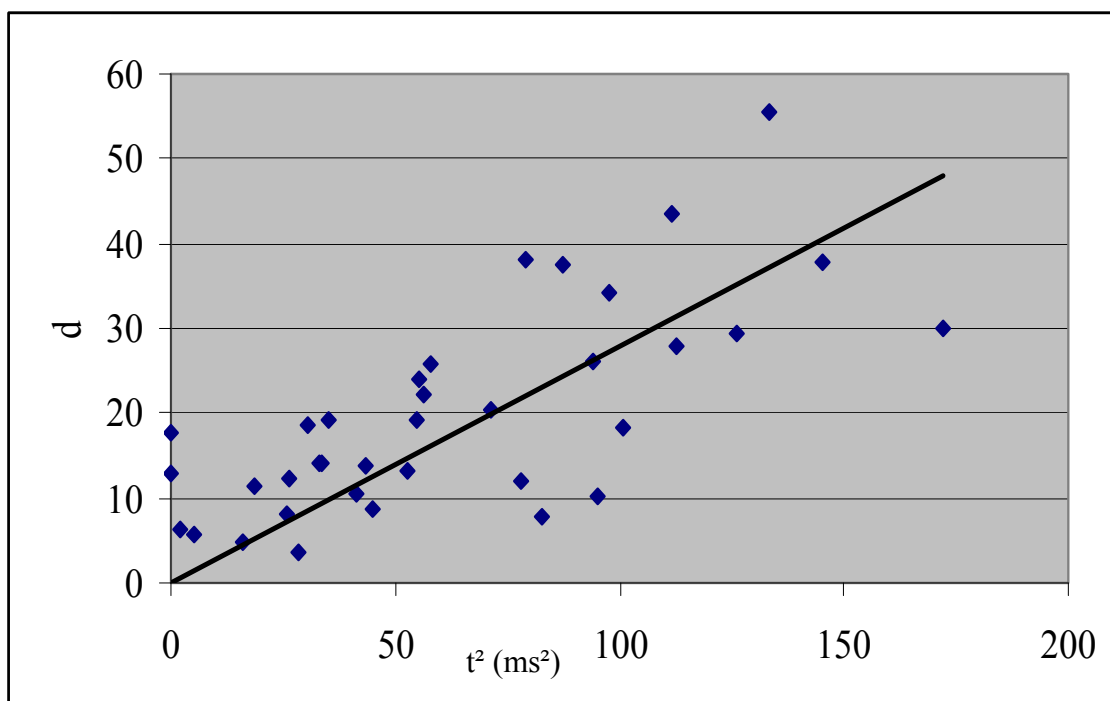


Figure 7.55 The time a bloodstain travelled through the air (t^2) before impacting a wall versus the amount of 3D error in the region of origin estimation (d) for Impact D.

7.2.4 Discussion

All four graphs show that as the time a blood drop is in the air increases, so does d , the 3D error in the region of origin estimation. This shows that the time of flight is the main parameter that contributes to the error in the Z coordinate of the region of origin estimate.

This result concurs with the results from section 7.1 where a strong correlation was seen between d and the gamma value. When the bloodstain had a gamma value close to 0 and 360°, the d value the smallest because the blood drop had not been significantly affected by gravity. The results of this experiment showed that the blood drops that were in the air for the longest time (meaning they have had more time to be affected by gravity) had the greatest d value.

The d and time square graphs for Impacts A - D did not correlate perfectly. There were points that were not on the trend line meaning gravity is not the only reason for errors in the region of origin estimate. Examples of other reasons include air resistance and measurement error.

The equations derived in this section allowed the time a blood droplet was in the air for to be calculated along with the velocity at which it was travelling. One of the main assumptions made when determining the region of origin is that the trajectory of the blood drops is a straight line. The trajectory is however parabolic meaning the Z coordinate of the region of origin is almost always overestimated. While this is generally accepted by analysts and is often mentioned when giving evidence, the way to minimise (or eliminate) this overestimation is to take into account the effect of gravity in region of origin calculations. In order to calculate the time of flight or the velocity of a blood drop, as was carried out in this section; the actual region of origin must be known. This is not the case when determining the region of origin at a crime scene and therefore the equation could not be applied to the current methods available for determining the region of origin. In the future however it may be possible to analyse a large number of bloodstains using an automated system and with the use of a computer estimate the region of origin. This estimate could then be used to calculate the time in flight of each blood drop and then the blood drops that have been in flight for the longest could be eliminated from the analysis. This would provide a

region of origin estimate accounting for the effect of gravity meaning the Z coordinate of the region of origin no would no longer exhibit such large uncertainty.

7.2.5 Conclusion

Overall this study has demonstrated that gravity is the principal reason for a systematic overestimation in the Z-axis when determining the region of origin. In order to minimise this overestimation, gravity needs to be accounted for in the region of origin calculations. Because of the complexity of the equations that allow gravity to be accounted for, it is likely that an automated method for bloodstain analysis would have to be developed before this extra step could be included in the analysis.

7.3 Investigation of stain selection theories

Three different theories for bloodstain selection are investigated in this section including the selection of well-formed bloodstains, the selection of an equal number of bloodstains from either side of an impact pattern and the number of bloodstains that should be selected from an impact pattern. The objective of this investigation is to assess whether each of these three theories should be considered when determining the region of origin.

7.3.1 Well-formed bloodstains

A well-formed bloodstain is a bloodstain that when divided along its major axis has an opposite half that looks identical to it (Fig. 7.56). Examples can be seen in Figure 7.57 (a-d).

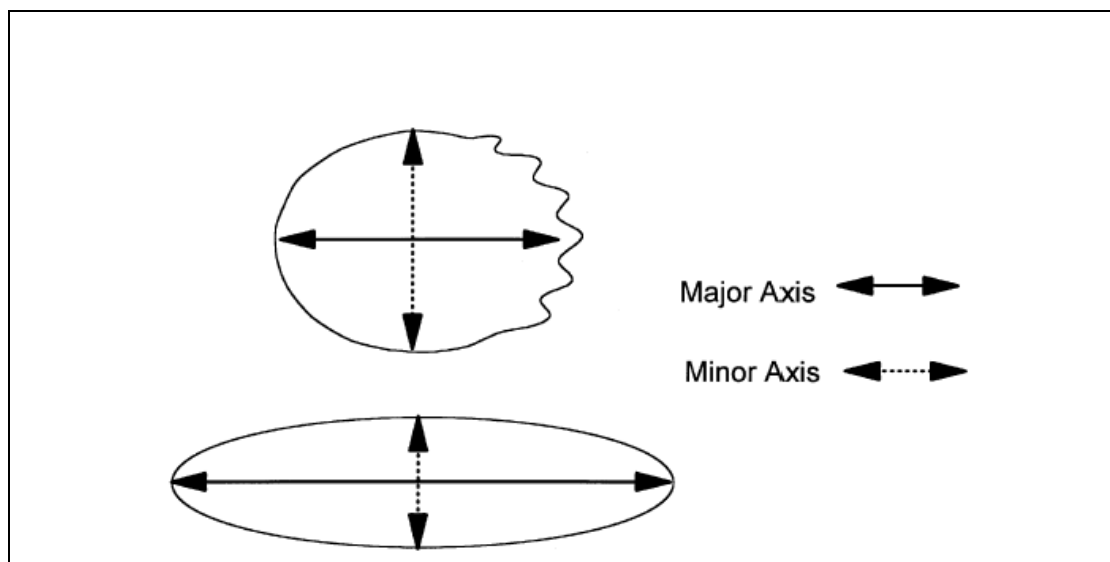


Figure 7.56 The concept of a well-formed bloodstain. If the bloodstain is divided along its major axis, the opposite halves would be equal to each other [30].

Well-formed bloodstains should be selected for an angle of impact calculation because the analyst can more accurately measure the width and length. Examples of bloodstains that are not well-formed are shown in Figure 7.58 (a-d).

- The perimeters of bloodstain **a** are very hard to distinguish.
- Bloodstains **b** and **c** are not symmetrical along the major axis.
- The perimeters of bloodstain **d** are very hard to distinguish because of the surface on which the blood landed. This bloodstain is also not symmetrical.

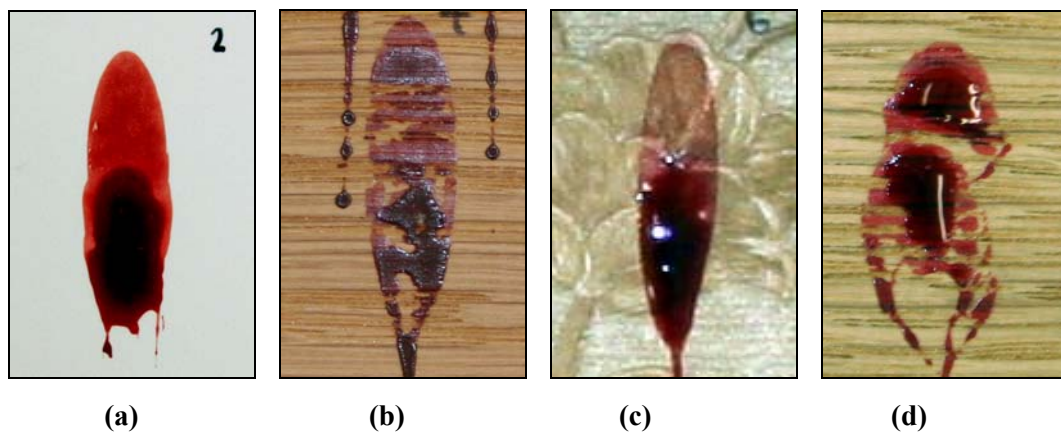


Figure 7.57 Examples of bloodstains that are not well-formed.

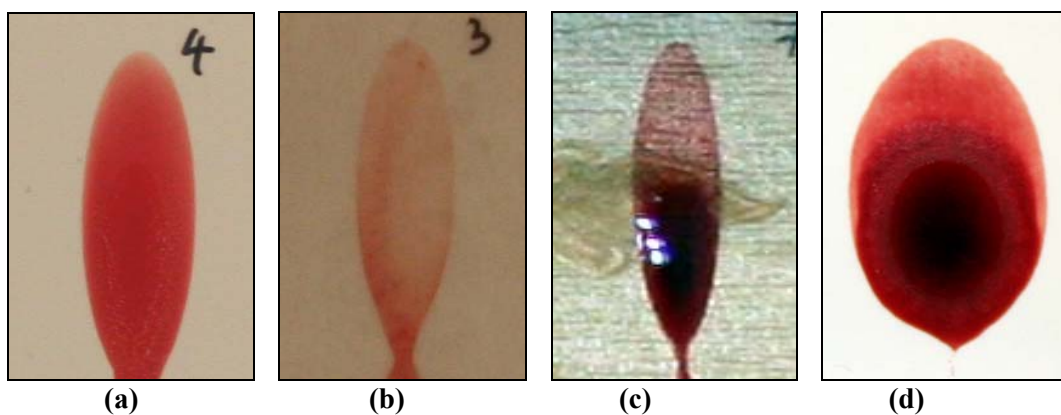


Figure 7.58 Examples of bloodstains that are well-formed.

Figure 7.59 shows examples of bloodstains with ellipses fitted to them. Bloodstain **b** is a well-formed stain and the ellipse was fitted easily and accurately to the bloodstain. Bloodstains **a** and **c** are not well-formed bloodstains and the ellipses could not be fitted easily or accurately.

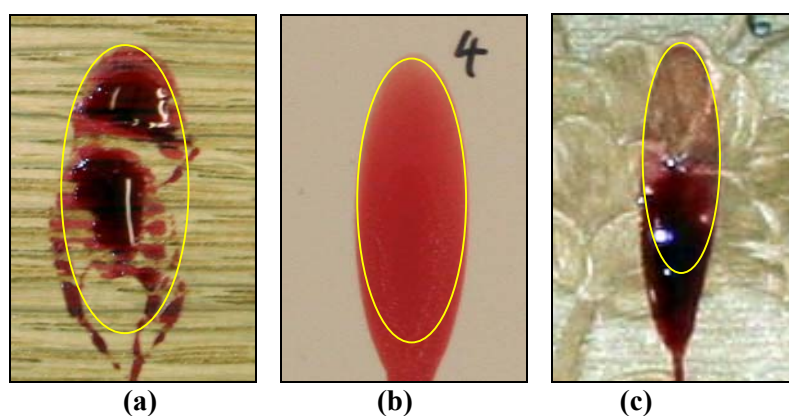


Figure 7.59 Examples of bloodstains with ellipses fitted to them. Bloodstain b is a well-formed stain and a and c are not.

In general when selecting bloodstains from an impact pattern, where available, well-formed bloodstains should be selected for analysis. This is because it is easier to fit an ellipse meaning that the width and length of the bloodstain can be more accurately measured.

7.3.2 The effect of selecting an equal number of bloodstains from an impact pattern when using a manual method to determine the region of origin

7.3.2.1 Introduction

In the survey described in Chapter 6, 10 out of 14 analysts stated that they would select an equal number of bloodstains from each side of the impact spatter pattern. The reason for this was not provided in the surveys but may be to ensure that the region of origin result is as accurate as possible, especially when manual methods are used.

7.3.2.2 Method

An impact spatter pattern was generated by striking a 5 ml pool of blood with a hammer. The blood was placed on Parafilm on a 10 cm² block of wood, at a known position in three-dimensional space. The impact pattern was labelled Impact 1 and twenty bloodstains were labelled with a scale, a number and a vertical line (Appendix 2). The bloodstains were then photographed individually and the photos were transferred to a computer for analysis. The gamma angle of each bloodstain was determined using Microsoft ® Office Visio ® Professional 2003. A photograph was also taken of each impact pattern from a distance so that the position of each bloodstain relative to the other bloodstains could be visualised. The actual point of origin for Impact 1 was $x = 32$ cm, $y = 135.5$ cm and $z = 50.2$ cm. All values are ± 2 cm due to the position at which the blood was struck with the hammer differing from the point measured, which was the point at the exact centre of the 5 ml blood pool.

An image of the entire spatter pattern was opened in Microsoft ® Office Visio ® Professional 2003 and lines were drawn through a number of bloodstains at the gamma angle. This allowed an area of convergence to be visualised. This process was repeated using first a balanced selection of bloodstains (2 from each side of the

pattern) and then with an unbalanced selection (2 from one side and four from the other side).

7.3.2.3 Results

Figure 7.60 shows the area of convergence when an equal number of bloodstains were selected from each side of the impact pattern and Figure 7.61 shows the area of convergence when an unequal number were selected.

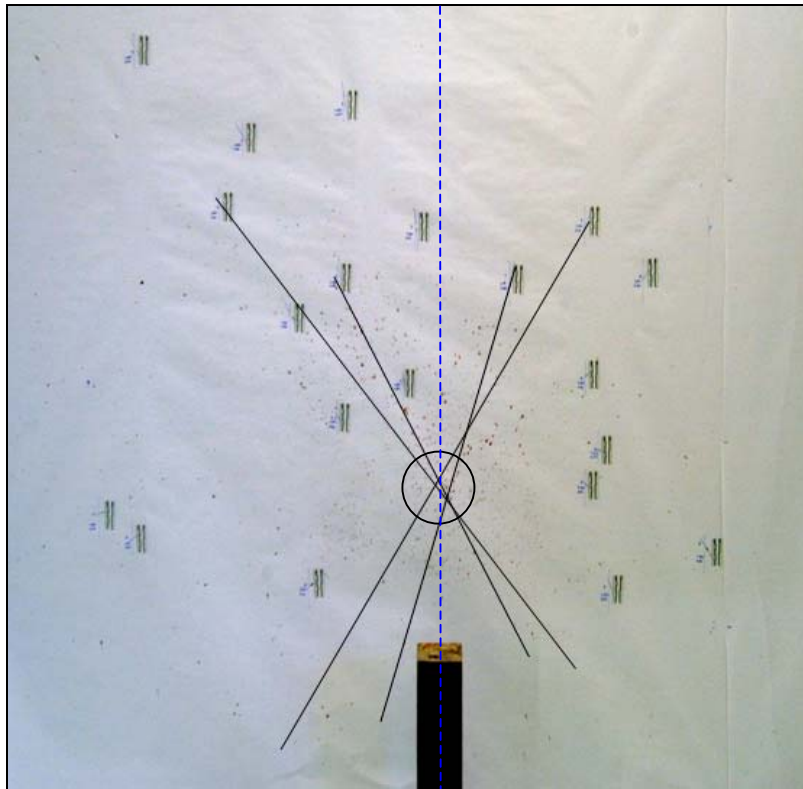


Figure 7.60 The area of convergence when an equal number of bloodstains were selected from each side of the impact pattern.

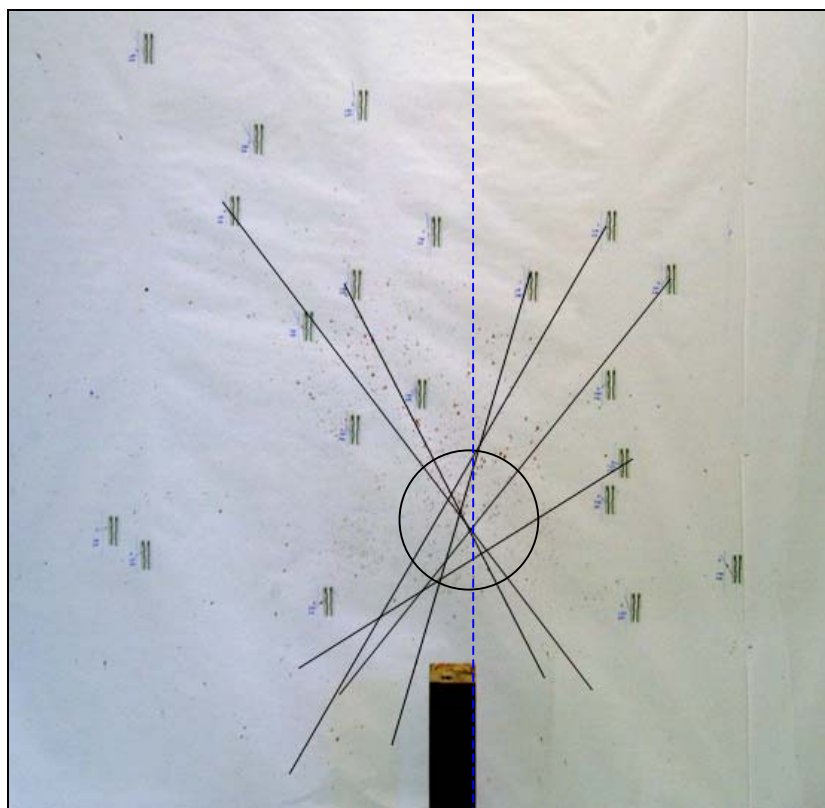


Figure 7.61 The area of convergence when an equal number of bloodstains were selected from each side of the impact pattern.

7.3.2.4 Discussion

The result of using an unbalanced selection of bloodstains was that the position of the point of convergence changed. When a balanced selection was used, the area of convergence was smaller and closer to the actual point of convergence and when an unbalanced number of bloodstains were selected from each side of the impact pattern the area of convergence shifted and increased in area (Figures 7.60 and 7.61).

One of the effects of an inaccurate point of convergence estimate is that the Y and Z coordinate estimates would be inaccurate. Because of this the D measurements, (distance from a bloodstain to the point of convergence) which are made in order to calculate the region of origin using the tangent method, would be inaccurate.

Therefore the overall effect of selecting an unequal number of bloodstains from each side of an impact pattern is that the X, Y and Z coordinate estimates of the region would be less accurate they would be if an equal number of bloodstains was selected from each side the pattern.

In conclusion when using a manual method to determine the region of origin, an equal number of bloodstains should be selected from each side of the impact pattern.

7.3.3 Assessing whether the accuracy of a region of origin estimate improves as the number of bloodstains selected for the analysis increases

7.3.3.1 Introduction

The survey carried out in Chapter 6 revealed that some analysts would select as little as 8 bloodstains for a region of origin analysis, while others would select up to 24 for this purpose.

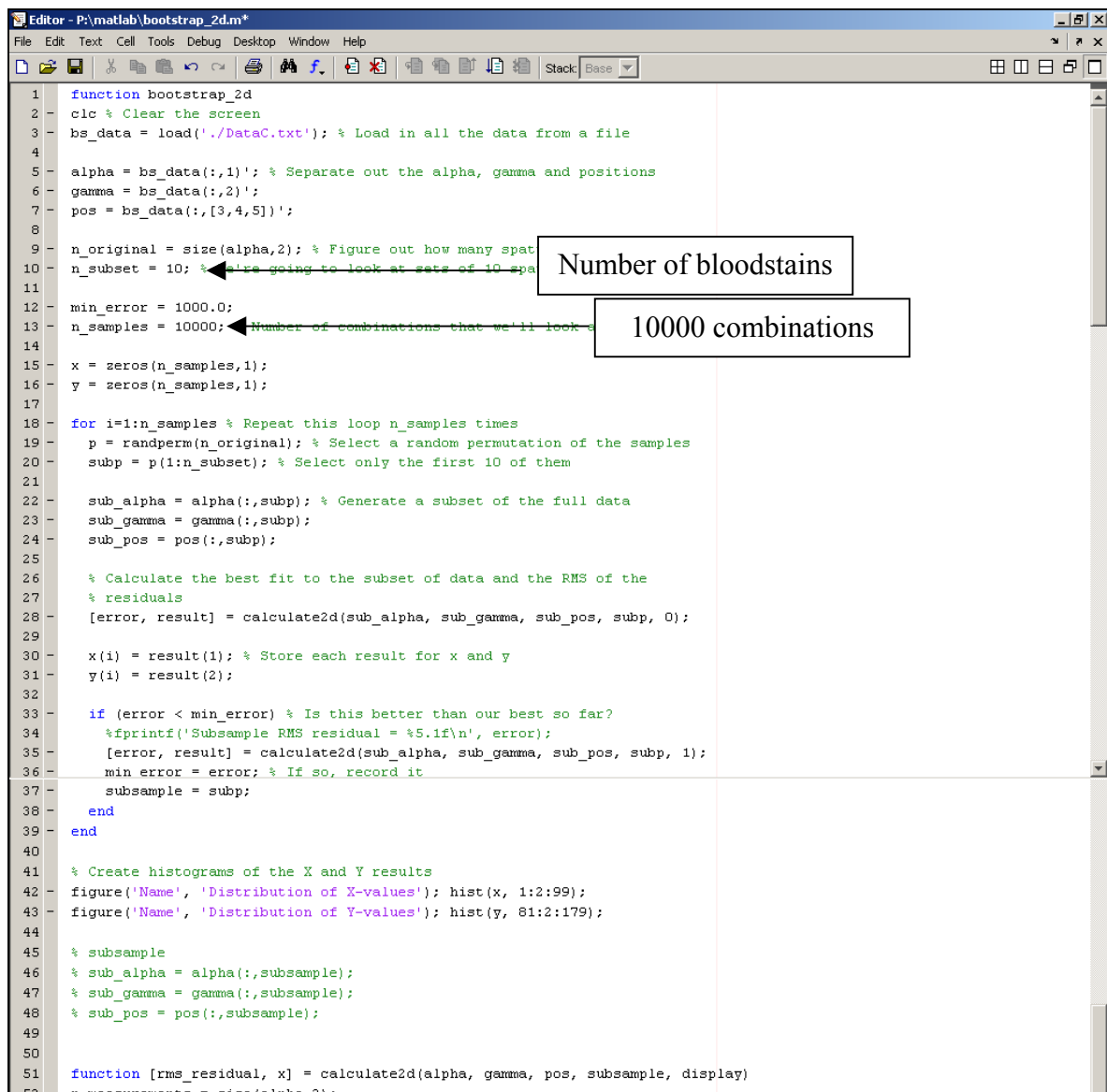
The objective of this experiment is to determine if the X, Y coordinates of the region of origin become more accurate as the number of bloodstains selected for the analysis increases.

The X and Y coordinates were evaluated in this experiment and the Z coordinate was not. This is because it has already been established that there is a systematic overestimation of this value and increasing sample size does not reduce systematic errors. The X and Y coordinates should however only exhibit random error and it is therefore expected that as the number of bloodstains selected increases, so too will the accuracy of the X and Y coordinates.

7.3.3.2 Method

Because of the large sample sizes and time restrictions, MATLAB® was used to analyse the angle of impact, gamma angle and X, Y and Z position of 80 bloodstains (see Appendix 2). Data from Impact C was used and the details for the generation of this pattern is given in Table 7.1 of this chapter.

The number of combinations used was 10000. The number of bloodstains selected varied from 10 – 40 (Fig. 7.62). Histograms of the distribution of each of the coordinates were generated in MATLAB®. The results represented a situation where 10000 people randomly selected a set of bloodstains (10, 20, 30 or 40) from the 80 bloodstains documented from Impact C.



```

1 function bootstrap_2d
2 clc % Clear the screen
3 bs_data = load('./DataC.txt'); % Load in all the data from a file
4
5 alpha = bs_data(:,1)'; % Separate out the alpha, gamma and positions
6 gamma = bs_data(:,2)';
7 pos = bs_data(:,[3,4,5])';
8
9 n_original = size(alpha,2); % Figure out how many spat
10 n_subset = 10; % Number of bloodstains
11
12 min_error = 1000.0;
13 n_samples = 10000; % 10000 combinations
14
15 x = zeros(n_samples,1);
16 y = zeros(n_samples,1);
17
18 for i=1:n_samples % Repeat this loop n_samples times
19     p = randperm(n_original); % Select a random permutation of the samples
20     subp = p(1:n_subset); % Select only the first 10 of them
21
22     sub_alpha = alpha(:,subp); % Generate a subset of the full data
23     sub_gamma = gamma(:,subp);
24     sub_pos = pos(:,subp);
25
26     % Calculate the best fit to the subset of data and the RMS of the
27     % residuals
28     [error, result] = calculate2d(sub_alpha, sub_gamma, sub_pos, subp, 0);
29
30     x(i) = result(1); % Store each result for x and y
31     y(i) = result(2);
32
33     if (error < min_error) % Is this better than our best so far?
34         fprintf('Subsample RMS residual = %5.1f\n', error);
35         [error, result] = calculate2d(sub_alpha, sub_gamma, sub_pos, subp, 1);
36         min_error = error; % If so, record it
37         subsample = subp;
38     end
39 end
40
41 % Create histograms of the X and Y results
42 figure('Name', 'Distribution of X-values'); hist(x, 1:2:99);
43 figure('Name', 'Distribution of Y-values'); hist(y, 81:2:179);
44
45 % subsample
46 % sub_alpha = alpha(:,subsample);
47 % sub_gamma = gamma(:,subsample);
48 % sub_pos = pos(:,subsample);
49
50
51 function [rms_residual, x] = calculate2d(alpha, gamma, pos, subsample, display)
52 % measurements = size(alpha,2);

```

Figure 7.62 MATLAB® editor showing the number of combinations and bloodstains selected.

7.3.3.3 Results

Figures 7.63 – 7.70 are histograms showing the X and Y distribution for Impact C when different numbers of bloodstains were randomly selected 10000 times. As the number of bloodstains selected increased, both the X and Y distribution decreased.

Impact C: Actual region of origin: X = 25 cm, Y = 138 cm

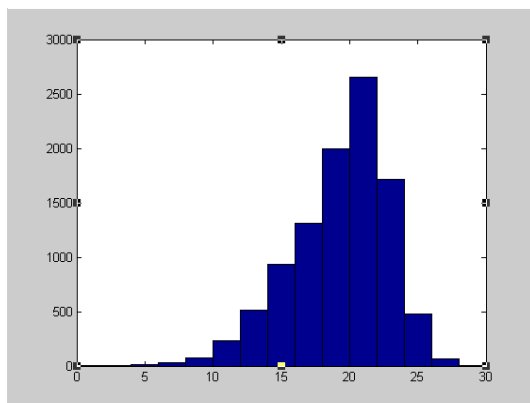


Figure 7.63 The X distribution when 10000 groups of 10 bloodstains were randomly selected from Impact C.

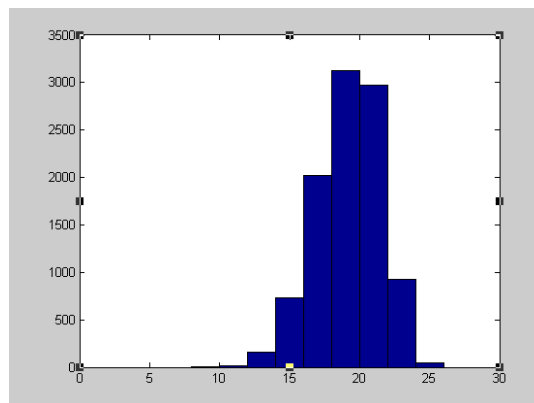


Figure 7.64 The X distribution when 10000 groups of 20 bloodstains were randomly selected from Impact C.

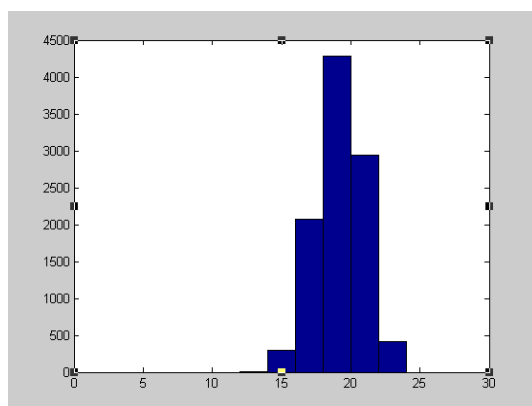


Figure 7.65 The X distribution when 10000 groups of 30 bloodstains were randomly selected from Impact C.

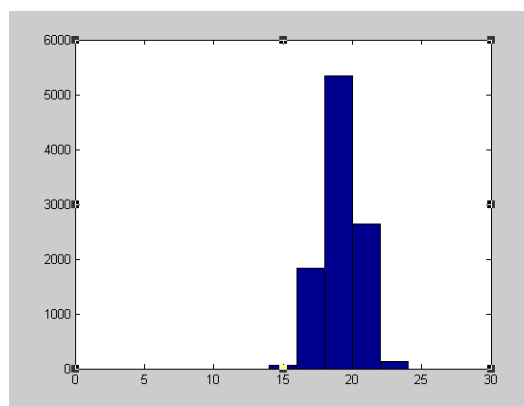


Figure 7.66 The X distribution when 10000 groups of 40 bloodstains were randomly selected from Impact C.

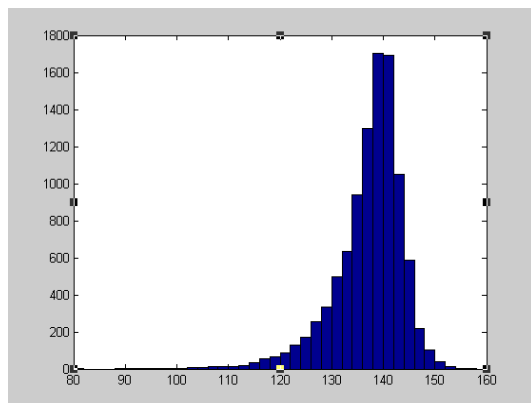


Figure 7.67 The Y distribution when 10000 groups of 10 bloodstains were randomly selected from Impact C.

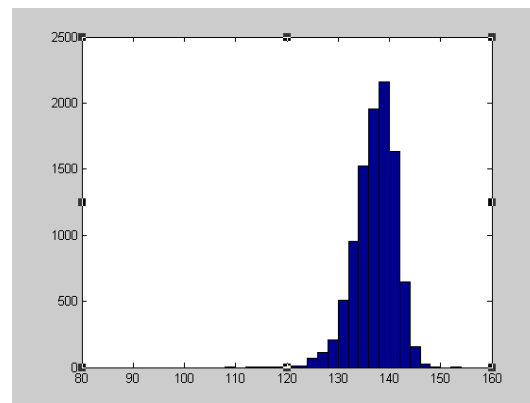


Figure 7.68 The Y distribution when 10000 groups of 20 bloodstains were randomly selected from Impact C.

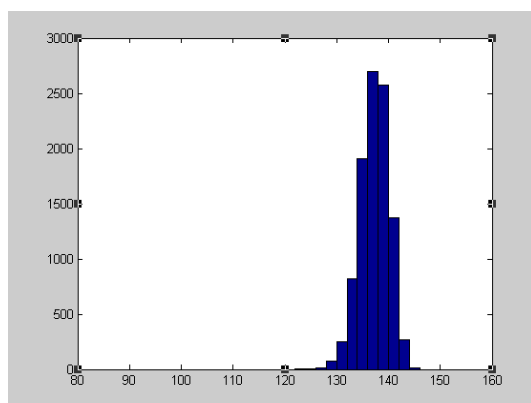


Figure 7.69 The Y distribution when 10000 groups of 30 bloodstains were randomly selected from Impact C.

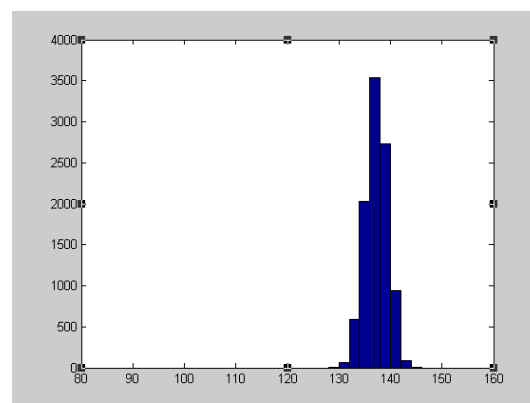


Figure 7.70 The Y distribution when 10000 groups of 40 bloodstains were randomly selected from Impact C.

7.3.3.4 Discussion

The results show that as the number of bloodstains randomly selected increased the X and Y distribution decreased (Fig 7.71). As the distribution decreased, the peak of the histograms more closely represented the true point of origin.

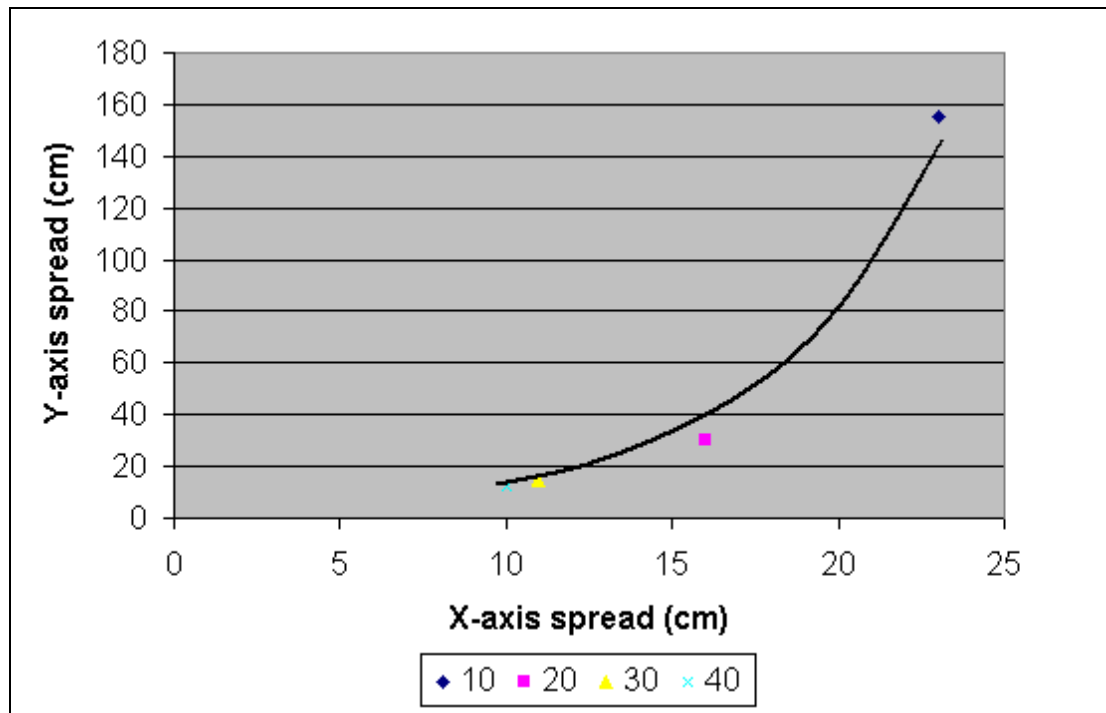


Figure 7.71 As the number of bloodstains randomly selected increased from 10 – 40 the spread of the X and Y-axis distribution decreased.

For Impact C, the Y peak was at about 140 cm and the actual point of origin coordinate was 138 cm. For Impact D the Y peak was at about 145 cm and the actual point of origin was at 146 cm. Therefore by selecting a greater number of bloodstains from the impact pattern the X and Y coordinates of the region of origin became more accurate, even when the bloodstains were selected randomly.

For Impact C, the X peak was at about 20 cm and the actual point of origin coordinate was 25 cm. The reason for this underestimation of the X coordinate may be due to the dynamics that occur when blood is struck in an impact situation. It was seen with high-speed photography that the blood travelled away from the impact site before beginning to travel upwards and split into droplets (Chapter 4). This would result in an underestimation of the X coordinate, which was what was observed here

These results show that even if bloodstains are selected randomly, as the number selected increases, so too does the accuracy of the X and Y estimates of the region of origin. Bloodstain pattern analysts would be likely to use some stain selection, which should result in even greater accuracy than the results seen here.

When an analyst is selecting bloodstains for a region of origin analysis they should be aware that the greater the number selected, the more accurate the X and Y estimates of the region of origin are likely to be.

The information from the survey (Chapter 6) showed that analysts generally select between 8 and 24 bloodstains for a region of origin analysis. The data from this study showed that selecting 20 bloodstains ensured the spread of the X and Y coordinates was reasonably small (Fig. 7.63). Selecting more than 20 did not significantly decrease the spread of the X and Y distribution, however selecting less than 20 did. Therefore if time allows approximately 20 bloodstains should be selected for the analysis. Given that the bloodstains were randomly selected in this experiment, stain selection would decrease the spread of the data even more making the results all the more accurate.

7.3.3.5 Conclusions

It was demonstrated in section 7.3.1 that well-formed bloodstains are a good choice when selecting stains for a region of origin determination. It is easier to fit an ellipse to a well-formed bloodstains meaning the width and length measurements of the bloodstain are likely to be more accurate, resulting in a more accurate angle of impact calculation. This in turn gives a more accurate result in the X-axis of the region of origin estimate.

It was demonstrated in section 7.3.2 that when using a manual method to determine the region of origin, an equal number of bloodstains should be selected from each side of the impact pattern. This minimises the amount of error in the X and Y coordinate estimates of the region of origin.

In section 7.3.3 it was demonstrated that as the number of bloodstains selected for a region of origin analysis is increased, the X and Y coordinate estimates become more accurate. This is because the X and Y coordinates exhibit random error and

consequently increasing the number of samples makes the results more accurate. Approximately 20 bloodstains should be selected from an impact pattern for a region of origin analysis.

Overall this section demonstrated why well-formed bloodstains should be selected from an impact pattern when determining the region of origin, why an equal number of bloodstains should be selected from each side of an impact pattern when using a manual method to determine the region of origin and why the maximum number of bloodstains should be selected from an impact pattern to get the most accurate region of origin result.

7.4 Bloodstain selection criteria

This research has identified a number of factors that are important when selecting bloodstains for a region of origin determination. Because every impact pattern is different, a very important part of the analysis is considering the factors that have contributed to the formation of the pattern. These include:

- The dynamics of the impact that the pattern resulted from.
- The surface on which the pattern is.
 - Whether it is a vertical or horizontal surface or a surface at another angle.
- The likely area of convergence.
- How many convergences there might be.
- The height and distance from the area of convergence of the furthest away bloodstains.
- The number of bloodstains available for analysis.
- Any other relevant factors.

Once the pattern has been considered as a whole, stain selection can begin at an individual-stain level. This research has investigated practical parameters that can be considered by an analyst when selecting bloodstains for a region of origin determination. Taking into account what was found in this research two separate sets of criteria are presented. One set for when a manual method is used to determine the region of origin and one for when directional analysis is used. In general however, the following parameters have been shown to be important when selecting bloodstains for a region of origin determination:

- How well the bloodstain has formed on the target surface.
- The directionality of the bloodstain (gamma)
- The size of the bloodstain
- The angle of impact
- The position of the bloodstain relative to the area of convergence.
- The number of bloodstains that are selected.
- Whether an equal number of bloodstains are selected from each side of the impact pattern.

Criteria for when a manual method/ directional analysis is used is given below. A reference to the section the relevant rational can be found in is given alongside each criterion.

MANUAL METHOD CRITERIA

- Well-formed bloodstains should be selected (7.3.1).
 - Upward moving bloodstains should be selected (7.1).
 - The gamma value of the bloodstains should be $> 280^\circ$ or $< 80^\circ$ (7.1).
 - If using a manual method to measure the width and length of the bloodstain, larger bloodstains should be selected. If small bloodstains are included in the analysis, a computer-based method should be used to fit an ellipse for measuring the width and length (5.1).
 - Bloodstains that are within about 50 % of the distance to the furthest out stain in the Y-axis should be selected (7.1).
 - An equal number of bloodstains from each side of the pattern should be selected (7.3.2).
 - Approximately 20 bloodstains should be considered in the analysis (7.3.3).
 - Elliptical bloodstains with an angle of impact less than 60° (7.1, 5.2 &).
-

DIRECTIONAL ANALYSIS CRITERIA

- Well-formed bloodstains should be selected (7.3.1).
 - Elliptical bloodstains with an angle of impact less than 60° (7.1 & 5.2).
 - *When only the X and Y coordinates are being calculated, the following criteria do not need to be considered. When Z is being calculated they should.*
 - Upward moving bloodstains should be selected (7.1).
 - The gamma value of the bloodstains should be $> 280^\circ$ or $< 80^\circ$ (7.1).
 - Bloodstains that are within about 50 % of the distance to the furthest out stain in the Y-axis should be selected (7.1).
 - Approximately 20 bloodstains should be considered in the analysis (7.3.3).
-

7.4 Selection strategies identified in bloodstain pattern analyst survey (Chapter 6)

In Chapter 6, a number of selection strategies were described by analysts with respect to how they select bloodstains from an impact pattern for a region of origin analysis. This section assesses whether these strategies are important in light of the results from this research.

The first point to comment on is the fact that only two analysts noticed that there was more than one area of convergence. This was because the impact device was dropped twice and although it was dropped from the same site, because the point of origin was ± 2 cm the two origins were each slightly different from each other. The two analysts that indicated that there was more than one convergence identified them by drawing reverse azimuths through the major axis of a number of bloodstains and visualising two distinct areas of convergence.

Two analysts indicated that they would select 'fast moving' bloodstains for analysis. While this research confirmed that fast moving bloodstains do provide the most accurate region of origin results, there is currently no way to determine which bloodstains were fast moving and which were not so this should not be stated as a reason for selecting bloodstains.

Three analysts indicated that they would select an equal number of bloodstains from each side of the impact pattern for analysis. Given that a much larger number said they would analyse the pattern using a manual method this may be a factor that needs to be given more consideration.

The positions from which the analysts selected the bloodstains from on the wall shows that they are mainly selecting them from the area around the area of convergence. This is consistent with the results from this research and should result in the most accurate results.

The number of stains selected by the analysts ranged from 8 – 24 and the results from this study showed that selecting approximately 20 for the analysis is satisfactory. Therefore the number of bloodstains that analysts are selecting may need to be

increased for the greatest precision to be achieved, especially from an impact pattern like the one that was given in the survey, consisting of a large number of bloodstains.

Several analysts indicated that they would select larger stains for analysts. This is good if the method used to fit the ellipse is a manual method. If a computer-based method is being used the size of the stains is not important.

Overall the analysts indicated the way in which they would select bloodstains for a region of origin analysis and the strategies were in many cases consistent with the results of this research. This reflects the experience of the participants in the survey, who were all practicing bloodstain pattern analysts.

Chapter conclusions

- The factors that were identified in this research as important when selecting bloodstains from an impact pattern for a region of origin analysis are:
 - How well the bloodstain has formed on the target surface.
 - The directionality of the bloodstain (gamma)
 - The size of the bloodstain
 - The position of the bloodstain relative to the area of convergence.
 - The number of bloodstains that are selected.
 - Whether an equal number of bloodstains are selected from each side of the impact pattern.
- If a manual method is used for the analysis the following criteria should be applied:
 - Well-formed bloodstains should be selected.
 - Upward moving bloodstains should be selected.
 - The gamma value of the bloodstains should be $> 280^\circ$ or $< 80^\circ$.
 - If using a manual method to measure the width and length of the bloodstain, larger bloodstains should be selected.
 - If small bloodstains are included in the analysis, a computer-based method should be used to fit an ellipse for measuring the width and length.
 - Bloodstains that are within about 50 % of the distance to the furthest out stain in the Y-axis should be selected.

- An equal number of bloodstains from each side of the pattern should be selected.
 - Approximately 20 bloodstains should be considered in the analysis.
 - Elliptical bloodstains with an angle of impact less than 60°
-
- When using directional analysis the following criteria should be applied:
 - Well-formed bloodstains should be selected.
 - Upward moving bloodstains should be selected.
 - The gamma value of the bloodstains should be $> 280^\circ$ or $< 80^\circ$.
 - Bloodstains that are within about 50 % of the distance to the furthest out stain in the Y-axis should be selected.
 - Approximately 20 bloodstains should be considered in the analysis.
 - Elliptical bloodstains with an angle of impact less than 60° .

CHAPTER EIGHT: FUTURE DIRECTIONS

This chapter discusses the questions that arose during the research that could be investigated in future work.

Future work on blood dynamics

Blood drops impacting different surfaces, blood drops impacting the same surface at different angles and impact events were recorded with a high-speed camera in this research. High-speed photography could be used to record impact events occurring in a more realistic situation like, for example, a weapon impacting skin. A wider view would also be useful to allow the path the blood droplets travel to be visualised.

Future work on the angle of impact

This research established that there is a significant difference between angle of impact results of blood drops that are on different surfaces. Further research is required to determine the exact amount of error for surfaces that are commonly found at crime scenes so the analyst can take this into account when determining the region of origin. The contact angle of blood on different surfaces could more accurately be measured using a goniometer.

Different surfaces could be fully characterised and then the angle of impact results related to different surface characteristics. A scanning electron microscope could be used to allow the surfaces to be characterised.

Future work on bloodstain selection

A survey was carried out in this research to establish the strategies employed by analysts to determine the region of origin. Each analyst circled the bloodstains that they would have selected and the impact pattern has been stored and thoroughly documented. This means that the region of origin could be calculated using the bloodstains each analyst selected to determine how well the strategy they employ works. The calculation for velocity, introduced in this research, could be integrated into a computer program for calculating the region of origin, in order to take into account gravity, providing a much more accurate region of origin result. In order to make this functional, an automated method for collecting data from the impact pattern would need to be developed. Finally the bloodstain selection criteria presented in this research could be validated in a validation study.

APPENDIX 1: HEALTH AND SAFETY PROCEDURES

General Health and Safety Procedures

Protective Clothing

Protective clothing was worn to cover the skin, eyes and mucus membranes, preventing contact with blood or any other chemical or hazardous substance used or exposed to.

Footwear was worn at all times to provide ‘protection to the top of the foot, support the fore foot and heel, and have a non-slip sole’ [ESR Health & Safety Guidelines].

Eyewear was worn when in any lab (as per university lab safety standard). Eyewear included glasses for general lab work and a full-face shield during experiments or any other time when there is a risk of blood being splashed into the face.

In the *blood spatter labs* disposable gloves were worn at all times. During preparation of blood or work that did not involve blood spatter, safety glasses and disposable overalls or a disposable lab coat were worn. When blood spatter was involved disposable booties, overalls with hood up, gloves, and full-face shield were worn.

General Hygiene

Hands were washed in soapy water before leaving any lab. Two buckets, one containing soapy water and the other containing clean water, were taken down to the basement lab on each experimental day for hand washing (there is no basin in the basement).

Gloves, overalls, lab coats and protective clothing were taken off before leaving the basement lab. If bloody equipment was being brought up to the main lab fresh overalls and gloves were put on immediately before coming upstairs.

Disposable items were disposed of in the medical waste bin in the lab. All other items remained in the basement lab, unless they were being removed for cleaning/ scanning etc.

Equipment & Equipment Hygiene

Separate equipment was used for blood spatter experiments and that equipment kept in the lab in which it was used, unless specifically required to be removed (i.e. for cleaning).

Disposable items were disposed of into a medical waste bin, or medical 'sharps' bin as appropriate, which were located within the labs and refreshed as necessary.

Glassware was washed down with detergent between uses and autoclaved before being put back for general use in the lab.

All other *reusable items* were washed down with detergent and wiped down with hypochlorite solution.

Blood***Transport, Packaging & Labelling***

All containers used for collecting blood were labelled with: the contents (i.e. pigs blood and EDTA), when it was collected and the batch number. Bottles used for collecting blood were sealed in a plastic bag, during transit from the abattoir.

Disposal

Excess blood is to be washed down the sink with a large amount of water, and bleach added if necessary.

Containment

The exterior of items that contained blood or had come into contact with blood were wiped down and kept as clean as possible to prevent the spread of blood to non-bloody items.

When items containing blood or that were bloody were brought up to the main lab for cleaning they were contained in a plastic or metal tray, and on a trolley.

Blood was kept in a designated refrigerators in the laboratories, no substance that was not blood or not related to experiments with blood was permitted in this refrigerator.

Health & Safety Procedures Specific to Pig's Blood

An Internet search revealed a number of zoonotic diseases that can be contracted from pigs. However, the majority of these are contracted from faecal contamination or by eating uncooked pork and therefore will not be an issue when handling blood. The major zoonotic disease that can be contracted from pig's blood is brucellosis. The *Brucella* organism can be life threatening to humans and can cause severe fever, lesions on the spine and may even result in sterility in males. In order to prevent infection it was recommended that gloves should be worn at all times whenever handling pig's blood, hands should be washed with hot soapy water after handling, and food or drink should never be consumed in the laboratory.

Alliance Group Ltd, Sockburn, the supplier of the blood used in these experiments advised that *Leptospirosis* was the only zoonotic disease that they encounter and take precautions for. The primary route of transmission is via contact with pig urine and precautions include the use of safety glasses, gloves and ensuring all cuts are covered. As this disease is not transmitted via blood it should not be hazardous in the context of our use.

In all experiments involving the use of pig's blood a minimum of gloves should be worn at all times, and whenever blood is to be spattered, overalls, booties, and protective face and eye wear should be adorned.

Injury or Accident

Appropriate first aid should be applied and the incident reported to the Health & Safety Officer. All accidents or injuries, no matter how minor - including blood splashed onto skin, face, eyes, or mouth – must be reported to the Health & Safety Officers for the Forensic Group, as soon as possible.

Spills

Spills should be cleaned up immediately, or contained and assistance sort. Large spills must be reported to a Health & Safety Officer as soon as possible.

APPENDIX 2: RESULTS TABLES AND DATA

The tables of the data collected during this research have been put onto the CD on the back cover of this thesis. The following are the results from the experiment carried out in section 5.2.

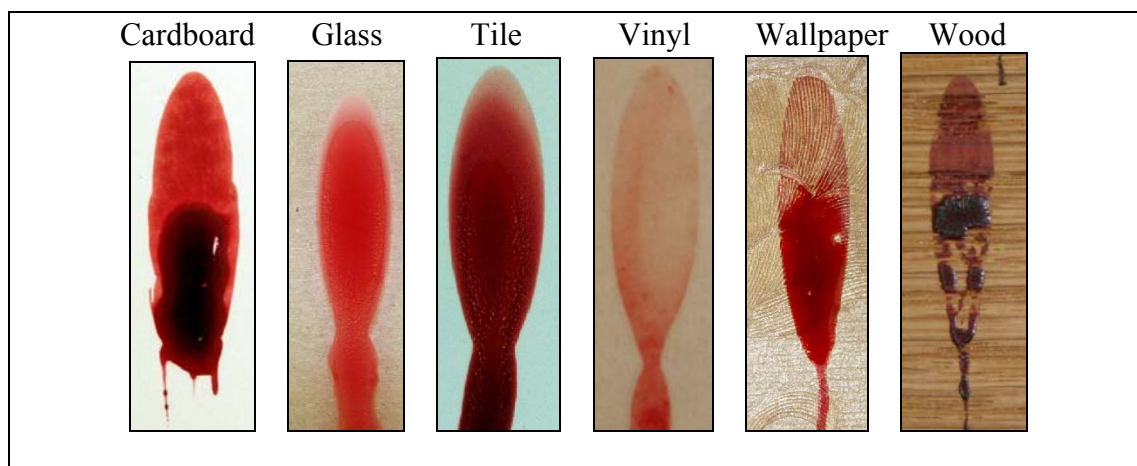


Figure A2-1 Examples of photographs taken of bloodstains formed on different surfaces at 20 degrees.

Table A2-1: The average angle of impact calculated using Microsoft® Office Visio® Professional 2003 for different target surfaces including the standard deviation and observed minus expected value (difference between the average and known angle of impact). The actual angle of impact was 20 degrees.

Target Surface	Average Angle (°)	O-E	Std dev of angle
Cardboard	19.3	-0.7	2.2
Glass	20.5	0.5	1.2
Tile	20.9	1.0	1.1
Vinyl	19.6	-0.4	2.5
Wallpaper	17.7	-2.3	2.0
Wood	15.3	-4.7	2.0

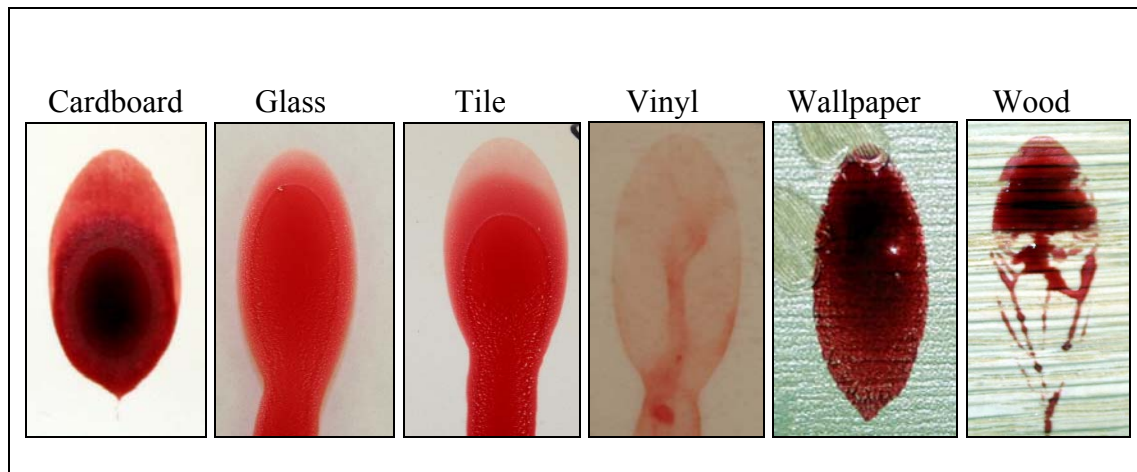


Figure A2-2 Examples of photographs taken of bloodstains formed on different surfaces at 30 degrees.

Table A2-2 The average angle of impact calculated using Microsoft® Office Visio® Professional 2003 for different target surfaces including the standard deviation and observed minus expected value (difference between the average and known angle of impact). The actual angle of impact was 30 degrees.

Target Surface	Average Angle (°)	O-E	Std dev of angle
Cardboard	33.4	3.4	1.0
Glass	31.2	1.2	1.5
Tile	31.8	1.8	1.5
Vinyl	32.9	2.9	1.7
Wallpaper	29.9	-0.1	2.6
Wood	24.6	-5.4	1.9

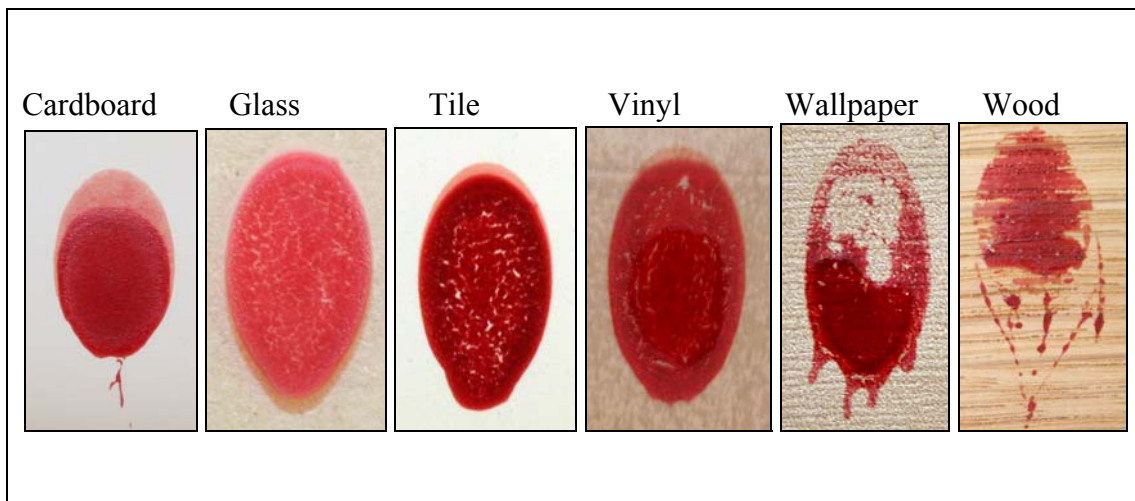


Figure A2-3 Examples of photographs taken of bloodstains formed on different surfaces at 40 degrees.

Table A2-3 The average angle of impact calculated using Microsoft® Office Visio® Professional 2003 for different target surfaces including the standard deviation and observed minus expected value (difference between the average and known angle of impact). The actual angle of impact was 40 degrees.

Target Surface	Average Angle (°)	O-E	Std dev of angle
Cardboard	41.9	1.9	2.9
Glass	39.9	-0.1	1.9
Tile	41.6	1.6	2.8
Vinyl	39.1	-0.9	1.3
Wallpaper	35.6	-4.4	3.5
Wood	35.7	-4.3	3.1

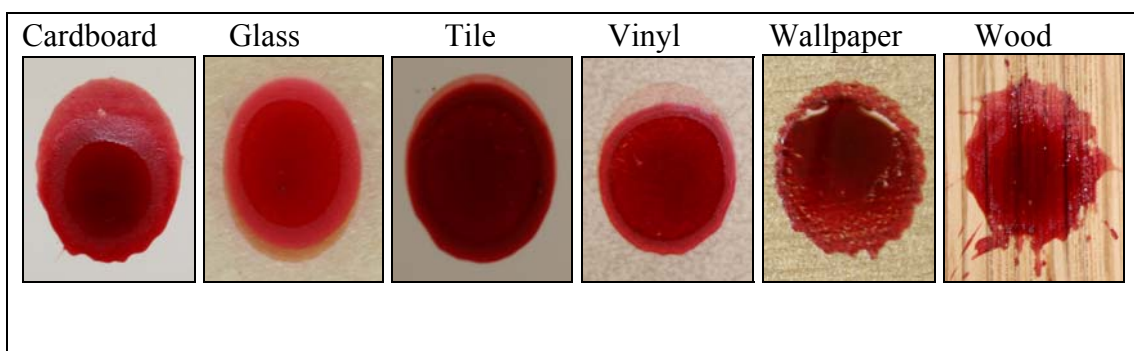


Figure A2-4 Examples of photographs taken of bloodstains formed on different surfaces at 60 degrees.

Table A2-4: The average angle of impact calculated using Microsoft® Office Visio® Professional 2003 for different target surfaces including the standard deviation and observed minus expected value (difference between the average and known angle of impact). The actual angle of impact was 60 degrees

Target Surface	Average Angle (°)	O-E	Std dev of angle
Cardboard	59.1	-0.9	3.5
Glass	61.7	1.7	2.1
Tile	61.6	1.6	3.8
Vinyl	60.3	0.3	2.4
Wallpaper	62.4	2.4	3.7
Wood	59.3	-0.7	3.7

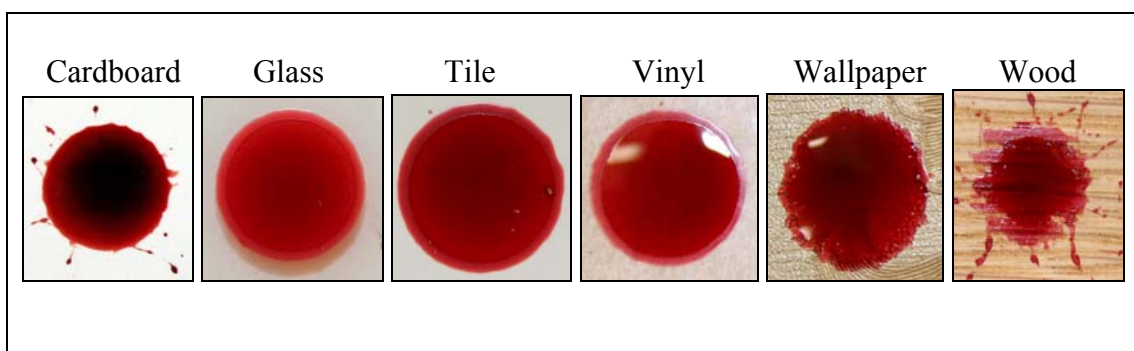


Figure A2-5 Examples of photographs taken of bloodstains formed on different surfaces at 80 degrees.

Table A2-5: The average angle of impact calculated using Microsoft® Office Visio® Professional 2003 for different target surfaces including the standard deviation and observed minus expected value (difference between the average and known angle of impact). The actual angle of impact was 80 degrees.

Target Surface	Average Angle (°)	O-E	Std dev of angle
Cardboard	75.6	-4.4	3.9
Glass	80.2	0.2	3.1
Tile	77.8	-2.2	3.1
Vinyl	79.7	-0.3	3.8
Wallpaper	78.3	-1.7	4.0
Wood	73.9	-6.1	8.7

REFERENCES

1. Wilson, F.E., Schuessler, D.R., *Geometric bloodstain pattern interpretation using a computer program*. Crime Laboratory Digest, 1987. 14(3): p. 95-97.
2. MacDonell, H.L., *Bloodstain Pattern Interpretation*. Corning, New York, Laboratory of Forensic Science, 1982.
3. James, S.H., Kish, P. E., Sutton, T. P., *Principles of bloodstain analysis: theory and practice*. Practical aspects of criminal & forensic investigation, ed. K. Stuart H. James, P. E., T. Paulette Sutton. 2005, Boca Raton, Fla: CRC Press. xxv, 542 p.
4. Bevel, T. and R.M. Gardner, *Bloodstain pattern analysis: with an introduction to crime scene reconstruction*. 2nd ed. CRC series in practical aspects of criminal and forensic investigations. 2001, Boca Raton: CRC Press. xxvi, 391.
5. James, S.H. and W.G. Eckert., *Interpretation of bloodstain evidence at crime scenes*. 2nd ed ed. CRC series in practical aspects of criminal and forensic investigations. 1999, Boca Raton: CRC Press. xiv, 324.
6. IABPA. *International Association of Bloodstain Pattern Analysts - Terminology list*. [cited 2006 4 March]; Available from: <http://www.iabpa.org/Terminology.pdf>.
7. Wonder, A., *Blood dynamics*. 2001, London: Academic Press. viii, 168.
8. Richardson, S., *It's All in the Blood*. Pony Express, 1997. 22(4): p. 25-27.
9. Slemko, J. *Bloodstain pattern analysis tutorial*. [cited 5 May 2006]; Available from: <http://www.bloodspatter.com/BPATutorial.htm>.
10. Rizer, C., *Blood drop patterns*. Police, 1960. 4(3): p. 18-19.
11. Carter, A.L., et al., *Validation of the BackTrack suite of programs for bloodstain pattern analysis*. Journal of Forensic Identification, 2006. 56(2): p. 242-254.
12. Carter, A.L., *The directional analysis of bloodstain patterns: theory and experimental validation*. Journal of the Canadian Society of Forensic Science, 2001. 34(4): p. 173-189.
13. Carter, A.L. *Bloodstain Pattern Analysis* <http://www.physics.carleton.ca/~carter/index.html>. 2004 [cited June 2006; Available from: <http://www.physics.carleton.ca/~carter/index.html>.
14. Carter, A.L., *Bloodstain pattern analysis with a computer*, in *Scientific and legal applications of bloodstain pattern interpretation*, S.H. James, Editor. 1998, CRC Press: Boca Raton, Florida.
15. Carter, A.L., et al., *Further validation of the BackTrack computer program for bloodstain pattern analysis - Precision and accuracy*. IABPA News, 2005. 21(3): p. 15-22.
16. MacDonell, H.L., *Bloodstain patterns*. 1993, Corning, New York: Laboratory of Forensic Science. xvi, 182.
17. *Daubert et al., v Merrell Dow Pharmaceuticals Inc*. 1993, United States Supreme Court.
18. Willis, C., et al., *Errors in the estimation of the distance of fall and angles of impact of blood drops*. Forensic Science International, 2001. 123(1): p. 1-4.
19. Raymond, M.A., *Trajectory reconstruction from bloodstains at a crime scene. Thesis submitted in fulfillment of the requirements for the degree of Doctor of Philosophy*. 1997, La Trobe University: Australia.
20. Rowe, W.F., *Errors in the determination of the point of origin of bloodstains*. Forensic Science International, 2005. In Press, Corrected Proof.

21. Laturnus, P. *Measurement survey*. in *International Association of Bloodstain Pattern Analysts*. 1991. Montreal: IABPA News.
22. Liesegang, J., *Bloodstain pattern analysis - Blood source location*. Journal of the Canadian Society of Forensic Science, 2004. 37(4): p. 215-222.
23. Raymond, M., E. Smith, and J. Liesegang, *Oscillating blood droplets - implications for crime scene reconstruction*. Science & Justice, 1996b. 36(3): p. 161-171.
24. Pace, A., *The relationship between errors in ellipse fitting and the increasing degree of error in angle of impact calculations*. IABPA News, 2005. 21(3): p. 12-14.
25. Carter, A.L. and E.J. Podworny, *Bloodstain pattern analysis with a scientific calculator*. Journal of the Canadian Society of Forensic Science, 1991. 24(1): p. 37-42.
26. Janes, W.L., *Developments in the practical reconstruction of blood spatter events*, in *Forensic Science Program, Department of Chemistry*. 2001, The University of Auckland: Auckland.
27. Raymond, M., E. Smith, and J. Liesegang, *The physical properties of blood - forensic considerations*. Science & Justice, 1996a. 36(3): p. 153-160.
28. Rein, M., *Phenomena of liquid drop impact on solid and liquid surfaces*. Fluid Dynamics Research, 1993. 12: p. 61-93.
29. Pizzola, P.A., S. Roth, and P.R. De Forest, *Blood droplet dynamics. I*. Journal of Forensic Sciences, 1986a. 31(1): p. 36-49.
30. Bevel, T. and R.M. Gardner, *Bloodstain pattern analysis: with an introduction to crime scene reconstruction*. CRC series in practical aspects of criminal and forensic investigations. 1997, Boca Raton: CRC Press.
31. Reynolds, M., *Personal communication*. 2006.
32. Slemko, J.A., *Bloodstains on Fabric: The Effects of Droplet Velocity and Fabric Composition*. IABPA News, 2003. December: p. P3-11.
33. *AST Products Inc.* [cited 2006 October]; Available from: www.labkorea.com.
34. KSV. *Powder Wettability - Application note #104*. Jan 28 2005 [cited 2006 10 April]; Available from: http://www.ksvinc.com/powder_wetting.htm.
35. Bussmann, M., Mostaghimi, J., and Chandra, S., *On a three-dimensional volume tracking model of droplet impact*. Physics of Fluids, 1999. 11(6): p. 1406-1417.
36. Pasandideh-Fard, M., Qiao, Y. M., Chandra, S. and Mostaghimi, J., *Capillary effects during droplet impact on a solid surface*. Physics of Fluids, 1996. 8(3).
37. Ford, R.E., Furnidge, C. G. L. *Impact and spreading of spray drops on foliar surfaces*. in *Colloid and Surface Chemistry Group of the Society of Chemical Industry*. 1967. Bristol.